Assessment of Impacts of Groundwater Salinity on Regional Groundwater Resources, Current and Future Situation in Mewat, Haryana – Possible Remedy and Resilience Building Measures (NIH-4_2016_5)

National Hydrology Project
Department of Water Resources, River Development and Ganga Rejuvenation, Ministry of Jal Shakti, New Delhi

National Institute of Hydrology, Roorkee
Department of Water Resources, River Development and Ganga Rejuvenation, Ministry of Jal Shakti, New Delhi

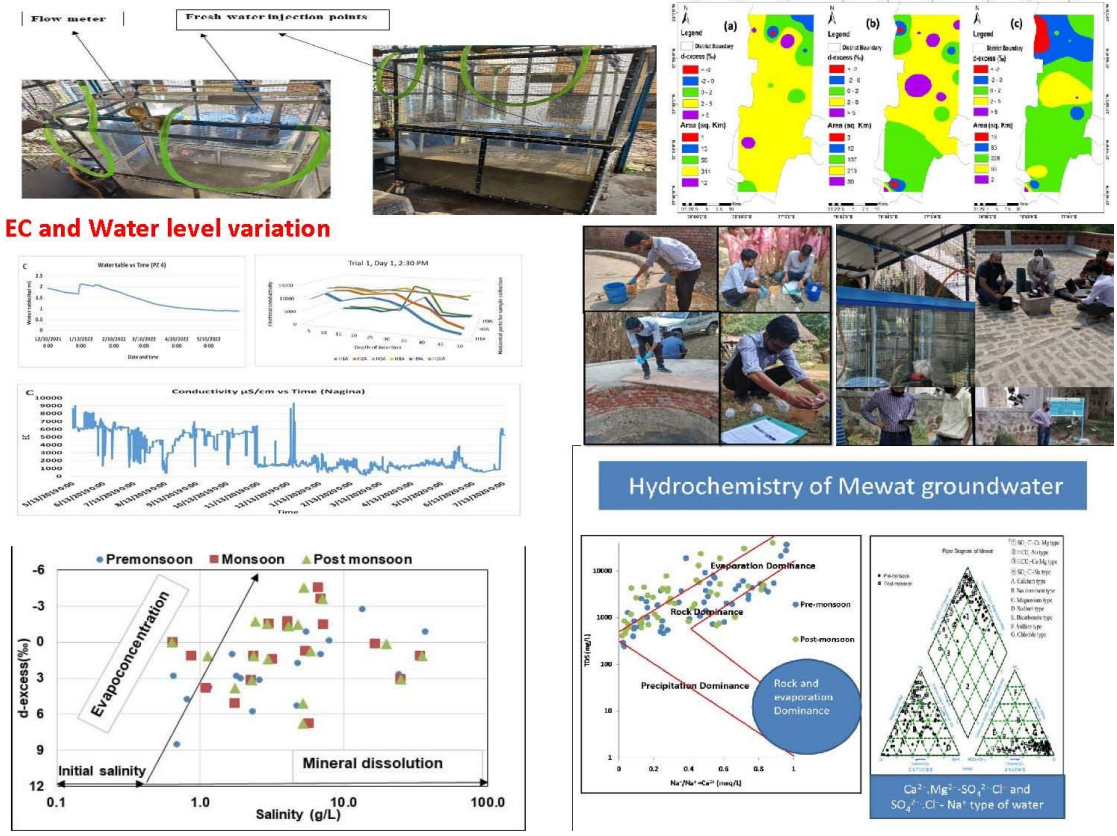

NATIONAL INSTITUTE OF HYDROLOGY, ROORKEE 247667, UTTARAKHAND
July 2022

Dr. J V Tyagi
Director

National Institute of
Hydrology, Roorkee-
247667
Uttarakhand

PREFACE

Groundwater salinity is a widespread problem in many productive agricultural areas in India, including many districts of Haryana. Aquifer salinization gradually affects the agro-economy, livelihoods, and drinking water supply on a local and regional scale due to the lowering of groundwater levels. Salinity is the main factor limiting the continued use of groundwater in surface water-scarce areas, and future reliance on groundwater is further diminished as groundwater levels decline, creating increases in salinity and exploitation costs. Systematic groundwater development and management that fulfills the technical needs of supply-side and demand-side components can arrest the aggravation of salinity and provide a sustainable solution to the problem.

This study aims to take a comprehensive view of hydrological and hydrogeological features together with chemistry and isotopic characteristics of groundwater for evaluating the causes of aquifer salinity, including its aggravation and effect on agro-economy, drinking water supply, and livelihoods, considering the problem of Mewat district in Haryana as the pilot study area. A few demonstrative schemes as resilience-building measures towards arresting the aggravation of salinity and increase of managed aquifer recharge together with their impact assessment on overall groundwater resources have also been successfully carried out in the controlled as well as field conditions. The development of an experimental model to predict changes in groundwater salinity as a result of aquifer recharge and extraction is another focus of the study.

The work was carried out by the Ground Water Hydrology Division of the Institute. It was led by Dr. Gopal Krishan, Scientist D, as the Principal Investigator in association with other team members. I appreciate all the work associated with the study.

Place: Roorkee
Date 29-07-2022 (J V Tyagi)

Project Team

Lead organization	National Institute of Hydrology, Roorkee-247667, Uttarakhand
	Dr. Gopal Krishan, Scientist D (PI) Dr. N.C. Ghosh, Scientist G & Ex-Head, GHWD (Co-PI up to March 2019) Er. C.P. Kumar, Scientist G & Ex-Head, GHWD (Co-PI up to September 2020) Dr. Surjeet Singh, Scientist F (Co-PI) Er. S.K. Verma, Scientist D (Co-PI up to February 2020) Dr. M.S. Rao, Scientist F (Co-PI from March 2020)
Partner organization	Irrigation and Water Resources Department, Haryana, Sector 5, Panchkula
	Executive Engineer, Nuh
Consultants	Indian Institute of Technology-Roorkee. Roorkee-247667, Uttarakhand
	Prof. M.L. Kansal Prof. Brijesh Kumar Yadav
	Sehgal Foundation, Gurgaon Sh. L.M. Sharma
Co-consultants	Prof. Allen Bradley, University of Iowa, USA Prof. Marian Muste, University of Iowa, USA

The Document Control Sheet

Title	Assessment of Impacts of Groundwater Salinity on Regional Groundwater Resources, Current and Future Situation in Mewat, Haryana – Possible Remedy and Resilience Building Measures
PDS number	NIH-4_2016_5
Date of approval	December 04, 2017
Budget in time of original approval (For Partner and Lead)	65 lakhs
Revised Budget (For Partner and Lead)	NA
Date of commencement	December 04, 2017
Date of completion	July 2022
Number of pages	
Number of figures and tables	

Abstract

Evaluation of groundwater quality parameters and their controlling processes are very important for the sustainable utilization of groundwater in any region. In the present study, more than 300 groundwater samples were collected during the years 2018 and 2019 from the tube wells and public water supply wells in the Mewat district, Haryana to investigate the water quality parameters to ascertain suitability for drinking purposes, and also to understand hydro geochemical processes by considering an integrated approach and salinity mechanisms. Different methods namely, conventional hydro-geochemical analysis, isotope analysis, ion ratio, etc. were applied. The results showed that the groundwater of Mewat is highly saline. Silicate weathering, evaporation, and cation exchange were the three factors controlling the geochemical composition of groundwater in Mewat district.

As remediation and management solutions, Aquifer Storage and Recovery (ASR) - a water management technique for storing excess freshwater during wet periods and recovering stored water during dry periods has been studied and recommended. The proposed method presents a viable option to harness the full potential of groundwater especially, in the saline groundwater zones of Mewat.

Originating unit	National Institute of Hydrology, Roorkee
Keywords	Groundwater salinity, mechanism, remedial and management solutions, Mewat (Nuh), Haryana
Security classification	~~Restricted~~/ Unrestricted
Distribution	~~Restricted~~/ General

List of Contents

List of Figures

List of Tables

ACKNOWLEDGEMENT

Groundwater is a hidden resource and its potential, availability, and contamination are based on the observations, formations, aquifer materials, etc., and more importantly, sample analysis. In this study, extensive fieldwork was carried out to survey, and sampling, and through analysis and monitoring massive database was generated to come to any inference since this is very significant and relevant especially when a problem is associated with drinking and irrigation.

First and foremost I express my sincere and humble gratitude to NIH Directors, Sh. R.D. Singh, Dr. Sharad Jain, and Dr. JV Tyagi for providing all kinds of cooperation and support. Heads of Groundwater Hydrology Division, Dr. N.C. Ghosh, Er. C.P. Kumar, and Dr. M.K. Goel, for all your encouragement throughout the project. I would like to thank Dr. Sanjay Jain, Nodal officer, NHP for his constant guidance.

I, on behalf of the institute and study team thankfully acknowledge Haryana Irrigation Department particularly Er. Rajiv Bansal, EIC for entrusting the task to NIH in the form of Purpose Driven Study through the World Bank-aided National Hydrology Project and for allowing us to address such a significant problem. Thanks to all the support received from Sehgal Foundation, Gurgaon in the form of logistic support which was much needed for conducting the work properly in the fields. Thanks to PDS coordinators Er. C.P. Kumar, Er. D.S. Rathore, Dr. Manohar Arora. Thanks to Dr. AK Lohani for coordinating training under this PDS.

My gratitude would be incomplete without mentioning the names of Profs. M.L. Kansal, Brijesh Yadav, IIT-Roorkee; Sh. Lalit Sharma, Sehgal Foundation, Gurgaon; Dr. M.S. Rao, Sh. Vishal Gupta, Sh. Vipin Agarwal for isotope analysis and Sh. Ram Chander, Sh. C.S. Chauhan, NIH Roorkee for field investigations. Thanks to Mr. Sanjay Mittal for the heavy metal analysis. Thanks to all project staff namely Pankaj, Mamta, Gokul, Priyanka, Ravi, Mohit, Rahul, Ankur, and Archit for sample collection, fieldwork, and analysis. Thanks to Zafar and his team for help in locating sampling points in the field.

Thanks to Profs. Marian Muste and Prof. Allen Bradley, the University of Iowa for helping in the study by providing data generated from the piezometers developed by Iowa university in the initial phases of the study. Thanks to Dr. Peter Ravencraft for his valuable suggestions on salinity identifications. Data received from the Groundwater water cell, Haryana irrigation, and rainfall data from the revenue department is duly acknowledged. Thanks to students Johnnes Medik (HTWD, Germany) Abhishek, Ashutosh (MMIT, Gorakhpur), Jayprakash (NIT-Manipur), Radhye (CU, Mahendergarh), Gokul, Gayatri (KUFOS, Kerala).
I also take this opportunity to thank all the staff of the Groundwater Hydrology division, NHP office (procurement), finance, and bill section for extending all support during the project work.

Date: July 29, 2022
Place: Roorkee **(Gopal Krishan)**

1.0INTRODUCTION

1.1 **General**

Groundwater

Groundwater is the water that is found below the earth's surface and is stored in the cracks and spaces in soil, sand, and porous rocks. Most groundwater comes from rain that has infiltrated through the ground and accumulated over thousands of years. Water covers seventy percent area of the earth and is requisite for all life-supporting processes vital for all biological communities. Amongst all forms of water, groundwater is the most used in different sectors like domestic, industrial, and agricultural throughout the world (Yang et al., 2016; Yousefi et al., 2018). The water table is the depth at which soil pore spaces or fractures and voids in rock become completely saturated with water. Groundwater is recharged from the surface; it may discharge from the surface naturally as springs and seeps and can form oases or wetlands. Groundwater is often withdrawn for agricultural, municipal, and industrial use by constructing and operating extraction wells.

Issues and challenges

With the rapid population explosion, many water-related needs have increased with time. In many parts of the world, groundwater has been exploited at a speedy rate, resulting in groundwater levels and quantity depletion. Water scarcity problems have almost existed in all arid and semi-arid regions of the world during the last decades. The dependence of human and ecological communities on groundwater and their respective challenges varies substantially across the globe. The communities' dependence on groundwater can be seasonal or episodic; for example, the resource may become critical to survival during a severe drought when surface water resources run dry. There are countries, such as Belgium, Denmark, Saudi Arabia, and Austria, where over 90 % of total water consumption is sourced from aquifers (Zektser and Everett, 2004). However, on average, groundwater comprises approximately 20 % of the world's water use. In many humid regions, such as Japan and northern Europe, groundwater is mainly used for industrial and domestic purposes (Villhoth and Giordano, 2007). In most countries outside the humid intertropical zone, groundwater is predominantly used for agricultural purposes, especially irrigation (Zektser and Everett, 2004). Many large aquifers vital to Agriculture, notably in India, Pakistan, Saudi Arabia, the USA, China, Iran, and Mexico, are under threat from over-exploitation (Gleeson et al., 2012; Wada et al., 2012).

Where groundwater abstraction exceeds recharge over long periods and extensive areas, the subsequent decline in water table level affects natural groundwater discharge, which may have harmful impacts on groundwater-dependent streams, wetlands, and ecosystems (Wada et al. 2010). The groundwater issues are shown in fig. 1.1.

Regions with sustainable groundwater balance are shrinking day by day throughout the world. Three problems dominate groundwater use: depletion due to overdraft;

waterlogging and salinization primarily due to inadequate drainage and insufficient conjunctive use; and pollution due to agricultural, industrial, and other human activities. In regions of the world, especially with high population density, dynamic tube-well-irrigated agriculture, and insufficient surface water, many consequences of groundwater overdevelopment are becoming increasingly evident.

The most common symptom is a secular decline in water tables. Besides depletion, waterlogging and the pollution of aquifers through human activity constitute another major groundwater challenge. Waterlogged areas in India are estimated at 6 million hectares; in 12 major irrigation projects with a design command of 11 million hectares, 2 million hectares were three waterlogged, and another million hectares were salinized (Mudrakartha, 1999).

1.2 Groundwater salinity

Salinization is a global issue of grave concern because it reduces the potential productivity and use of land and water resources. In coastal regions that are close to the sea, salinization may lead to changes in the chemical composition of natural water resources, degrading the quality of water supply to the domestic, agriculture, and industrial sectors, loss of biodiversity, taxonomic replacement by halo-tolerant species, loss of fertile soil, the collapse of agricultural and fishery industries, changes in local climatic conditions, and creating health problems; thus, affecting many aspects of human life and posing a major hindrance to the economic development of the region.

Groundwater salinity may arise from natural and artificial sources, resulting in a change in the chemistry of the aquifer. The natural sources include water-rock interactions, salts dissolution, the geology of the aquifer, and geogenic weathering. In contrast, anthropogenic sources like wastewater disposal on the surface and over-extraction of groundwater may lead to saline water intrusion and irrigation in dry areas where improper drainage networks are used. Decreasing groundwater levels due to overexploitation of coastal aquifers, in particular in regions under arid and semi-arid conditions, can result in saline water intrusion (Louvat et al., 1999; Edmunds and Milne, 2001; Kim et al., 2003; Cartwright et al., 2004; Pulido-Leboeuf, 2004; Bouchaou et al., 2008).

1.2.1 Types of salinity

Changes in land use, seasonal variations in our weather, and long-term climate changes can all affect the surface water, groundwater, the flows between them, and the amounts of salt that they contain. The term "salinity" refers to the concentration of salts in water or soils. Salinity can take three forms, classified by their causes: primary salinity (also called natural salinity); secondary salinity (also called dryland salinity), and tertiary salinity (also called irrigation salinity).

1.2.2 **Primary salinity (natural salinity)**

Primary salinity is caused by natural processes such as the accumulation of salt from rainfall over many thousands of years or from the weathering of rocks. When rain falls on a landscape, some evaporates from the soil, vegetation surfaces, and water bodies, some infiltrate into the soil and the groundwater, and some enter streams and rivers and flow into lakes or oceans. The small amounts of salt brought by the rain can build up in soils over time (especially clay soils) and can also move into the groundwater, increasing the salts content of the aquifer.

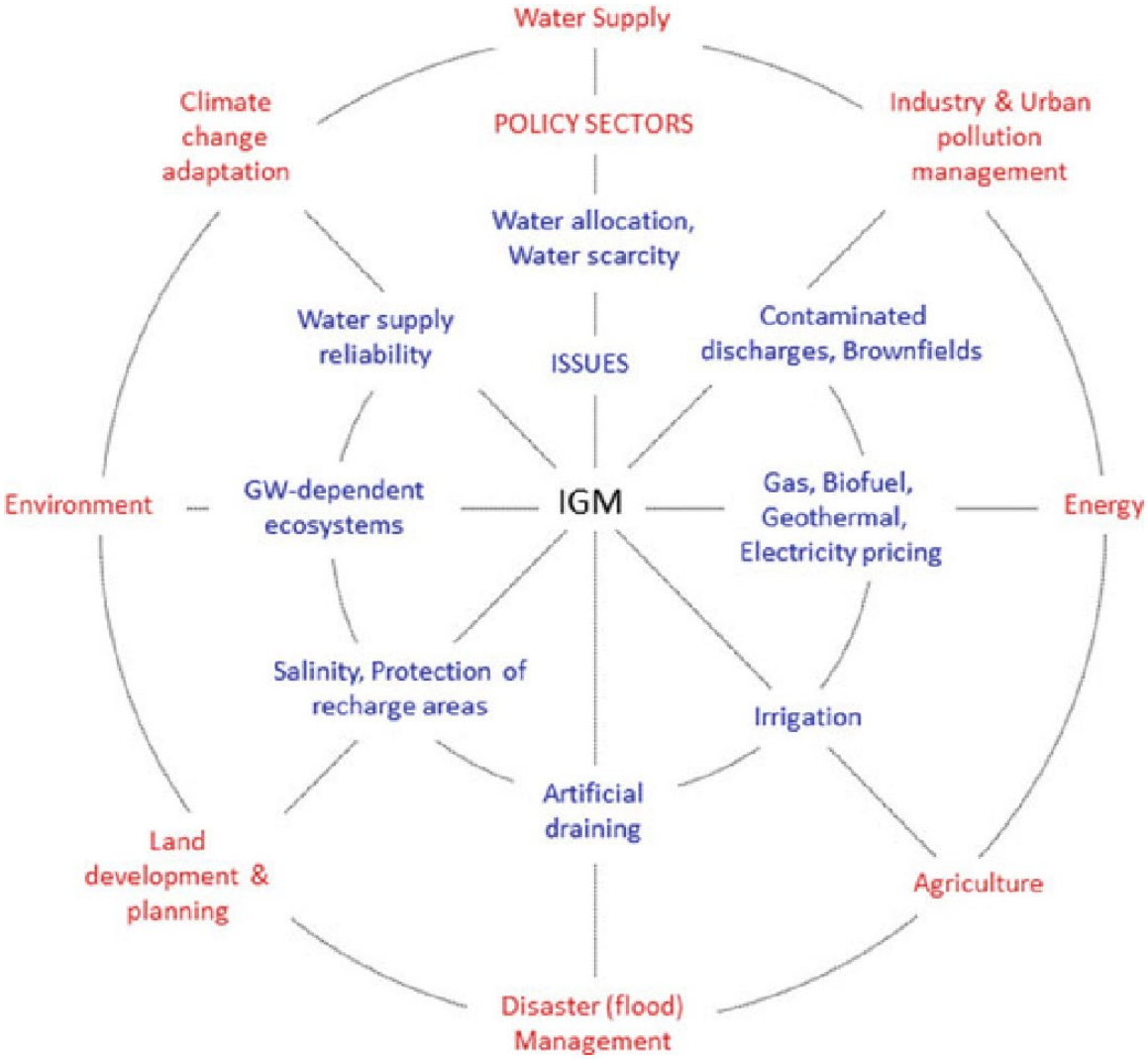

Fig. 1.1 Diverse issues related to groundwater and their relevant policy sectors (A.J. Jakeman et al., 2016)

1.2.3 **Secondary or dryland salinity**

Secondary salinity is caused when groundwater levels rise, bringing salt accumulated through primary salinity processes to the surface. This is caused by the clearing of perennial

(long-lived) vegetation in drier areas, i.e. areas that accumulate salt in the soil profile and groundwater over time. When foliage is cleared, as happened extensively in the Western Australian wheat belt, the amount of water lost from the landscape through plants is drastically reduced. Instead, more water enters the groundwater, and groundwater levels rise. As groundwater levels rise, they bring the salt into the groundwater and dissolve the salt in the previously unsaturated part of the soil profile. Eventually, low-lying areas of valley floors may become fully saturated (especially during winter), and the amount and duration of flow in streams and rivers increases. The discharging saline groundwater mixes with the fresher surface water to cause flows that vary between marginal to brine. As these saturated areas dry out after the wet season, salt crystals can be left behind, causing a salt scald.

1.2.4 Tertiary or irrigated salinity

Tertiary salinity occurs when water is re-applied to crops or horticulture over many cycles, either directly or by filtering into the groundwater before pumping it out for re-application. Each time the water is applied, some of it will evaporate. The salts in the water remaining will become more concentrated, and very high salt concentrations can result from multiple cycles of reuse.

1.3 Salinity problem in the world

A study on groundwater salinization and associated co-contamination risk increase and severe drinking water vulnerabilities on the southwestern coast of Bangladesh was carried out by Rakib et al. (2019) and the mean value of measured EC was found to be approximately 7100 µS/cm in the coastal aquifer, which exceeded the water quality standards for both drinking and agriculture purposes. The extremely high values of EC in the southwestern coastal area of the country indicated the occurrence of significant seawater intrusion in the aquifer. Dang et.al (2020) investigated the evolutionary process of saline groundwater influenced by palaeo-seawater trapped in coastal deltas: A case study in Luanhe River Delta, China, and reported that vertical salinity gradient observed through an EC profile showed rapid incremental changes in the aquifer stratum. Major ions/ chloride ratios show an original marine source of salinity in the saline and brine groundwater. The relationship between the radiocarbon activity and chloride further revealed that paleo-seawater's primary source of salinity.

Salinity enrichment, sources, and its contribution to elevated groundwater arsenic and fluoride levels in Rachna Doab, Punjab, Pakistan was studied by Parvaiz et al. (2020) and it was observed that mineral dissolution, ion exchange processes, and partial input of evaporation were identified as the factors affecting groundwater salinity in the region. Van Gend et al. (2021) characterized groundwater type and sources of salinity in the study area. They reported major ion chemistry and 87Sr/86Sr isotope ratios which indicate that salts present in the groundwater are linked to dry deposition of marine aerosols and ion-exchange reactions in soils in the alluvial aquifer systems.

1.4 Salinity problem in India

The most important factor affecting the quality of groundwater in coastal aquifers is seawater, which contains several chemical constituents in very high concentrations compared to groundwater. The shallow groundwater is a major part of the west coast between Daman (UT) and Thiruvananthapuram (Kerala) exhibits EC less than 750 µS/cm except in a few patches around Raigarh in Maharashtra and Udupi in Karnataka, where higher EC up to 3000 µS/cm is observed. Further north, along the coast of Gujarat, the EC of shallow groundwater, in general, ranges from 1500 to 4500 µS/cm except in the area between Sikka and Hadiyana of the Jamnagar coast. However, certain coastal tracts of Kachchh and Saurashtra coasts and parts of the Gulf of Kachchh and the Gulf of Khambat show EC values above 4500 µS/cm. EC is up to about 20000 µS/cm near Vinjhan (Kachchh coast), 6000 µS/cm around Dwarka, 15000 to 18000 µS/cm, around Mangrol-Veraval (Saurashtra coast), 11000 to 12000 µS/cm near Shikarpur-Kumbhariya (Gulf of Kachchh) and 6000 to 12000 µS/cm near Jantram and Bhavnagar (Gulf of Khambat) (CGWB, 2014). Along the east coast, the EC of groundwater in the shallow aquifers varies, in general, from 750 to 3000 µS/cm except for a few patches with EC less than 750µS/cm around Digha on the coast of West Bengal and Kendrapara and Puri on the coast of Odisha (Table 1.1). In the northern part of Andhra Pradesh coast, the EC is mainly in the range of 750 to 1500 µS/cm, while in the southern part, it is mainly in the field of 1500 to 3000 µS/cm, although there are patches with EC values in the field of 3000 to 4500 µS/cm on the coast of Andhra Pradesh and Tamil Nadu. Shallow aquifers with very high EC in the field of 7000 to 22000 µS/cm are encountered only in the southern coastal districts of Tamil Nadu, viz., Pudukkottai, Ramanathapuram, Tuticorin, and Tirunelveli (Table 1.2). Thus, the quality of groundwater in coastal aquifers shows considerable variation from place to place, depending on a host of factors, including climate, geomorphology, geology, hydrogeological setting, and extent of anthropogenic influence (CWC 2017).

Groundwater in coastal areas occurs under unconfined to confined conditions in a wide range of unconsolidated and consolidated formations. Normally, saline water bodies owe their origin to entrapped sea water (connate water), seawater ingress, seepage from navigation canals constructed along the coast, leachates from salt pans, etc. In general, the following situations are encountered in coastal areas.

i. Saline water overlying freshwater aquifer
ii. Freshwater overlying saline water
iii. The alternating sequence of fresh water and saline water aquifers

Mewat is a semi-arid region, that exhibits high groundwater salinity and 65% of the surface water is also highly saline (ICAR, 2012). Groundwater salinity in many districts in Haryana has given rise to water scarcity for irrigation and domestic uses (CGWB, 2007). The increase in illegal extraction of groundwater from freshwater zones has forced the government to intervene for stopping such extractions. Mewat district lacks perennial surface water resources and thus, groundwater is being used as the source for irrigation and domestic water, which has resulted in aggravation of salinity. If exploited at the current

rate, the depleting fresh groundwater in the district can turn into serious water scarcity in the next 10-15 years (CGWB, 2007).

Table 1.1 Area-wise inland groundwater salinity and related causes in India

S. No.	Place/Block/ District/State		Area (km^2)	Aquifer Depth bgl(m)	Salinity Value/ Range (µS/cm)	Causes/Factors of Salinity	Data Source
	State	District					
1	Haryana	Mewat	1507	2 - 35	57968	Mineral dissolution and Evapo-concentration	Krishan et. al 2020
2	Punjab	Muktsar	2630	30	5980	Terrestrial origins, mineral dissolution	CGWB 2013
3	Delhi	NCT Delhi	1483	>30	37500	Evaporative enrichment, dissolution, and leaching of salt	Kumar et al. 2015
4	Rajasthan	Jalore, Bikaner, Bundi, Nagaur, Jodhpur, Sikar and Tonk	98928	0.01-121.3	3000 - 23000	Geogenic and mineral dissolution	CGWB 2019-20 and Krishan et al. 2020
5	Uttar Pradesh	Mathura	3340	50	> 4000	Geogenic/mineral dissolution	Misra and Mishra 2007

Saline aquifer zones can expand to a larger area over time and the saline water in the deeper zones may rise and reach closer to the ground surface due to several factors related to the regional geomorphology and human intervention, such as excessive groundwater withdrawal for irrigation from the upper, freshwater zones. Other factors affecting the increasing salinity of shallow aquifers include the natural higher salt content of the soil horizons in the semi-arid region, combined with high evapotranspiration and low annual rainfall (for aquifer recharge), excessive use of chemical fertilizers, and poor drainage conditions (Saini et al., 2016). Uncontrolled irrigation or excessive pumping of groundwater, in particular, is also the cause of declining water levels in northwest India (Krishan et al., 2013, 2014; Lapworth et al., 2015; MacDonald et al., 2016; Rodell et al., 2009; Rao et al., 2014). Similar conditions of salinity and depleting groundwater are reported in Mewat, a district of Haryana (Thomas et al., 2014). The availability of fresh groundwater has already reached a critical category (around 67%) in the Mewat district (CGWB, 2012; Saini et al., 2016), and the remaining aquifer must be protected against further deterioration and permanent loss that has occurred due to lack of suitable aquifer management strategies.

Several factors are responsible for the rapid depletion of freshwater aquifers in Mewat; some of which are attributable to Mewat's ground conditions. First, saline aquifers in Mewat are located in low-lying areas that contain saline soil. Second, a good amount of runoff generated from the Aravalli Hills in the district flows down into these low-lying saline groundwater areas, recharges the saline aquifers, and raises the saline water tables.

Table 1.2 Area-wise coastal groundwater salinity and related causes in India

S. No.	Place/Block/District/State		Area (km^2)	Aquifer Depth bgl (m)	Salinity Value/Range (µS/cm)	Causes/Factors of Salinity	Data Source
	State	District/s					
1	Gujarat	Kachchh	456.52	40	1500 - 4500	Seawater ingress	CWC Report 2017
2	Maharashtra	Thane, Raigarh, Ratnagiri, and Sindhudurg	24781	10–20	4000 - 4400	Seawater ingress	CWC Report 2017
3	Karnataka	Uttara Kanada,DakshinaKanada and Udupi	18730		4230	Marine deposits and tidal influence	CWC Report 2017
4	Kerala	Kozhikode,Kasaragod,Kannur, Malappuram and Thrissur	1492.62	12	>3000	Geogenic factors and long residence time	CWC Report 2017
5	Tamil Nadu	Coimbatore, Chennai, Cuddalore, Dindigul, Dharmapuri, Ramanathapuram,	23739	11-103	7000 - 22000	Seawater ingress	CWC Report 2017 and CGWB 2008
6	Andhra Pradesh	Prakasam	17626	100	46000	Seawater intrusion	CWC Report 2017
7	Odisha	Puri	530.16	135- 200	3000	Geogenic origin	CWC Report 2017
8	West Bengal	Haldia	683.9	70-360	3000	Seawater (Cannate water)	CWC Report 2017
9	Puducherry (UT)	Puducherry	492	2-12	30000	Seawater contamination	CWC Report 2017
10	Goa	North Goa and South Goa	3702	22	-	Marine deposits and tidal influence	CWC Report 2017

Third, most fresh groundwater tables are contained in foothills with higher ground gradients. Although a large amount of runoff is generated from the uphill areas passes through these areas but it flows rapidly due to the high-gradient freshwater areas. Because of its low concentration time, freshwater percolation into the ground is minimal here. The result is the poor recharging of fresh groundwater pockets. Fourth, fresh groundwater tables are found deeper than saline groundwater tables. Due to the difference in depth between the two groundwater tables, saline groundwater flows toward fresh groundwater tables. As

a result, to attain the equilibrium condition, saline groundwater spreads and encroaches over freshwater pockets and thereby existing limited freshwater pockets are shrinking.

With these unfavorable circumstances, more than 95% of the population in the district live in rural pockets and predominantly depend on agriculture as their occupation. The district also lags behind all other districts of Haryana in terms of almost all development indicators, such as education, health, livelihood, etc. The percentage of rural households living Below the Poverty Line (BPL) in the Mewat area is almost double that of all other districts in the state. The literacy rate in the district is quite low (41.7%), and has an unequal female to male ratio (907:1000), high infant mortality rate, and poor maternal health.

Given the high level of salinity that worsens the impoverishment in the Mewat and similar regions elsewhere, there is a growing realization to better understand the role of salinity on existing socio-economic conditions of the region so that appropriate policy initiatives could be undertaken to address the high level of poverty in the region. Though there is a vast body of literature available on vulnerable indicators in the district, there are limited studies that offer insight into the impact of high groundwater salinity on the socio-economic vulnerabilities in the district. Groundwater salinization has been cited as the biggest single threat to aquifer sustainability (Foster and Chilton, 2003). Salinization can be caused by saltwater intrusion resulting from aquifer drawdown (primary salinization), or by agricultural intensification (secondary salinization). It has been estimated that 20% of the world's irrigated areas are affected by secondary salinization, with India, China, Pakistan, and Australia accounting for some of the most salinized soils.

The saline groundwater villages are dependent on surrounding fresh groundwater villages for their water demands. So another factor for the rapid freshwater depletion is the extraction of fresh groundwater to meet the domestic and agricultural water demands of these and surrounding saline groundwater villages at a rate that outpaces that of natural water recharge. Further exacerbating the situation, some villagers indiscriminately use available fresh water for domestic and agricultural purposes. For example, wealthier farmers purchase small patches of land located above fresh groundwater tables, install tube wells and transport the fresh water through an underground pipeline to irrigate fields located in saline groundwater areas. The result of these combined factors is enlarging saline groundwater areas, which poses a challenge to the water resource management in Mewat.

Taking into account the twin problem of declining water levels in fresh groundwater areas and the increasing spread of saline groundwater, this joint study is proposed by the National Institute of Hydrology, Roorkee along with the Indian Institute of Technology, Roorkee to assess (i) groundwater resources, (ii) salinity and (iii) development of the remediation measures; and SM Sehgal foundation is included to assess the impacts of groundwater salinity on socio-economic aspects; and demonstrations and promotion of resilience building measures.

Objectives

This proposed investigation included the following key components.

1. Assessment of lowering of the water table (depletion in groundwater level) in the salinity impacted area using the historical data.
2. Detailed qualitative analysis of the area and the aquifer depth impacted by higher salinity levels, and preparation of maps.
3. To monitor the influx of saline groundwater into the freshwater zone.
4. To assess the impact of groundwater salinity on socio-economic aspects.
5. To develop and demonstrate the management and resilience-building measures.

2.0 REVIEW OF LITERATURE

In Australia's Murrumbidgee Irrigation Areas, the influence of the water table, water-conducting soil qualities, climatic variables, and groundwater salinity on the salinization of soils was investigated by (Talsma, 1963). Between May 1960 and October 1961, average daily capillary flow rates were computed based on salinity measurements (through sampling). Using suction readings from tensiometers, potential gradients were determined. For the examined soils, the proportion of accessible water varied from 8 to 14%. There was a strong correlation between auger hole-measured hydraulic conductivity and capillary conductivity computed from chloride buildup (measured monthly sampling). The correlation between field data and the theory of steady-state flow across unsaturated soils was excellent when evaporation by the soil's moisture-conducting properties was not restricted. Where potential evaporation surpassed maximum probable flow, soil evaporation was equal to or less than the profile's expected maximum flow. Under these conditions, evaporation was reduced by either the creation of a natural mulch or the formation of a salt crust over the top. It was determined that the "critical depth" of the water table corresponded to the water table at which the flow rate through the soil profile decreased to around 0.1 cm per day. In general, the water table should be maintained lower in soils with an intermediate texture than in soils with fine or coarse textures.

The stable-isotopic (δD, $\delta^{18}O$) and chemical composition of Mexicali Valley waters are utilized to investigate the genesis of groundwater salinity (Payne, 1979). It is hypothesized that the present-day stable isotopic composition of the Colorado River when it reaches the valley is more enriched than it was three or four decades ago as a result of evaporation from reservoirs erected on the river during this period. This has resulted in unique isotopic identifiers for "ancient" and "modern" Colorado River water. The sample reveals no evidence that the salinity is the result of partial mixing with saltwater. There is evidence that a portion of the salinity is related to the dissolution of evaporitic deposits, while infiltration from the surface-water system is the primary salinity control.

In the study of (Konikow et al., 1985) the Arkansas River basin of southern Colorado, changes in the salinity of groundwater and surface water are mostly attributable to irrigation techniques. To compute salinity variations in response to geographically and temporally changing pressures, a solute transport model was used for an 11-mile stretch of the valley. In 1973, the model was calibrated using field measurements taken in 1971 and 1972. In 1973, the calibrated model was used to estimate that the observed irrigation methods would lead to a steady long-term rise in groundwater salinity of around 2–3 percent per year. During the winter of 1982, the research region was resampled to see whether or not long-term increases in salinity are happening. Utilizing nonparametric and parametric statistical tests, the significance of observed variations in groundwater salinity was evaluated. Between the winters of 1971 and 1972, these tests reveal a statistically significant rise in salinity (the model calibration period). Nonetheless, a comparison of the data from winter 1972 and winter 1982 reveals that there has been no substantial net change in salinity during the last decade. The examination of the scant available historical data (1895, 1923, 1959–1964, and 1964) supports the idea that the groundwater salinity in this irrigated region has attained a long-term dynamic equilibrium as a result of irrigation

methods. Because the calibration period occurred during a short-term annual trend of increasing salinity in the river (and, consequently, in leaky irrigation canals and applied irrigation water), which was not representative of the long-term trend, the model's predictions of long-term salinity increases were likely invalid.

The influence of agricultural activities on water quality has mostly been studied with a focus on surface water. Compared to surface waterways, groundwater impacts are significantly more difficult to assess. This is owing to longer transit durations to and within groundwater compared to surface fluids and the difficulty of collecting accurate samples of groundwater. Despite these problems in quantifying, the effects on both groundwater and surface water are crucial. In non-irrigated regions, agriculture frequently increases recharge, resulting in the occasional leakage of unsaturated zone salts into groundwater. In irrigated locations, groundwater salinization may come from irrigation with salty water, saltwater intrusion due to groundwater pumping, downward migration of salts in the unsaturated zone or dissolution of saline minerals, and the inevitable concentration of salts due to plant water intake. The link between surface and groundwater must include both water quality and quantity. Optimization of water resources necessitates concurrent usage, which necessitates consideration of water quality across the whole system. In (Suarez, 1989), examples are provided to illustrate how river salinity reduction efforts might result in groundwater salinization, which may not be the optimal management method.

McNeill (1990) for the first time introduced the use of electromagnetic methods in groundwater salinity investigation. By measuring differences in the electrical conductivity of the earth, inductive electromagnetic survey techniques are commonly utilized to map near-surface geology today. Changes in soil structure (porosity), clay content, the conductivity of the soil water, and the degree of water saturation produce these fluctuations. Very low frequency (VLF, including VLF resistivity), audio-magnetotelluric, controlled-source audio-magnetotelluric, and Slingram are frequency-domain techniques that may be used to map terrain conductivity (including ground conductivity meters and borehole induction loggers). Methods in the time domain may utilize either a fixed or a moving loop structure. Each technique's benefits and drawbacks are explained in sufficient depth for a potential user to choose which method is best suitable for a particular groundwater situation. Case studies are provided to highlight the use of electromagnetic techniques for groundwater research, mapping industrial toxins in groundwater, mapping groundwater quality, and mapping soil salinity concerning crop development (McNeill, 1990).

de Monty (2008) did the hydro-chemical and isotopic investigation of the confined aquifer of Camargue, France which reveals that the groundwater results from mixing between Mediterranean seawater and a freshwater end-member, intermediate between the Rhône river and the Crau aquifer. The respective influence of these two freshwater sources has to be specified in the future, especially because of the possible increasing exploitation of the Crau aquifer for water supply. The calculated mixing percentage of seawater in the groundwater varies widely from North to South and reaches up to 98% in the most southern part of the aquifer, at about 8 km from the shoreline. The confined aquifer of Camargue is thus subject to significant seawater intrusion. This evolution of the aquifer is recent. Indeed, the salinity of the groundwater has strongly increased since 1970. The seawater

intrusion induces modifications of the groundwater chemistry by cation exchange or SO_4 reduction due to the presence of fossil organic matter in the aquifer. These reactions increase Ca^{2+} and HCO_3 contents in the water. Moreover, seawater intrusion causes high Mg^{2+} in groundwater. The increase of Ca^{2+}, Mg^{2+}, and HCO_3 shifts the carbonate equilibrium and leads to dolomite and/or magnesium calcite precipitation. Moreover, the major ion deviation regarding a pure two end-member mixing highlight that different geochemical processes occur according to the degree of seawater contribution. In the part of the aquifer containing less than 20% of seawater, cation exchange seems to prevail while SO_4 reduction and precipitation phenomena prevail in the most saline part of the aquifer (seawater contribution >20%) and could influence the permeability. The evolution of the intrusion in the Camargue delta and especially its consequences on the permeability of the aquifer needs further monitoring in the context of sea level rise.

Varadaraj's (2010) investigations seek to comprehend the saline state of the Gokak, Mudhol, Bilgi, and Bagalkot taluks of the Ghataprabha command region in Karnataka, India. The command area consists of semiarid and drought-affected regions. In 2007, samples were obtained from 25 open wells and 41 bore wells throughout the pre and post-monsoon seasons. A chemical study reveals that open wells contain more EC than deep bore wells. The EC is an effective indicator of salinity danger. In the present research region, EC values range from 280 mS/cm to 6500 mS/cm during pre-monsoon and from 290 mS/cm to 9020 mS/cm during post-monsoon. According to the categorization of natural water based on EC concentration, water ranges from mild to extremely high salinity. The examination of factors was conducted for both seasons. For further study, the first five factors for pre-monsoon and the first six components for post-monsoon were discovered. Factor 1 of both pre-monsoon and post-monsoon seasons exhibits 38.70 percent and 33.35 percent variance with high positive loadings of EC, Na, Mg, Cl, Ca, and SO4 as a representation of salinity, which may be the result of a combination of hydro-geochemical processes that contribute more mineralized water, rock weathering, and agricultural activities.

Dhar et al. (2010) investigated the saltwater intrusion phenomenon in the Piyali river aquifer located in the South of West Bengal, India. They mentioned that the sluice gate is connected to the Malta river which in turn is connected to the Bay of Bengal. So at different distances from the sluice gate, samples were collected and analyzed for variation in TDS, EC, PH, etc. They also discussed the variation of chloride content of soil samples. They concluded that maximum values of salinity occurred near the sluice gate of the Piyali river. Values are reduced at a distance of 10 km away from the sluice gate. For the coastal community of the Piyali river saltwater intrusion is a significant concern. The values of PH decrease as the distance from the sluice gate increases.

Shah and Patel (2011) developed linear regression equations to predict the concentration of water quality constituents having a significant correlation coefficient with the electrical conductivity of groundwater in Anand district, Gujarat. Groundwater samples from the Anand district were collected by the grab sampling method during the pre-monsoon (May 2008) and post-monsoon seasons (October 2008). Physico-chemical analysis was conducted following standard methods (IS: 10500:1983). The linear regression analysis

between electrical conductivity and strongly correlated TDS and Cl^- in water showed that these constituents can be estimated from electrical conductivity values in the Anand district.

Rina et al. (2012) suggested that the groundwater resources' characteristics and distribution vary from location to location and within the parts of an area. The integration of hydrochemistry with GIS has been beneficial in understanding the factors governing the groundwater quality in the studied parts of the Sabarmati basin. The anthropogenic activities that induced contributions of contaminants are the dominant processes governing the groundwater quality in the study area, in addition to the natural processes such as silicate and carbonate weathering, ion exchange, and reverse ion exchange. In both pre-monsoon and post-monsoon, %Na is very high. The majority of the samples showed that the Na–Cl type of hydro-chemical species indicates the presence of highly saline water in the area. High nitrate concentration in groundwater shows the impact caused by leaching of agrichemicals from intensive agricultural activity in the area. Except for a few locations, in most places, groundwater is suitable for irrigation purposes. However, over-exploitation of groundwater is causing more saline groundwater to get mixed with less saline water, thereby depleting freshwater availability. To protect the good quality water from further depletion and pollution, appropriate measures need to be taken to control indiscriminate and unplanned groundwater exploitation, fertilizers, and disposal of industrial wastes in the affected areas.

Dimitriadou et al. (2018) presented the interpretation of the groundwater chemical composition of the granular formations, which revealed useful information about the type of the aquifers that host them, their area, and their way of recharging their movement, their relationship with other groundwater and surface water bodies. Thus, selecting and using the appropriate research methodologies plays a key role in the extraction of fruitful conclusions. This study used classic methodological approaches, including distribution maps, hydro-chemical and isotopic diagrams, and R-mode factor analysis.

In a study carried out by Sahour et al. (2020), the purpose was to develop and evaluate a methodology for mapping the groundwater salinity in the Caspian sea's southern coastal aquifer using available hydrogeology hydrometeorology data, as well as statistical and machine learning techniques. First, they determined the variables that affect groundwater salinity and then randomly divided the dataset into three subsets for training, testing, and verification. The relationship between groundwater salinity and its controlling factors was established using three methods. Finally, the optimum model was applied to the set of known input variables to map the spatial variation of groundwater salinity across the Caspian sea's southern coastal plain, and the final map was verified using the verification subset. The results indicated that due to the EGB method's superior performance on the testing subset, consideration should be given to it. An in-depth analysis of the variables revealed that the most critical parameter affecting groundwater salinity in the region is aquifer transmissivity. The approach adopted here could be applied to groundwater management in other study areas and similar settings. The results indicate that while the groundwater level in the center of the groundwater depression cone has recovered somewhat since 1993 as a result of existing groundwater protection measures, the

horizontal area of the groundwater depression cone (defined as the area bounded by the 1100 m groundwater level contour) has increased significantly, reaching 310.51 km^2 by 2019. Groundwater samples from the phreatic aquifer were predominantly SO_4Cl–CaMg and HCO_3–CaMg, whereas those from the confined groundwater were predominantly SO_4Cl–Na and HCO_3–CaMg North-West India and central Pakistan have some of the world's most heavily exploited groundwater systems. However, the current and well-documented decline has not been contextualized previously.

Mosavi et al. (2021) used the machine learning application in site suitability mapping groundwater salinity. The study describes machine learning (ML) model application in groundwater salinity modeling using dichotomous forecasts. The aquifer salinity is postulated utilizing k-fold cross-validation and the critical elements (identified by the simulation result annealing attribute selection technique). To map aquifer salinity, six ML models were used: mixture discriminant analysis (MAD), flexible discriminant analysis (FDA), random forest (RF), boosted regression tree (BRT), multivariate adaptive regression spline (MARS), and support vector machine (SVM). The results showed that the SVM model performed much better than the other models. Soil sequence, groundwater withdrawal, rainfall, land use, and altitude contribute to aquifer salinity modeling.

MacAllister et al. 2022 presented a regional analysis of post-monsoon groundwater levels from 1900 to 2010 using a long-term observation-well dataset. They demonstrated that human activity in the early 20^{th} century increased groundwater availability before the late 20th century onset of large-scale exploitation. In the 20^{th} century, net groundwater accumulation was estimated at least 420 km^3 at 3.6 cm/yr in regions with adequate information. The progression of the area's extensive irrigation canal network, which accelerated groundwater recharge, was instrumental in the buildup of groundwater in the 20th century. Between 1970 and 2000, groundwater levels balanced due to the contrasting effects of above-average annual precipitation and the beginning of irrigation tube well development. In the first decade of the 21st century, approximately 70 km^3 of groundwater was lost at a rate of 2.8 cm/yr due to a combination of low rainfall and increased tube well development. The findings demonstrate how ancient groundwater trends have been influenced by both human and climatic factors.

Elmeknassi et al. (2022) used a variety of chemical and isotopic samples from the Bou-areg coastal aquifers to track down the source of water salinity and to expose the mechanisms of the multiple pollution sources. The hydro-chemical analysis of water samples showed that $Cl > HCO_3 > SO_4^{2-} > NO_3$ and $Na^+ > Ca^{2+} > Mg^{2+} > K^+$ were the most abundant elements, as well as extremely high salinity levels (EC up to 22000 µS/cm). Ion ratio diagrams, isotopic results, and graphical comparisons indicate that carbonate dissolution, evaporite dissolution, ion exchange, and sewage invasion all influence the mineralization of groundwater in the area. These scientific findings provide decision-makers with additional information to help them improve the sustainable management of groundwater in water-stressed regions. Chemical and isotopic tracers have demonstrated their utility in such areas where systematic monitoring is lacking.

The combination of these methods resulted in the conceptual model of the area, the use of which not only leads to a better understanding of the area's aquifers but also documented planning of future projects. The distribution maps pinpointed areas with particular characteristics, on the interpretation of which much of the analysis that followed was focused. The classification of the samples, combined with their geographical distribution, pointed out mechanisms that control their quality. This classification was particularly useful in the construction of scatter plots because the samples were not plotted all together and thus the hydro-chemical processes for each group were made clearer. Although indications of the groundwater origin had already emerged from the above analysis, groundwater origin was further investigated and documented using the isotopic data of preliminary research conducted in the broader area.

3.0 STUDY AREA AND DATA USED

3.1 General

Mewat, a newly formed district, is one of the 22 districts of Haryana state in North India. It lies between $27^0$39' to 28^0 20' North latitude and $76^0$51' to $77^0$20' East longitude as shown in Fig 3.1. The district covers an area of 1507 sq km. The area is largely occupied by alluvial plains, traversed by elongated ridges of Delhi quartzites. The groundwater in the district area is saline and salinity increases with depth. The district is socio-economically backward. Agriculture, the base economic activity of the people is deprived of irrigation. There is no river and the area is drained by artificial drains namely Nuh, Ujina, and Kotla drain. They carry rainwater into the Yamuna river. Gurgaon canal carries water to the area which is distributed through Nuh, Firozpur Jhirka, Uttar, Mandkola, Hathin, and Chhyansa distributaries. Potable drinking water is still a problem except in the areas at the base of ridges and hillocks of the district. The Central Ground Water Board has carried out hydrogeological investigations, groundwater exploration, geophysical studies, and micro-level studies of waterlogged areas in the district.

3.2 Demography

Mewat is a historical region of Haryana and Rajasthan states in North-Western India. The main center areas of Mewat are Firozpur Jhirka, Nuh, Ramgarh, Paharisikri and Punahana. Mewat region lies in between Delhi-Jaipur-Agra. The total population of Mewat is 1089263 (2011 Census), which represents 4.30 % of the Haryana state population (fig 3.2). Out of the total Mewat population for the 2011 census, 11.39 percent live in urban regions of the district. In total, 124,106 people live in urban areas, of which males are 65,076 and females are 59,030. The Sex ratio in the urban region of Mewat district is 907 as per 2011 census data. Similarly, the child sex ratio in Mewat district was 890 in the 2011 census. The child population (0-6) in the urban region was 23,059, of which males and females were 12,201 and 10,858. This child population figure of Mewat district is 18.75 % of the total urban population. The average literacy rate in Mewat district as per census 2011 is 69.42 %, of which males and females are 80.09 % and 57.71 % literate, respectively. As per the 2011 census, 88.61 % population of Mewat districts lives in rural areas of villages (fig 3.3). The total Mewat district population living in rural areas is 965,157, of which males and females are 506,086 and 459,071, respectively. In rural areas of the Mewat district, the sex ratio is 907 females per 1000 males. If child sex ratio data of Mewat district is considered, the figure is 908 girls per 1000 boys. The child population in the age 0-6 is 225,069 in rural areas, of which males were 117,967 and females were 107,102. The child population comprises 23.31 % of the total rural population of Mewat district. The literacy rate in rural areas of Mewat district is 51.99 % as per census data 2011. Gender-wise, male and female literacy stood at 68.56 and 33.71 percent respectively.

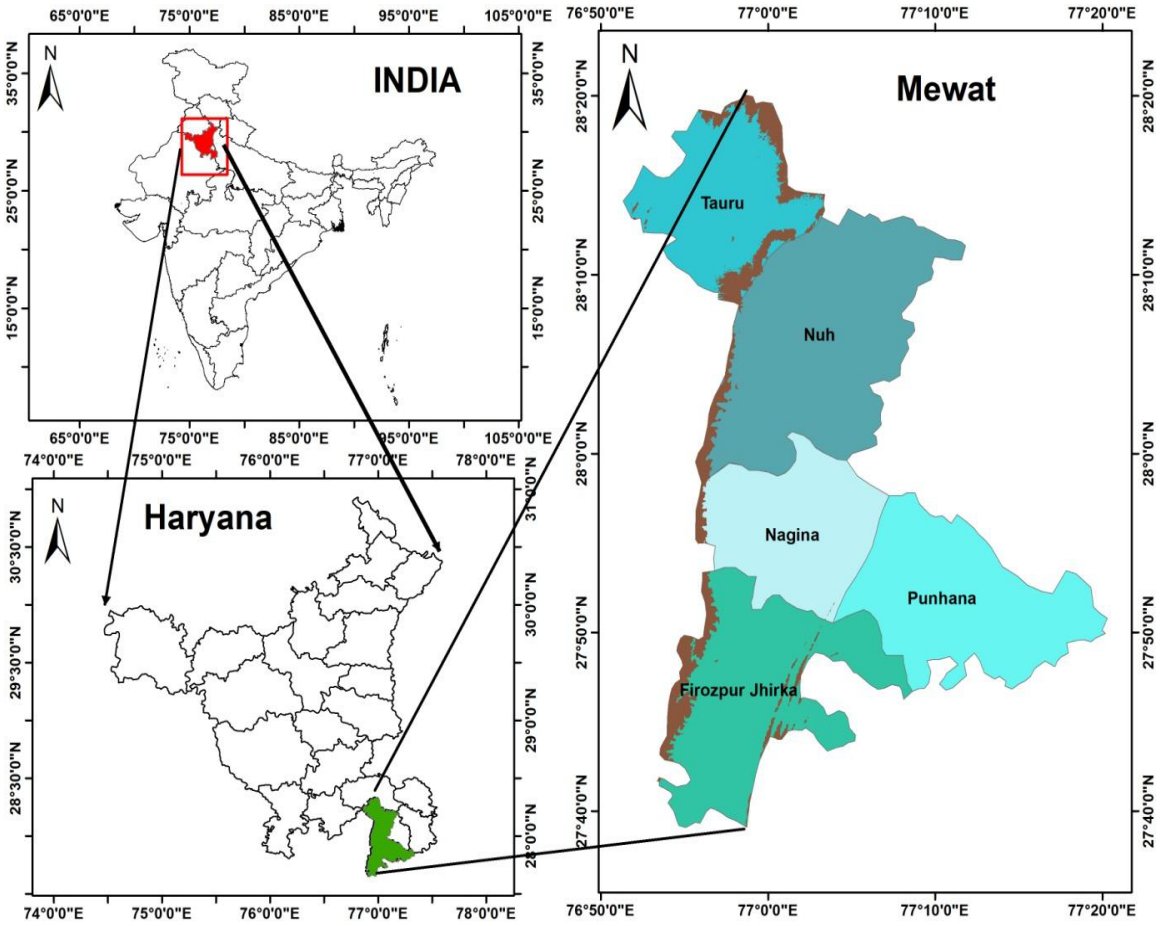

Fig 3.1 Location of the study area

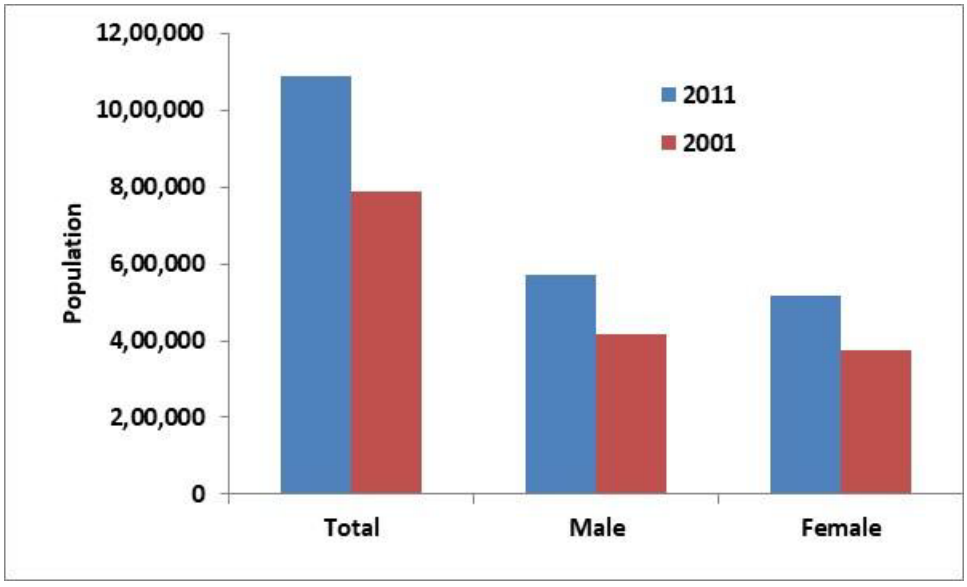

Fig 3.2 Population changes during the last two censuses (2001 to 2011).

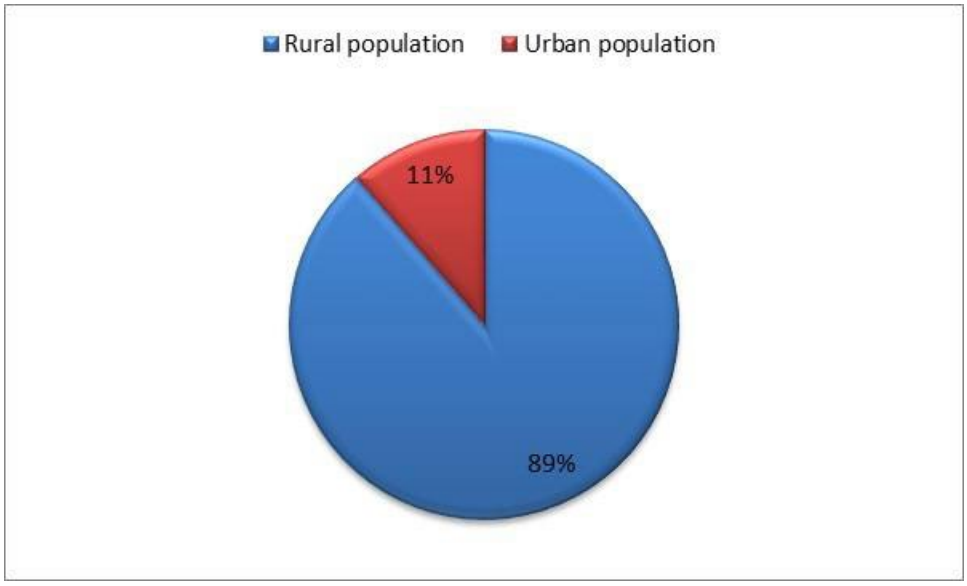

Fig 3.3 Population proportion (census 2011) of Mewat (male and female)

3.3 Climate and rainfall

The climate of the study area is semi-arid type, which is characterized by hot summer and cold winter. During three months of South-West monsoon from July to September, the moist air of oceanic origin penetrates the district and causes high humidity, cloudiness, and monsoon rainfall. The period from October to December constitutes the post-monsoon season. The cold weather season prevails from January to the beginning of March and is followed by the hot weather or summer season which prevails up to the last week of June. The temperature ranges from 5.1 ºC (minimum) to 40.0ºC (maximum) where the minimum temperature falls in January and the maximum rise in May and June months. The district receives an average annual rainfall of 594 mm whereas 75% of the total rainfall occurred with average monsoon rainfall of 494 mm. The South-West monsoon sets in the last week of June and withdraws towards the end of September. July and August are the wettest months and 25% of the annual rainfall occurs during the non-monsoon months in the wake of thunderstorms and western disturbances.

3.4 Land use/land cover

Agriculture is the main occupation of the people in the study area, as evident from land use data that consists of 64 percent agricultural land, 12 percent build-up area (human settlements including the residential sites), 18 percent under hills, 1 percent under water bodies, and 5 percent under fallow area without perennial rivers (Fig.3.4) and a normal semi-arid and arid drainage. The major crops are rabi such as wheat, gram, rice, etc. The economy of this region depends on agriculture because there is no industrial setup in this region. Agriculture demands high irrigational water but available water bodies do not make the requirements. This creates stress on present water supplies in the study area.

3.5 Hydrogeology

Mewat district area is mainly alluvium quaternary age, in which most of the groundwater exists. However, some portion of groundwater also occurs in joints, crevices, and fractures of the hard rocks. The alluvium thickness varies from 90 to 300 m bgl, whereas central and eastern parts show a maximum of 300 m, and the remaining lies within 90 m. The depth to water level varies from 2 – 32 m BGL (Below Ground Level). The district area has undulating topography and thus, no general slope can be defined. In the western part, the slope is toward NW-SE and on the North-South side, the slope is NE-SW direction. The location of litholog and the fence diagram is shown in fig 3.5.

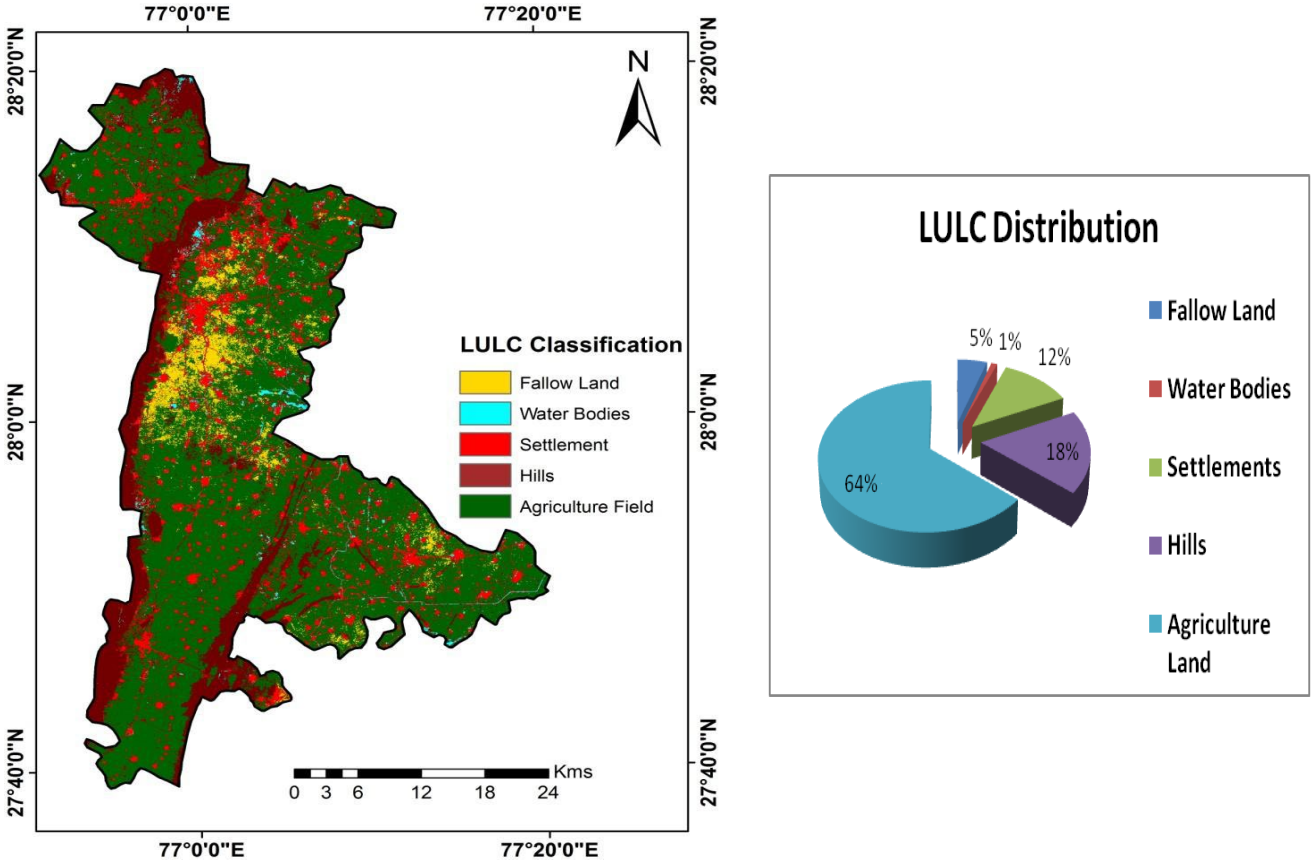

Fig 3.4 Land Use Land Cover classification and distribution in Mewat

3.6 Geology

The Mewat district of Haryana is a part of the Aravalli craton and settles over the gneissic banded complex. The district is surrounded by the Delhi-Aravalli fold belt of paleo-Meso Proterozoic time. The Delhi fold belt encloses Mewat from the East, West, and South directions. The major lithology is quartzite, schist, and phyllites of the Alwar and Ajabgarh group. The weathering of these Proterozoic mobile belts form the overlying younger

quaternary deposits of the Pleistocene-Holocene period, deposited as aeolian deposits in the form of loose oxidized sand and silt. The detailed geology of the region is given in table 3.1 and fig 3.6.

Table 3.1 Detailed stratigraphy of Mewat, Haryana

Super group	Group	Formation	Lithology
Quaternary Alluvial Sediments	Newer alluvium	Loharu/Aeolian Deposits	Yellowish brown loose sand
	Older Alluvium	Varanasi, Ambala, Ludhiana	Oxidized silt clay and micaceous sand
Mesoproterozoic Delhi fold belt	Ajabgarh	Arauli	Carbonaceous phyllite
		Bharkol	Phylite, quartzite
		Asarwas	Feldspathic Quartzite and schist
		Undefined	Phyllite, slate, limestone, quartzite, schist
	Alwar	Pratapgarh	Feldspathic Quartzite

3.7 Geomorphology

The elevation of the study area is 100 m to ~550 m (Fig. 3.7). Higher elevations are found in the Aravalli ranges. Two major soil types, vertisols, and salanchalks are found in the study area. These soil types generally have medium-textured loamy sand. Due to the recurring lack of rainfall during the monsoon season and the scarcity of freshwater resources, farmers are forced to plant crops that require less water, such as wheat, millet, and mustard. The district has a rolling topography with an urn-shaped structure. Topographically, the study area is mainly made up of alluvium of Quaternary and Pale-oproterozoic age groups. The most dominant is the Quaternary age group alluvium, with a polycyclic sequence composed of sand, silt, and clay with kankar. The Geomorphologic map of the study area is shown in fig 3.8. Three types of soils, which depend upon three types of the terrain of the state, constitute the morphology of the district; soils of the hilly terrain are rocky; the upper hills are mostly barren and the terrain in the plains has fertile soils which are light in texture particularly, sandy, sandy loam and clay loam. Soils of the district are mostly salt-affected. Some topographic depressions have given rise to natural lakes in the area (Krishan et al. 2020).

3.8 Area drainage network map

The area-drainage network map has been prepared using the downloaded SRTM data from the internet and analyzed through the Soil and Water Assessment Tool (SAWT) including watershed delineation using watershed delineation tool. The drainage network map is presented in fig 3.7. There are no natural drains in the district with no natural lakes and ponds. The drains represented in the figure use interflows which originate from the natural

hill barriers which are parts of a wide range of Aravali hills. These interflows move from every direction with trees like multiple tangles. The whole area falls under the vast Ganga basin and these interflows contribute to the Yamuna river in the East. Micro watersheds are also drawn using the SWAT water delineation tool which uses Digital Elevation Model (DEM) data to differentiate the watershed using surface elevation. The prominent micro watershed which artificially drains the water is found in Nuh, Punhana, and Firozpur blocks.

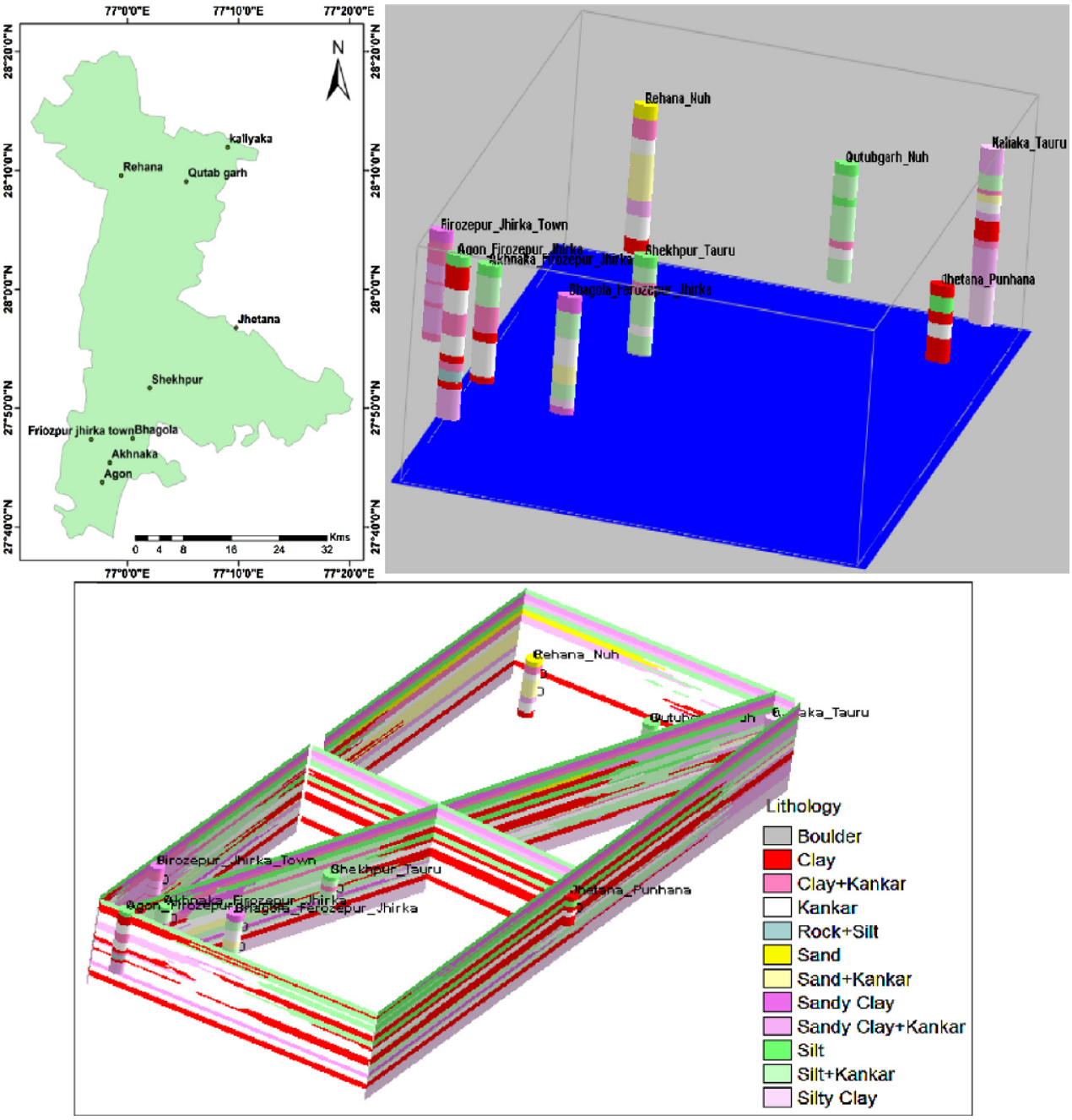

Fig 3.5 Lithologs of the bore logs and fence diagram

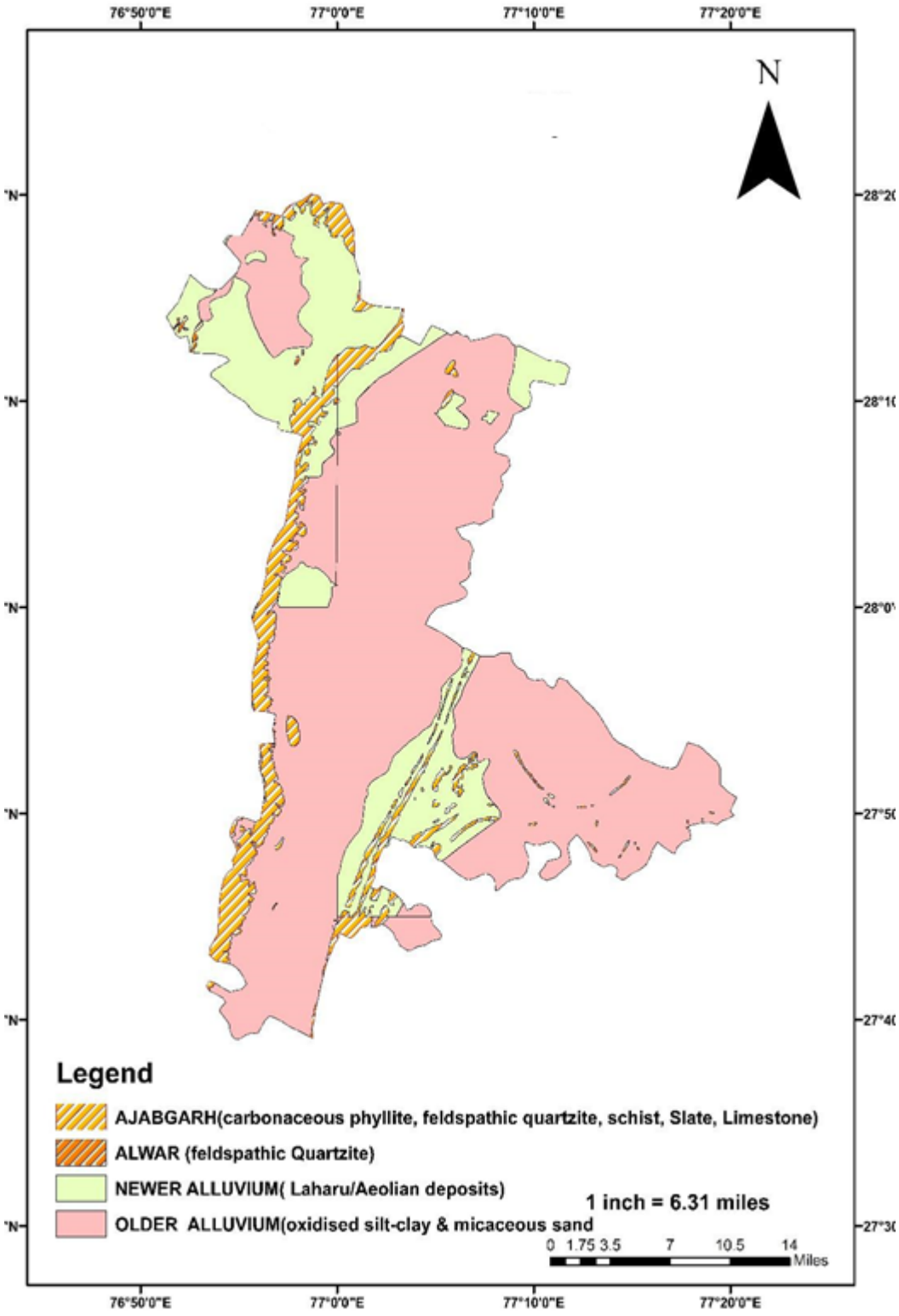

Fig 3.6 Geological map of Mewat, Haryana

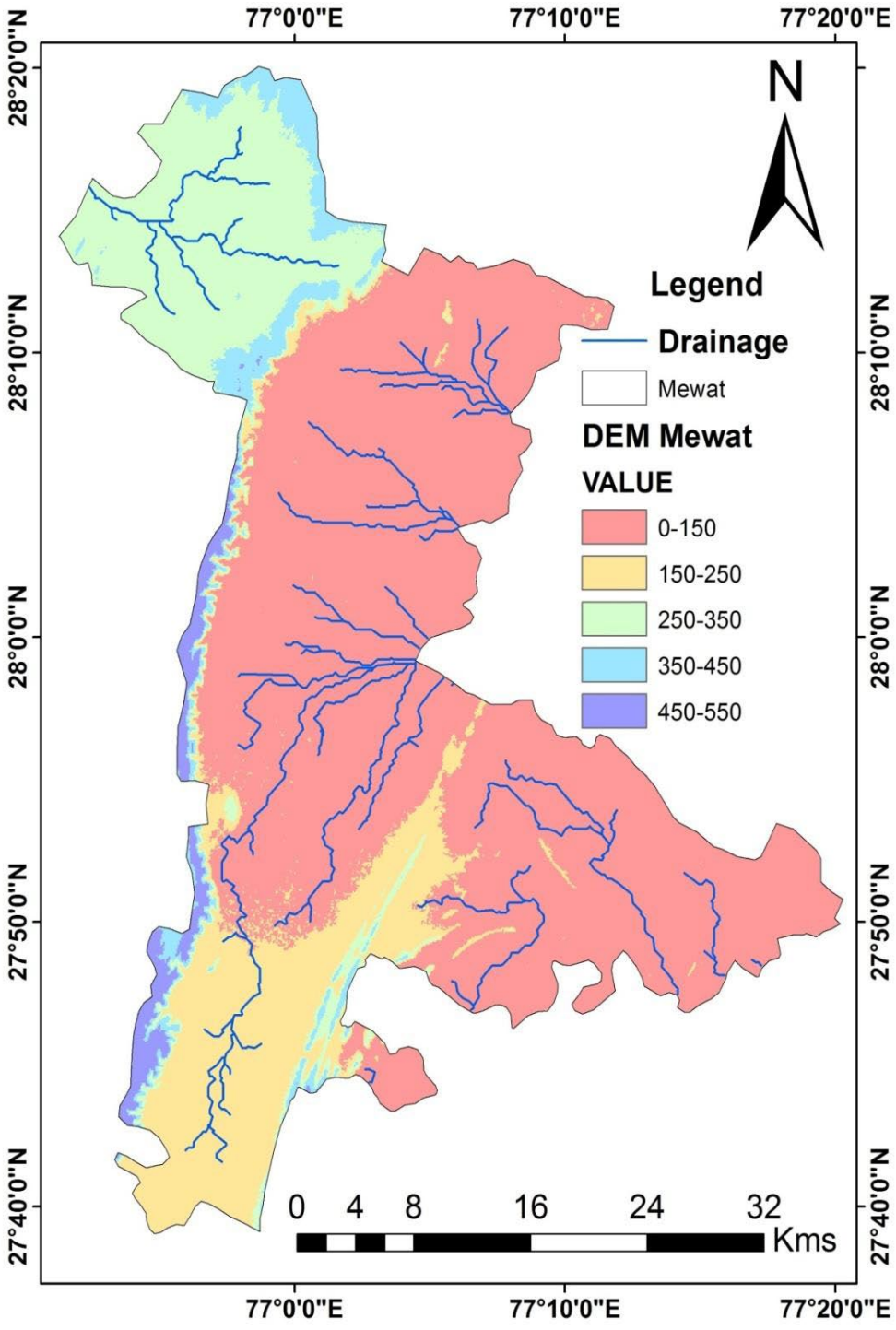

Fig 3.7 Digital Elevation Model showing drainage of Mewat, Haryana

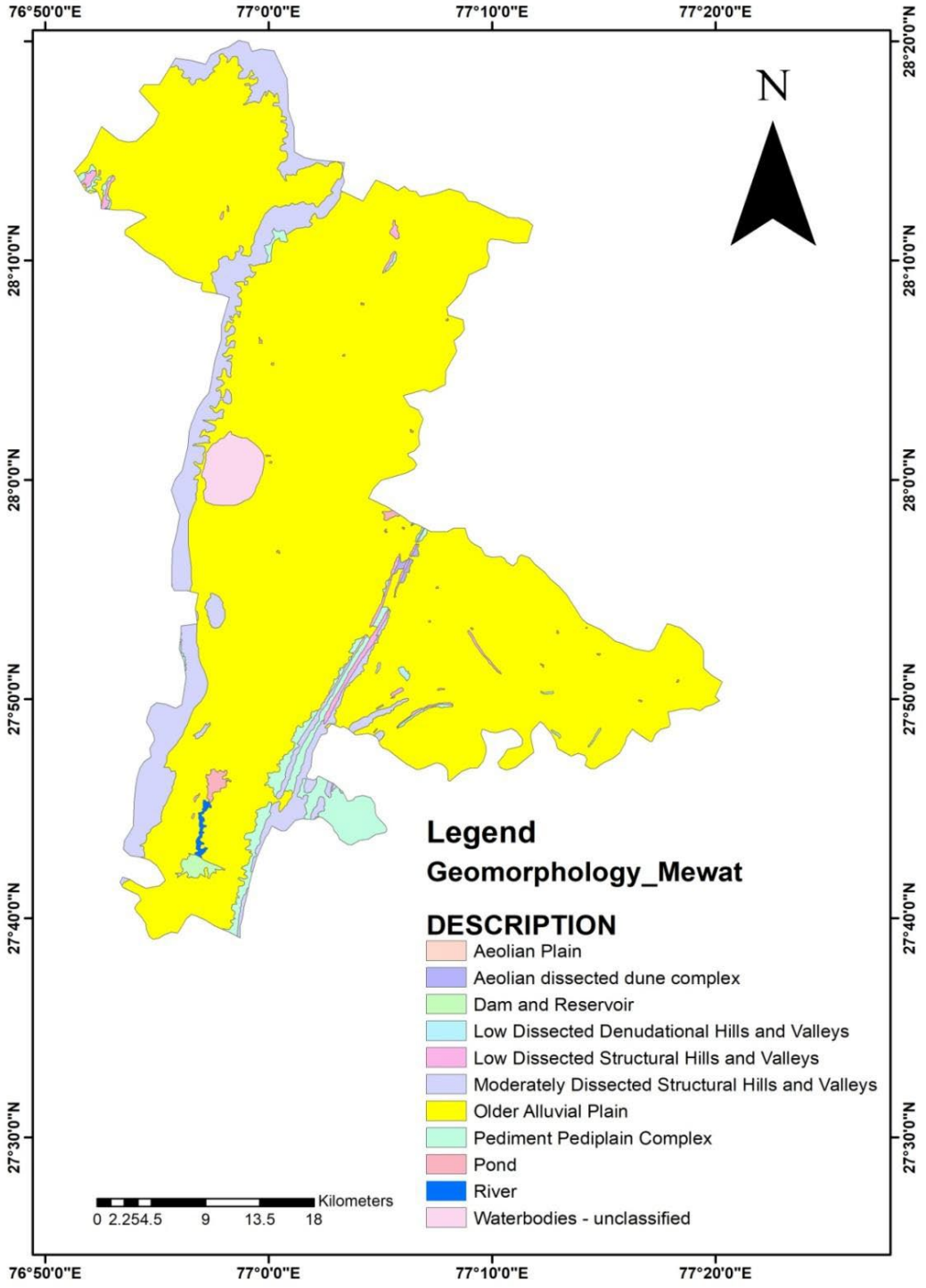

Fig 3.8 Geomorphology of Mewat, Haryana

4.0 METHODOLOGY

Salinity is a severe problem that is detrimental to soil quality and agricultural yields. High salinity water has a major adverse impact on the key aspects of livelihood, such as agriculture income, crop yield, and incidence of severe health problems. This further influences the living standards of the community, in particular, and the overall socio-economic conditions of the people living in the region, in general. The present study fills an important void because the number of scientific investigations in the highly saline regions in India, such as Mewat, that highlight the impact of salinity on the socio-economic conditions has been quite limited thus far. This work has been accomplished in five phases as identified below:

4.1 Socio-economic survey

In Phase 1, a socio-economic-based survey was carried out to find out the impact of salinity on the socioeconomic condition of the people based on a list of indicators given in the table below (Table 4.1). The findings of the study will help in initiating the development activities as coping strategies for the survival of humankind in the presence of salinity in the Mewat district.

Table 4.1 Socio-economic indicators

Themes	Indicators
Domestic consumptions	Low availability of fresh drinking water
	Health problems
	Women drudgery
	Low farm income
	Limited occupation opportunity
	High Expenditure
	Poor education indices
Agriculture	Degradation of land quality
	Poor quality of crop produce
	Limited crops variety
	Poor crop yield
	The low capital value of land
	The decline in fodder production

The study has employed both qualitative and quantitative methods. Under the quantitative method, a well-structured coded interview schedule was used. Focus Group Discussion (FGD), as a qualitative method, was administered to collect information on the above socio-economic characteristics of the farmers.

4.2 Development of Hydrogeological framework of the aquifer system in Mewat

Phase 2 of our proposed study began with the development of a hydrogeological framework of the aquifer system in Mewat district based on all existing lithologic, stratigraphic and hydrologic information that was available from various agencies. The saline areas in the district were mapped. Litholog data for 5 sites in Tauru (Shekhpur and Kaliaka), Nuh (Qutubgarh and Rehana), and Firozepur Jhirka (Agon) blocks were obtained from Groundwater Cell, Haryana Agriculture Department, Gurgaon office and for one site in Tauru, it was obtained from L&T office at Sohna. Making use of 'Rockworks' software - a comprehensive software program for creating 2D and 3D maps, logs and cross sections, geological models, general geology diagrams, etc - the bore logs data were analyzed for delineation of the lithological profiles and aquifer characterization. Piezometers and data logger installation was done at different locations in the study area as per details given in table 4.2.

Table 4.2 Details of piezometers and data loggers installed in the study area

Data logger Installation Details				
S. No.	**Installation date**	**Location**	**No. of Piezometers**	**Parameters measured**
1	13/05/2019	Nagina	1	Water level, Barometric pressure, Conductivity, and Temp.
2	14/05/2019	Uleta	1	Water level, Barometric pressure, Conductivity, and Temp.
3	14/05/2019	Saini Shikhsa Niketan	1	Water level, Barometric pressure, Conductivity, and Temp.
4	30/12/2019	Karhera	1	Water level, Barometric pressure, Conductivity, and Temp.
5	20/07/2020	Karhera	4	Water level, Barometric pressure, Conductivity, and Temp.

4.3 Hydro-chemical and isotope characterization

Phase 3 of the study included hydro-chemical characterization (based on anions, cations, physicochemical characteristics, etc.) and quantification of salinity. Representative samples were collected from the salinity-affected areas based on the salinity map of Thomas et al. (2014) using the sampling protocol during pre-monsoon (May), monsoon (August), and post-monsoon (November) seasons for the years 2018 and 2019 for ions and stable isotope analysis. A total of 24 groundwater samples were collected in pre-monsoon (May) 2018, 29 groundwater samples collected in monsoon (August) 2018, and 29 groundwater samples collected in post-monsoon (November) 2018. And during the year 2019, a total of 150 groundwater samples were collected 50 each in the pre-monsoon; monsoon, and post-monsoon seasons respectively (Table 4.3). The locations were selected from the high saline zone of the Nagina block and the freshwater zone in the Firozepur Jhirka, and Taoru blocks. Samples from Punhana blocks were not taken as baseline data was already collected in a study carried out by NIH in the year 2016.

Table 4.3 Details of sample collection and analysis

Season/ Year	Pre-monsoon			Monsoon			Post-monsoon		
	Number of samples	Analysis	Method / Instrument used	Number of samples	Analysis	Method / Instrument used	Number of samples	Analysis	Method /Instrument used
2018	24	HCO_3^- Ca^{++}, Mg^{++} Cl^-	Titration	29	HCO_3^- Ca^{++}, Mg^{++} Cl^-	Titration	29	HCO_3^- Ca^{++}, Mg^{++} Cl^-	Titration
	24	Na^+, K^+	Flame photometer	29	Na^+, K^+	Flame photometer	29	Na^+, K^+	Flame photometer
	24	SO_4^{--},F^- ,NO_3^-	UV-visible spectroscopy	29	SO_4^{--},F^- ,NO_3^-	UV-visible spectroscopy	29	SO_4^{--}, F-, NO_3	UV-visible spectroscopy
	24	Isotopes	DI IRMS (Isoprime GV instruments, U.K)	29	Isotopes	DI IRMS (Isoprime GV instruments, U.K)	29	Isotopes	DI IRMS (Isoprime GV instruments, U.K)
2019	50	HCO_3^- Ca^{++}, Mg^{++} Cl^-	Titration	50	HCO_3^- Ca^{++}, Mg^{++} Cl^-	Titration	50	HCO_3^- Ca^{++}, Mg^{++} Cl^-	Titration
	50	Na^+, K^+	Flame photometer	50	Na^+, K^+	Flame photometer	50	Na^+, K^+	Flame photometer
	50	SO_4^{--},F^- ,NO_3^-	UV-visible spectroscopy	50	SO_4^{--},F^- ,NO_3^-	UV-visible spectroscopy	50	SO_4^{--},F^- ,NO_3^-	UV-visible spectroscopy
	50	Isotopes	DI IRMS (Isoprime GV instruments, U.K)	50	Isotopes	DI IRMS (Isoprime GV instruments, U.K)	50	Isotopes	DI IRMS (Isoprime GV instruments, U.K)
	-	-	-	-	-	-	50	Heavy metals	ICP-OES
	6	Tritium	Liquid Scintillation Spectrometry	-	-	-	3	Tritium	Liquid Scintillation Spectrometry
2020	8	Isotopes	DI IRMS (Isoprime GV instruments, U.K)	4	Isotopes	DI IRMS (Isoprime GV instruments, U.K)	4	Isotopes	DI IRMS (Isoprime GV instruments, U.K)
	-	-	-	4	Tritium	Liquid Scintillation Spectrometry	-	-	-
2021	-	-	-	-	-	-	4	Isotopes	DI IRMS (Isoprime GV instruments, U.K)
2022	26	F^-	Ion meter (Thermo Fischer)	-	-	-	-	-	-

Groundwater samples were collected from hand pumps using outside taps after thoroughly flushing the water for at least 15 minutes or until temperature measurements indicated that all onsite storage was purged and water originated from the good bore or aquifer. All sampling containers were rinsed three times with sample water before collecting the final sample. The samples were collected in acid-washed LDPE (Low-Density Polyethylene) tarson bottles as shown in fig. 4.1. The samples for heavy metal analysis were preserved by the addition of nitric acid by adding 5 ml of concentrated HNO_3 for one liter of sample to acidify the sample to maintain pH < 2 in the field itself. Samples for analysis of major anions (bicarbonate, sulfate, fluoride, chloride, and nitrate) and cations (sodium, potassium, calcium, and magnesium) were collected as unpreserved.

In addition to these, four rainwater samples were also collected during the monsoon period. These samples were pre-filtered with 0.45 µm filter paper and collected in poly tetra fluoro ethylene (PTFE) sample bottles. EC was recorded in the field using Hach, HQ30d portable meter.

HCO_3 was measured using the acid titration method. The samples were preserved in an ice box at 4°C and analyzed in the laboratory at the earliest. The samples were analyzed for Na^+, K^+, Ca^{++}, Mg^{++}, F^-, Cl^-, SO_4^{--} and NO_3^- using APHA (2005) procedures in the laboratory. The Ca^{++} and Mg^{++} were determined titrimetrically using the standard EDTA method, and Na^+, K^+ by flame photometry. The Cl^- concentration was determined by $AgNO_3$ titration and SO_4^{--} and NO_3^- values by spectrophotometer. The ratios of heavy stable isotopes ($\delta^{18}O$ and δD) were measured using a Dual Inlet Isotope Ratio Mass Spectrometer-DI IRMS (Isoprime GV instruments, U.K) with automatic sample preparation units at the Nuclear Hydrology Laboratory of National Institute of Hydrology, Roorkee. The measured errors (precision) in estimates were within the limits of ± 0. 1% for $\delta^{18}O$ and ± 1.0% for δD. The isotope ratio $^{18}O/^{16}O$ and D/H were expressed per mil units using the δ notation relative to VSMOW.

Electrical Conductivity variation and distribution

Electrical conductivity is used to measure the salinity of the water samples. The groundwater salinity data for the year 2018 and 2019 were obtained physically by taking groundwater samples from the site. Samples were collected for pre-monsoon (March-May), monsoon (July – August), and post-monsoon (September to November) seasons. There were initially 24 well sites marked for monitoring in 2018 pre-monsoon which were increased (up to 50 sites in 2019) as more and more detailed investigations were conducted on the field. Coordinates of these 50 sample sites were extracted using a handheld Global Positioning System (GPS) device. The coordinates were fed into GIS for collector application in a tablet to examine the location of the wells.

The spatial maps for EC (µS/cm), TDS, salinity, and water quality parameters were prepared using ArcGIS 10.4. The point data were interpolated by IDW (Inverse distance weighting) using a raster interpolation tool. Data converted to raster were classified by providing a meaningful range for visualization. A similar procedure was used for each

season and different spatial plots were generated as shown in the flow diagram below (figure 4.2).

Fig 4.1 Sample collection in the field

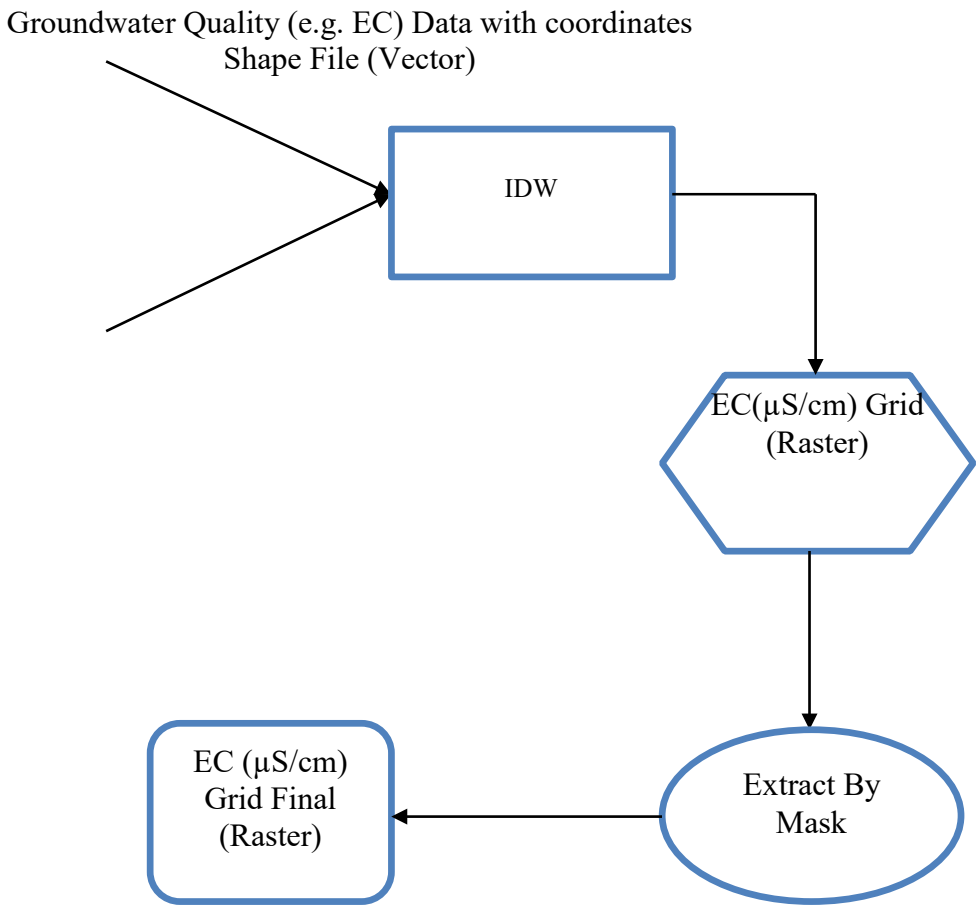

Fig 4.2 Flow chart showing the preparation of spatial maps using the GIS tool

As mentioned earlier the sample locations were used thrice a year based on the season (pre-monsoon, monsoon, and post-monsoon) to collect groundwater samples. Below are the maps which show the sampling locations for the years 2018 and 2019 (Fig 4.3 and Fig 4.4). These maps figure shows the sampling point's location for the year 2018 where the sample points for the pre-monsoon season started at 24 and grew up to 29 number for monsoon and post-monsoon seasons afterward. Subsequently, the sampling locations were increased up to 50 in the year 2019.

Data Logger

A data logger is an electronic device that is used to record data at specific intervals. A data logger can either have in-built sensors to record the data, or a few of them are also interfaced with external sensors to log information. Most of them are small, lightweight, battery-operated, portable, and equipped with a microprocessor and internal memory for data storage. Some even interface with a personal computer and use data logger software to activate the data logger and view and analyze the collected data. At the same time, others can also be used as a standalone device.

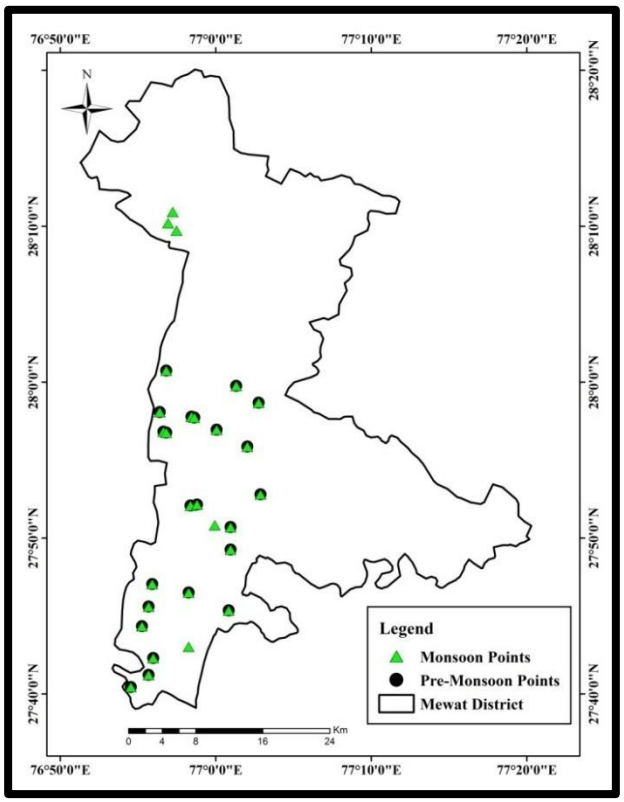

Fig 4.3 Pre-monsoon, monsoon, and post-monsoon sampling points during 2018

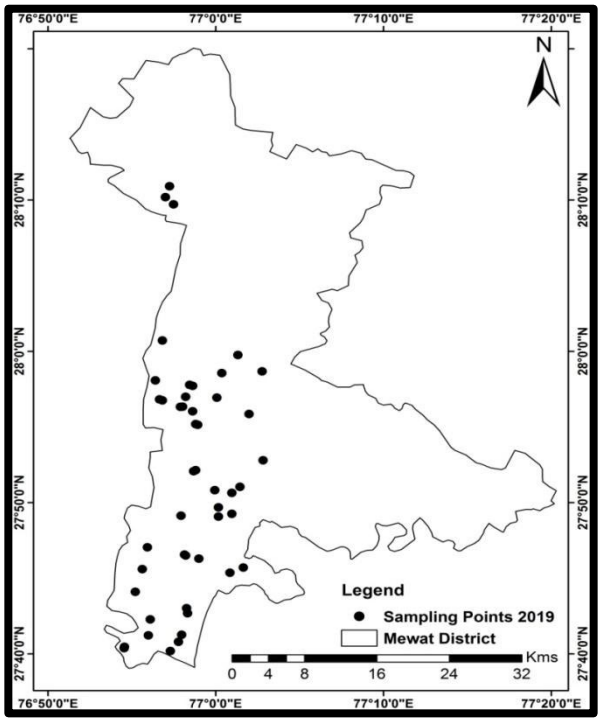

Fig 4.4 Pre-monsoon, monsoon, and post-monsoon sampling points during 2019

For the study area total of 4 data loggers were purchased from ENCARDIO RITE. For borewell/piezometers' water level monitoring and measuring conductivity, an automatic data logger for the SDI-12 interface sensor (model ESDL-30) was selected for well monitoring and measuring conductivity. The ESDL-30 data logger is designed to log data from any sensor with an SDI-12 digital interface. It can be programmed to measure data at 5 seconds, initial for 168 hours in a linear model. All the measured data were stored together with the current date, time, and battery voltage in the internal non-volatile memory of the data logger. It can record four parameters: water level, barometric pressure, electrical conductivity, and temperature.

To measure electrical conductivity, temperature, and water level, a conductivity sensor (model ECTD-60) was provided with the ESDL-30 box connected with a wire of length 10m.

Onsite data monitoring and usage

A total of four data loggers were installed in the study area, and sites were selected based on the depth of water level at the well. Since the height of the wire holding the sensor is fixed to 10m, the wells were determined to have a water level depth of fewer than 10m with a fluctuation of ±15% in the well. Figs 4.5 and 4.6 show the sites selected for data loggers and installation.

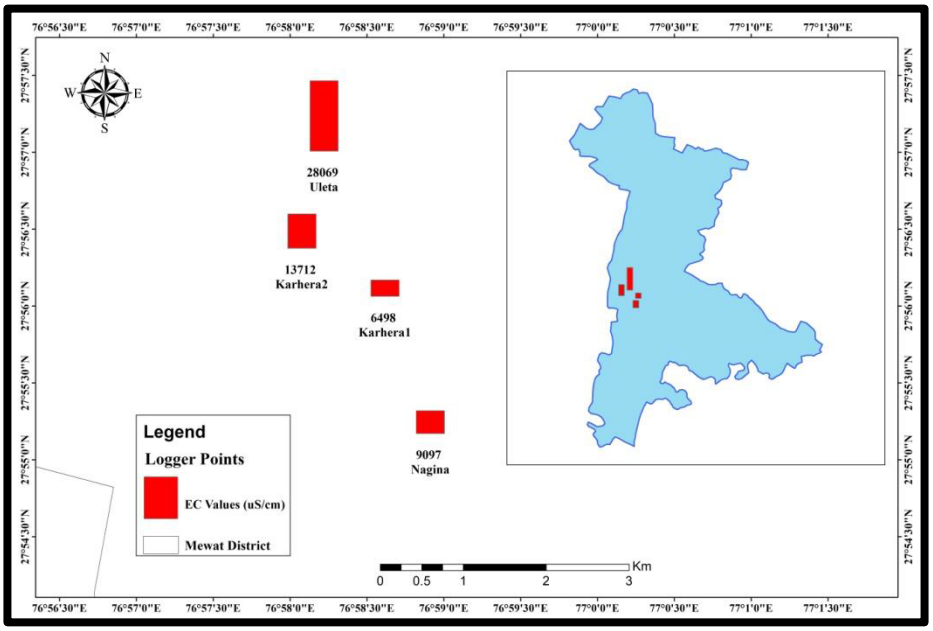

Fig 4.5 Map displaying the locations and values of conductivity of data loggers

a. b.

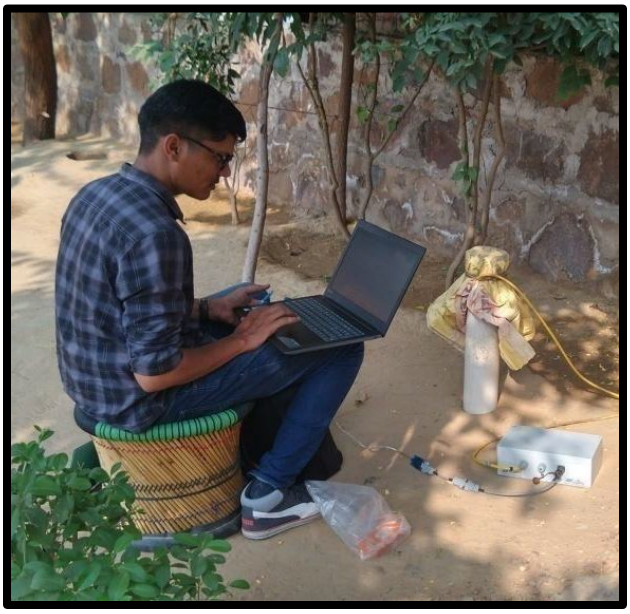

c.

Fig 4.6 (a, b, c) Setting up and installation of data logger on site in Mewat

ESDL-30 data logger is equipped with Duracell Ultra Alkaline D Battery (2 Pieces) which provides a battery life of 1.5 years to the logger. It also has a memory sim card slot for remote access to the logger.

Rain Gauge

The data logging rain gauge consists of two major components: a tipping bucket rainfall collector, and a HOBO® event/temperature data logger. The collector consists of a black-anodized aluminum knife-edged ring, screen, and funnel assembly that diverts rainwater to a tipping-bucket mechanism located in the aluminum housing. The housing is coated with a white baked enamel surface designed to withstand years of exposure to the environment. The tipping-bucket mechanism is designed such that one tip of the bucket occurs for each 0.01" (RG3) or 0.2 mm (RG3-M) of rainfall (Fig 4.7). Each bucket tip is detected when a magnet attached to the tipping bucket actuates a magnetic switch as the bucket tips, thus

effecting a momentary switch closure for each tip. The spent rainwater then drains out of the bottom of the housing. The switch is connected to a HOBO event/temperature data logger, which records the time of each tip. The data logger is a rugged, weatherproof event logger with a 10-bit temperature sensor. It can record 16,000 or more measurements and tips. It uses a coupler and optical base station with a USB interface for launching and data readout by a computer. Data shuttle options are also available.

Fig 4.7 Installation of tipping bucket rain gauge in the field (July 2020)

Field calibration

The tipping-bucket mechanism is a simple and highly reliable device. Accurate rain gauge calibration can be obtained only with laboratory equipment, but an approximate field check can be quickly done. The rain gauge must be calibrated with a controlled rate of flow of water through the tipping bucket mechanism. The maximum rainfall rate that the rain gauge smart sensor can accurately measure is one inch of rain per hour (36 seconds between bucket tips). Therefore, the rain gauge should be field calibrated using a water flow rate equivalent to, or less than, one inch of rain per hour (more than 36 seconds between bucket tips). If the flow rate increases, a properly calibrated instrument will read low. Decreasing the rate of flow will not materially affect the calibration. This is obvious if the tipping bucket assembly is observed in operation. With water falling into one side of the tipping

bucket, there comes the point when the mass of the water starts to tip the bucket. Sometimes, the bucket must tip (a few milliseconds). During the first 50% of this tipping time, water flows into the filled bucket; the last 50% of this tipping time, water flows into the empty bucket. The amount of water flowing during the first 50% of the time is an error, the faster the flow rate the greater the error. At flow rates of one inch per hour (25 mm/hr) or less, the water drips into the buckets rather than flowing. Under this condition, the bucket tips between drips, and no error water is added to a full moving bucket.

a. Battery

The logger requires one 3-Volt CR-2032 lithium battery. Battery life varies based on the temperature and the frequency at which the logger is recording data (the logging interval). A new battery typically lasts one year with logging intervals greater than one minute or if used for rainfall logging only. Deployments in extremely cold or hot temperatures, or logging intervals faster than one minute, may significantly reduce battery life. Continuous logging at the fastest logging rate of one second will deplete the battery in as little as two weeks.

b. Data Storage

The data logger has 64,000 bytes of non-volatile data storage. The logger records a time stamp for each tipping-bucket tip. Data storage requirements per tip are a function of enabled channels and logging intervals. When tips are 3 to 12 days apart, 32 bits are required to record a single tip (16,000 tips). When tips are less than 16 seconds apart, only 22 bits are required to record a single tip (23,000 tips). In most cases, 25,000 to 30,000 data points (including tips, temperature, and/or battery measurements) can be logged. For most rain gauge applications, battery life, not memory capacity, will be the factor that limits deployment duration.

4.4 Statistical analysis and software used for data processing

Statistical analysis was carried out using Microsoft Excel, and SPSS software and spatial distribution maps were created using Arc GIS Software. Principal component analysis and descriptive analysis were carried out for 2018 and 2019 data using SPSS software. Rockworks software was used for creating 2D and 3D maps, logs and cross sections, geological models, general geology diagrams, etc.

4.5 Aquifer Storage and Recovery

Phase 4 targeted the areas surrounding the drinking water wells that showed the presence of salinity in Phase 2 using existing and new tube wells. Further, the water extracted from tube wells within and down-gradient from the industrial areas was examined where untreated wastewater may have been disposed of on the surface (e.g., in infiltration ponds) or injected into the subsurface. The main purpose of the study in Phase 3 was to identify cause/source areas using isotopes (release locations).

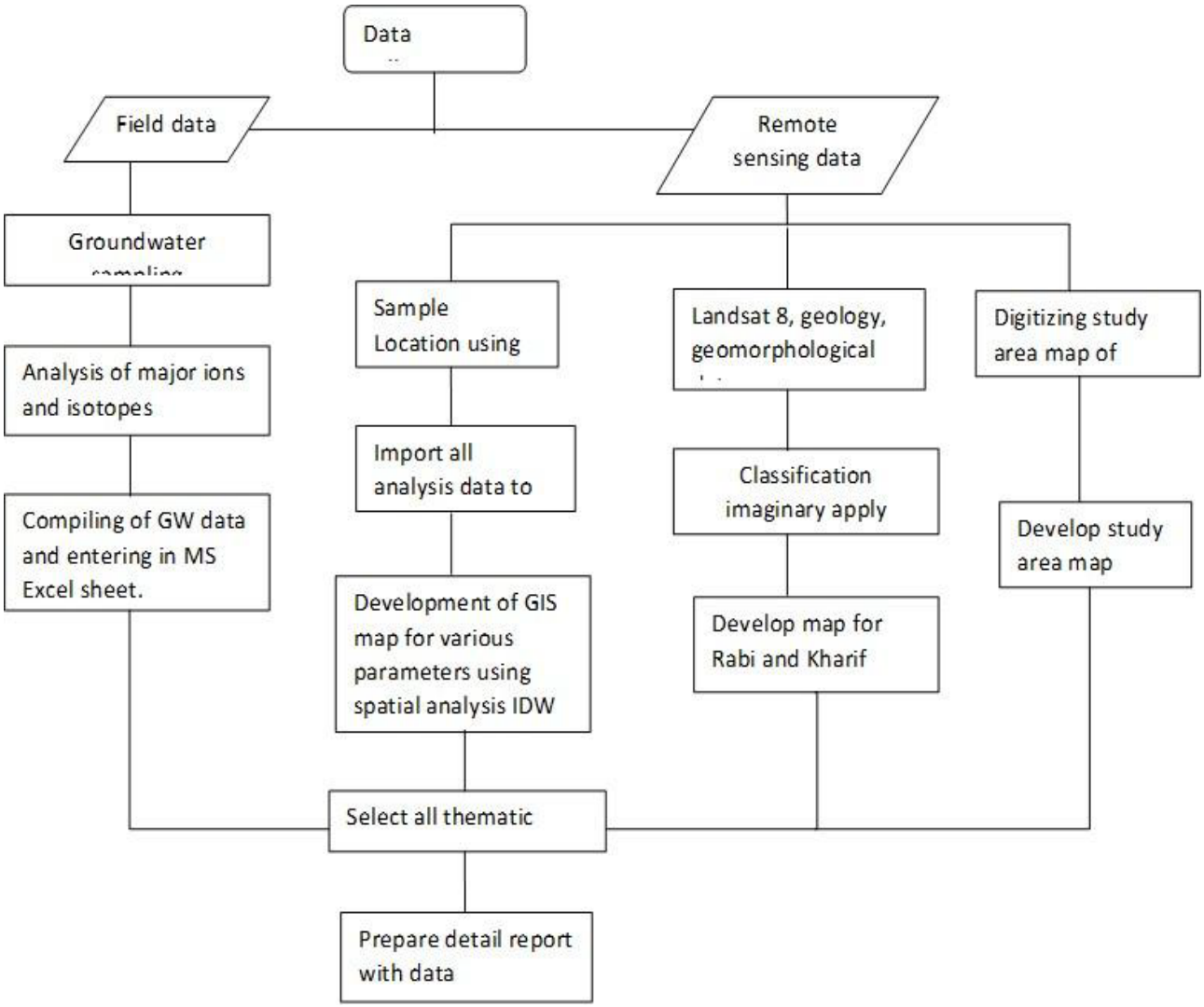

Fig 4.8 Flow chart of the methodology

The laboratory experimentation was performed to measure the viability of Aquifer Storage and Recovery (ASR) as a remediation method in the saline plains of Mewat, Haryana. This experiment was conducted in an experimental model having dimensions: length of 125 cm, width58 cm, and height of 153 cm (Fig. 4.9). Two self-prime regenerative pumps were used for injecting and extracting water. For experimenting, a saline solution of concentration 8500 µs/cm was prepared from sodium chloride (NaCl). The experimental model layout is given in fig 4.9. The temperature was measured with an EC meter (Eutech). 100 liters of this salt solution at a temperature of 25°C was inserted into the layer of the sand with a size ranging between 0.075 to 1.00 mm till saturation. Sand is kept in the experimental model for a prototype artificial aquifer. The sand with a volume of 0.479 m^3 was filled to the mid-section up to a height of 66 cm. After saturating these with saline water, freshwater was injected and simultaneously recovered at a certain time

interval of 1, 1.5, 2, 2.5, 3, 3.5, 4, 4, 8 24, 48, 72, 96, 120, 144, and 168 hours. The cumulative hours are 768.30. The freshwater carrier pipe was connected to the freshwater tank above the experiment model to maintain the gravity flow (Fig 4.10). 60 liters of fresh water with an average EC of 467.50µs/cm and an average temperature of 24.91°C was injected through the freshwater carrier pipe which was regulated through a tap. Two pipes were fixed up to the bottom of the sand bed. The recovery pipe was connected to the pump with a chuck valve in between to retain water in the pipe (Fig 4.10).

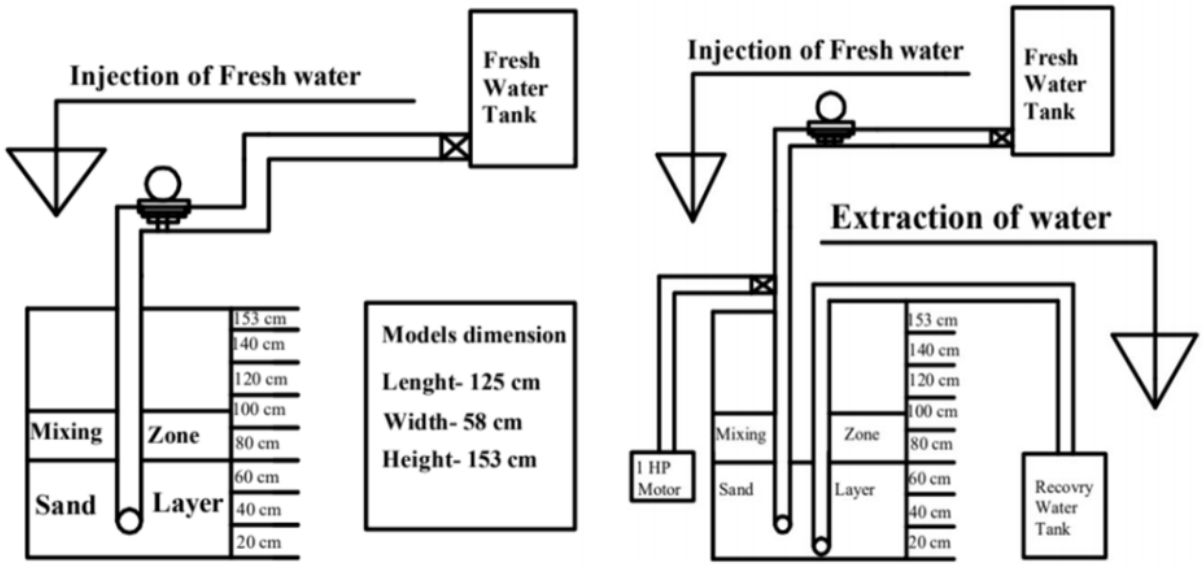

Fig 4.9 Experimental model layout of ASR

The model was further upgraded and modified to represent the Aquifer Storage and Recover process in much detail and with scientific temporum. The dimension of the new models is 120 cm in length, 60 cm in width, and 120 cm in height (Fig 4.10). Instead of one injection and recovery well, separate fresh and saline water injection sources were built. Two sprinklers were used to create saline saturated conditions and four injection wells were used to inject fresh water into the aquifer. The wide distribution of injection wells allows four different pockets of freshwater to observe the ASR phenomenon.

Phase 5 included the suggestions and development of resilience-building measures. Some proposed measures may be the construction of the hydraulic barrier, solid barriers (clay); high-pressure recharge.

One of the proposed models to be considered is a recharge well raised to roof height, leaving a margin to accommodate a pre-filter to remove suspended and floating materials coming with rainwater from the roof (Fig 4.11). This way, the hydro-static pressure for recharging is increased by about three meters. The rainwater harvested from the roof is directed under the ground through recharge wells penetrating below the groundwater table to form a pocket of fresh water.

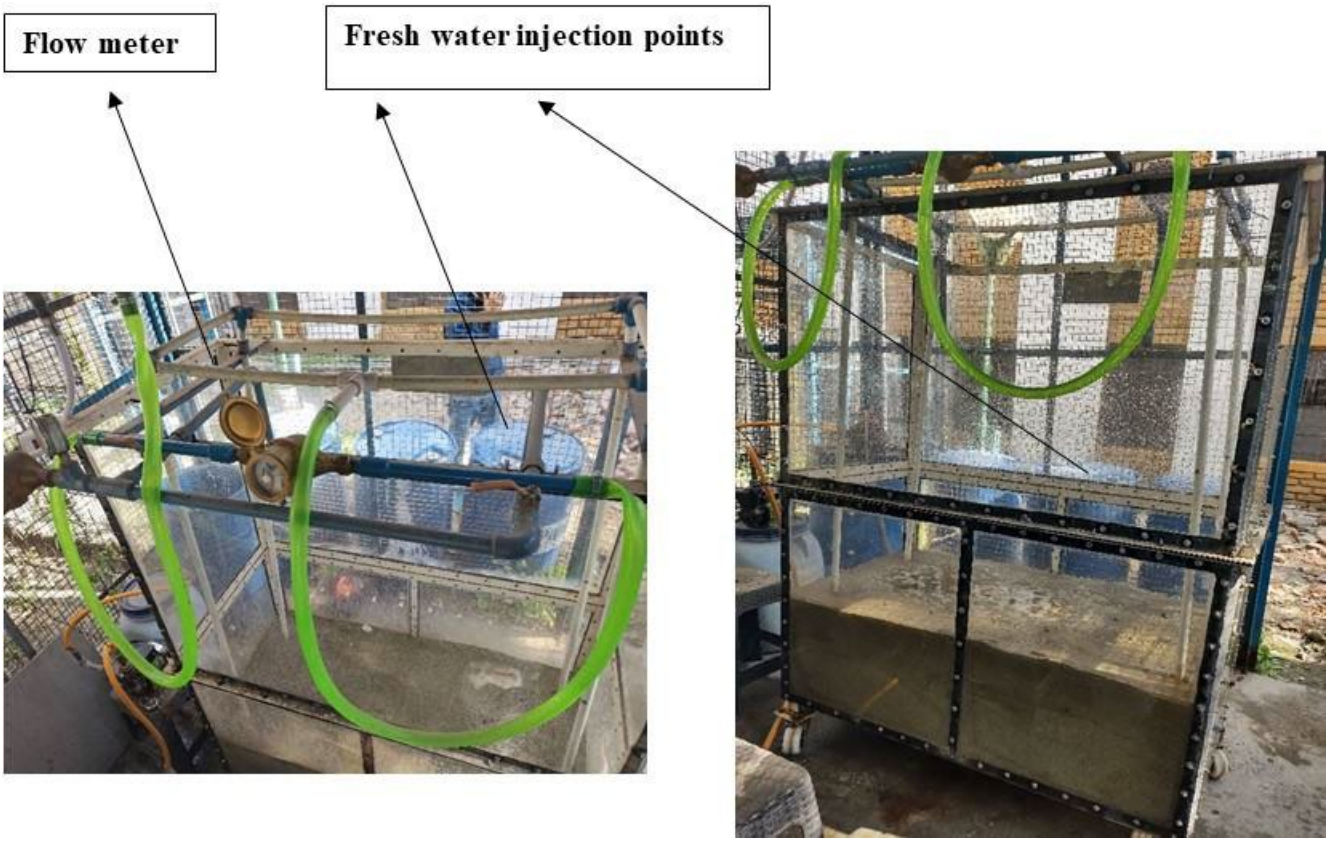

Fig 4.10 The ASR model with labeled parts

4.6 Remediation/Resilience building measures

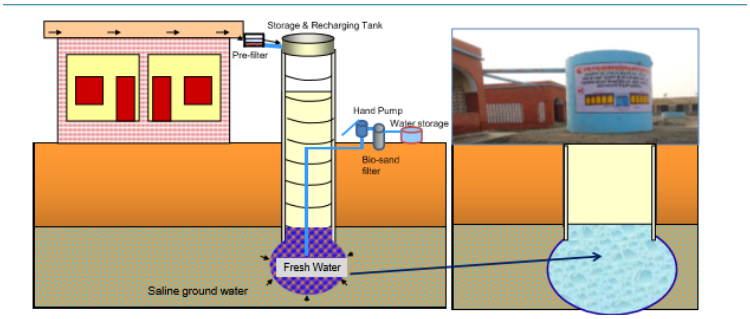

Fig 4.11 Model for freshwater bubble

For this, the experiment was conducted in controlled conditions where the periodic water sampling of the recharged water and subsequent quality analysis were carried out to find out any mixing of the saline water.

5.0 RESULTS AND DISCUSSIONS

Studies have established that water salinity creates massive vulnerabilities in the environment, destroys the ecosystem, degrades the soils and thereby productivity, and generates health problems, and so on. Salinity also results in severe socio-economic problems such as poverty, illiteracy, malnutrition, and structural problems in India (Mustari and Karim, 2014).

Fresh groundwater is available only in a few pockets at the foothills of the Aravallis, and most other groundwater sources are saline. Lack of freshwater can have far-reaching consequences that affect the district's economy, socio-political setup, and the health status of its inhabitants. Agriculture is the main occupation in the area, but the water scarcity limits farming to rain-fed cropping. The quality of groundwater is not fresh in shallow or deeper horizons in most parts of the district. Larger parts of Nuh (formerly called Mewat), Nagina, and Firozpur Jhirka blocks are underlain with brackish/saline groundwater even at shallow levels. For improving the understanding of local issues, resource uses and management systems, a socio-economic survey was conducted in the study area.

5.1 Socio-economic survey

One of the study's objectives is to analyze the impact of salinity on the socio-economic indices of the rural inhabitants in the Mewat district of Haryana. A theory-based approach forms the yardstick that is constructed to identify the thrust areas affected directly or indirectly by water salinity. The conceptual framework has been guided by a thorough literature review of the impact variables of water salinity (Fig 5.1). The impact of water salinity is studied vis-à-vis availability, accessibility, sufficiency, and mitigation strategies at the household level.

5.1.1 Socio-economic characteristics of respondents

With a population of 1.1 million, Nuh is a recently formed district, carved out of Gurugram and Faridabad, two districts of Haryana that border Delhi, India's capital. Compared to most districts in the state, Nuh lags on several socio-economic indicators. For instance, the female literacy rate is as low as 36 percent (Census, 2011), and access to improved water and sanitation is very poor (Mehta et al. 2015).

The socio-economic profiling of the respondent households helps in deconstructing the social, economic, and cultural contexts of a region. The information on caste category, ration card holding pattern, occupational engagements, and demographics across water salinity levels help to identify vulnerable groups. The inhabitants of the study region are predominately Muslim (traditionally called *Meos*). The minority group is categorized as "Other Backward Caste" per the Indian Constitution. The sample represents the dominance of Meos in the region with some representation from the Hindu population majorly from the Tauru block (Fig 5.2). The ration card holding pattern is identical across three water salinity categories with the majority of respondents holding APL (Above Poverty Line) card (Fig 5.2). The gender ratio is highly variant across these categories. While district Nuh

performs better in terms of gender ratio than the state of Haryana, the respondents in the moderately saline villages are found to have the lowest level of gender ratio. Based on the respondents' data, the gender ratio is relatively better in both highly saline and sweet villages.

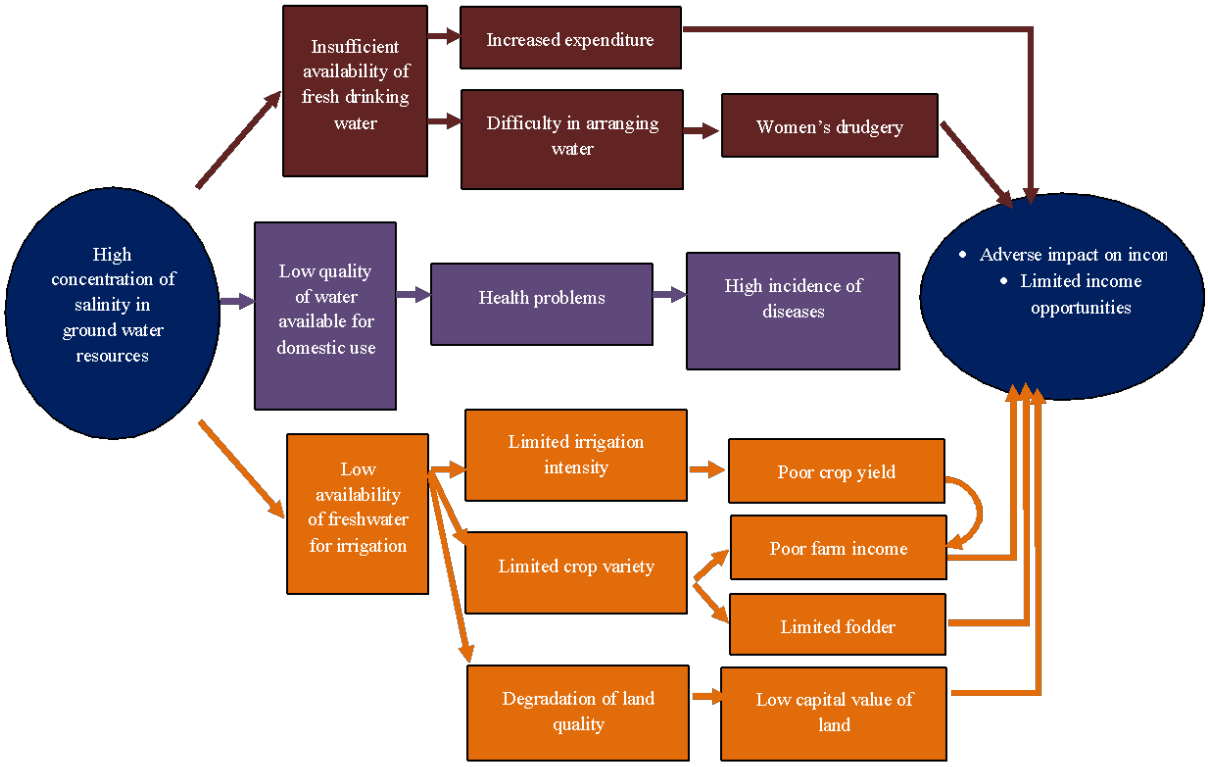

Fig 5.1Theory of the change model

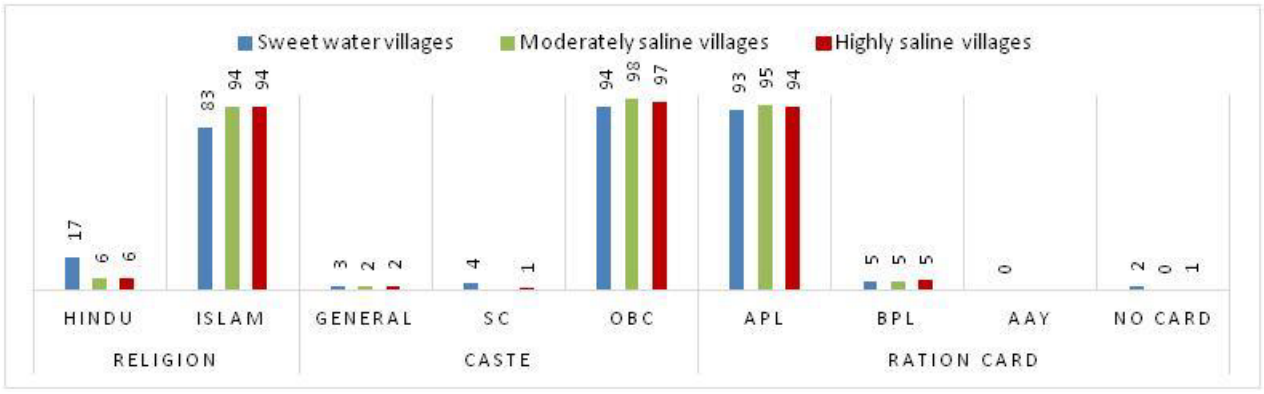

Fig 5.2 Social classification of respondent households (in percentages)

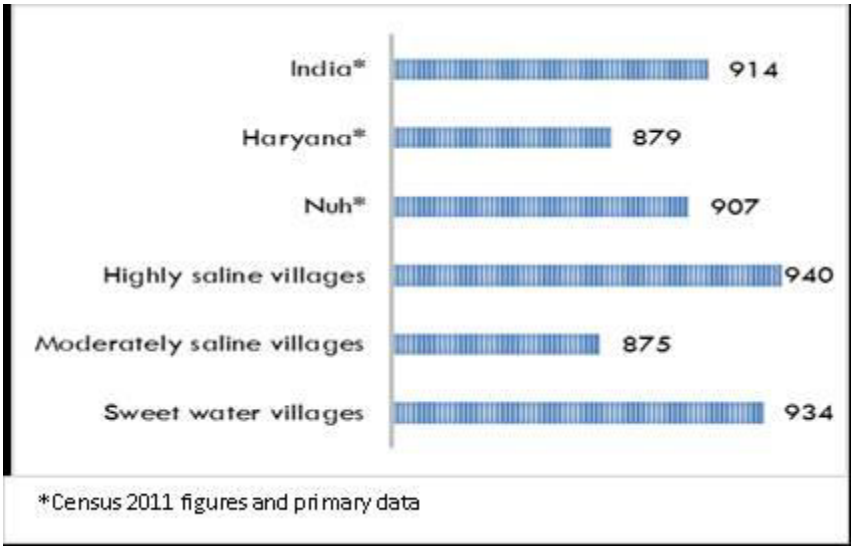

Fig 5.3 Gender ratio (number of females per 1,000 males)

5.1.2 Availability of water for irrigation

Irrigation is a very important input for crop growth in agriculture. Irrigation is the process through which controlled amounts of water can be supplied through artificial means such as pipes, ditches, sprinklers, etc. The main objective of irrigation systems is to help agricultural crop growth by providing adequate soil moisture, especially to reduce the effect of inadequate rainfall (Roy and Shah, 2002).

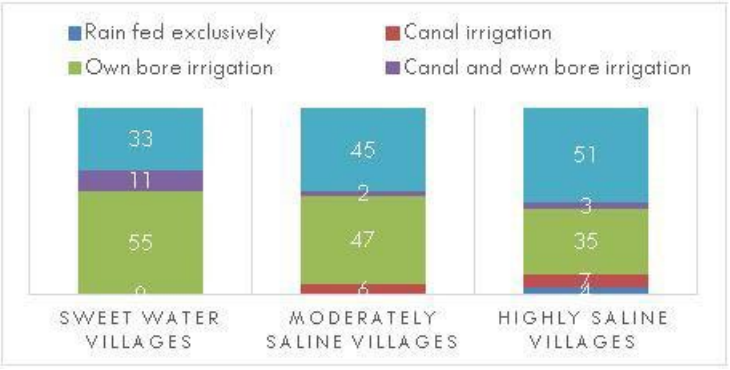

Fig 5.4 Irrigation sources (percentage of respondent farming households)

The results of the study reveal that the overall irrigation pattern in the study region is primarily dependent on groundwater resources. However, the proportion of farmers owning irrigation sources declines with increasing salinity levels. Across all the salinity groups, only 3 percent of farmers were found to be exclusively dependent on rain for irrigation (Fig 5.4). It is interesting to note that 35 percent of farmers in the high-salinity

region irrigate using groundwater.[1] These farmers are cultivating wheat, mustard, and cotton using groundwater for irrigation. For the few farmers who are using saline water for irrigation, it is important to note that the process of saline irrigation increases the salt content in the soil, which limits its production potential. Although crops like wheat and cotton are salt tolerant to a certain extent, it has implications on the quality of the produce. Due to limited freshwater sources in saline regions, the dependence on purchased water sources can be seen increasing with increased salinity levels. In highly saline regions, freshwater is available in the form of canals (in Nuh and Punhana blocks) or lines connecting bore wells from the nearest sweet village. In the absence of the same, farmers either practice rain-fed cultivation, saline irrigation, or cultivation through purchased water.

5.1.3 Availability of drinking water

Water is essential for the survival of human beings. Salinity could prove to be a great threat to the availability of safe drinking water. In the study region, the drinking water sources found varied across the villages with different levels of salinity. In the Nuh district, sweet water is mostly found in the villages lying at the foothills of the Aravalli range. But the cost of extracting the groundwater is high, hence a lot of villagers are unable to invest resources for a private bore well. In this section, we explore the impact of salinity on the availability of water for drinking and other domestic purposes in the region.

The percentage of households purchasing drinking water is highest in the high-saline villages with 54 percent of the respondents buying water, while for moderately saline villages, the percentage stands at 8 percent and for sweet water villages, it stands at 20 percent (Fig 5.5). These households are getting water from multiple sources and when their total water requirements are not met, they purchase water. In the sweet water category, respondents of two villages, Santawadi and Hasanpur bilonda, purchase water due to the insufficiency of safe drinking water. This has resulted in a higher percentage of villagers purchasing water in sweet villages as compared to moderately saline villages.

Private bore wells are the major source of drinking water for households with access to groundwater sources. These sources are most prevalent in moderately saline villages with 55 percent of the respondent households utilizing the source for drinking water, followed by 51 percent for sweet water villages, and 11 percent for highly saline villages. The prevalence of private bore wells is dependent on the cost of installing the bore, which increases with the depth and is not viable for households with economic constraints.

Use of government-supplied water was observed to be the most in high-saline villages with 22 percent of the respondents using it for drinking purposes. The sweet water villages have similar figures with 21 percent of the households using the government water supply, followed by moderately saline villages with 10 percent of the respondents relying on the government water supply for drinking water.

[1], There are pockets of freshwater (sweet) beneath the ground in nearby villages or within some pockets of the village, therefore they use bore well for irrigation. Very few farmers are also using saline water for irrigation.

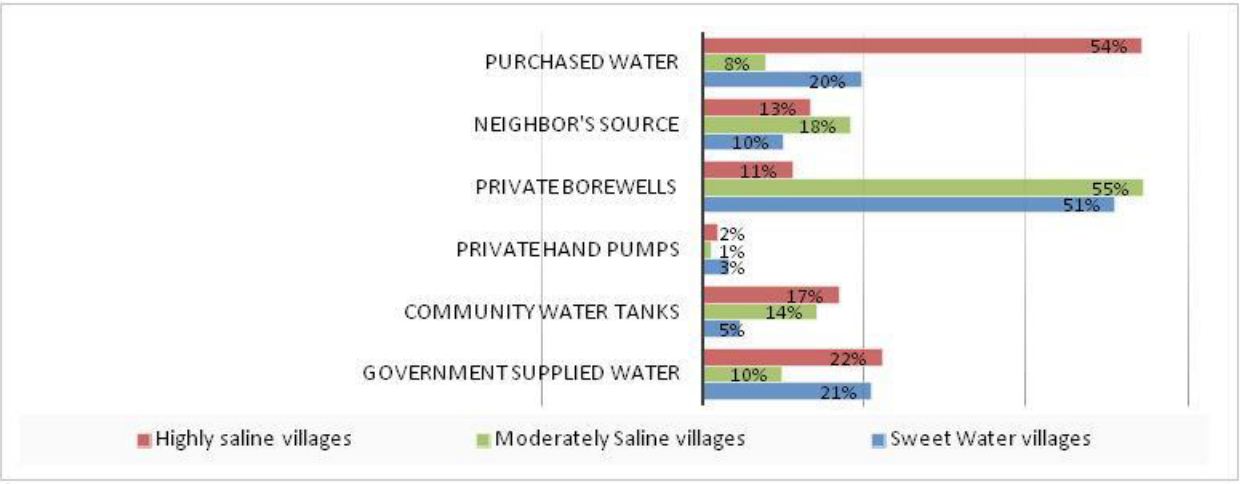

Fig 5.5 Sources of drinking water

5.1.4 Water for household use

The figures for the household sources of water were mostly the same as the drinking water sources of highly saline villages. In the case of water for household purposes, 21 percent use water from a private bore well and 39 percent of the respondents purchase water to meet the water demand for household purposes. As a trend, it was seen that people usually end up constructing underground water tanks and filling them from purchased tankers that usually last 20–25 days. In other regions, households mostly do not rely on purchased water to meet their domestic demands. On average, the cost of purchased water is highest in the sweet water villages, with the average cost being 1,264 per month, followed by high-saline villages with an average cost being 1,088 per month, followed by moderately saline villages with the cost of water being 1,057 per month.

5.1.5 Collection of water

Lack of water availability at the household level means that people have to find alternative sources to fulfill their needs. An improved water supply can bring significant change in water-use behavior. For example, the supply of water to households has been linked to the use of toilets and personal hygiene.[2] Lack of water supply makes people defecate in the open even though they have a toilet constructed at home, as it is difficult to fetch a large quantity of water at home. The results reveal that in the sweet water villages, the percentage of respondents with a source outside the village was 10 percent and 19 percent in moderately saline and highly saline villages (Fig 5.6).

The general trend in the region is that if the water was available in nearby villages and not within the household premises, then women and girls are mostly responsible for fetching water. In case, water was not available in the village, villagers either construct an underground tank, which is filled up by purchased tanker services that are easily available,

[2]See https://doi.org/10.1371/journal.pone.0071977.

or they buy filtered water using the reverse osmosis (RO) technique in a twenty-liter plastic dispenser as per the trend in high-saline villages, the average distance traveled to collect water was found to be the most, followed by the moderately saline villages and the least was in sweet water villages. Whenever there is a greater water burden and a sudden or unexpected scarcity of water, it is found that in the highly saline villages, the households tend to use all the means almost equally, such as buying water, managing with less water, taking neighbors help, and fetching the water. In moderately saline villages, most of the respondents cope by fetching water from far away; and in sweet water villages, households buy water to mitigate the lack of water availability.

Fig 5.6 Average distance from the source of water (in meters)

5.2 Water level variations

The groundwater levels data for the period 1974 to 2016 was taken from Groundwater Cell, Haryana Agriculture Department. The database of groundwater level data for the period 1974 to 2016 was analyzed for the changes and trends during the period of observations (Fig 5.7).

The pre-monsoon and post-monsoon groundwater levels for the period 2004-2017 were plotted as time-series plots (Fig 5.8) to check the annual rate of groundwater variation. Spatial distribution maps for the study area for the period of 2010-2019 were prepared. To explore the seasonal effect on groundwater level, monthly data have been categorized into seasonal data with respective two distinct seasons i.e. Post monsoon (November) and Pre-monsoon (May) from annual data (Jan-Dec). Different graphical presentations of the groundwater level were used to interpret the temporal variation in groundwater level in the district. Groundwater level fluctuation was studied by subtracting the groundwater level with ground elevation from 2010 to 2019 at the different wells (Fig 5.9).

Fluctuation of groundwater level provides crucial information on the dynamics of recharge and discharge in short duration and aquifer conditions (in terms of ground potential/depletion) in long term. The long-term (10 years) average water level trend indicates that the water level ranges from 150 m to 230 m, amsl during pre-monsoon, and 150 m to 240 m during post-monsoon. The maximum decline has been noticed in the South-Western part of the district (Firozpur Jhirka block) and the minimum decline in the Northern part of the district.

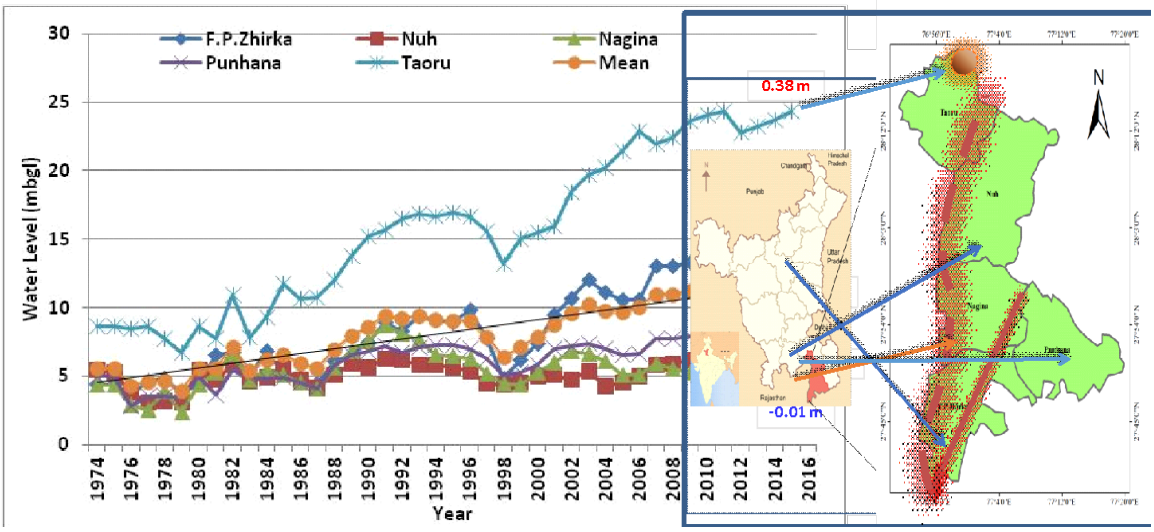

Fig 5.7 Groundwater level variations from 1974 to 2016

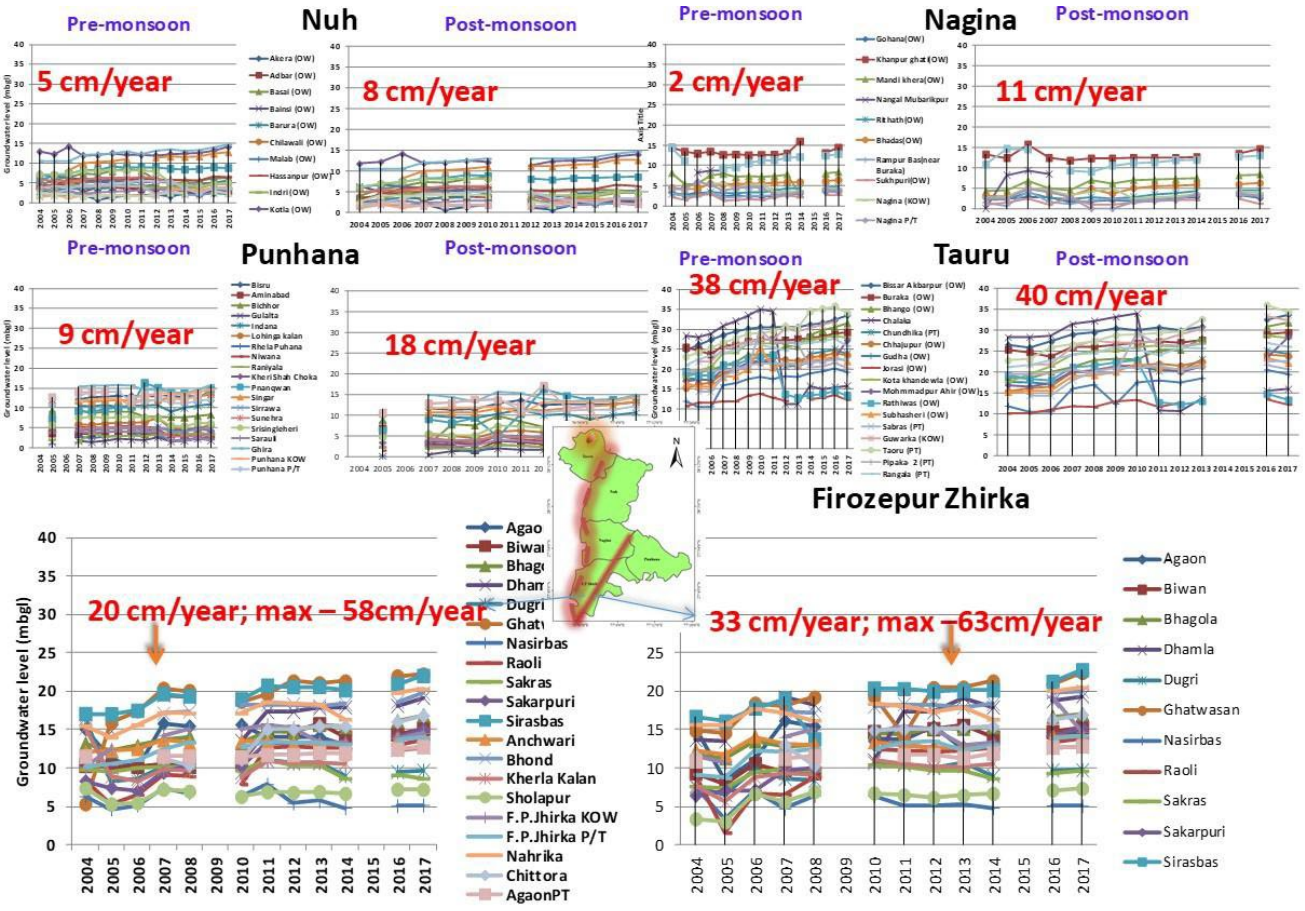

Fig 5.8 Groundwater level variations for pre-monsoon and post-monsoon seasons for the period 2004 to 2017

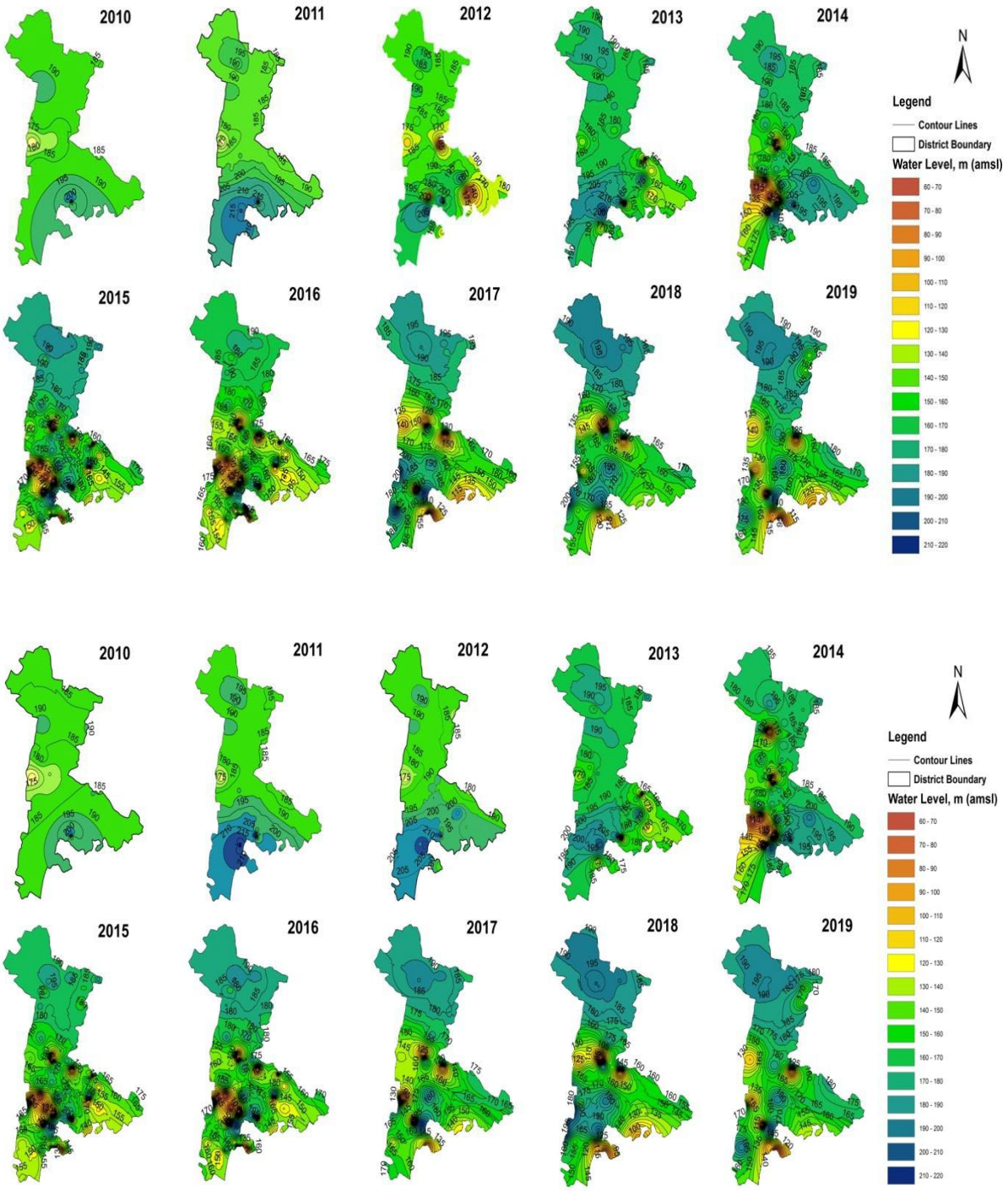

Fig 5.9 Spatial groundwater level variations from 2010 to 2019 in Mewat

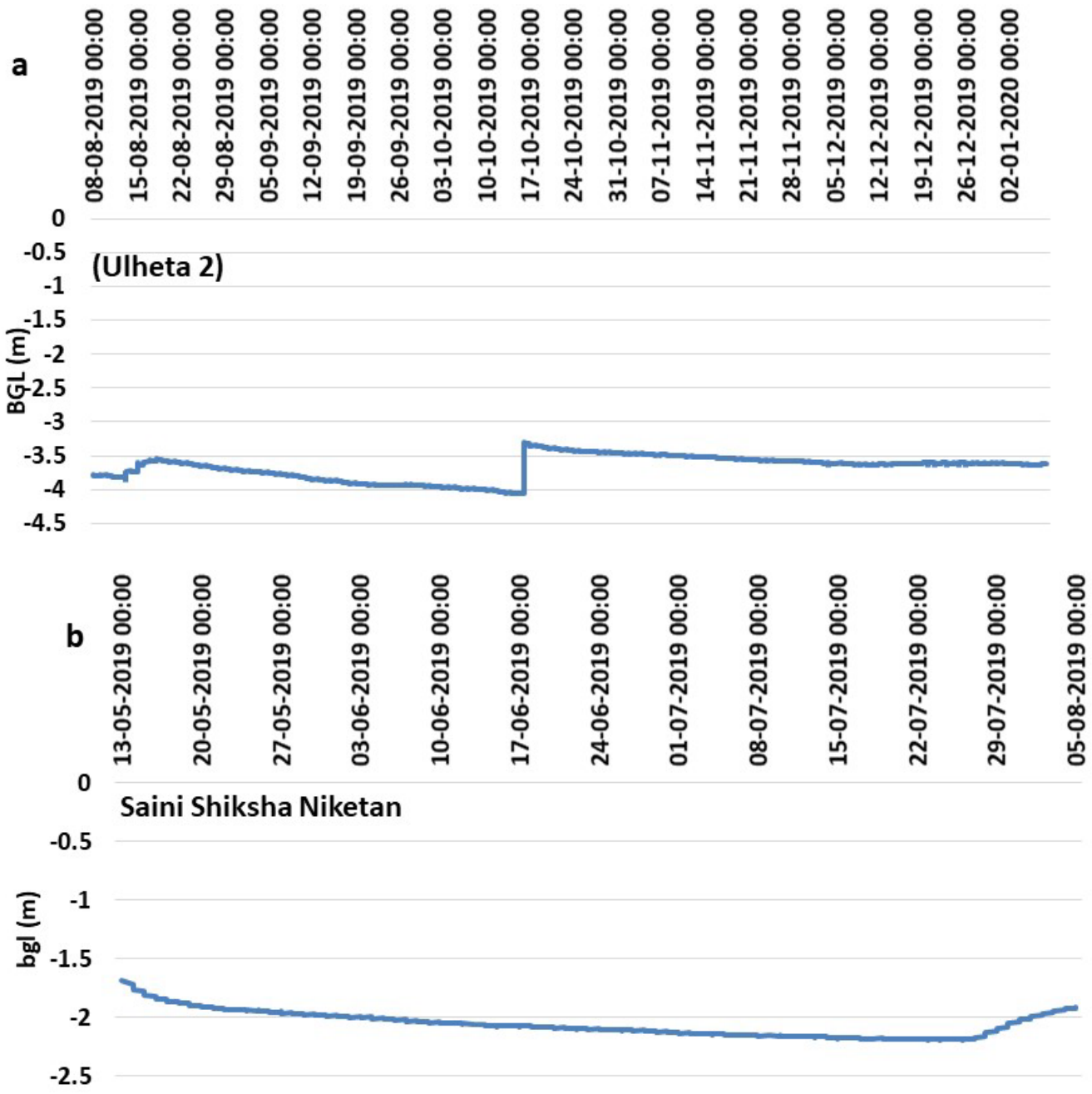

From figure 5.8, it is clear that the water levels in Tauru block depleting at a faster rate i.e 0.40 m/year, followed by Firozepur Jhirka block depleting at the rate of 0.33m/year. These 2 blocks have sweet water and the groundwater extraction is maximum. Minimum depletions are found in Nuh (0.08m/year) and Nagina (0.11 m/year) blocks due to groundwater salinity issues in large pockets.

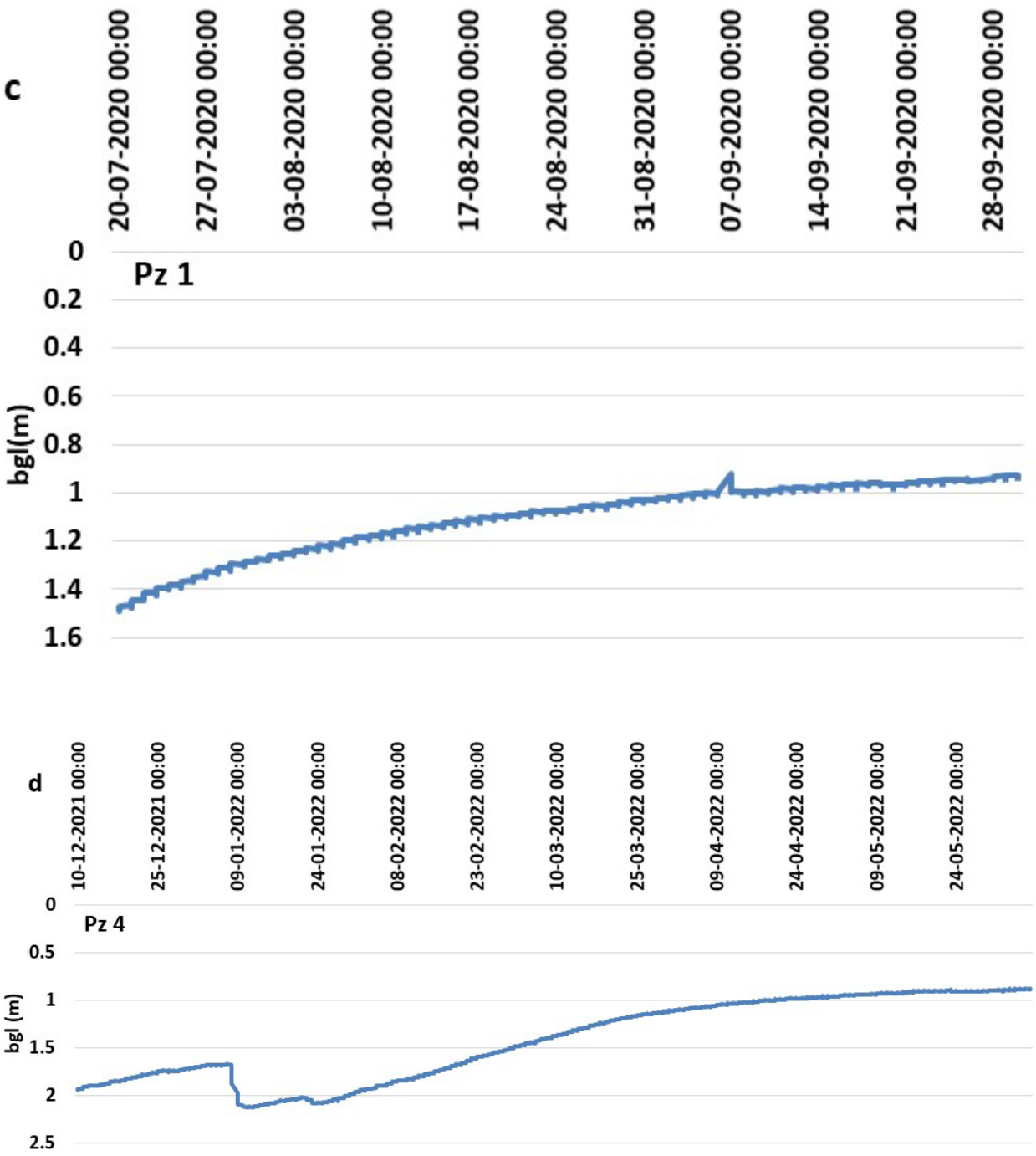

Figure 5.10 Variation in water level with time (a to d) at different sites

Water level loggers were also installed in the field and found that the behavior of fluctuations was different in all the wells (Figs. 5.10).

5.3 Salinity variations

For temporal salinity variations, historical data for total dissolved solids (TDS) in groundwater for the representative 15 wells for the time period 2012-2016 was taken from Sehgal Foundation Gurgaon, and the distribution of these points is shown in fig 5.11.

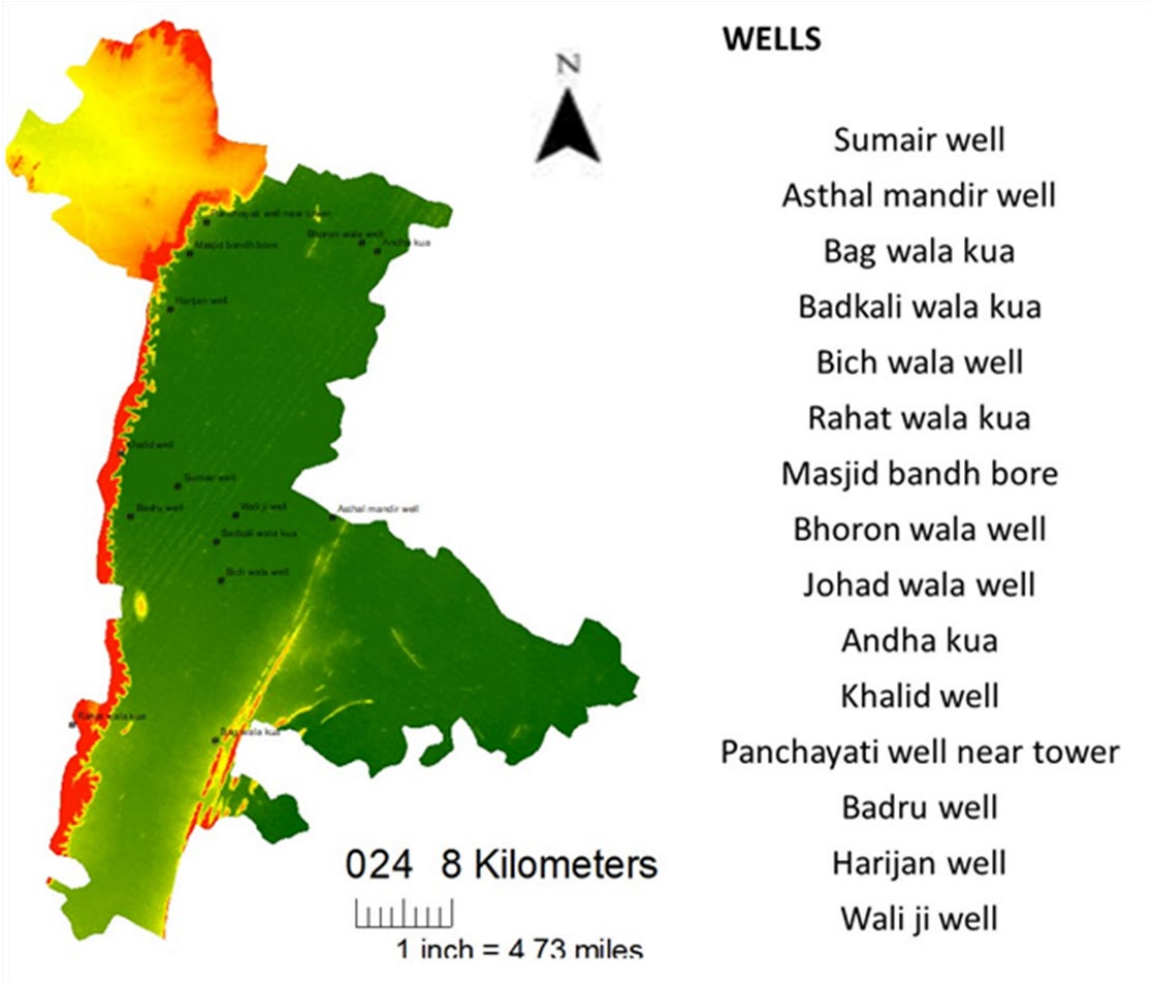

Fig 5.11 Locations of wells for salinity variations during the years 2012 to 2016

It was found that TDS increases per annum varied from 2% (Bichwala well) to 48% (Khalid well). Another notable increase of 37% was found in Badru well followed by 20% in Bag walakua. The spatial distribution is shown in fig 5.12. TDS increase in 74% of the area was in the range of 500-1000 mg/l TDS while in 35% of the area, it was in the range of 1500-2000 mg/l TDS.

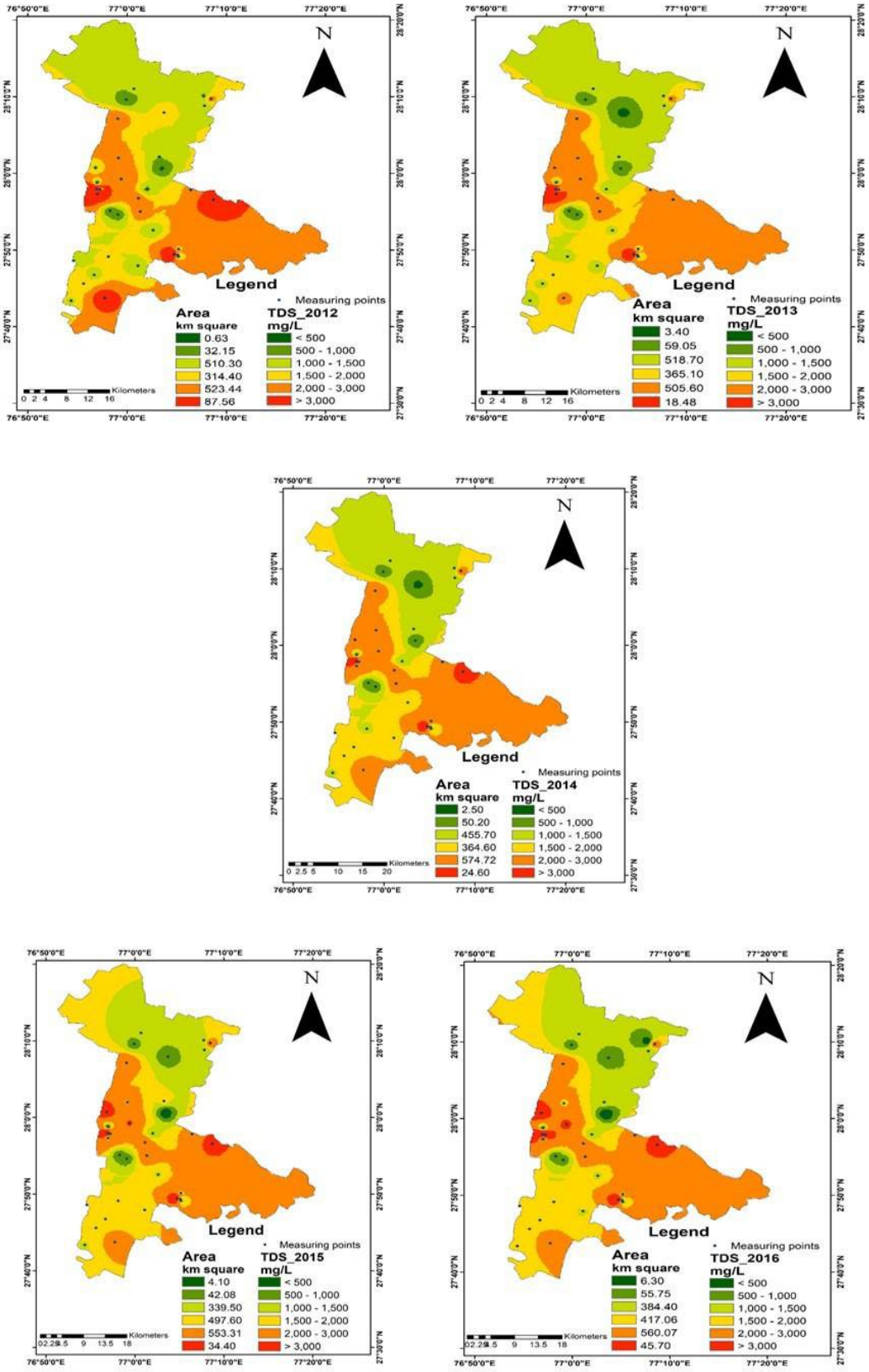

Fig 5.12 Temporal and spatial variation of TDS during the years 2012 to 2016

Table 5.1 Variation in groundwater salinity at different locations during the period from 2012 to 2016

S. No.	Location/ Village	TDS values in various years					Change during 2012-16
		2012	2013	2014	2015	2016	
1	Panchayati well near the tower	1060	1156	1163	1304	1500	41.50
2	Badru well	1402	1215	1343	1523	3000	113.98
3	Harijan well	2625	2846	2858	2896	2905	10.66
4	Wali Ji well	923	1002	1099	1117	1120	21.34
5	Sumair well	2827	2815	2925	3099	3200	13.19
6	Asthal mandir well	2014	2058	2153	2362	2425	20.41
7	Bag wala Kua	371	422	501	591	638	71.96
8	Badkali wala Kua	2355	2422	2549	2658	2735	16.13
9	Bich wala well	2736	2672	2705	2837	2900	6.02
10	Rahat wala Kua	1458	1541	1663	1728	1780	22.08
11	Masjid bandh bore	616	670	712	733	740	20.12
12	Bhoron wala well	883	979	1033	1083	1105	30.23
13	Johad wala well	436	551	556	561	681	56.19
14	Andha Kua	2249	2334	2525	2548	2590	15.16
15	Khalid well	1384	2330	3024	3923	4020	190.46

Table 5.2 Change in the area covered under fresh/saline groundwater distribution during the period from 2012 to 2016

S. No.	TDS Range	Area covered in Km^2 (values in bracket shows the area in %)					% change
		2012	2013	2014	2015	2016	
1	**< 500**	0.04	0.23	0.17	0.27	0.43	975
2	**500-1000**	2.18	4.01	3.41	2.86	3.8	74
3	**1000-1500**	34.74	35.27	30.95	23.08	26.14	-
4	**1500-2000**	21.0	24.83	24.76	33.82	28.4	35
5	**2000-2500**	35	34.38	39.03	37.61	38.12	7
6	**>3000**	6	1.26	1.67	2.33	3.13	-
Total		100	100	100	100	100	

Recent data from data loggers have been collected and variation in EC concerning the time at different sites in the study area is shown in fig 5.13(a to g). The salinity plots show notable fluctuations in salinity levels. Monitoring and observations for longer durations are required to find the causes of these variations.

a

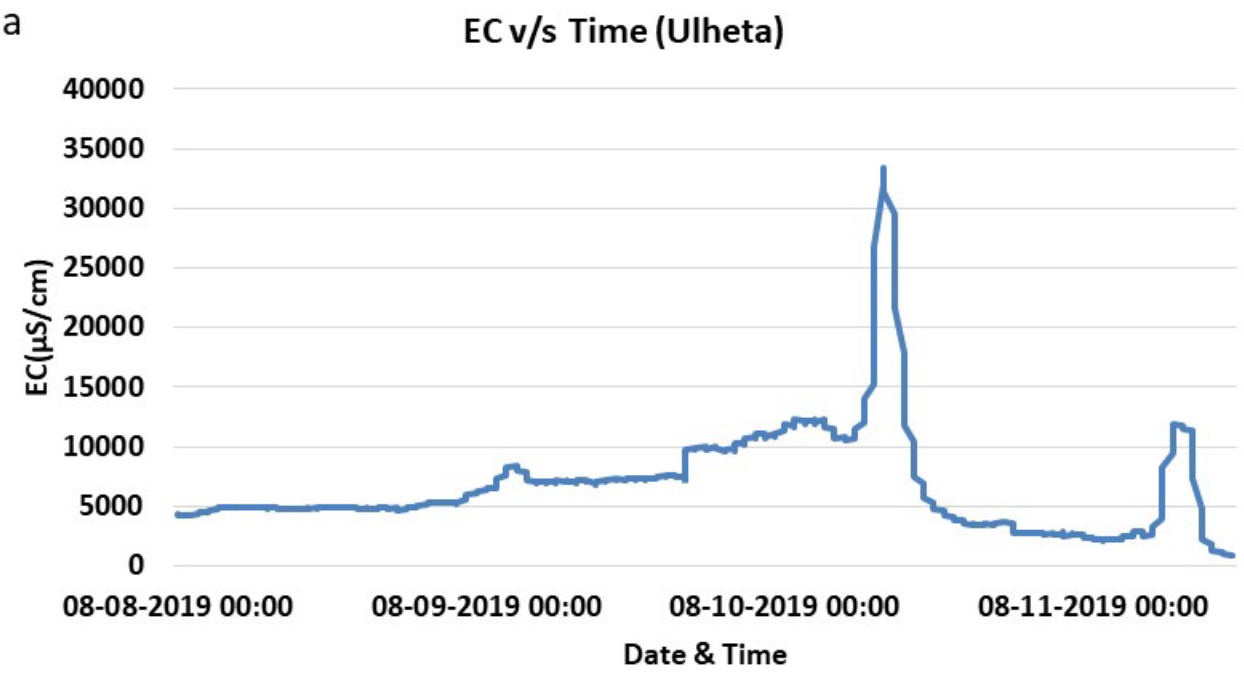
EC v/s Time (Ulheta)
40000
35000
30000
25000
20000
15000
10000
5000
0
EC(µS/cm)
08-08-2019 00:00
08-09-2019 00:00
08-10-2019 00:00
08-11-2019 00:00
Date & Time

b

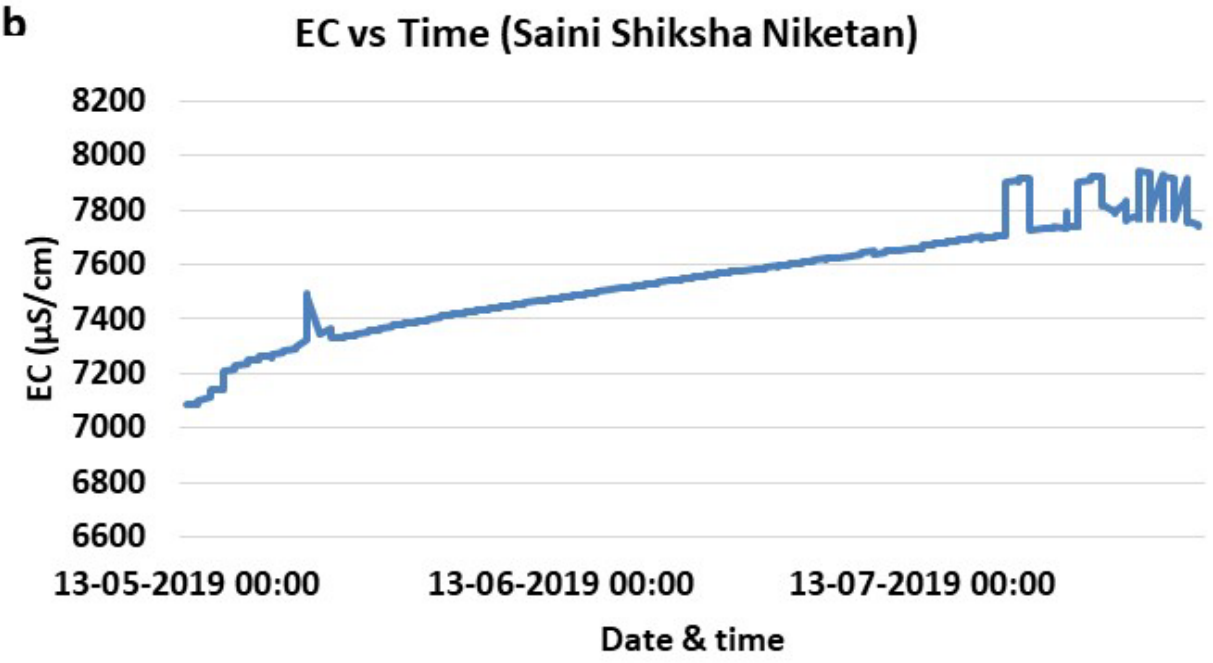
EC vs Time (Saini Shiksha Niketan)
8200
8000
7800
7600
7400
7200
7000
6800
6600
EC (µS/cm)
13-05-2019 00:00
13-06-2019 00:00
13-07-2019 00:00
Date & time

b

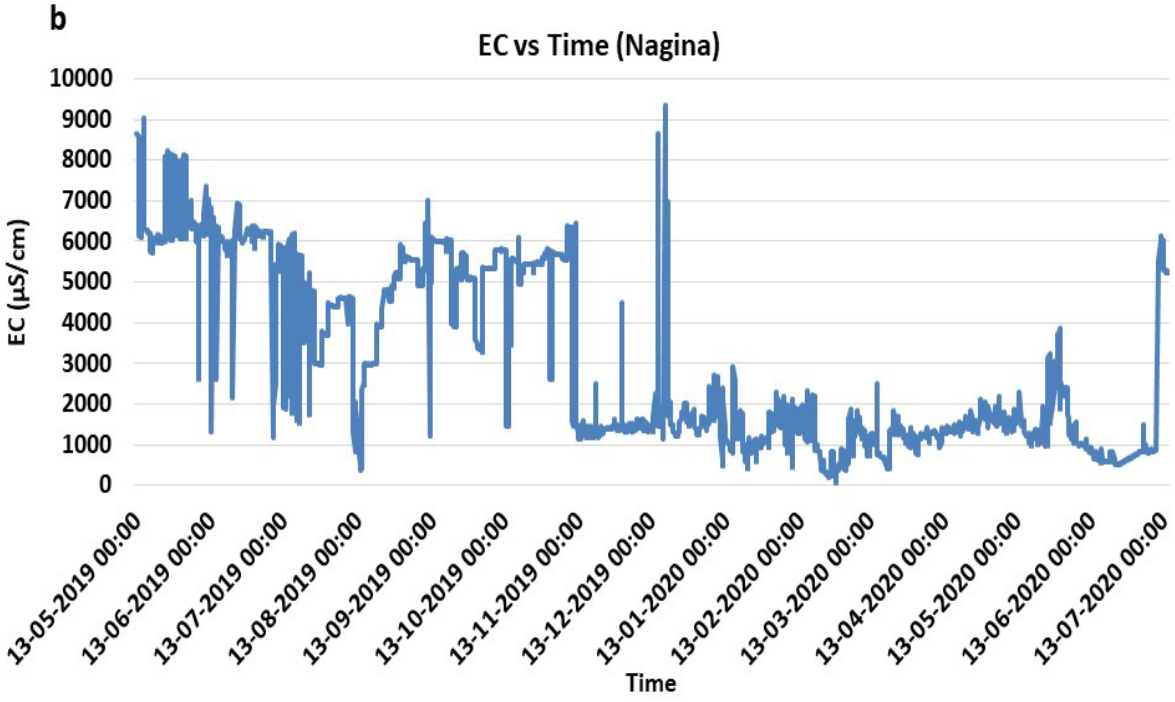
EC vs Time (Nagina)
EC (µS/cm)
10000
9000
8000
7000
6000
5000
4000
3000
2000
1000
0
13-05-2019 00:00
13-06-2019 00:00
13-07-2019 00:00
13-08-2019 00:00
13-09-2019 00:00
13-10-2019 00:00
13-11-2019 00:00
13-12-2019 00:00
13-01-2020 00:00
13-02-2020 00:00
13-03-2020 00:00
13-04-2020 00:00
13-05-2020 00:00
13-06-2020 00:00
13-07-2020 00:00
Time

d

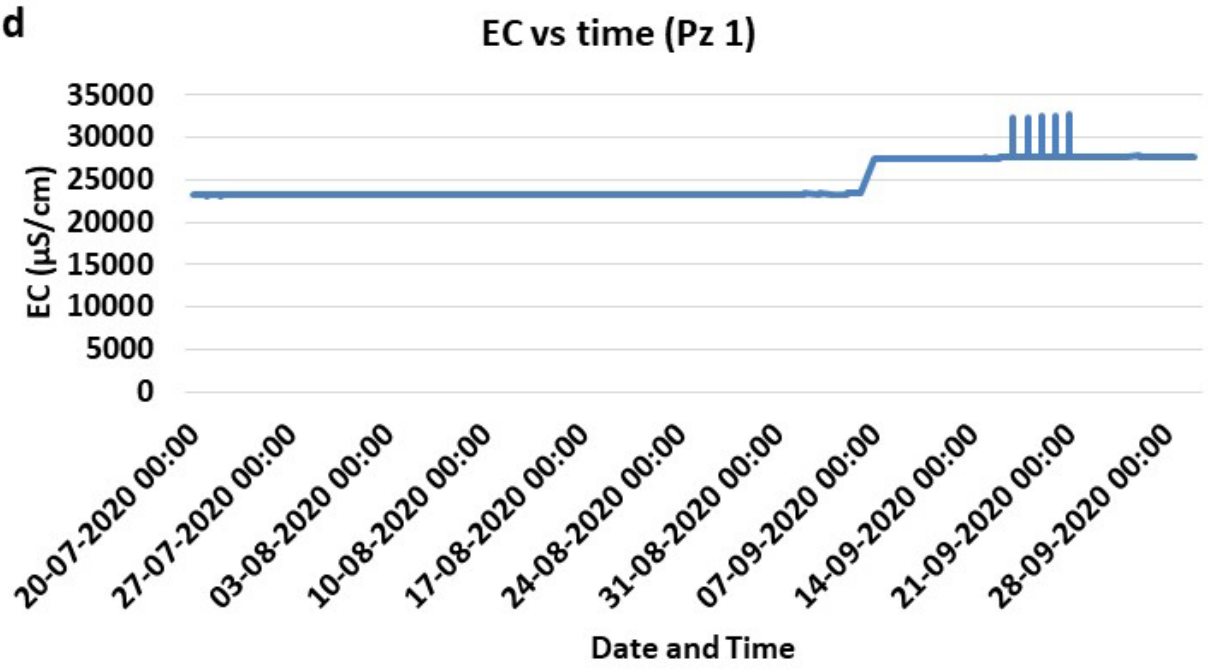
EC vs time (Pz 1)
EC (µS/cm)
35000
30000
25000
20000
15000
10000
5000
0
20-07-2020 00:00
27-07-2020 00:00
03-08-2020 00:00
10-08-2020 00:00
17-08-2020 00:00
24-08-2020 00:00
31-08-2020 00:00
07-09-2020 00:00
14-09-2020 00:00
21-09-2020 00:00
28-09-2020 00:00
Date and Time

e

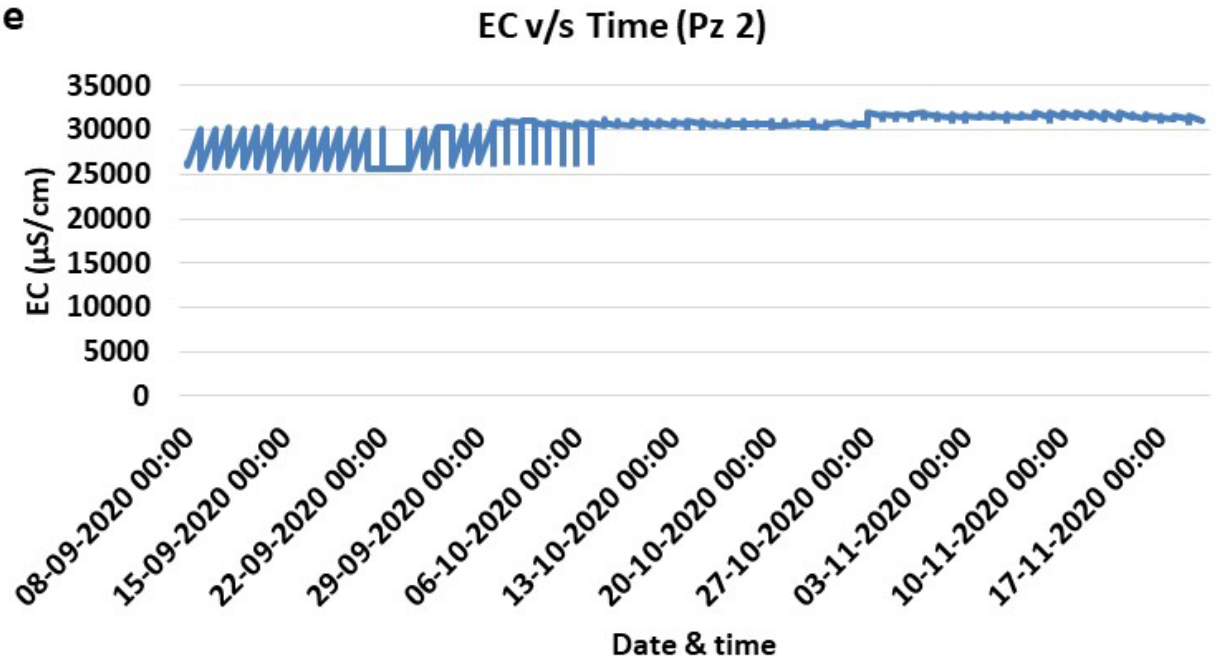
EC v/s Time (Pz 2)
35000
30000
25000
20000
15000
10000
5000
0
EC (µS/cm)
08-09-2020 00:00
15-09-2020 00:00
22-09-2020 00:00
29-09-2020 00:00
06-10-2020 00:00
13-10-2020 00:00
20-10-2020 00:00
27-10-2020 00:00
03-11-2020 00:00
10-11-2020 00:00
17-11-2020 00:00
Date & time

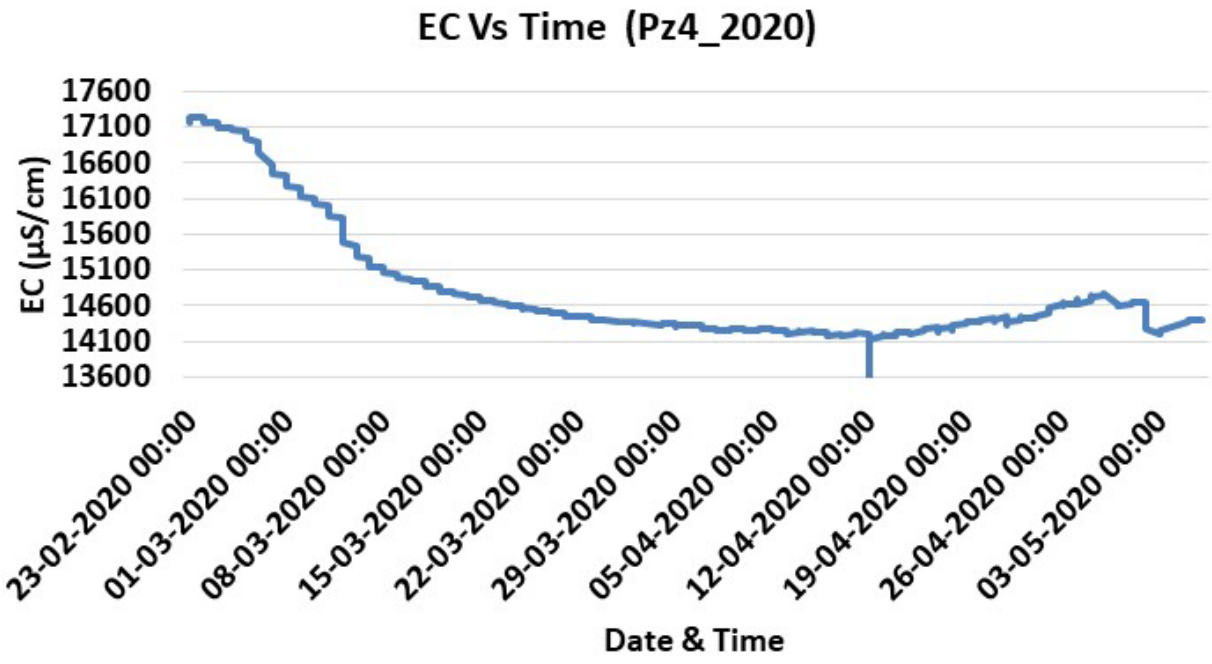
EC Vs Time (Pz4_2020)
17600
17100
16600
16100
15600
15100
14600
14100
13600
EC (µS/cm)
23-02-2020 00:00
01-03-2020 00:00
08-03-2020 00:00
15-03-2020 00:00
22-03-2020 00:00
29-03-2020 00:00
05-04-2020 00:00
12-04-2020 00:00
19-04-2020 00:00
26-04-2020 00:00
03-05-2020 00:00
Date & Time

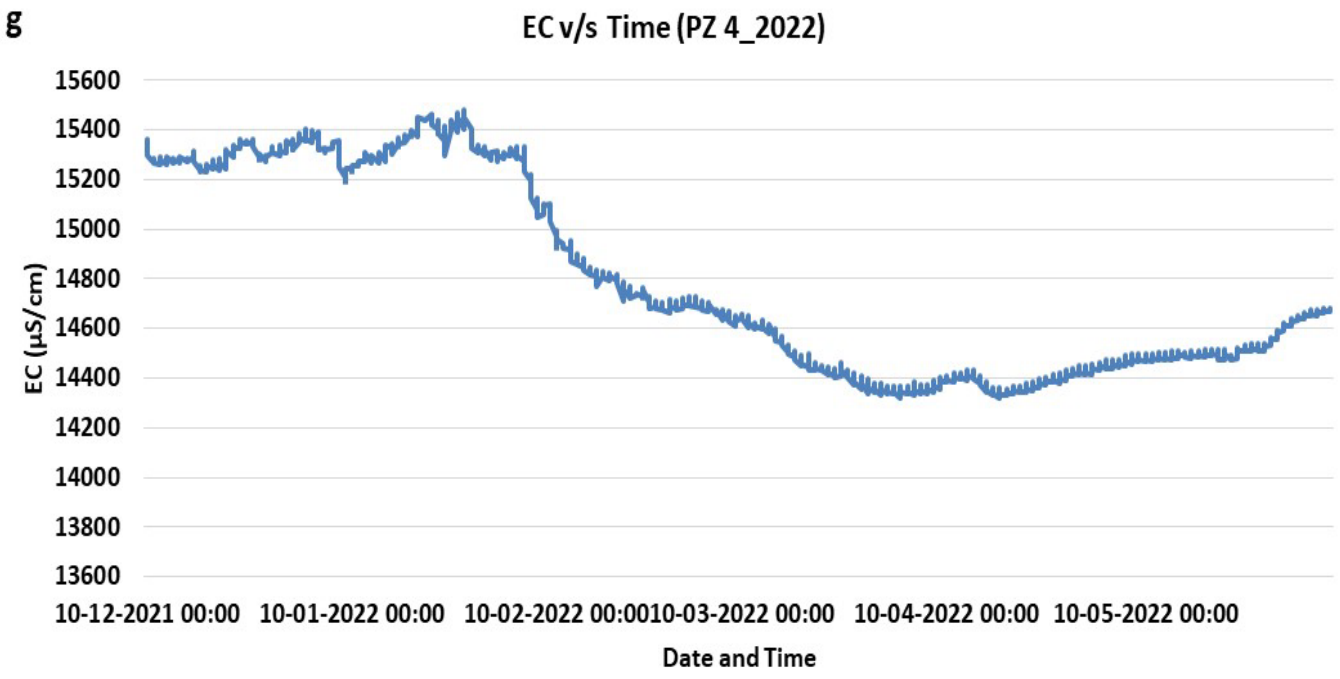

Figure 5.13 Variation in EC to time (a to g) at different sites.

5.4 Hydro-geochemical analysis

The comparative analysis of results for hydro-geochemical parameters for the years 2018-2019 was carried out for all the sampling locations based upon BIS: 10500 (BIS, 2012) standards for acceptable and permissible limits of various water quality parameters and checked the charge balance error.

5.4.1 Analysis for the year 2018

A total of 24 groundwater samples in the pre-monsoon (April) and from each of the 29 selected sites were collected during the monsoon (July), and post-monsoon (October) seasons in 2018 from hand pumps, open wells, and bore wells (Fig 4.3) with a depth range of 4-92 m. The water level in the open well (meters) was recorded using a water level indicator. GPS readings were taken for recording latitude and longitude. For each sampling site, samples were taken in 125 ml capacity acid-washed LDPE (Low-Density Polyethylene) tarson bottles. Electrical Conductivity (EC) and pH were measured using a portable handheld Hach, HQ30d EC meter, and total dissolved solids (TDS) were estimated from measured EC values and expressed in mg/L. The samples collected in 125 ml bottles were analyzed for cations (Ca^{2+}, Mg^{2+}, Na^{+}) and anions (HCO_3^-, SO_4^{2-}, Cl^-) in the water quality laboratory of the groundwater hydrology division of NIH, as per standard methodology. The unpreserved 0.45µm filtered water samples were used for the analysis of cations (Ca^{2+}, Mg^{2+}, Na^{+}) and anions (HCO_3^-, SO_4^{2-}, Cl^-). Ca^{2+} and Mg^{2+} were determined titrimetrically using standard EDTA. Cl^- was determined by the standard $AgNO_3$ titration method. HCO_3^- was determined by titration with H_2SO_4. Na^+ was

measured by flame photometry at a wavelength of 589 nm, and SO_4^{2-} by spectrophotometric turbidimetry by HACH spectrophotometer. All concentrations are expressed in milligrams per liter (mg/L).

5.4.1.1 Water Quality evaluation for drinking purposes

5.4.1.1.1 General Characteristics

The general characteristics of the hydro-geochemical analysis for the pre-monsoon, monsoon, and post-monsoon seasons are given in Table 5.3.
The pH values in the groundwater of the study area mostly fall within a range of 6.94 to 8.93 during the pre-monsoon season, 7.0 to 8.3 during the season, and 7.1 to 8.4 during the post-monsoon in the year 2018. The pH values for most of the samples are well within the limits prescribed by BIS (2012) and WHO (2007) for various uses of water, including drinking and other domestic supplies.

In the study area, the values of total dissolved solids (TDS) in the groundwater vary from 53 to 37051 mg/L with an average value of 6146 mg/L during the pre-monsoon season, 421-34170 mg/L with an average value of 4921 mg/L during the monsoon season; and 309 to 35108 mg/L with an average value of 5066 mg/L during the post-monsoon season in the year 2018. About 54%, 93%, and 62% of the samples were found above the maximum permissible limit of 2000 mg/L in pre-monsoon, monsoon, and post-monsoon seasons respectively. And about 8%, 7%, and 14% of samples were found within the acceptable limit of 500 mg/L in the pre-monsoon, monsoon, and post-monsoon seasons in the year 2018. Water containing more than 500 mg/L of TDS is not considered desirable for drinking water supplies, though more highly mineralized water is also used where better water is not available. For this reason, 500 mg/L as the acceptable limit and 2000 mg/L as the maximum permissible limit have been suggested for drinking water (BIS, 2012).

Alkalinity in natural water is mainly due to the presence of carbonates, bicarbonates, and hydroxides. Alkalinity as bicarbonate in the ground water varies from 34 to 540 mg/L with an average value of 273 mg/L during the monsoon season, 104 to 670 mg/L with an average value of 313 mg/L during the monsoon season, and 122 to 552 mg/L with average value 244 mg/L post-monsoon season in the year 2018. About 71%, 3%, and 0% samples were found above the maximum permissible limit of 600 mg/L in pre-monsoon, monsoon, and post-monsoon seasons respectively. And about 29%, 21%, and 41% of samples were found within the acceptable limit of 200 mg/L in the pre-monsoon, monsoon, and post-monsoon seasons of the year 2018 respectively.

The presence of calcium and magnesium, along with their carbonates, sulfates, and chlorides, is the main cause of hardness in the water. A limit of 200 mg/L as an acceptable limit and 600 mg/L as a permissible limit has been recommended for drinking water (BIS, 2012). Hardness in the ground water varies from 144 to 1590 mg/L with an average value of 709 mg/L during the pre-monsoon season, 200 to 7900 mg/L with an average value of 1611 mg/L during monsoon, and 233 to 4187 mg/L with an average value 1047 mg/L during the post-monsoon season in the year 2018. About 50%, 52%, and 62% of the

samples were found above the maximum permissible limit of 600 mg/L in pre-monsoon, monsoon, and post-monsoon seasons respectively. And about 8%, 3%, and 0% of the samples were found within the acceptable limit of 200 mg/L in the pre-monsoon, monsoon, and post-monsoon seasons of the year 2018 respectively.

In the groundwater of the study area, the values of calcium range from 50 to 1340 mg/L with an average value of 333 mg/L during the pre-monsoon season, 100 to 3080 mg/L with an average value of 683 mg/L during the monsoon; and 167 to 1700 mg/L with average value 552 mg/L during the post-monsoon season in the year 2018. About 54%, 79%, and 69% of samples were found above the maximum permissible limit of 200 mg/L in pre-monsoon, monsoon, and post-monsoon seasons respectively. And about 8%, 0%, and 0% samples were found within the acceptable limit of 75 mg/L in pre-monsoon, monsoon, and post-monsoon seasons in the year 2018 respectively. For magnesium, a limit of 30 mg/L as an acceptable limit and 100 mg/L as a permissible limit has been recommended for drinking water (BIS, 2012). In the groundwater of the study area, the values of magnesium range from 6 to 880 mg/L with an average value of 376 mg/L during the pre-monsoon season, 10 to 5560 mg/L with an average value of 928 mg/L during monsoon, and 13 to 3020 mg/L with average value 495 mg/L during post-monsoon seasons in the year 2018. About 83%, 79%, and 76% of samples were found above the maximum permissible limit of 100 mg/L in pre-monsoon, monsoon, and post-monsoon seasons respectively. And about 4%, 7%, and 3% of samples were found within the acceptable limit of 30 mg/L in pre-monsoon, monsoon, and post-monsoon seasons in the year 2018 respectively. In groundwater, the calcium content generally exceeds the magnesium content by their relative abundance in rocks.

The concentration of sodium in the study area varies from 2.4 to 10286 mg/L with an average value of 1298 mg/L during the pre-monsoon season; 0 to 5842 mg/L with an average value of 487 mg/L during the monsoon season; and 2.7 to 5168 mg/L with an average value of 643 mg/L during the post-monsoon season in the year 2018. The high sodium values in the study area may be attributed to a base-exchange phenomenon causing sodium hazards. Groundwater with high sodium content is not suitable for irrigation purposes. The concentration of potassium in the study area varies from 0.14 to 1323 mg/L with an average value of 75 mg/L during the pre-monsoon season, 0.2 to 1266 mg/L with an average value of 48 mg/L during the monsoon and 0 to 427 mg/L with an average value of 19 mg/L during the post-monsoon season of the year 2018.

The concentration of chloride in the study area varies from 135 to 8041 mg/L with an average value of 1819 mg/L during the pre-monsoon season, 13 to 14936 mg/L with an average value of 1909 mg/L during monsoon, and 150 to 11700 mg/L with an average value 2049 mg/L during the post-monsoon season of the year 2018. About 78%, 68%, and 72% of samples were found above the maximum permissible limit of 1000 mg/L in pre-monsoon, monsoon, and post-monsoon seasons respectively. And about 17%, 31%, and 21% of samples were found within the acceptable limit of 250 mg/L in the pre-monsoon, monsoon, and post-monsoon seasons of the year 2018 respectively.

The concentration of sulfate in the study area varies from 13 to 450 mg/L with an average value of 188 mg/L during the pre-monsoon season, 33 to 980 mg/L with an average value of 356 mg/L during monsoon, and 20 to 900 mg/L with an average value of 395 mg/L during the post-monsoon season in the year 2018. About 17%, 34%, and 51% of samples were found above the maximum permissible limit of 400 mg/L in pre-monsoon, monsoon, and post-monsoon seasons respectively. And about 17%, 34%, and 51% of samples were found within the acceptable limit of 200 mg/L in pre-monsoon, monsoon, and post-monsoon seasons in the year 2018 respectively.

The concentration of nitrate in the study area varies from 0.8 to 10.7 mg/L with an average value of 4.68 mg/L during the pre-monsoon season, 0.1 to 49.5 mg/L with an average value of 10 mg/L during monsoon, and 0.35 to 90 mg/L with average value 17 mg/L during the post-monsoon season in the year 2018. Almost all samples (more than 93%) of the study area fall within the permissible limit of 45 mg/L during all three seasons.

The concentration of fluoride in the study area varies from 0.12 to 2.82 mg/L with an average value of 0.91 mg/L during the pre-monsoon season, 0 to 12.7 mg/L with an average value of 1.21 mg/L during monsoon, and 0.1 to 8 mg/L with average value 2.35 mg/L during the post-monsoon season in the year 2018. About 13%, 14%, and 72% of samples were found above the maximum permissible limit of 1.5 mg/L in pre-monsoon, monsoon, and post-monsoon seasons respectively. And about 63%, 62%, and 24% of samples were found within the acceptable limit of 1 mg/L in pre-monsoon, monsoon, and post-monsoon seasons in the year 2018 respectively.

Table 5.3 Hydro-geochemical data of groundwater samples collected during pre-monsoon, monsoon, and post-monsoon seasons (2018)

Sr. no.	Parameters	Range			Average			BIS Limit	
		Pre	Monsoon	Post	Pre	Monsoon	Post	Acceptable	Permissible
1.	**pH**	6.94-8.93	7-8.3	7.1-8.4	7.95	7.55	7.61	6.5-8.5	No Relaxation
2.	**EC (S/cm)**	790-55300	628-51000	462-52400	9173	7345	7500	-	-
3.	**TDS (mg/L)**	442-37051	421-34170	309-35108	**6146**	**4921**	**5066**	500	2000
4.	**Hardness (mg/L)**	144-1590	200-7900	233-4187	**709**	**1611**	**1047**	200	600
5.	**Na (mg/L)**	2.4-10286	2.7-5168	0-5842	1298	643	487	-	-
6.	**K (mg/L)**	0.14-1323	0.2-1266	0-427	75	48	19	-	-
7.	**Ca (mg/L)**	50-1340	100-3080	167-1700	**333**	**683**	**552**	75	200
8.	**Mg (mg/L)**	6-880	10-5560	13-3020	**376**	**928**	**495**	30	100
9.	**HCO_3 (mg/L)**	35-540	104-670	122-552	273	313	244	-	-
10.	**Cl (mg/L)**	135-8041	13-14936	150-11700	**1819**	**1909**	**2049**	250	1000
11.	**SO_4 (mg/L)**	13-450	33-980	20-900	188	356	395	200	400
12.	**NO_3 (mg/L)**	0.8-10.7	0.1-49.5	0.35-90	5	10	17	45	No Relaxation
13.	**F (mg/L)**	0.12-2.82	0-12.7	0.1-8	0.9	1.21	**2.35**	1.0	1.5

5.4.1.1.2 Water quality evaluation for irrigation purposes

Water quality plays an important role in irrigated agriculture. Many problems arise during the inefficient management of water for agricultural use. The concentration and composition of dissolved constituents in water determine its quality for irrigation use. Quality of water is an important consideration in any appraisal of salinity or alkali conditions in an irrigated area. Under good soil and water management practices, good quality water can cause maximum yield. The quality of irrigation water is assessed by the following characteristics:

1. Salinity
2. The relative proportion of sodium to other cations (SAR)
3. Residual Sodium Carbonate (RSC)

Salinity

Salinity is expressed in terms of total dissolved solids (TDS) and thereby electrical conductivity (EC). If the salt concentration in water increases, the soil salinity also increases and it becomes difficult for plants to extract water. The salts present in water, besides affecting the growth of the plants directly, also affect the soil structure, permeability, and aeration, which indirectly affect plant growth. Soil water passes into the plant through the root zone due to osmotic pressure. As the dissolved solid content of the soil water in the root zone increases, it becomes difficult for the plant to overcome the osmotic pressure and the plant root membrane can assimilate water and nutrients. Thus, the dissolved solid content of the residual water in the root zone also has to be maintained within limits by proper leaching. The safe limits of electrical conductivity for crops of different degrees of salt tolerances under varying soil textures and drainage conditions are given in Table 5.4. The quality of water is commonly expressed by classes of relative suitability for irrigation with reference to salinity levels.

Table 5.4 Safe limits of electrical conductivity for irrigation water

S.No.	Nature of soil	Crop growth	The upper permissible safe limit of EC, µS/cm
1.	Deep black soil and alluvial soils having clay content of more than 30%, fairly to moderately well drained	Semi-tolerant	1500
		Tolerant	2000
2.	Having textured soils having clay contents of 20-30%, well-drained internally, and have a good surface drainage system	Semi-tolerant	2000
		Tolerant	4000
3.	Medium textured soils have clay content of 10-20%, are internally very well-drained, and have a good surface drainage system	Semi-tolerant	4000
		Tolerant	6000
4.	Light textured soils having clay content of less than 10%, excellent internally and surface drainage system	Semi-tolerant	6000
		Tolerant	8000

Sources: CGWB and CPCB (2000).

The relative proportion of sodium to other cations

The clay minerals in the soil absorb divalent cations, like calcium and magnesium ions from irrigation water. Whenever the exchange sites in clay are filled with divalent cations, the soil texture is conducive to plant growth. Sodium reacts with soil to reduce its permeability. The sodium or alkali hazard in the use of water for irrigation is determined by the absolute and relative concentration of cations and is expressed in terms of Sodium Adsorption Ratio (SAR). If the proportion of sodium is high, the alkali hazard is high; conversely, if calcium and magnesium predominate, the hazard is less. There is a significant relationship between the SAR values of irrigation water and the extent to which sodium is absorbed by the soil. If the water used for irrigation is high in sodium and low in calcium, the cation-exchange complex may become saturated with sodium. This can destroy the soil structure owing to the dispersion of the clay particles. A simple method of evaluating the danger of high-sodium water is the sodium-adsorption ratio, or SAR (Richards, 1954):

$$SAR = \frac{Na^{+}}{\sqrt{(Ca^{2+} + Mg^{2+})/2}} \quad \text{.....(5.1)}$$

The sodium percentage is calculated as:

$$Na\% = \frac{Na^{+} + K^{+}}{Ca^{2+} + Mg^{2+} + Na^{+} + K^{+}} \times 100 \quad \text{.....(5.2)}$$

where all ionic concentrations are expressed in milli equivalents per liter. Calculation of SAR for given water provides a useful index of the sodium hazard of that water for soils and crops. A low SAR (2 to 10) indicates little danger from sodium; medium hazards for SAR values between 7 and 18, high hazards between 11 and 26, and very high hazards above that. The lower the ionic strength of the solution, the greater the sodium hazard for a given SAR (Richards, 1954).

Residual Sodium Carbonate

Water containing a high concentration of carbonate and bicarbonate ions tends to precipitate calcium and magnesium as carbonate, changing the residual water to high sodium water with sodium bicarbonate in solution. As a result, the relative proportion of sodium increases and gets concentrated in the soil thereby decreasing the soil permeability. This excess is denoted by Residual Sodium Carbonate (RSC) and is determined by the following formula:

$$RSC = (HCO_3^{-} + CO_3^{--}) - (Ca^{++} + Mg^{++}) \quad \text{.....(5.3)}$$

Where all ionic concentrations are expressed in epm. If the RSC exceeds 2.5 epm, the water is generally unsuitable for irrigation. Excessive RSC causes the soil structure to deteriorate, as it restricts the water and air movement through the soil. If the value is between 1.25 and 2.5, the water is of marginal quality, while values less than 1.25 epm indicate that the water is safe for irrigation.

The values of SAR in the study area vary from 0.05 to 71.07 epm with an average value of 11.05 epm during the pre-monsoon season, 0 to 15.07 epm with an average value of 2.36 epm during monsoon, and 0.04 to 29.28 epm with average value 4.18 epm during the post-monsoon season in the year 2018. The percentage of sodium in the study area varies from 1.43 to 92.5 with an average value of 35.5 during the pre-monsoon season, 0.24 to 56.91 with an average value of 14.52 during monsoon, and 1.17 to 65.63 with an average value 21.56 during the post-monsoon season in the year 2018. Almost all samples have SAR values below 10 indicating excellent quality for irrigation purposes, except for only 9 samples that have more than 10. Almost all samples were observed to have an RSC value below 1.25 suggesting suitability for irrigation purposes. The recommended classification with respect to electrical conductivity, sodium content, Sodium Absorption Ratio (SAR), and Residual Sodium Carbonate (RSC) are given in Table 5.5.

Table 5.5 Guidelines for evaluation of irrigation water quality

Water class	Na, %	EC, µS/cm	SAR	RSC, meq/l
Excellent	< 20	< 250	< 10	< 1.25
Good	20-40	250-750	10-18	1.25-2.0
Medium	40-60	750-2250	18-26	2.0-2.5
Bad	60-80	2250-4000	> 26	2.5-3.0
Very bad	> 80	> 4000	> 26	> 3.0

Source: CGWB and CPCB (2000).

5.4.1.1.3 Classification of Groundwater for quality

Different accepted and widely used graphical methods such as Piper trilinear diagram and U.S. Salinity Laboratory classification have been used in the present study to classify the groundwater in the study area. Piper trilinear (Piper, 1944) is used to express similarity and dissimilarity in the chemistry of water based on major cations and anions. U.S. Salinity Laboratory classification (Wilcox, 1955) has been used to study the suitability of groundwater for irrigation purposes. In the classification of irrigation waters, it is assumed that the water will be used under average conditions with respect to soil texture, infiltration rate, drainage characteristics, quantity of water used, climate, and salt tolerance of crop.

Piper trilinear classification

Piper (1944) has developed a form of trilinear diagram, which is an effective tool in segregating analyzed data with respect to sources of the dissolved constituents in groundwater, modifications in the character of water as it passes through an area, and related geochemical problems. The diagram is useful in presenting graphically a group of

analyses on the same plot. The Piper trilinear diagram combines three areas of plotting, two triangular areas (cations and anions) and an intervening diamond-shaped area (combined field). Using this diagram, water can be classified into different hydro-chemical facies. In pre-monsoon and post-monsoon seasons, the piper trilinear diagram shows that groundwater is of Ca-Cl/ Ca-SO_4 type and Na-SO_4-Cl type (Fig 5.14 and Fig 5.16). In the monsoon season, groundwater in the study area is of Ca-HCO_3 type and Ca-Cl/ Ca-SO_4 type (Fig 5.15).

Durov trilinear plot

The important geochemical processes that play a great role in the chemistry of groundwater in the study area have been evaluated using the Durov trilinear plot (Fig 5.17- 5.19) for all three seasons during the 2018 year. Ion-exchange and dissolution processes control the hydrochemistry of the aquifer during all three seasons.

U. S. Salinity Laboratory Classification

Sodium concentration plays an important role in irrigation-water classification because sodium reacts with the soil to create sodium hazards by replacing other cations. The extent of this replacement is estimated by Sodium Adsorption Ratio (SAR). The U.S. Regional Salinity Laboratory has developed a diagram for use in studying the suitability of groundwater for irrigation purposes about sodium adsorption ratio (SAR) as an index for sodium hazard S and electrical conductivity (EC) of water expressed in µS/cm as an index of salinity hazard C.

The chemical analysis data of groundwater samples of the study area have been analyzed as per the U.S. Salinity Laboratory classification for the groundwater quality data (Fig 5.20 to Fig 5.22). It is evident from the results that the majority of groundwater samples of the study area fall under water types C4-S1 followed by C3-S1 in pre-monsoon, monsoon, and post-monsoon seasons. C4-S1 water type (high salinity and low SAR) cannot be used directly on soils that have poor drainage. Moreover, even with adequate drainage special management for salinity control may be required and only salt-tolerant species are suitable for this type of water. The C3-S1 type water (medium salinity and low SAR) can be used if a moderate amount of leaching occurs. Plants with moderate salt tolerance can be grown in most cases without special practices for salinity control.

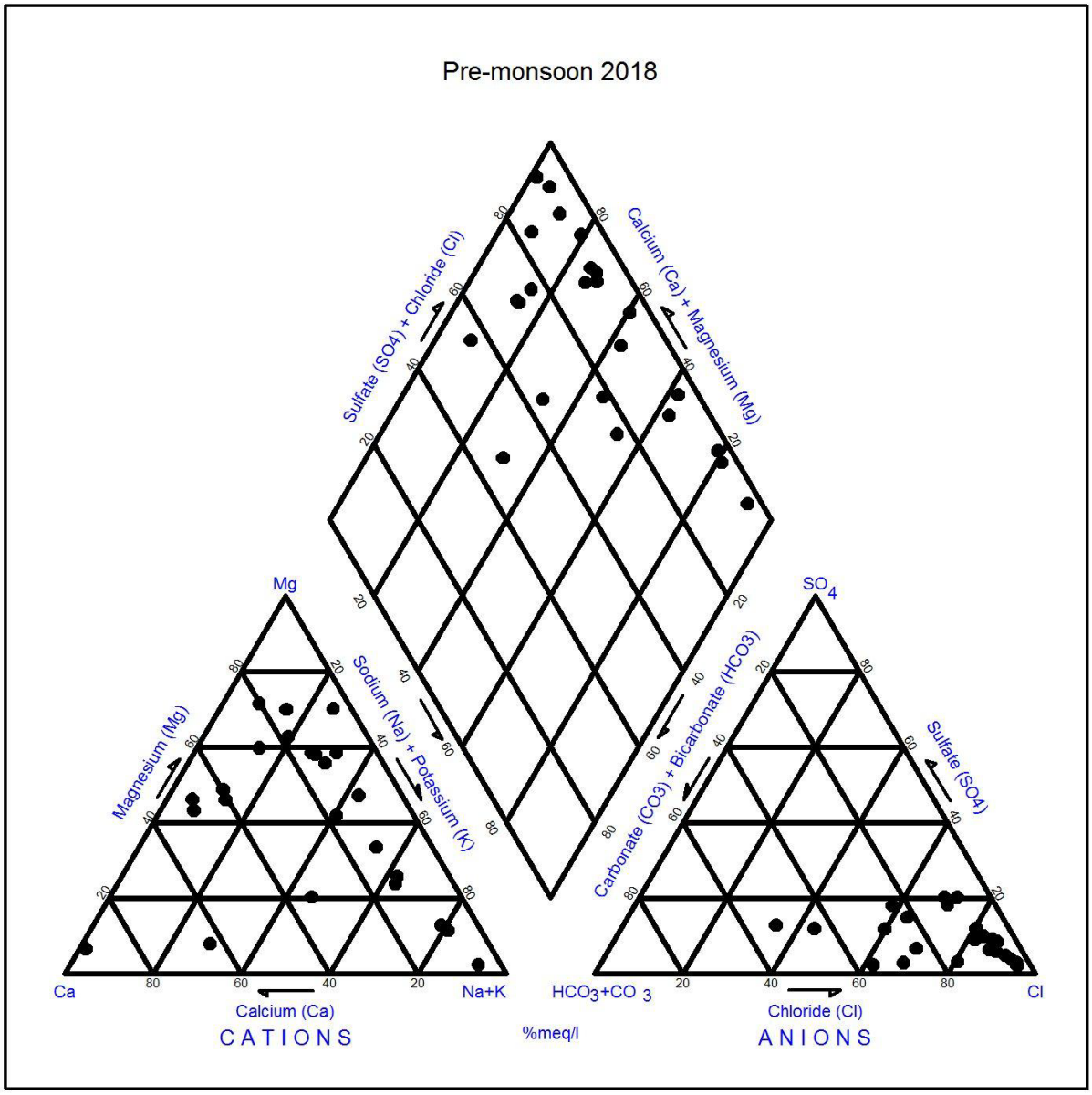

Fig 5.14 Piper trilinear diagram (Pre-monsoon 2018)

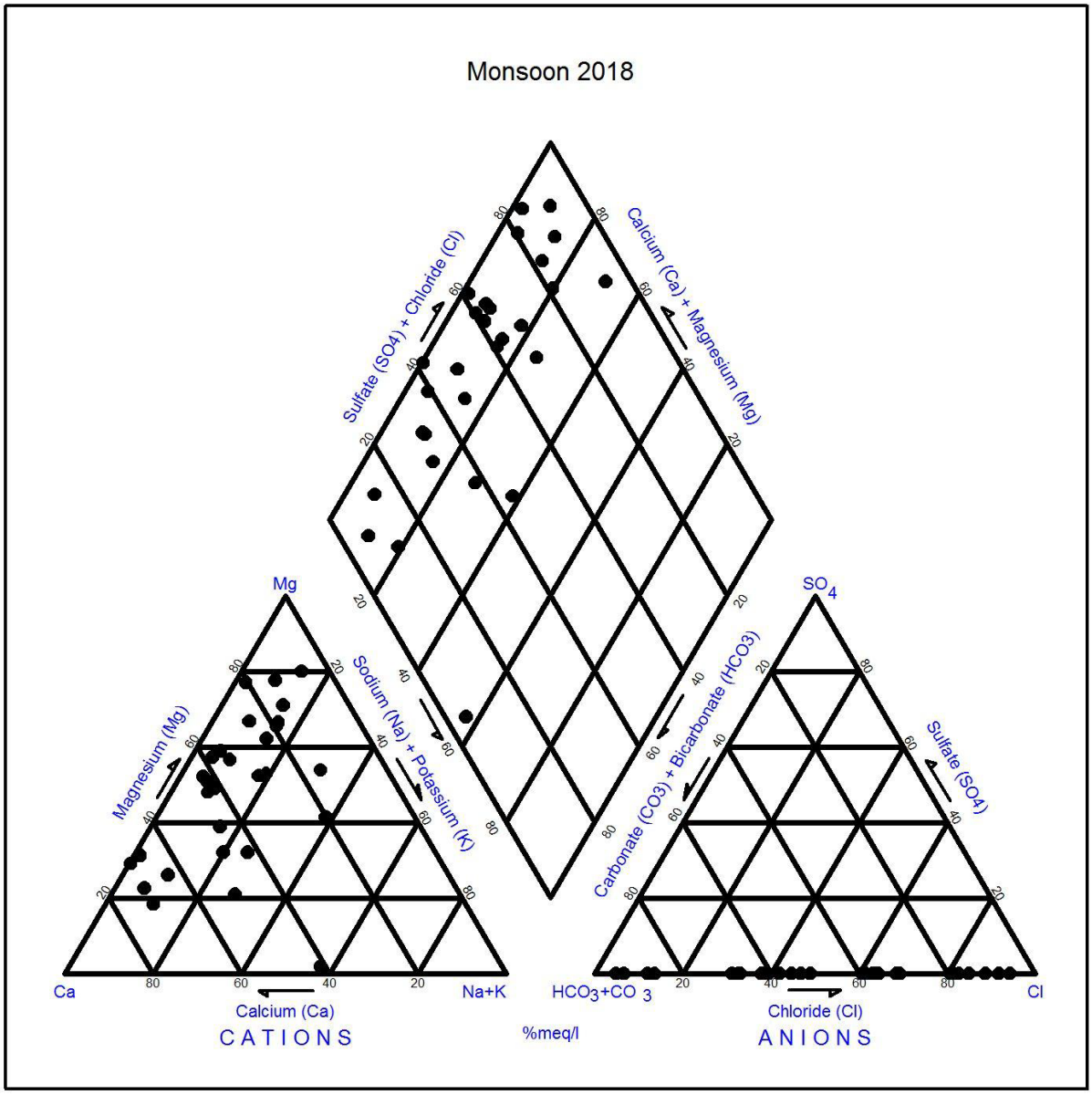

Fig 5.15 Piper trilinear diagram (Monsoon 2018)

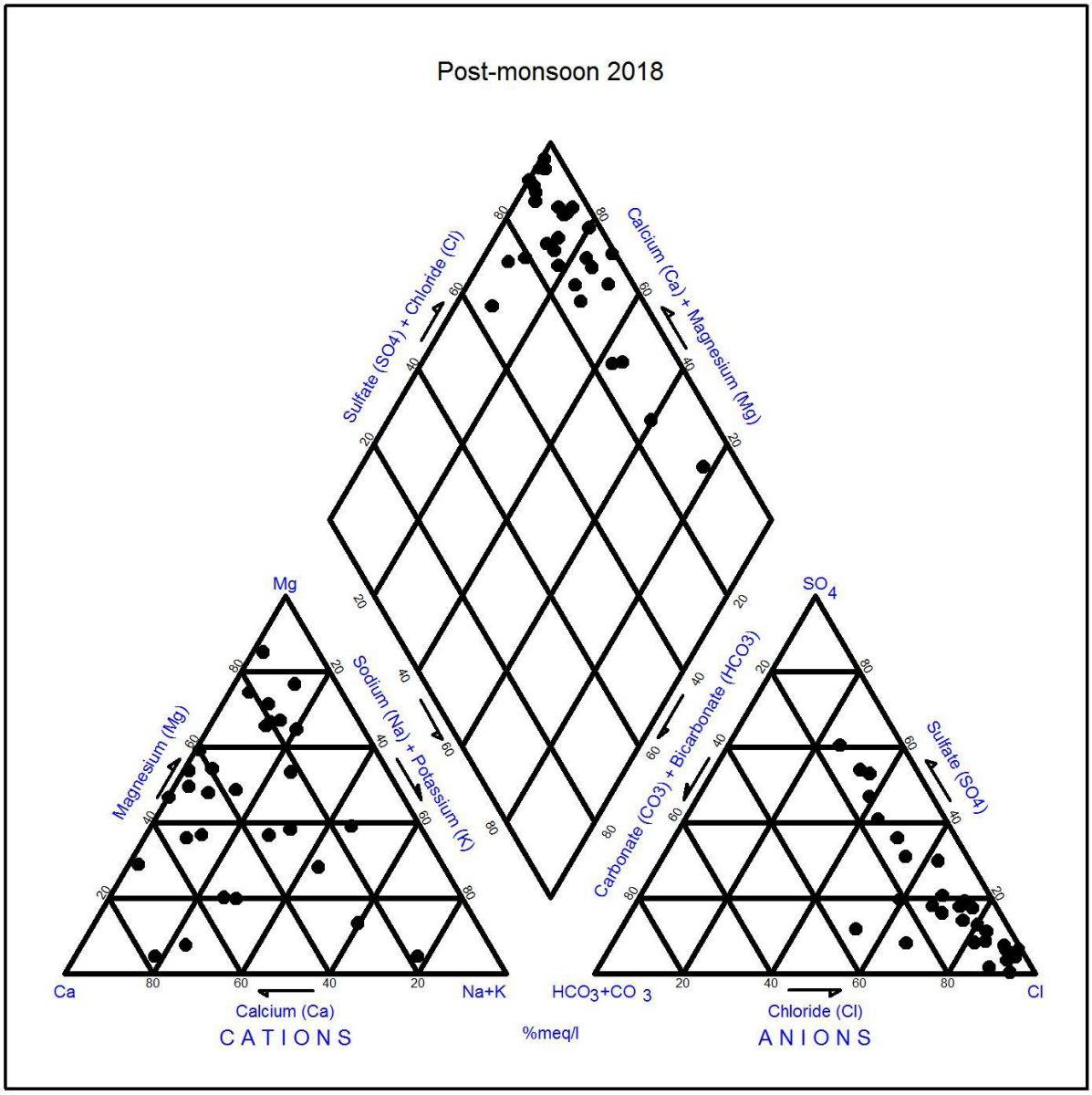

Fig 5.16 Piper trilinear diagram (Post-monsoon 2018)

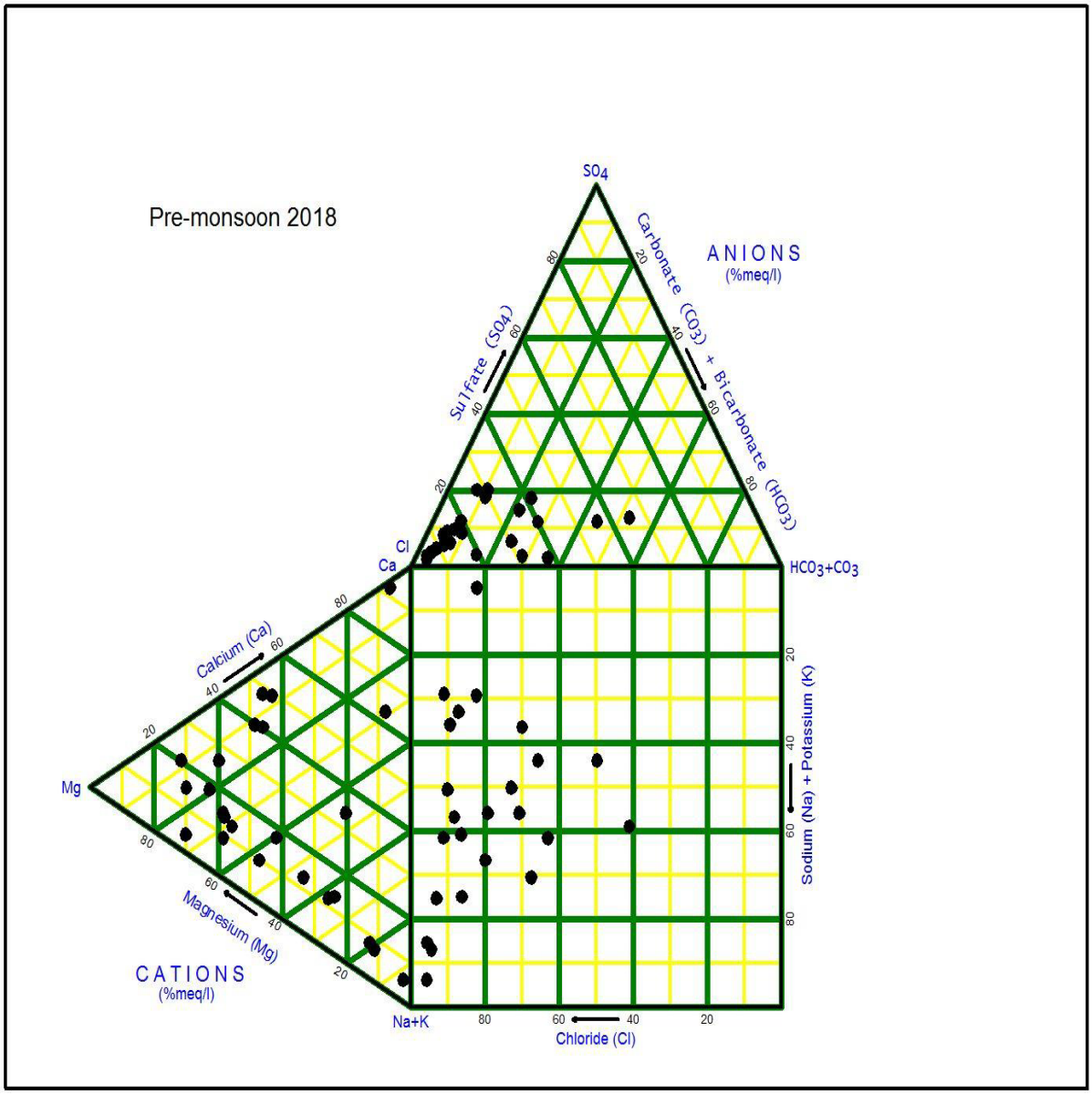

Fig 5.17 Trilinear Durov plot diagram (Pre-monsoon 2018)

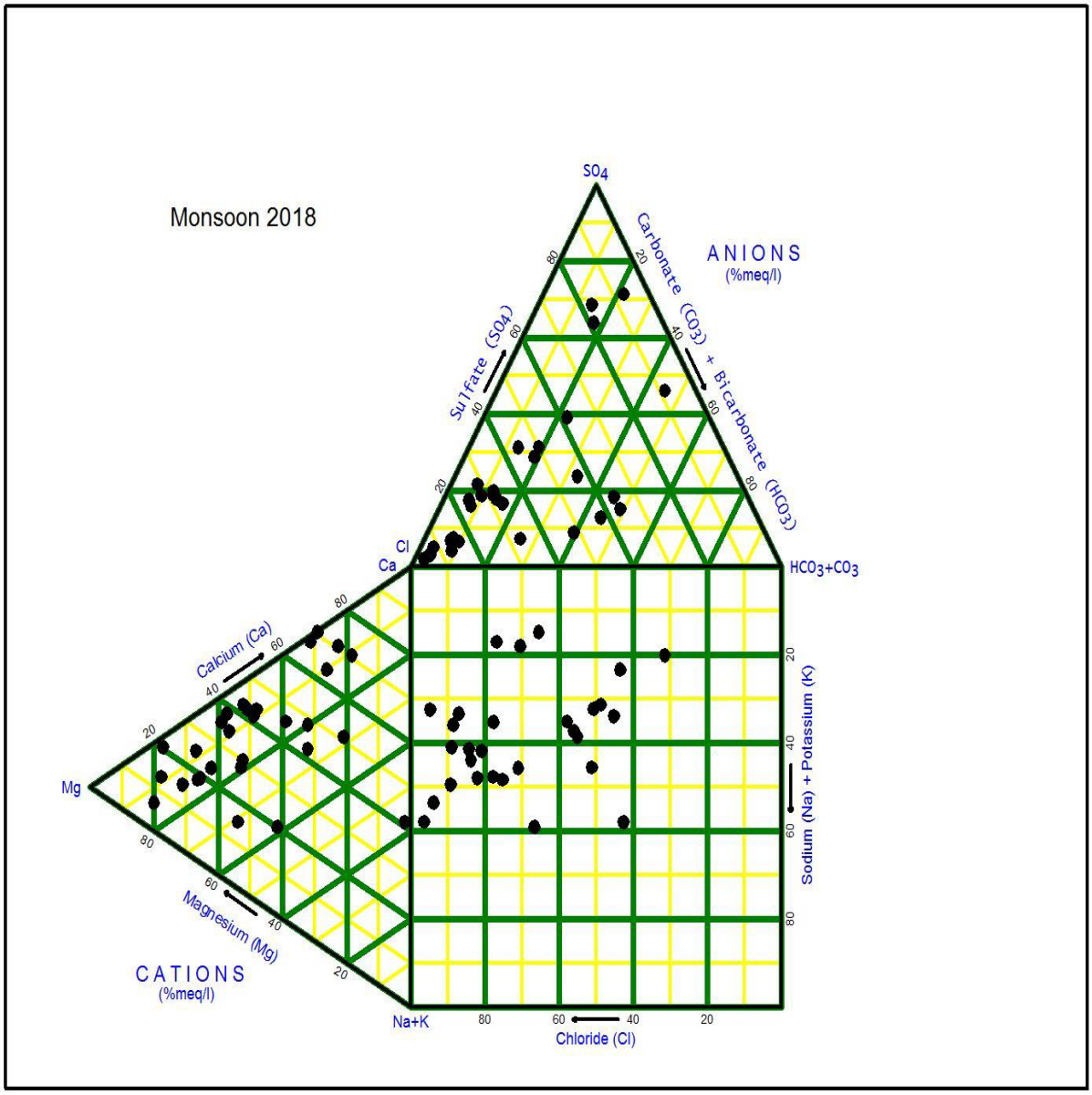

Fig 5.18 Trilinear Durov plot diagram (Monsoon 2018)

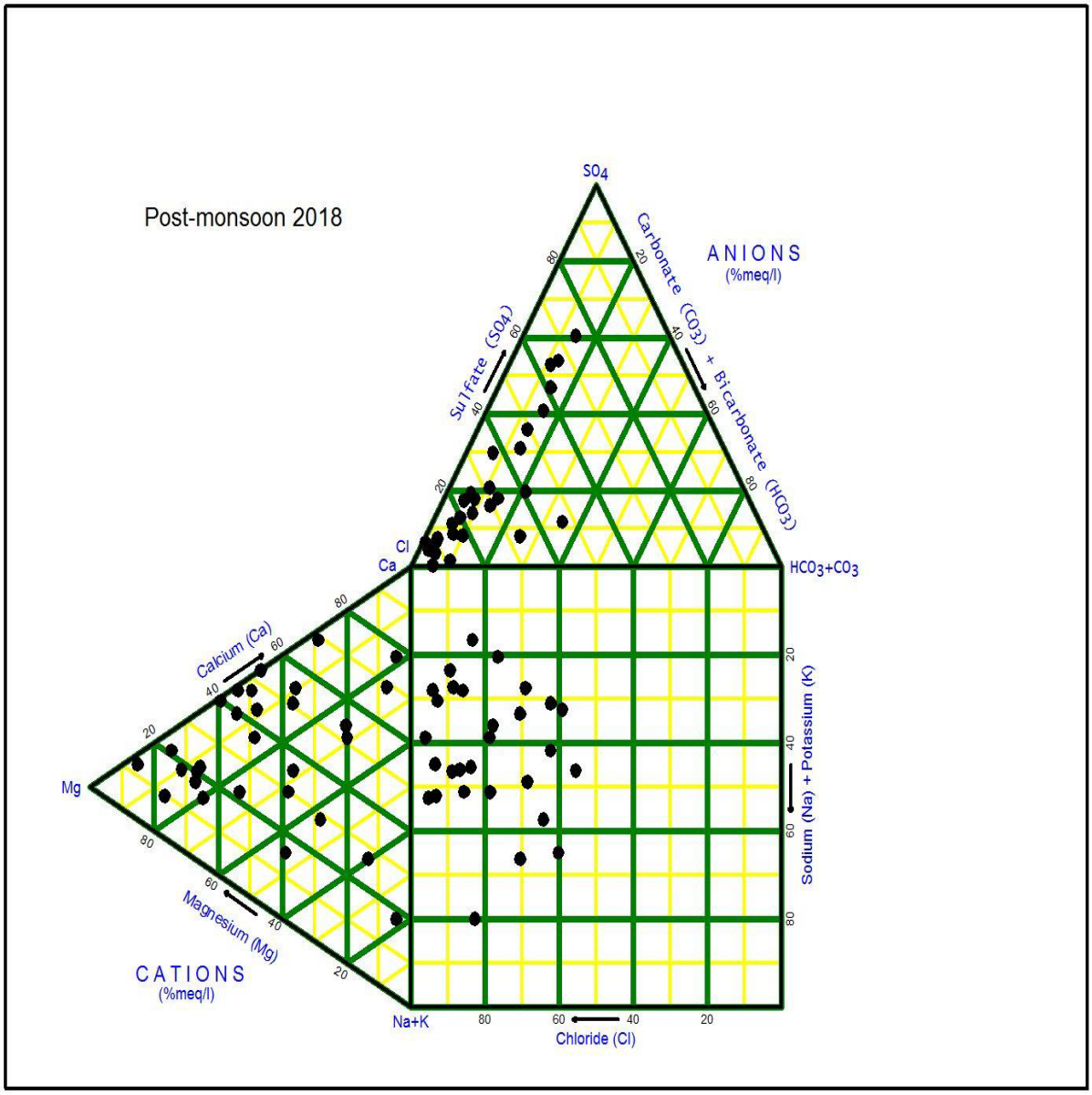

Fig 5.19 Trilinear Durov plot diagram (Post-monsoon 2018)

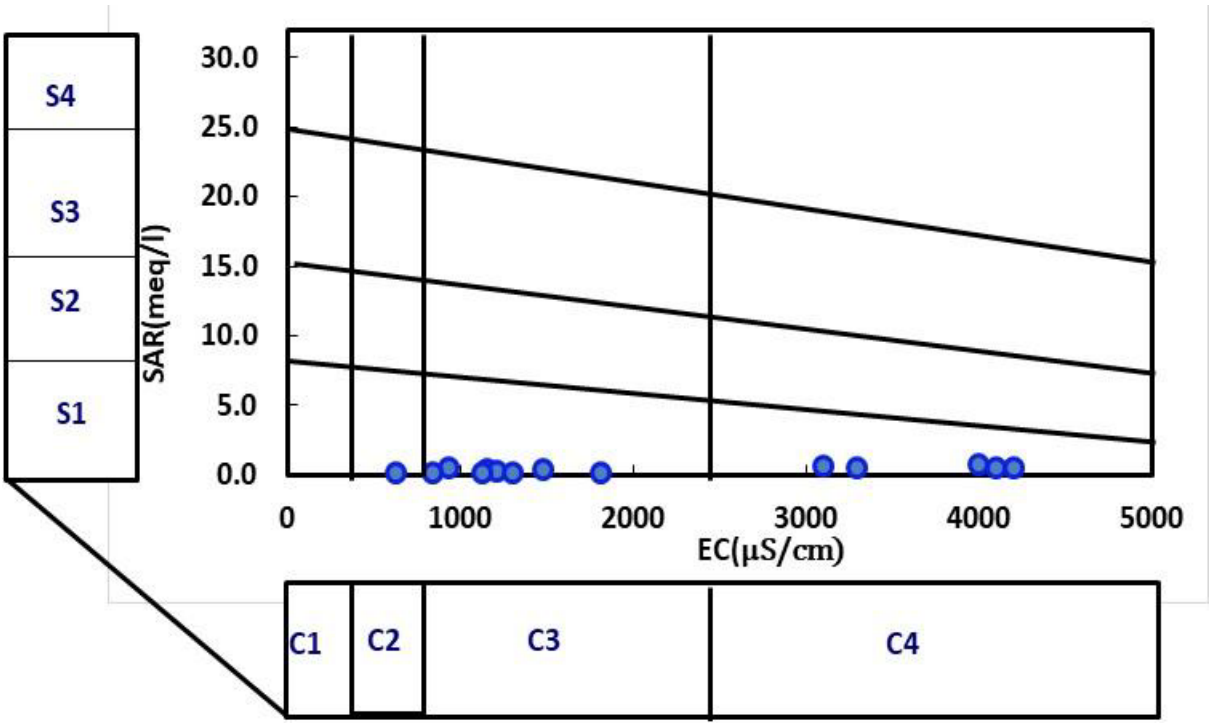

Fig 5.20 U.S. Salinity Laboratory classification (Pre-monsoon 2018)

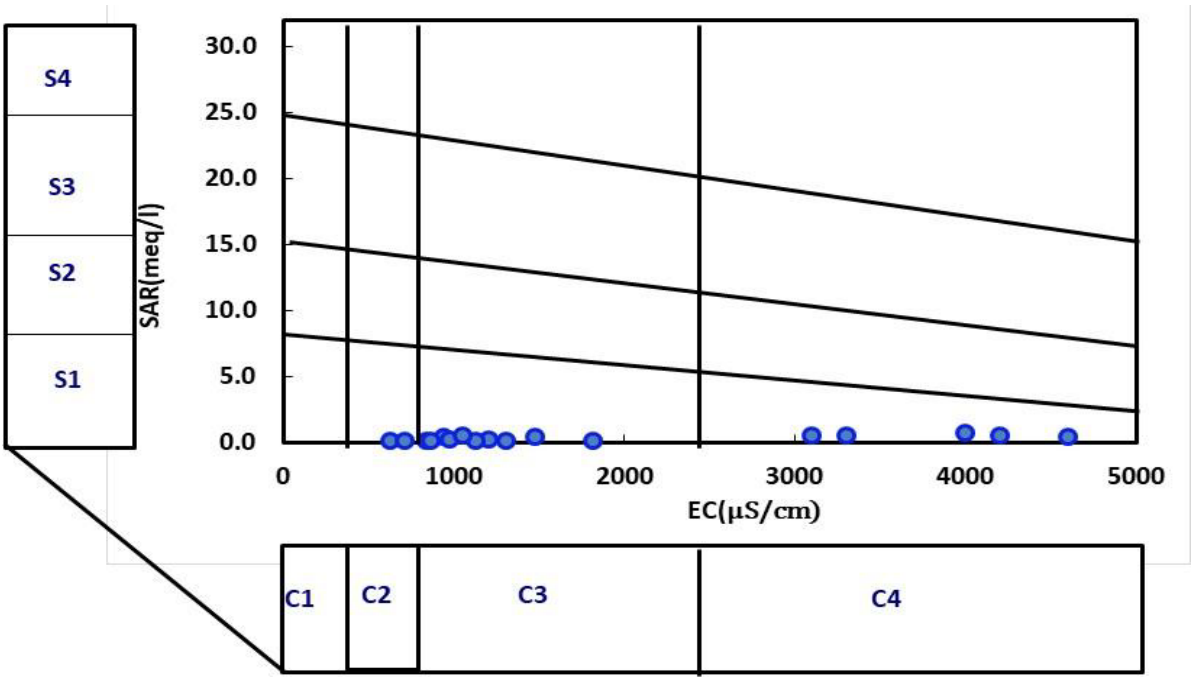

Fig 5.21 U.S. Salinity Laboratory classification (Monsoon 2018)

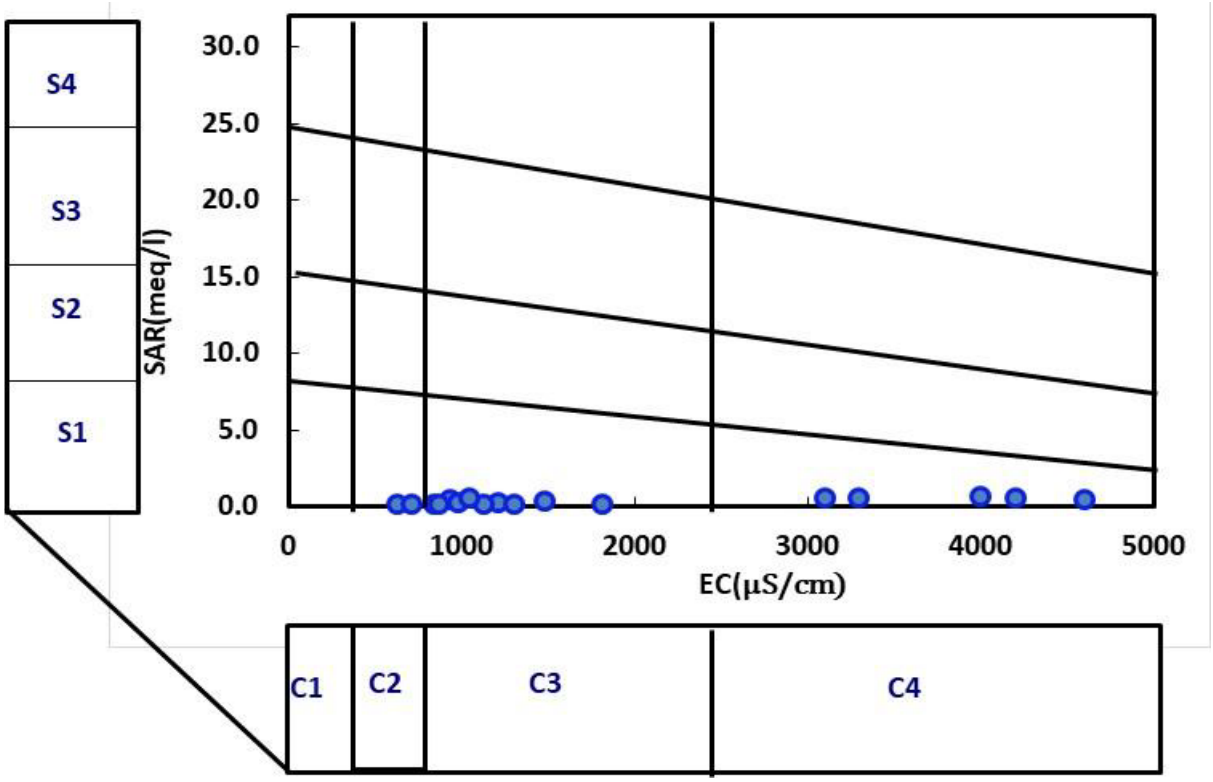

Fig 5.22 U.S. Salinity Laboratory classification (Post-monsoon 2018)

Gibbs diagram

Geo-environmental conditions have a marked influence on groundwater quality. Hydro-geochemical studies relevant to water quality explain the relationship of water chemistry to aquifer lithology. Such a relationship would help not only to explain the origin and distribution of dissolved constituents but also to elucidate the factors controlling the groundwater chemistry. Gibbs (1970) proposed a hypothesis to elucidate the major natural mechanisms controlling world water chemistry. Three mechanisms – atmospheric precipitation, rock dominance, and the evaporation-crystallization process – are the major factors controlling the composition of dissolved salts in world waters. The plot (Fig 5.23) shows the chemical weathering of rocks to form minerals as the major reason governing the groundwater chemistry in the study area.

Scattered plots for pre-monsoon 2018

The bivariate plot of $Ca^{2+}+Mg^{2+}$ vs $HCO_3^{-}+SO_4^{2-}$ is used to identify the parent rock responsible for the ion exchange process in the groundwater system (Maurya et al., 2019; Srinivasamoorthy et al., 2008). Most of the points for the present study are found to be above equiline (1:1), which indicates that carbonate weathering is the primary process of ion exchange. An area rich in feldspars and kankars (calcium-rich encrustations) reacts with carbonic acid that may contribute to these ions namely, Ca^{2+}, Na^{+} , HCO_3^{-} and H_4SiO_4 in groundwater (Guo and Wang, 2005). The scattered plot of Ca^{2+} + Mg^{2+} vs TZ^{+} (Total

cations) shows that almost all the water samples of the study area are above the equiline line (1:1), resulting in the weathering of carbonate minerals (Fig 5.24). Similarly, the relationship between $Na^+ + K^+$ vs TZ^+(Fig 5.24) shows that most of the samples are plotted well below the 1:1 equiline. This suggests that silicate weathering and anthropogenic inputs in soil salts contribute mainly Na^+ and K^+ ions to the water system (Stallard and Edmond 1983; Sarin et al., 1989; Datta and Tyagi, 1996).

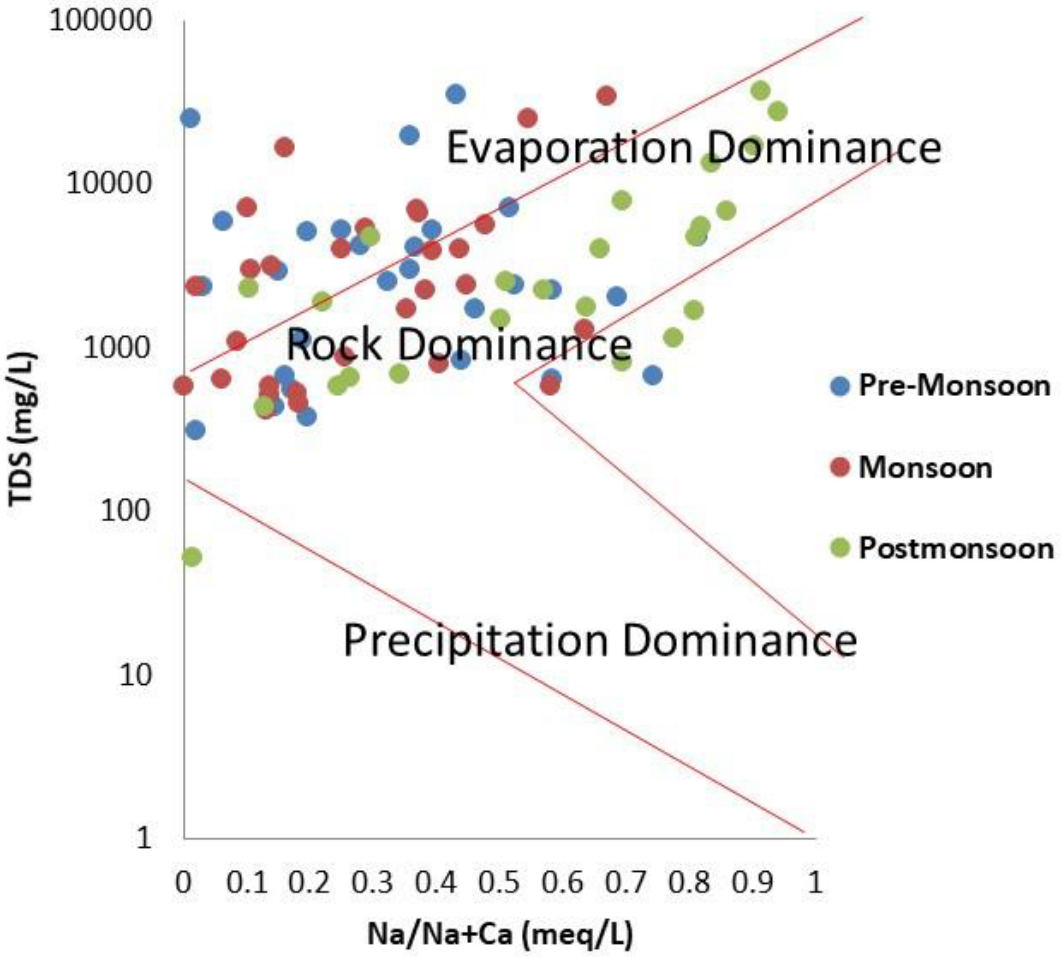

Fig 5.23 Gibbs plot showing mechanism controlling the chemistry of groundwater during the year 2018

The Na^+ vs Cl^- plot lie above the equiline (1:1) and it suggested that besides some silicate weathering Na^+ may be attributed to some anthropogenic sources such as sewage, and domestic and animal waste. The dominance of Cl^- over Na^+ indicates aquifer contamination by anthropogenic activities. The higher content of Cl^- in the groundwater may be attributed to the discharges of the untreated municipal and industrial effluents and leakage from the septic tanks.

The Na^+/Cl^- molar ratio was used to the identification of the source of salinity in groundwater. If this ratio is equal to 1, then the source of Na^+ is due to halite dissolution and if the ratio is greater than 1, then the source is silicate weathering (Meybeck 1987). Fig 5.25, it is showing that most of the samples are below the ratio of 1 and only 7 samples have a value greater than 1, indicating the silicate weathering was the source of Na^+ in the groundwater of Mewat.

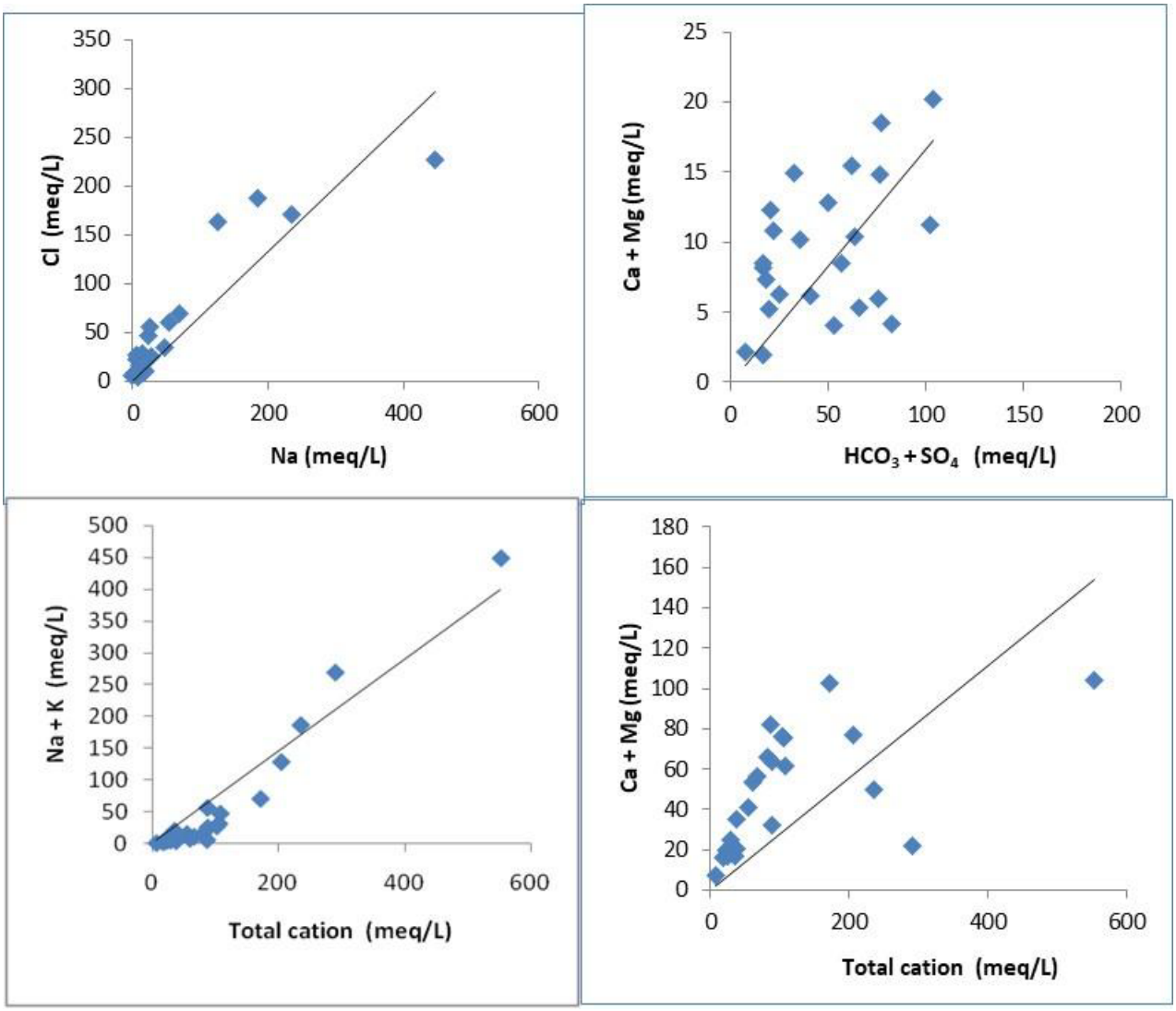

.Fig 5.24 Scattered plots of pre-monsoon 2018

The ratio of SO_4^{2-}/Cl^- ions was used as a marker to identify the potential pyrite dissolution in groundwater. SO_4^{2-}/Cl^- a ratio of more than 0.5, indicates pyrite oxidation **(**Okiongbo and Douglas 2015**)**. SO_4^{2-}/Cl^- ratio indicates that all points fall below 0.5, which confirmed that there is no pyrite oxidation in the aquifer (Fig 5.25). The ca/Mg ratio is also derived to evaluate the influence of carbonate and silicate weathering on groundwater chemistry. The Ca/Mg ratio equal to one indicates the dissolution of dolomite, while the ratio of more than one depicts the sources of these ions from the dissolution of calcite rocks (Mayo and

Loucks 1995). Ca/Mg >2 represents the dissolution of silicate minerals in the groundwater (Katz et al., 1997). Most of the points lie below 1 suggests that there is carbonate weathering in the groundwater of the study area (Fig 5.25).

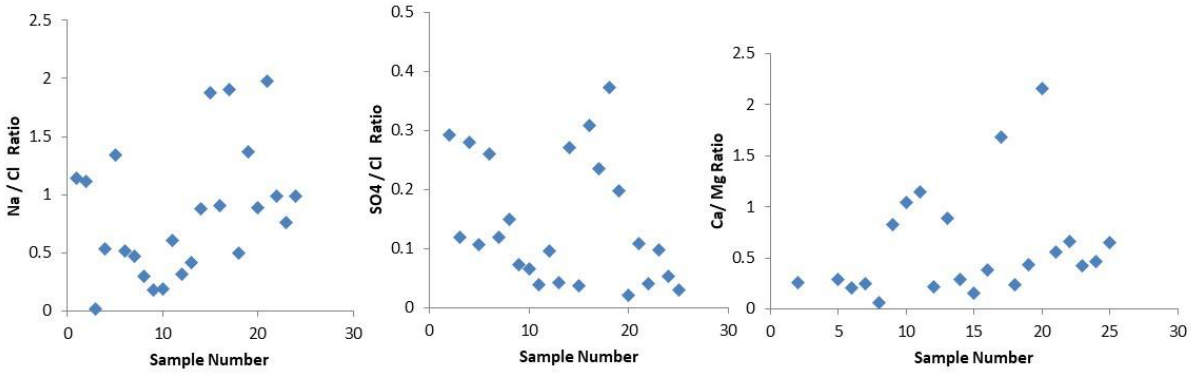

Fig 5.25 Ratio vs sample number during the pre-monsoon 2018

Scattered plots for monsoon 2018

Most of the points in the bivariate plot of $Ca^{2+}+Mg^{2+}$ vs $HCO_3^{-}+SO_4^{2-}$ are above equiline (1:1), which indicates that carbonate weathering is the primary process of ion exchange. The scattered plots of $Ca^{2+}+Mg^{2+}$ vs TZ^{+} (Total cations) show that almost all the water samples of the study area are above the equiline line (1:1), resulting in the weathering of carbonate minerals. Similarly, the relationship between $Na^{+}+ K^{+}$ vs TZ^{+} shows that most of the samples are plotted below the 1:1 equiline. This suggests that silicate weathering and anthropogenic inputs in soil salts contribute mainly Na^{+} and K^{+} ions to the water system (Fig 5.26).

The Na^{+} vs Cl^{-} plot lies above the equiline (1:1) and it suggested that besides some silicate weathering, Na^{+} may be attributed to some anthropogenic sources such as sewage, and domestic and animal waste (Fig 5.26). The dominance of Cl^{-} over the Na^{+} indicates aquifer contamination by anthropogenic activities. The higher content of Cl^{-} in the groundwater may be attributed to the discharges of the untreated municipal and industrial effluents and leakage from the septic tanks.

The Na^{+}/Cl^{-} molar ratio was used to identify the source of salinity in groundwater. In fig 5.27, it is clearly shown that most of the samples are below the ratio of one, and only six samples have a value greater than 1, indicating the silicate weathering was the source of Na^{+} in the groundwater of Mewat.

The ratio SO_4^{2-}/Cl^{-} ions ratio was used as a marker to identify the potential pyrite dissolution in groundwater. SO_4^{2-}/Cl^{-} the ratio of more than 0.5 indicates pyrite oxidation (Okiongbo and Douglas, 2015). SO_4^{2-}/Cl^{-} ratios indicate that all points fall below 0.5, which confirms no pyrite oxidation in the aquifer (Fig 5.27).

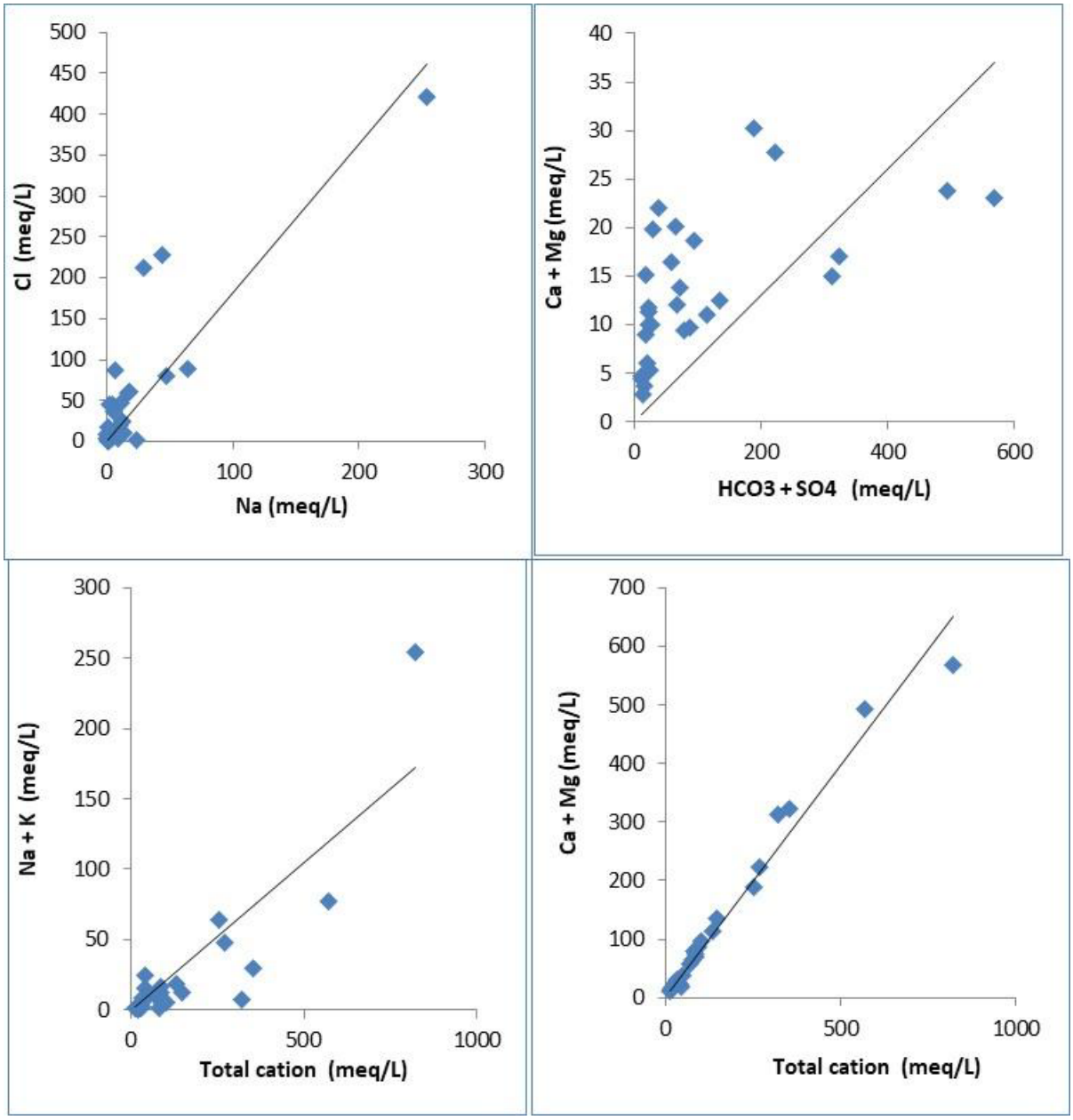

Fig 5.26 Scattered plots of monsoon 2018

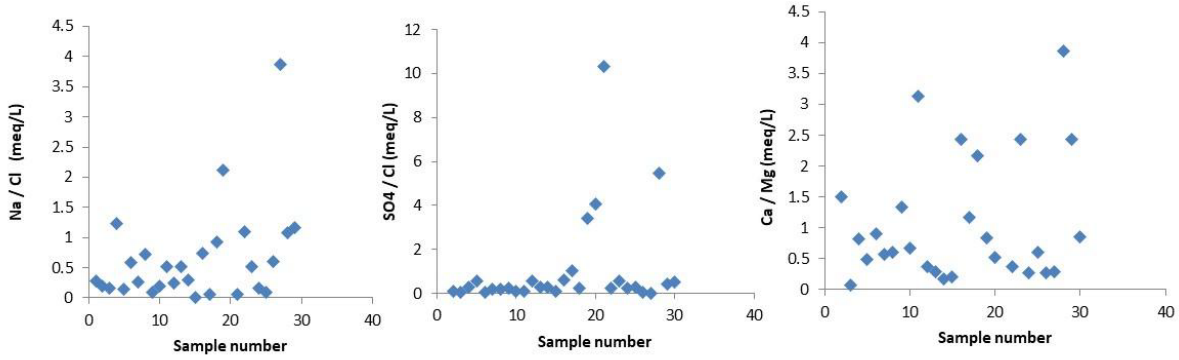

Fig 5.27 Ratio vs sample number during the monsoon 2018

The $Ca^{2+/}Mg^{2+}$ ratio is also derived to evaluate the influence of carbonate and silicate weathering on groundwater chemistry. The $Ca^{2+/}Mg^{2+}$ ratio equal to 1 indicates the dissolution of dolomite, while the ratio of more than 1 depicts the sources of these ions from the dissolution of calcite rocks (Mayo and Loucks 1995). Ca/Mg >2 represents the dissolution of silicate minerals in the groundwater (Katz et al., 1997). Most of the points lie below one suggests that there is carbonate weathering in the groundwater of the study area (Fig 5.27).

Scattered plots for post-monsoon 2018

Most of the points in the bivariate plot of $Ca^{2+}+Mg^{2+}$ vs TZ^{+} (Total cations) show that almost all the water samples of the study area are above the equiline line (1:1), which indicates that carbonate weathering as the primary process of ion exchange (Fig. 5.28).
The scatter plots of $Ca^{2+}+Mg^{2+}$ vs TZ^{+} (Total cations) show that almost all the water samples of the study area are above the equiline line (1:1), resulting in the weathering of carbonate minerals. Similarly, the relationship between $Na^{+}+ K^{+}$ vs TZ^{+} shows that the samples are plotted below the 1:1 equiline. This suggests that silicate weathering and anthropogenic inputs in soil salts contribute mainly Na^{+} and K^{+} ions to the water system (Fig 5.28).

The Na^{+} vs Cl^{-} plot lie above the equiline (1:1) and it suggested that besides some silicate weathering Na^{+} may be attributed to some anthropogenic sources such as sewage, domestic and animal waste (Fig 5.28). The dominance of Cl^{-} over the Na^{+} indicates aquifer contamination by anthropogenic activities. The higher content of Cl^{-} in the groundwater may be attributed to the discharges of the untreated municipal and industrial effluents and leakage from the septic tanks.

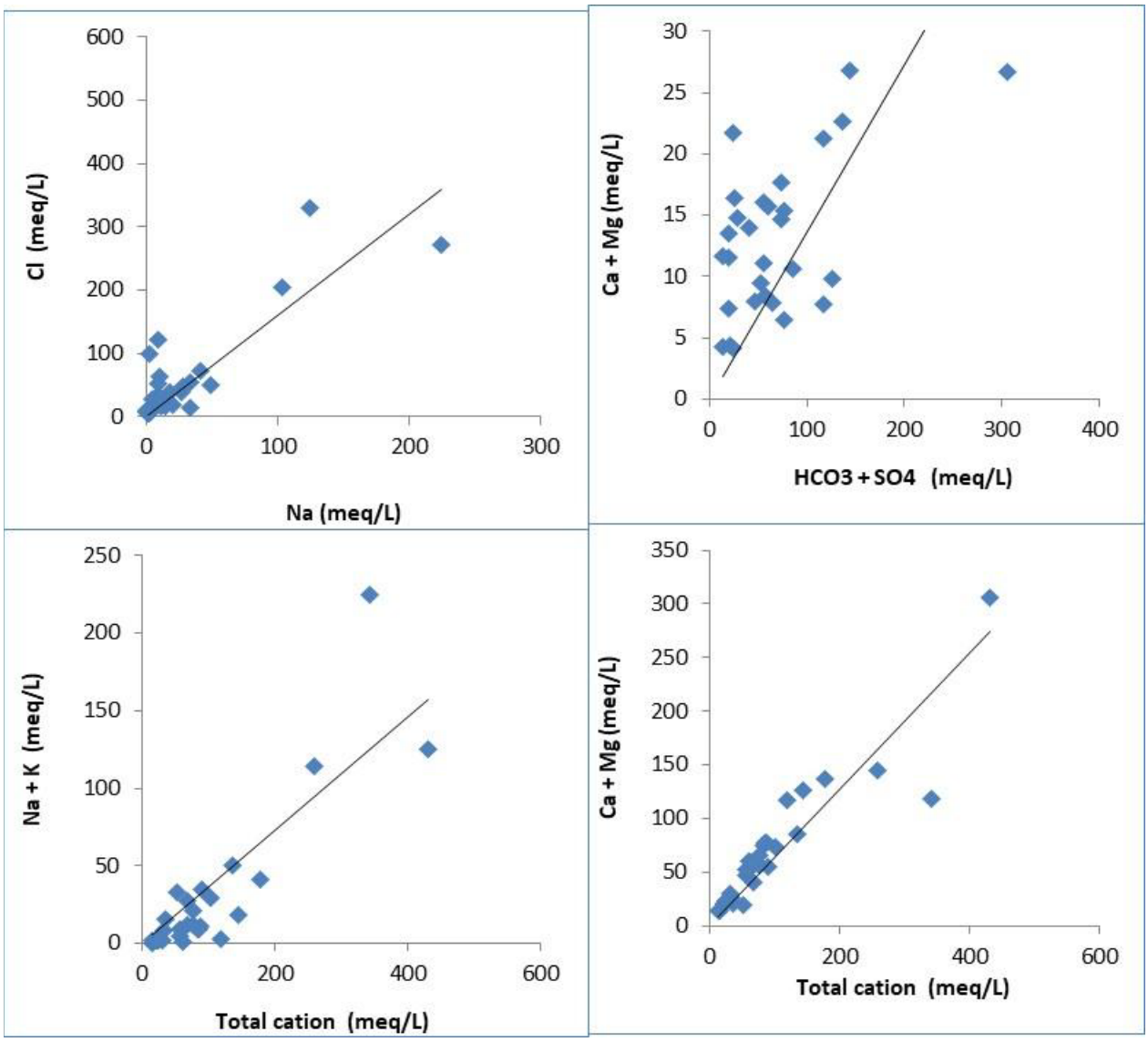

Fig 5.28 Scattered plots of post-monsoon 2018

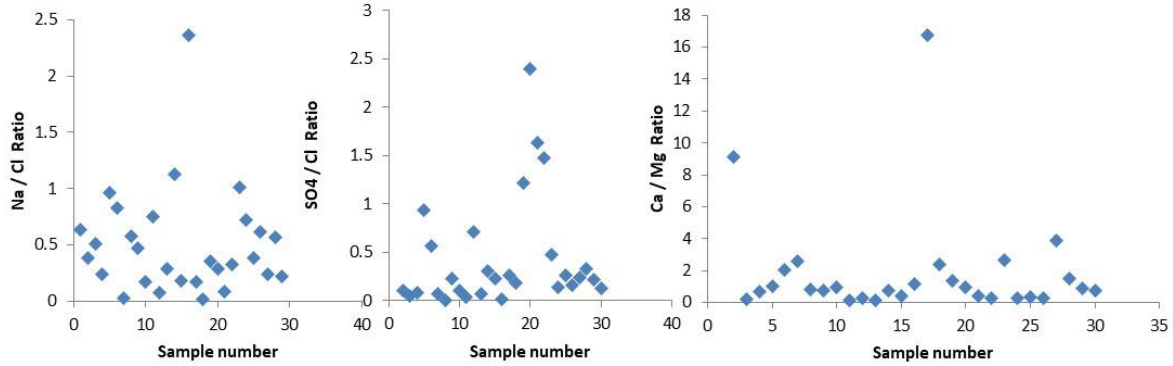

Fig 5.29 Ratio vs sample number during the post-monsoon 2018

The Na^+/Cl^- molar ratio was used to the identification of the source of salinity in groundwater. Fig 5.27, it is clearly showing that most of the samples are below the ratio of one and only4 samples have values greater than 1, indicating the silicate weathering was the source of Na^+ in the groundwater of Mewat.

The ratio of SO_4^{2-}/Cl^- ions ratio was used as a marker to identify the potential pyrite dissolution in groundwater. SO_4^{2-}/Cl^- the ratio of more than 0.5, indicates pyrite oxidation. SO_4^{2-}/Cl^- ratios computed for the present study indicate that all points fall below 0.5 which confirms that there is no pyrite oxidation in the aquifer (Fig 5.29).

The $Ca^{2+/}Mg^{2+}$ ratio is also derived to evaluate the influence of carbonate and silicate weathering on groundwater chemistry. The $Ca^{2+/}Mg^{2+}$ ratio equal to 1 indicates the dissolution of dolomite, while the ratio of more than 1 depicts the sources of these ions from the dissolution of calcite rocks (Mayo and Loucks 1995). Ca/Mg >2 represents the dissolution of silicate minerals in the groundwater (Katz et al., 1997). Most of the points lie below one suggests that there is carbonate weathering in the groundwater of the study area (Fig 5.29).

5.4.2 Analysis for the year 2019

A total of 50 groundwater samples in each of the selected sites were collected from pre-monsoon (April), monsoon (July), and post-monsoon seasons (October) in 2019 from hand pumps, open wells, and bore wells (fig 4.4) with a depth range of 4-92 m. The water level in the open well (meters) was recorded using a water level indicator. GPS readings were taken for recording latitude and longitude. For each sampling site, samples were taken in 125 ml capacity acid-washed LDPE (Low-Density Polyethylene) tarson bottles. Electrical Conductivity (EC) and pH were measured using a portable hand-held Hach, HQ30d EC meter, and total dissolved solids (TDS) were estimated from measured EC values and expressed in mg/L. The samples collected in 125 ml bottles were analyzed for cations (Ca^{2+}, Mg^{2+}, Na^+) and anions (HCO_3^-, SO_4^{2-}, Cl^-) in the water quality laboratory of the groundwater hydrology division of NIH as per standard methodology.
The unpreserved 0.45µm filtered water samples were used for the analysis of cations (Ca^{2+}, Mg^{2+}, Na^+) and anions (HCO_3^-, SO_4^{2-}, Cl^-). Ca^{2+} and Mg^{2+} were determined titrimetrically using standard EDTA. Cl^- was determined by the standard $AgNO_3$ titration method. HCO_3^- was determined by titration with H_2SO_4. Na^+ was measured by flame photometry at a wavelength of 589 nm, and SO_4^{2-} by spectrophotometric turbidimetry by HACH spectrophotometer. All concentrations are expressed in milligrams per liter (mg/L).

5.4.2.1 Water Quality Evaluation for Drinking Purpose

5.4.2.1.1 General Characteristics

The general characteristics of the hydro-geochemical analysis for the pre-monsoon, monsoon, and post-monsoon seasons (2019) are given in Table 5.6.

The pH values in the groundwater of the study area mostly fall within a range of 6.8 to 9.0 during the pre-monsoon season, 6.9 to 8.6 during the monsoon season, and 6.6 to 8.4 during the post-monsoon in the year 2019. The pH values for most of the samples are well within limits prescribed by BIS (2012) and WHO (1996) for various uses of water, including drinking and other domestic supplies.

In the study area, the values of total dissolved solids (TDS) in the groundwater vary from 243 to 36582 mg/L with an average value of 4435 mg/L during the pre-monsoon season, 504-43820 mg/L with an average value of 4482 mg/L during monsoon and 409 to 39845 mg/L with average value 4938 mg/L during the post-monsoon season in the year 2019. About 54%, 62%, and 58% of samples were found above the maximum permissible limit of 2000 mg/L in pre-monsoon, monsoon, and post-monsoon seasons. And about 8%, 0%, and 4% samples were found within the acceptable limit of 500 mg/L in pre-monsoon, monsoon, and post-monsoon seasons in 2019. Water containing more than 500 mg/L of TDS is not considered desirable for drinking water supplies, though more highly mineralized water is also used where better water is not available. For this reason, 500 mg/L as the acceptable limit and 2000 mg/L as the maximum permissible limit have been suggested for drinking water (BIS, 2012).

Alkalinity in natural water is mainly due to carbonates, bicarbonates, and hydroxides. Alkalinity as bicarbonate in the ground water varies from 99 to 692 mg/L with an average value of 322 mg/L during the pre-monsoon season, 14 to 790 mg/L with an average value of 274 mg/L during monsoon, and 43 to 645 mg/L with average value 334 mg/L during the post-monsoon season in the year 2019. About 2%, 6%, and 4% samples were found above the maximum permissible limit of 600 mg/L in pre-monsoon, monsoon, and post-monsoon seasons. And about 26%, 34%, and 18% of samples were found within the acceptable limit of 200 mg/L in pre-monsoon, monsoon, and post-monsoon seasons in 2019, respectively. The presence of calcium and magnesium and their carbonates, sulfates, and chlorides are the main cause of hardness in the water. A limit of 200 mg/L as an acceptable limit and 600 mg/L as a permissible limit has been recommended for drinking water (BIS, 2012). Hardness in the ground water varies from 120 to 3767 mg/L with an average of 856 mg/L during the pre-monsoon season, 123 to 11120 mg/L with an average value of 1300 mg/L during monsoon and 96 to 1017 mg/L with an average value 392 mg/L during the post-monsoon season in the year 2019. About 58%, 46%, and 16% of samples were found above the maximum permissible limit of 600 mg/L in pre-monsoon, monsoon, and post-monsoon seasons. And about 8%, 10%, and 16% of samples were found within the acceptable limit of 200 mg/L in pre-monsoon, monsoon, and post-monsoon seasons in 2019 respectively.

In the groundwater of the study area, the values of calcium range from 60 to 3292 mg/L with an average value of 465 mg/L during the pre-monsoon season, 14 to 2240 mg/L with an average value of 369 mg/L during monsoon, and 16 to 515 mg/L with average value 138 mg/L during the post-monsoon season in the year 2019. About 74%, 38%, and 20% of samples were found above the maximum permissible limit of 200 mg/L in pre-monsoon, monsoon, and post-monsoon seasons respectively. And about 2%, 14%, and 30% of samples were found within the acceptable limit of 75 mg/L in pre-monsoon, monsoon, and post-monsoon seasons in the year 2019 respectively. For magnesium, a limit of 30 mg/L

as an acceptable limit and 100 mg/L as a permissible limit has been recommended for drinking water (BIS, 2012). In groundwater of the study area, the values of magnesium range from 0 to 3010 mg/L with an average value of 390 mg/L during the pre-monsoon season, 14 to 2240 mg/L with an average value of 369 mg/L during monsoon, and 22 to 679 mg/L with an average value 254 mg/L during the post-monsoon season in the year 2019. About 68%, 90%, and 20% of samples were found above the maximum permissible limit of 100 mg/L in pre-monsoon, monsoon, and post-monsoon seasons respectively. And about 8%, 2%, and 30% of samples were found within the acceptable limit of 30 mg/L in pre-monsoon, monsoon, and post-monsoon seasons in the year 2019 respectively. In groundwater, the calcium content generally exceeds the magnesium content in accordance with their relative abundance in rocks.

The concentration of sodium in the study area varies from 12 to 11635 mg/L with an average value of 936 mg/L during the pre-monsoon season, 3 to 448 mg/L with an average value of 61 mg/L during monsoon, and 4 to 557 mg/L with an average value 84 mg/L during the post-monsoon season in the year 2019. The high sodium values in the study area may be attributed to the base-exchange phenomenon causing sodium hazards. Groundwater with high sodium content is not suitable for irrigation purposes. The concentration of potassium in the study area varies from 0.27 to 151 mg/L with an average value of 15 mg/L during the pre-monsoon season, 0.05 to 110 mg/L with an average value of 5 mg/L during monsoon, and 0.05 to 158 mg/L with an average value 7 mg/L during the post-monsoon season in the year 2019.

The concentration of chloride in the study area varies from 130 to 17042 mg/L with an average value of 1960 mg/L during the pre-monsoon season, 37 to 11886 mg/L with an average value of 1534 mg/L during monsoon, and 29 to 18460 mg/L with an average value 2076 mg/L during the post-monsoon season of the year 2019. About 54%, 38%, and 42% of samples were found above the maximum permissible limit of 1000 mg/L in pre-monsoon, monsoon, and post-monsoon seasons respectively. And about 8%, 36%, and 36% of samples were found within the acceptable limit of 250 mg/L in pre-monsoon, monsoon, and post-monsoon seasons in the year 2019 respectively.

The concentration of sulfate in the study area varies from 15 to 4280 mg/L with an average value of 434 mg/L during the pre-monsoon season and 7 to 3690 mg/L with an average value of 375 mg/L during monsoon and 9 to 3630 mg/L with an average value 363 mg/L during the post-monsoon season in the year 2019. About 22%, 32%, and 20% of samples were found above the maximum permissible limit of 400 mg/L in pre-monsoon, monsoon, and post-monsoon seasons respectively. And about 52%, 60%, and 60% of samples were found within the acceptable limit of 200 mg/L in pre-monsoon, monsoon, and post-monsoon seasons in the year 2019 respectively.

The concentration of nitrate in the study area varies from 1 to 53 mg/L with an average value of 10 mg/L during the pre-monsoon season, 0 to 10 mg/L with an average value of 3 mg/L during monsoon, and 0 to 9 mg/L with an average value of 3 mg/L during the post-monsoon season in the year 2019. Almost all samples (more than 98%) of the study area fall within the permissible limit of 45 mg/L during all three seasons.

The concentration of fluoride in the study area varies from 0 to 4.58 mg/L with an average value of 1.41 mg/L during the pre-monsoon season, 0.03 to 2.32 mg/L with an average value of 0.90 mg/L during monsoon, and 0 to 8 mg/L with average value 1.88 mg/L during the post-monsoon season in the year 2019. About 36%, 16%, and 40% of samples were found above the maximum permissible limit of 1.5 mg/L in pre-monsoon, monsoon, and post-monsoon seasons respectively. And about 46%, 58%, and 44% of samples were found within the acceptable limit of 1 mg/L in pre-monsoon, monsoon, and post-monsoon seasons in the year 2019 respectively.

Table 5.6 Hydro-chemical data of groundwater samples collected during pre-monsoon, monsoon, and post-monsoon seasons (2019)

S. No.	Parameters	Range			Average			BIS Limit	
		Pre	Monsoon	Post	Pre	Monsoon	Post	Acceptable	Permissible
1.	**pH**	6.8-9.0	6.9-8.6	6.6-8.4	7.66	7.62	7.57	6.5-8.5	No Relaxation
2.	**EC (µS/cm)**	363-54600	720-62600	630-61300	6619	6402	7597	-	-
3.	**TDS (mg/L)**	243-36582	504-43820	409 - 39845	4435	4482	4938	500	2000
4.	**Hardness (mg/L)**	120-3767	123 -11120	96 -1017	856	1300	392	200	600
5.	**Na (mg/L)**	12 -11635	3 - 447	3 – 557	936	61	84	-	-
6.	**K (mg/L)**	0.27-151	0.05 - 110	0.05-158	15.65	5.27	7.57	-	-
7.	**Ca (mg/L)**	60-3292	14 - 2240	16-515	465	369	138	75	200
8.	**Mg (mg/L)**	0-3010	14 - 2240	22-679	390	369	254	30	100
9.	**HCO_3 (mg/L)**	99 - 692	14 -790	43- 645	322	274	334	-	-
10.	**Cl (mg/L)**	130-17042	37 -11886	29-18460	1960	1534	2075	250	1000
11.	**SO_4 (mg/L)**	15-4280	7 - 3690	9-3630	433	375	363	200	400
12.	**NO_3 (mg/L)**	1-52.5	0-9.7	0-8.6	9.79	3.56	2.74	45	No Relaxation
13.	**F (mg/L)**	0-4.58	0.03-2.32	0-8.1	1.41	0.90	1.88	1.0	1.5

5.4.2.2 Water quality evaluation for irrigation purposes

Water quality plays an important role in irrigated agriculture. Many problems arise during inefficient management of water for agriculture use. The concentration and composition of dissolved constituents in water determine its quality for irrigation use. Quality of water is an important consideration in any appraisal of salinity or alkali conditions in an irrigated area. Under good soil and water management practices, good quality water can cause maximum yield. The quality of irrigation water is assessed by the following characteristics:

1. Salinity
2. The relative proportion of sodium to other cations (SAR)
3. Residual Sodium Carbonate (RSC)

Salinity

Salinity is expressed in terms of total dissolved solids (TDS) and thereby electrical Conductivity (EC). If the salt concentration in water increases, the soil salinity also increases and it becomes difficult for plants to extract water. The salts present in water, besides affecting the growth of the plants directly, also affect the soil structure, permeability, and aeration, which indirectly affect plant growth. Soil water passes into the plant through the root zone due to osmotic pressure. As the dissolved solid content of the soil water in the root zone increases, it becomes difficult for the plant to overcome the osmotic pressure and the plant root membrane can assimilate water and nutrients. Thus, the dissolved solid content of the residual water in the root zone also has to be maintained within limits by proper leaching. The safe limits of electrical conductivity for crops with different degrees of salt tolerances under varying soil textures and drainage conditions are given in table 5.3. The quality of water is commonly expressed by classes of relative suitability for irrigation with reference to salinity levels.

Residual Sodium Carbonate

Water containing high concentrations of carbonate and bicarbonate ions tends to precipitate calcium and magnesium as carbonate, changing the residual water to high sodium water with sodium bicarbonate in solution. As a result, the relative proportion of sodium increases and gets concentrated in the soil thereby decreasing the soil permeability. This excess is denoted by Residual Sodium Carbonate (RSC) and is determined by the following formula:

$$RSC = (HCO_3^- + CO_3^{--}) - (Ca^{++} + Mg^{++}) \quad \text{.....(5.4)}$$

Where all ionic concentrations are expressed in epm. If the RSC exceeds 2.5 epm, the water is generally unsuitable for irrigation. Excessive RSC causes the soil structure to deteriorate, as it restricts the water and air movement through the soil. If the value is between 1.25 and 2.5, the water is of marginal quality, while values less than 1.25 epm indicate that the water is safe for irrigation.

The value of SAR in the study area varies from 0.14 to 43.72 with an average value of 6.07 during the pre-monsoon season, 0.04 to 1.0 with an average value of 0.32 during monsoon, and 0.06 to 6.50 with an average value 0.98 during the post-monsoon season in the year 2019. The percentage of sodium in the study area varies from 2.12 to 73.80 with an average value of 28.80 during the pre-monsoon season and 0.62 to 12.78 with an average value of 3.25 during monsoon and 1.11 to 46.74 with an average value 11.56 during the post-monsoon season in the year 2019. Almost all samples have SAR values below 10 indicating excellent quality for irrigation purposes, except only 7 samples that have more than 10. Almost all of the samples were observed to have an RSC value below 1.25 suggesting suitability for irrigation purposes. The recommended classification with respect to electrical conductivity, sodium content, sodium Absorption Ratio (SAR), and Residual Sodium Carbonate (RSC) are given in Table 5.7.

Table 5.7 Guidelines for evaluation of irrigation water quality

Water class	Na, %	EC, µS/cm	SAR	RSC, meq/l
Excellent	< 20	< 250	< 10	< 1.25
Good	20-40	250-750	10-18	1.25-2.0
Medium	40-60	750-2250	18-26	2.0-2.5
Bad	60-80	2250-4000	> 26	2.5-3.0
Very bad	> 80	> 4000	> 26	> 3.0

Source: CGWB and CPCB (2000).

5.4.2.1.3 Classification of Groundwater for quality

Different accepted and widely used graphical methods such as Piper trilinear diagram and U.S. Salinity Laboratory classification have been used in the present study to classify the groundwater in the study area. Piper trilinear (Piper, 1944) is used to express similarity and dissimilarity in the chemistry of water based on major cations and anions. U.S. Salinity Laboratory classification (Wilcox, 1955) has been used to study the suitability of groundwater for irrigation purposes. In a classification of irrigation waters, it is assumed that the water will be used under average conditions with respect to soil texture, infiltration rate, drainage characteristics, the quantity of water used, climate, and salt tolerance of crops.

Piper trilinear classification

Piper (1944) has developed a form of trilinear diagram, which is an effective tool in segregating analyzed data with respect to sources of the dissolved constituents in groundwater, modifications in the character of water as it passes through an area, and related geochemical problems. The diagram is useful in presenting graphically a group of analyses on the same plot. The Piper trilinear diagram combines three areas of plotting, two triangular areas (cations and anions) and an intervening diamond-shaped area (combined field). Using this diagram, water can be classified into different hydro-chemical facies. In pre-monsoon and post-monsoon seasons, the piper trilinear diagram shows that groundwater is of Ca-Cl/ Ca-SO_4 type and Na-SO_4-Cl type (Fig 5.30 and Fig 5.32). In the monsoon season, the groundwater in the study area is of Ca-HCO_3 type and Ca-Cl/ Ca-SO_4 type (Fig 5.31).

Durov trilinear plot

The important geochemical processes that play a great role in the chemistry of groundwater in the study area have been evaluated using the Durov trilinear plot (Fig 5.33-5.35) for all three seasons during the 2019 year. Ion-exchange and dissolution processes control the hydrochemistry of the aquifer during all three seasons.

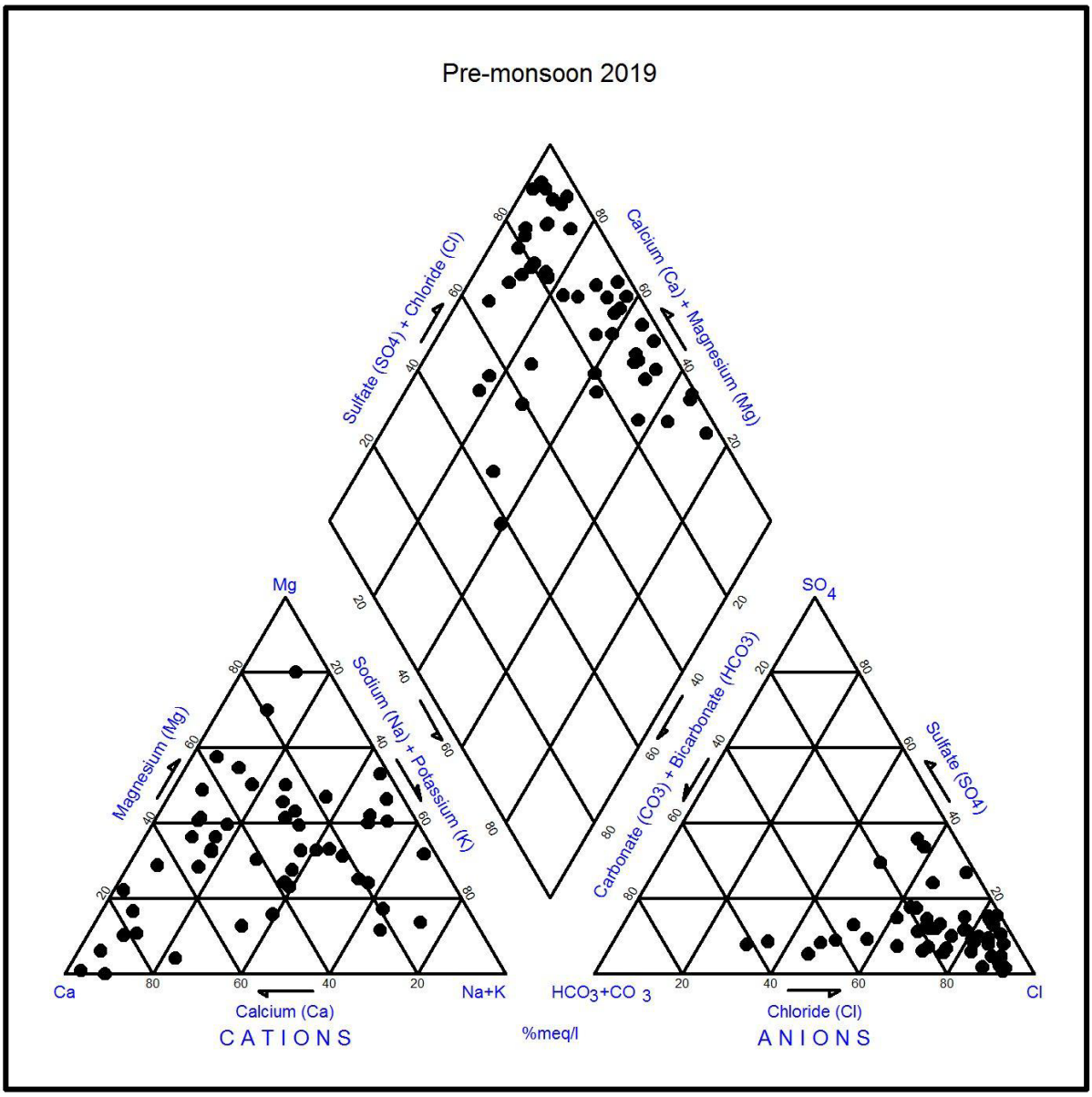

Fig 5.30 Piper trilinear diagram (Pre-monsoon 2019)

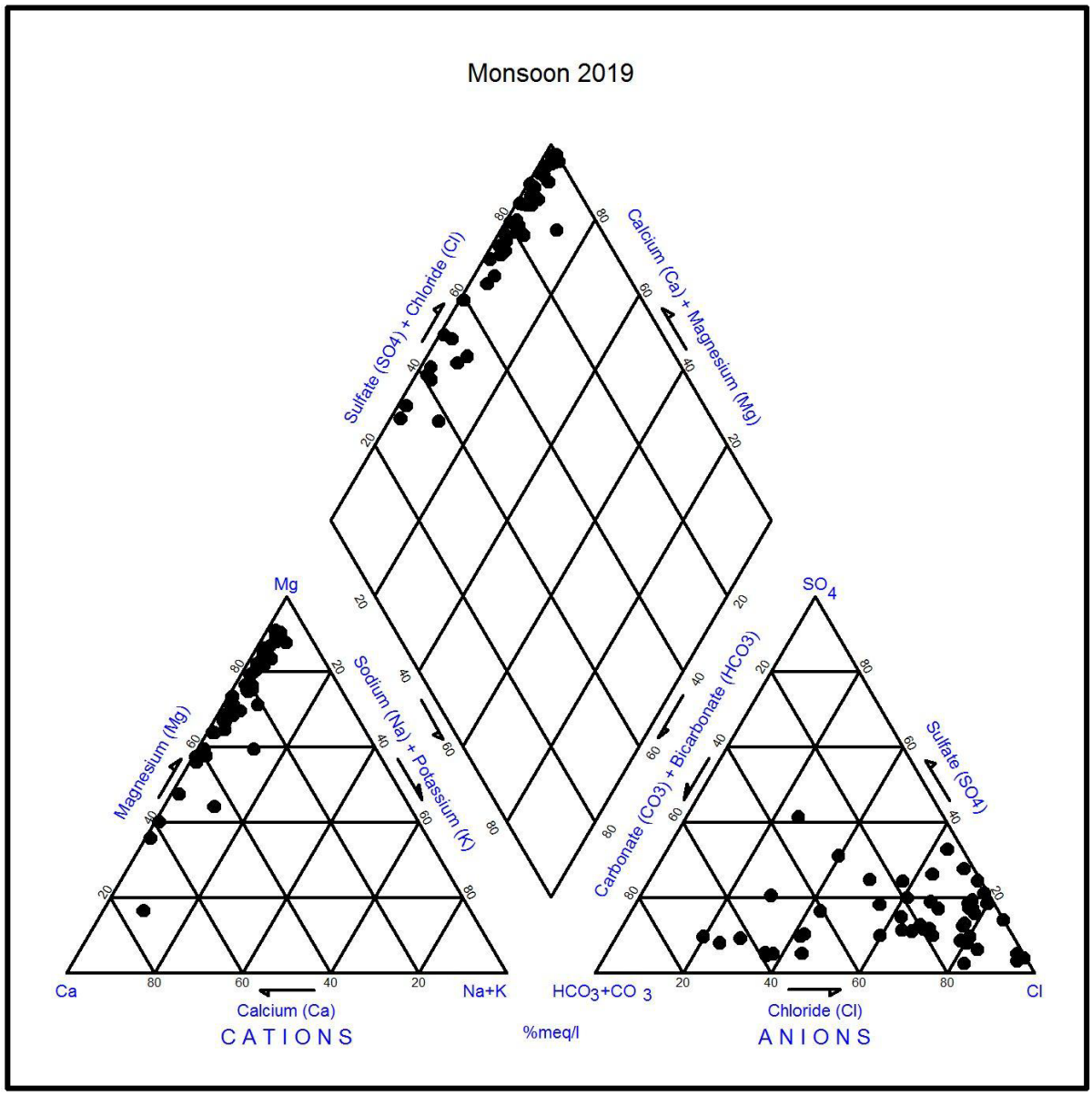

Fig 5.31 Piper trilinear diagram (Monsoon 2019)

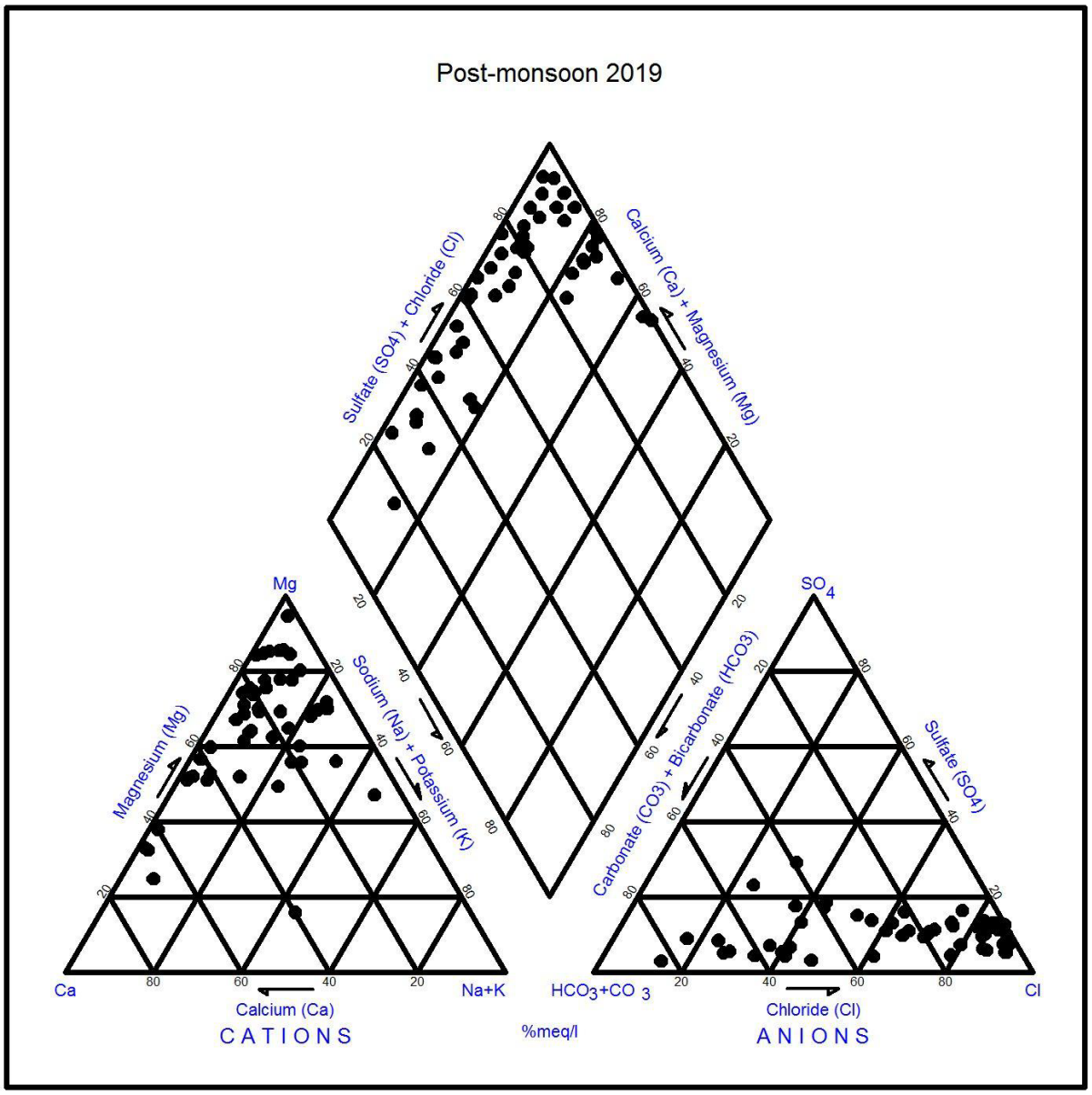

Fig 5.32 Piper trilinear diagram (Post-monsoon 2019)

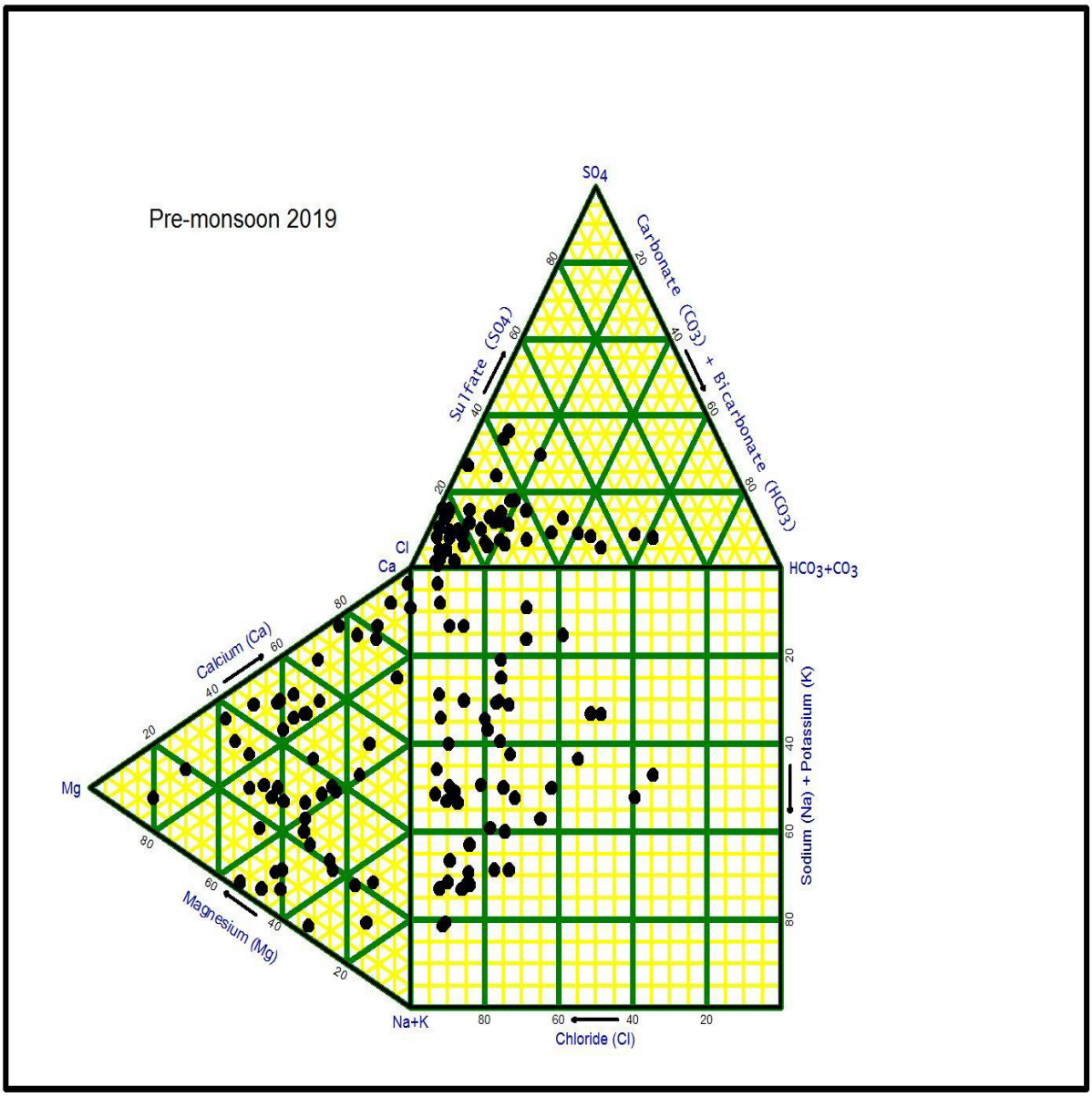

Fig 5.33 Trilinear Durov plot diagram (Pre-monsoon 2019)

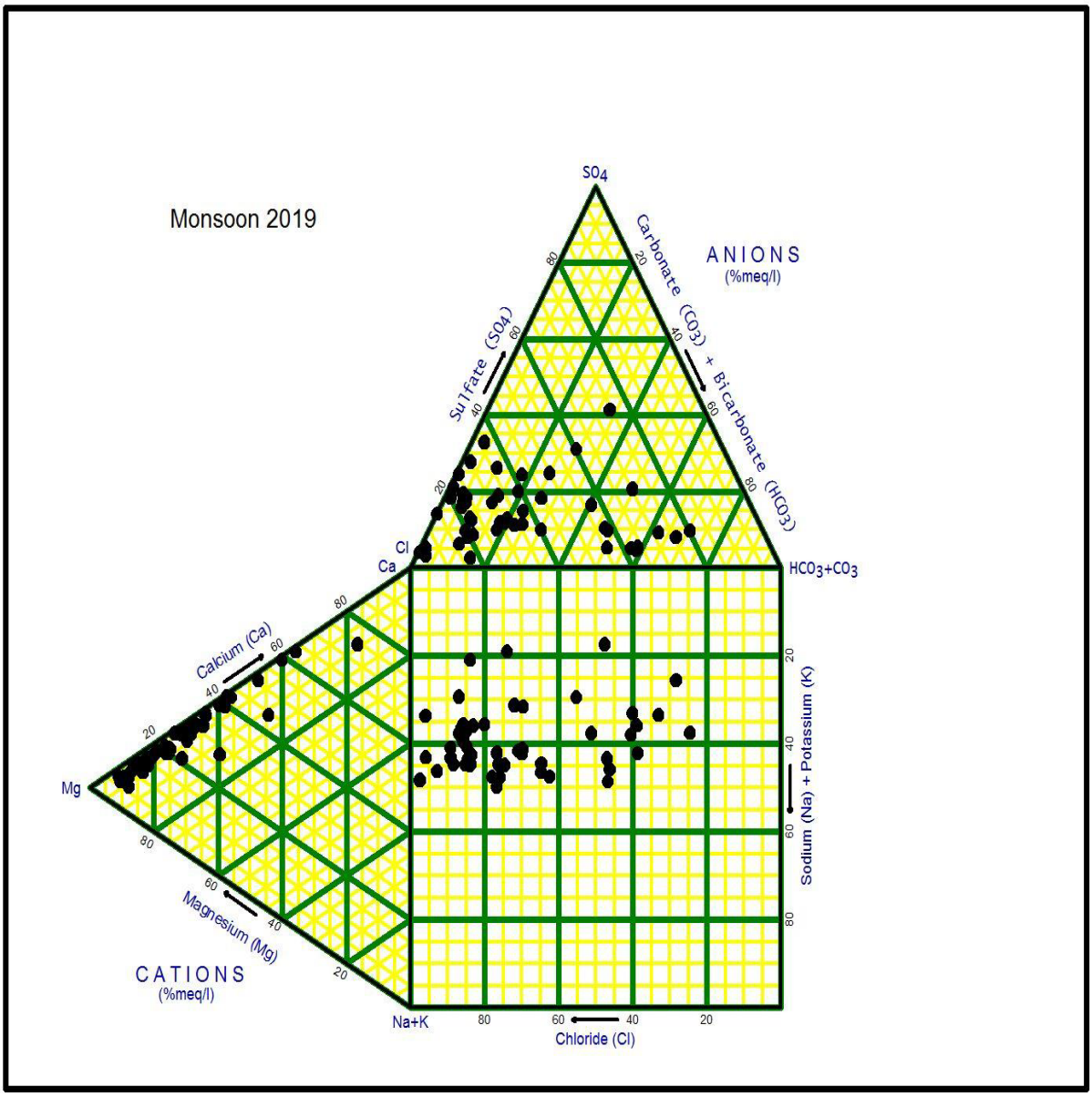

Fig 5.34 Trilinear Durov plot diagram (Monsoon 2019)

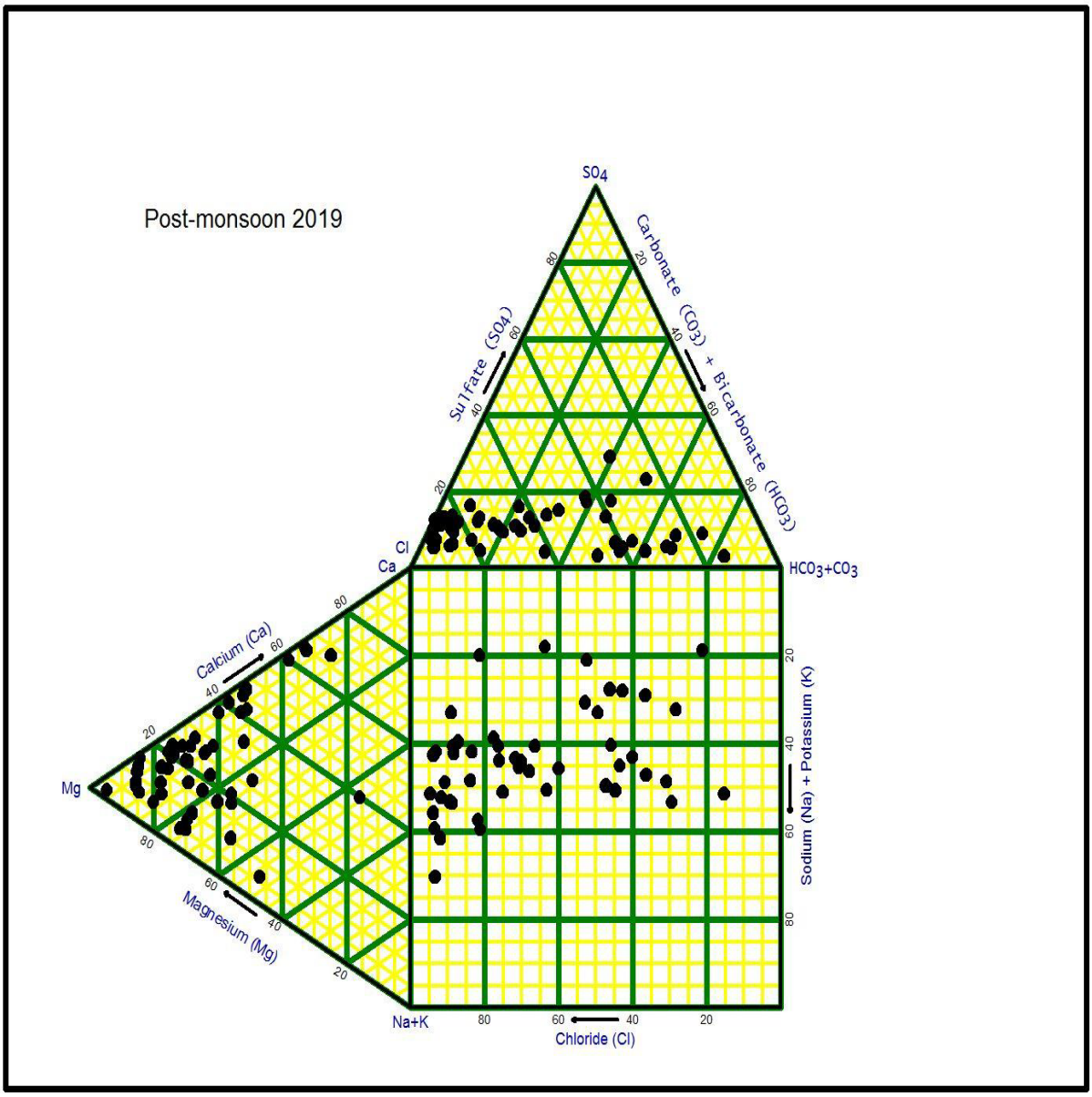

Fig 5.35 Trilinear Durov plot diagram (Post-monsoon 2019)

U. S. Salinity Laboratory Classification

Sodium concentration plays an important role in irrigation-water classification because sodium reacts with the soil to create sodium hazards by replacing other cations. The extent of this replacement is estimated by Sodium Adsorption Ratio (SAR). The U.S. Regional Salinity Laboratory has developed a diagram for use in studying the suitability of groundwater for irrigation purposes with reference to sodium adsorption ratio (SAR) as an index for sodium hazard S and electrical conductivity (EC) of water expressed in μS/cm as an index of salinity hazard C.

The chemical analysis data of groundwater samples of the study area have been analyzed as per the U.S. Salinity Laboratory classification for the groundwater quality data (Fig 5.36 to Fig 5.38). It is evident from the results that the majority of groundwater samples of the study area fall under water types C4-S1 followed by C3-S1 in pre-monsoon, monsoon, and post-monsoon seasons. C4-S1 water type (high salinity and low SAR) cannot be used directly on soils that have poor drainage. Moreover, even with adequate drainage special management for salinity control may be required and only salt-tolerant species are suitable for this type of water. The C3-S1 type water (medium salinity and low SAR) can be used if a moderate amount of leaching occurs. Plants with moderate salt tolerance can be grown in most cases without special practices for salinity control.

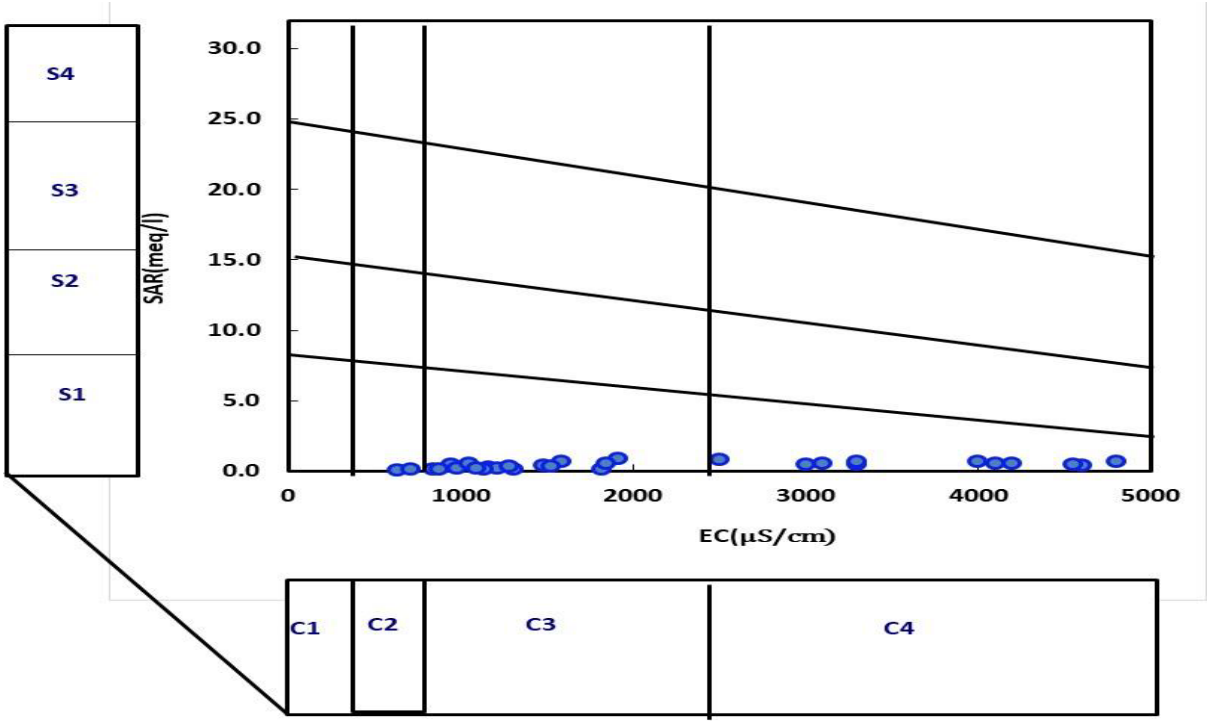

Fig 5.36 U.S. Salinity Laboratory classification (Pre-monsoon 2019)

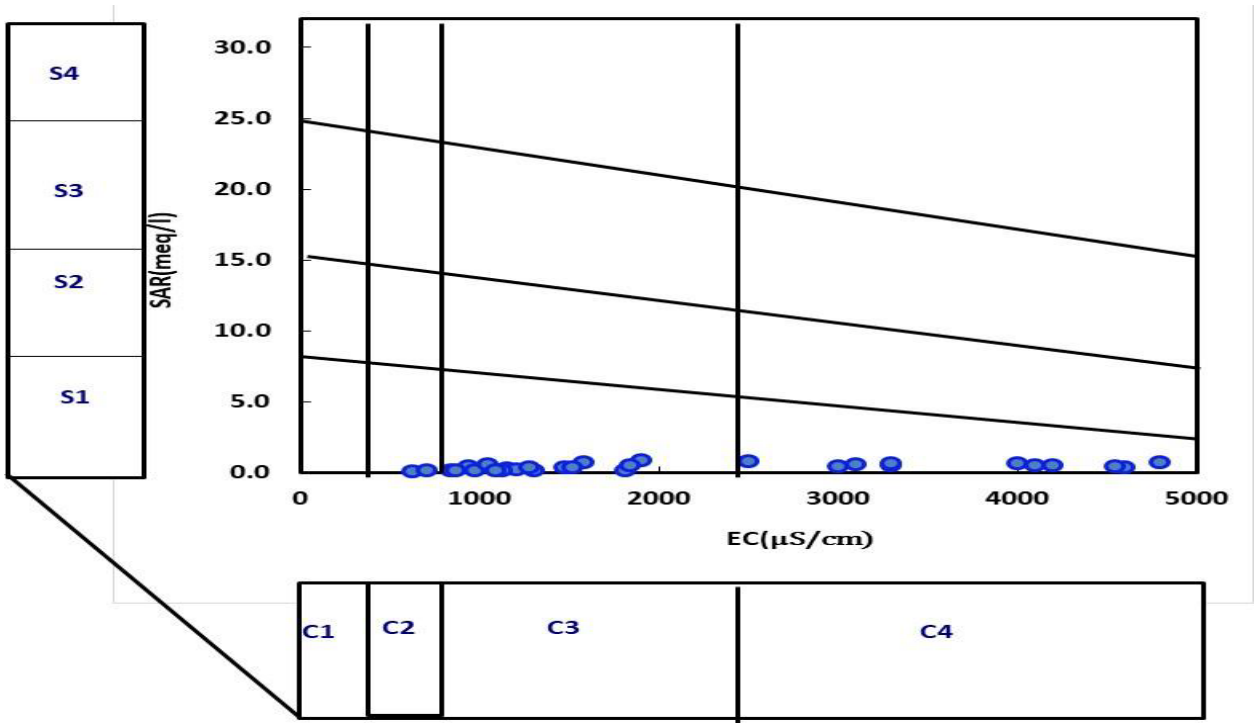

Fig 5.37 U.S. Salinity Laboratory classification (Monsoon 2019)

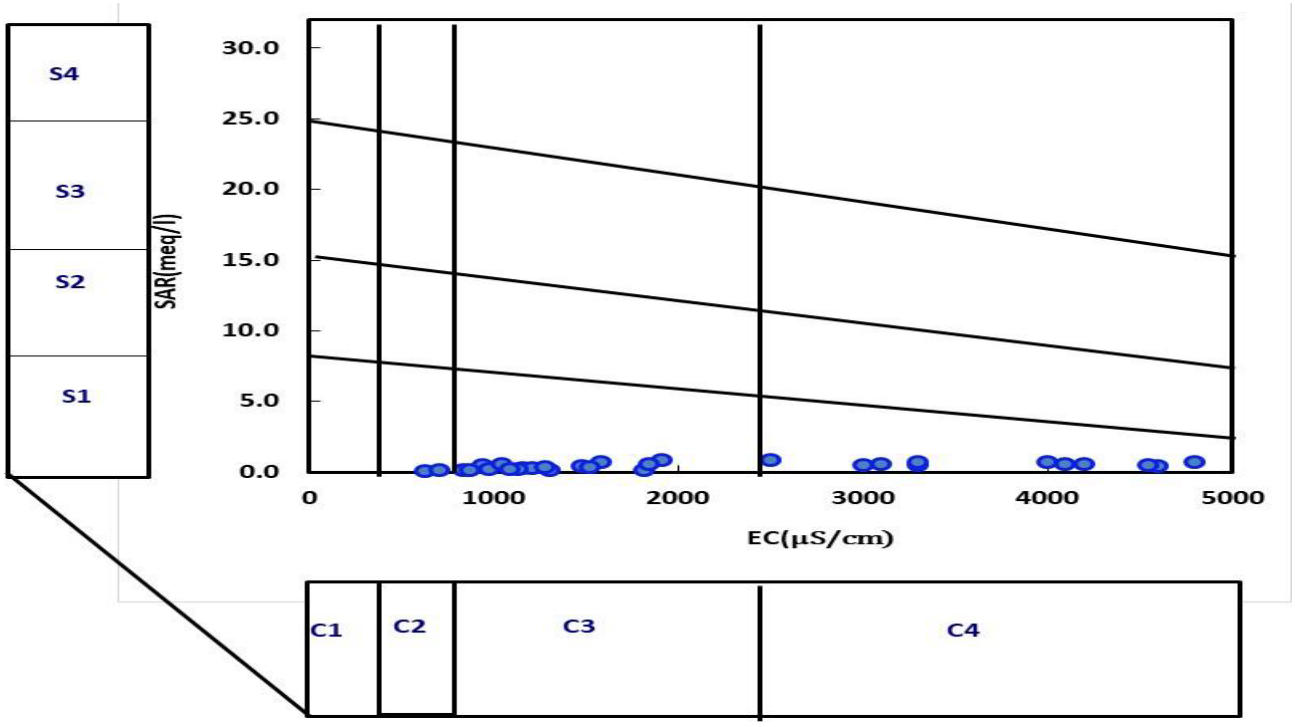

Fig 5.38 U.S. Salinity Laboratory classification (Post-monsoon 2019)

Gibbs diagram

Geo-environmental conditions have a marked influence on groundwater quality. Hydro-geochemical studies relevant to water quality explain the relationship of water chemistry to aquifer lithology. Such a relationship would help not only to explain the origin and distribution of dissolved constituents but also to elucidate the factors controlling the groundwater chemistry. Gibbs (1970) proposed a hypothesis to elucidate the major natural mechanisms controlling world water chemistry. Three mechanisms – atmospheric precipitation, rock dominance, and the evaporation-crystallization process – are the major factors controlling the composition of dissolved salts in world waters. The plot (Fig 5.39) shows the chemical weathering of rocks to form minerals as the major reason governing the groundwater chemistry in the study area.

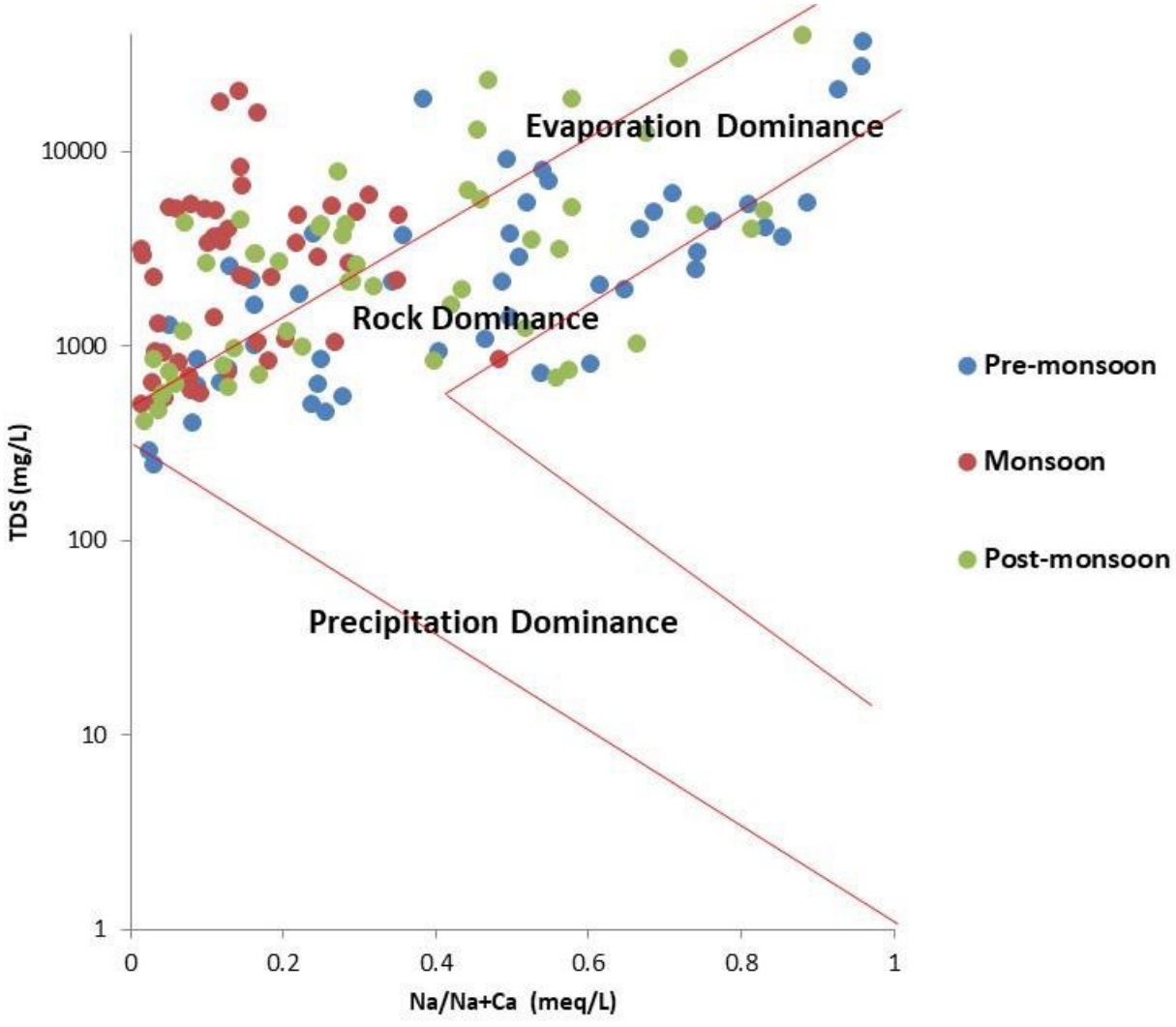

Fig 5.39 Gibbs plot showing mechanism controlling the chemistry of groundwater during the year 2019

Scatter plots for pre-monsoon 2019

The bivariate plot of $Ca^{2+}+Mg^{2+}$ vs $HCO_3^{-}+SO_4^{2-}$ is used to identify the parent rock responsible for the ion exchange process in the groundwater system. The abundance of $Ca^{2+} + Mg^{2+}$ over $HCO_3^{-} + SO_4^{2-}$ indicates carbonate weathering, whereas, the dominance of $HCO_3^{-} + SO_4^{2-}$ reflects silicate weathering as the primary process of ion exchange (Elango and Kannan 2007; Barzegar et al., 2016).

Areas rich in feldspars and kankars (calcium-rich encrustations) react with carbonic acid that may contribute to these ions namely, Ca^{2+}, Na^{+} and HCO_3^{-} and H_4SiO_4 in groundwater (Guo and Wang 2005).

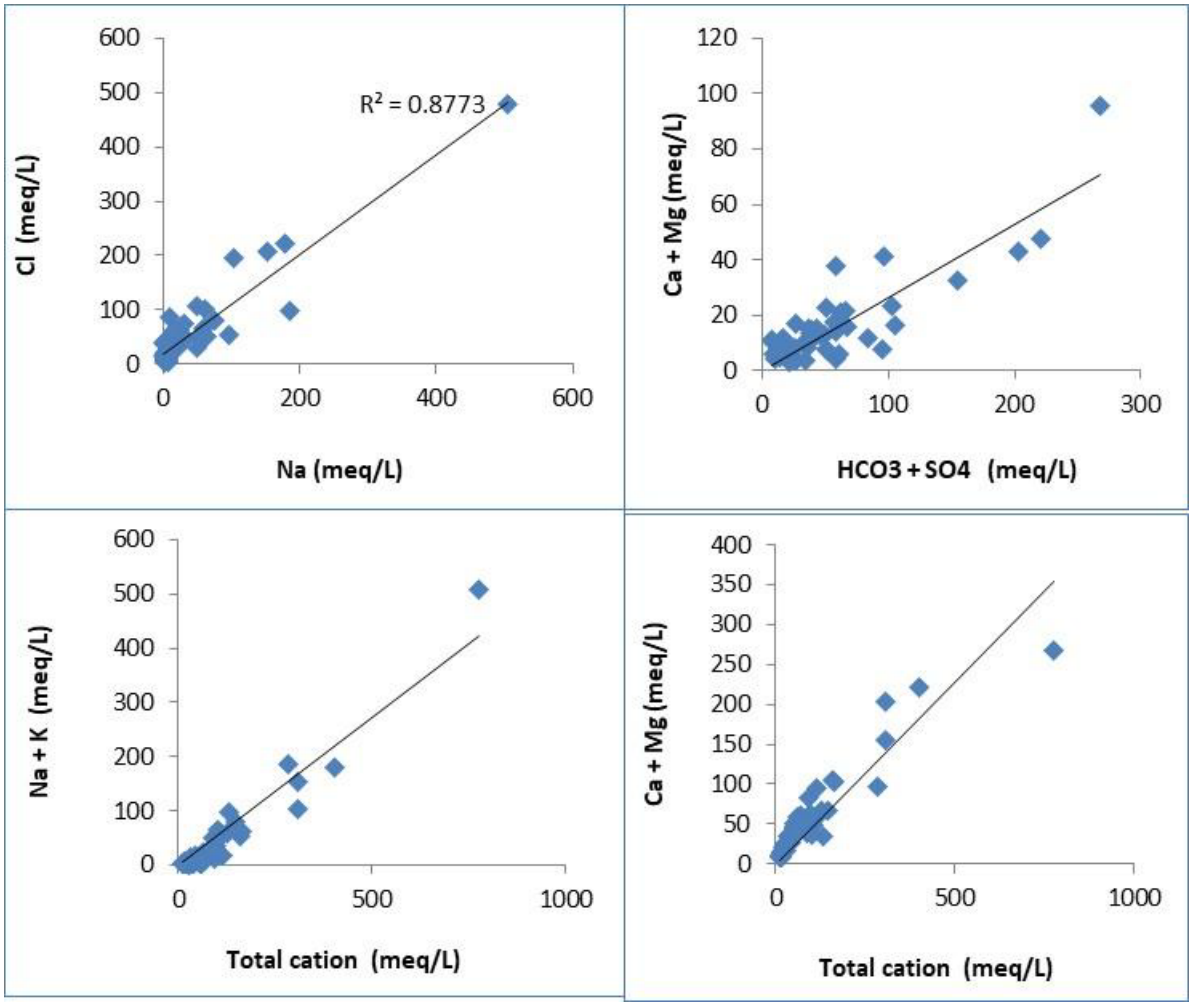

Fig 5.40 Scattered plots of pre-monsoon 2019

The scatter plot of the above Ca, Mg Vs. HCO3 and SO4 are indicating there is the dominance of the Carbonate type of rock in the area.

The scattered plot of Ca^{2+}+Mg^{2+} vs TZ^{+} (Total cations) shows that almost all the water samples of the study area are above the line (1:1), showing the weathering of carbonate minerals (Fig 5.40). Similarly, the relationship between Na^{+}+K^{+} vs shows that samples are plotted very well below the 1:1 line. This suggests that silicate weathering and anthropogenic inputs in soil salts contribute mainly Na^{+} and K^{+} ions to the water system.

The Na^{+} vs Cl^{-}plot lies above the line (1:1) though there is equal distribution little more Cl^{-} is there suggesting that besides some silicate weathering, Na^{+} may be due to some anthropogenic sources such as sewage, domestic and animal waste. Majority of Cl^{-} over Na^{+}indicating the contamination by anthropogenic activities. The higher content of Cl^{-} in the groundwater may be attributed to the discharges of industrial effluents and untreated municipal wastes (Fig 5.40).

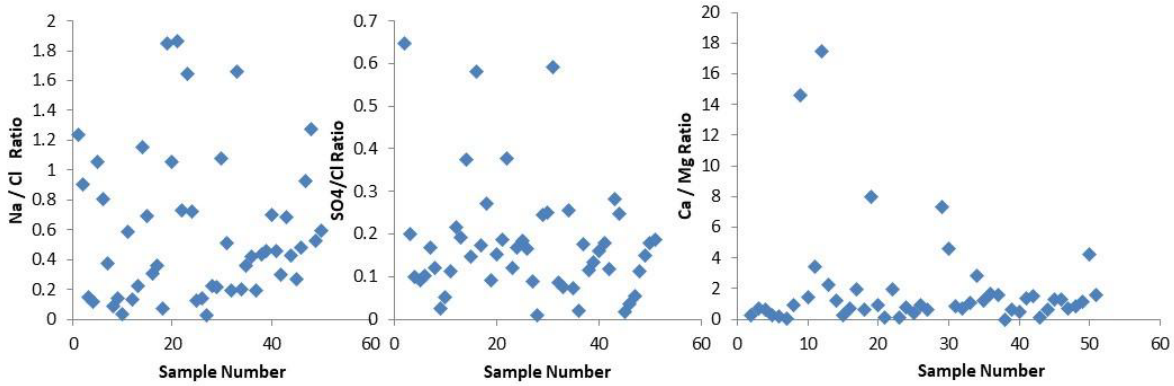

Fig 5.41 Ratio vs Sample number during the pre-monsoon 2019

The Na^{+}/Cl^{-} molar ratio was used to identify the source of salinity in groundwater. If Na^{+}/Cl^{-} ratio is equal to 1 then the source of Na^{+} is due to halite dissolution, if the Na^{+}/Cl^{-} ratio is greater than 1, the source of Na^{+} is silicate weathering (Meybeck 1987). Here the ratio is below 0.5 in almost the majority of samples hence there is no chance of silicate weathering (Fig 5.41).

The ratio of SO_4^{2-}/Cl^{-} ions was used as a marker to identify the potential pyrite dissolution in groundwater. SO_4^{2-}/Cl^{-} the ratio of more than 0.5, indicates pyrite oxidation **(**Okiongbo and Douglas 2015**)**. Here most of the values fall below the value of 0.5 hence no Pyrite dissolution is there in the study area.

The Ca/Mg ratio is also derived to evaluate the influence of carbonate and silicate weathering on groundwater chemistry. The Ca/Mg ratio equal to 1 indicates the dissolution of dolomite, while the ratio of more than 1 depicts the sources of these ions from the dissolution of calcite rocks (Mayo and Loucks 1995). Ca/Mg >2 represents the dissolution

of silicate minerals in the groundwater (Katz and Hicks, 1997). Here the majority of samples fall below the range of 1 which shows dissolution from dolomite (Fig 5.41).

Scatter plots for monsoon 2019

The bivariate plot of $Ca^{2+}+Mg^{2+}$ vs $HCO_3^{-}+SO_4^{2-}$ is used to identify the parent rock responsible for the ion exchange process in the groundwater system. The abundance of $Ca^{2+} + Mg^{2+}$ over $HCO_3^{-} + SO_4^{2-}$ indicates carbonate weathering, whereas, the dominance of $HCO_3^{-} + SO_4^{2-}$ reflects silicate weathering as the primary process of ion exchange (Elango and Kannan 2007; Barzegar et al., 2016).

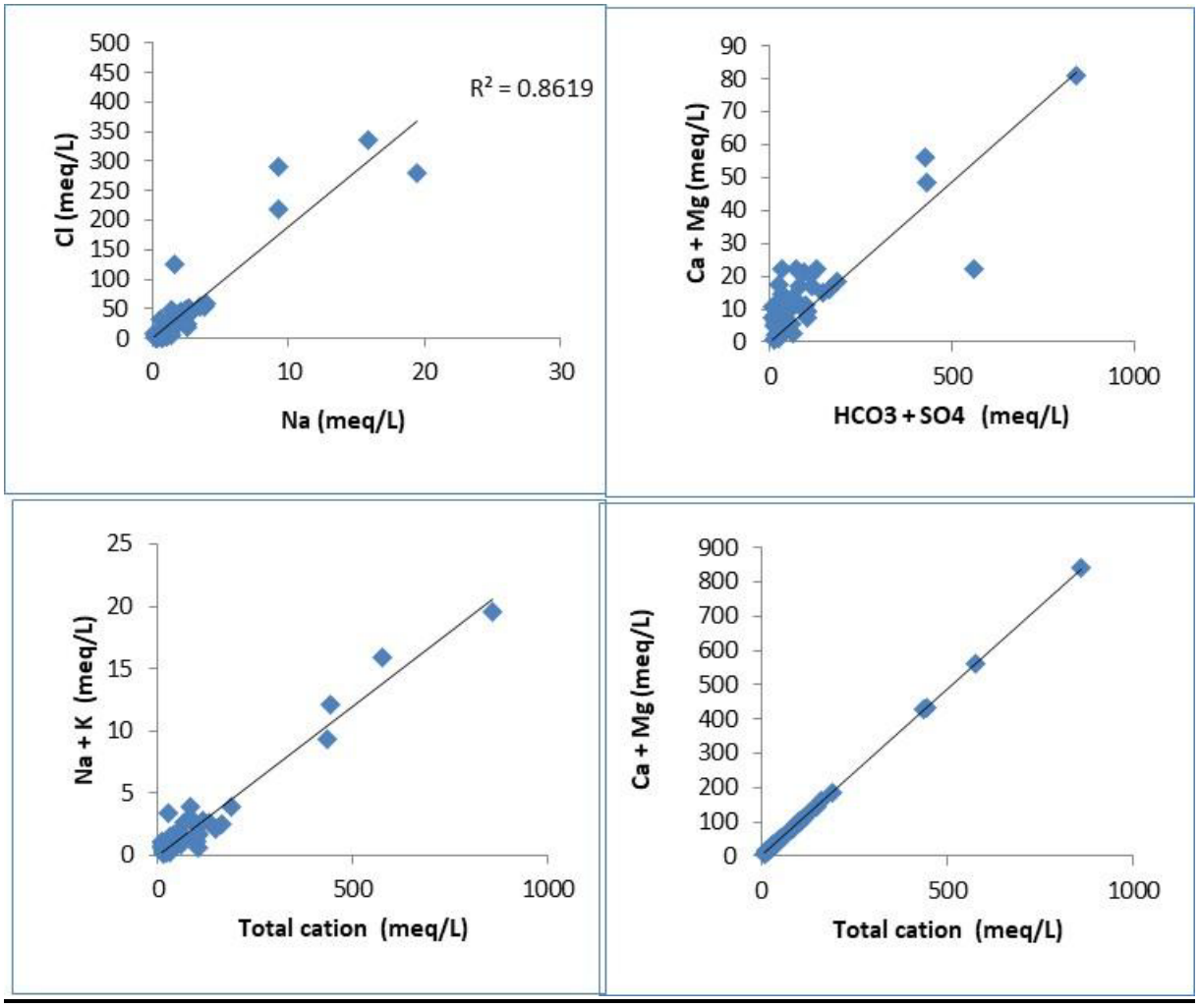

Fig 5.42 Scattered plots of monsoon 2019

The scatter plot of the above Ca, Mg vs. HCO3, and SO4 are indicating there is the dominance of the Carbonate type of rock in the area.

The scatter plots of $Ca^{2+}+Mg^{2+}$ vs TZ^{+} (total cations) show that all the water samples of the study area are coinciding with the line (1:1), showing the weathering of carbonate minerals (Fig 5.40). Similarly, the relationship between $Na^{+}+K^{+}$ vs shows that the samples are plotted below the 1:1 line. This suggests that silicate weathering and anthropogenic inputs in soil salts contribute mainly Na^{+} and K^{+} ions to the water system.

The Na^{+} vs Cl^{-} plot lie above the line (1:1) suggesting that besides some silicate weathering Na^{+} may be due to some anthropogenic sources such as sewage, and domestic and animal waste. The majority of Cl^{-} over Na^{+} indicates contamination by anthropogenic activities. The higher content of Cl^{-} in the groundwater may be attributed to the discharges of industrial effluents and untreated municipal wastes (Fig 5.42).

The Na^{+}/Cl^{-} molar ratio was used to identify the source of salinity in groundwater. If Na^{+}/Cl^{-} ratio is equal to 1 then the source of Na^{+} is due to halite dissolution, if the Na^{+}/Cl^{-} ratio is greater than 1, the source of Na^{+} is silicate weathering. Here the ratio is below 0.5 in almost the majority of samples hence there is no chance of silicate weathering. The ratio of SO_4^{2-}/Cl^{-} ions was used as a marker to identify the potential pyrite dissolution in groundwater. SO_4^{2-}/Cl^{-} the ratio of more than 0.5, indicates pyrite oxidation **(**Okiongbo and Douglas 2015**)**. Here most of the values fall below the value of 0.5 hence no Pyrite dissolution is there in the study area (Fig 5.43).

The Ca/Mg ratio is also derived to evaluate the influence of carbonate and silicate weathering on groundwater chemistry. The Ca/Mg ratio equal to one indicates the dissolution of dolomite, while the ratio of more than one depicts the sources of these ions from the dissolution of calcite rocks (Mayo and Loucks 1995). Ca/Mg >2 represents the dissolution of silicate minerals in the groundwater. Here the majority of samples fall below the range of 1 which shows dissolution from dolomite (Fig 5.43).

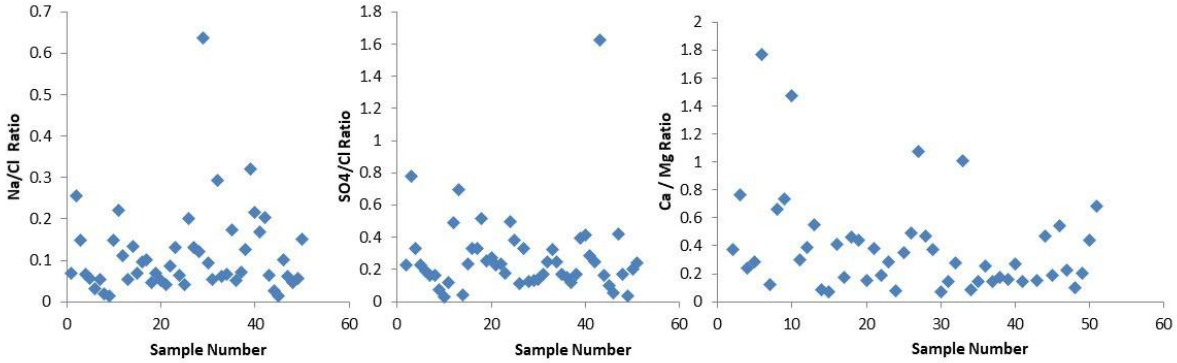

Fig 5.43 Ratio vs Sample number during the monsoon 2019

Scatter plots for post-monsoon 2019

The bivariate plot of $Ca^{2+}+Mg^{2+}$ vs $HCO_3^{-}+SO_4^{2-}$ is used to identify the parent rock responsible for the ion exchange process in the groundwater system. The abundance of

$Ca^{2+} + Mg^{2+}$ over $HCO_3^- + SO_4^{2-}$ indicates carbonate weathering, whereas, the dominance of $HCO_3^- + SO_4^{2-}$ reflects silicate weathering as the primary process of ion exchange (Elango and Kannan 2007; Barzegar et al., 2016).

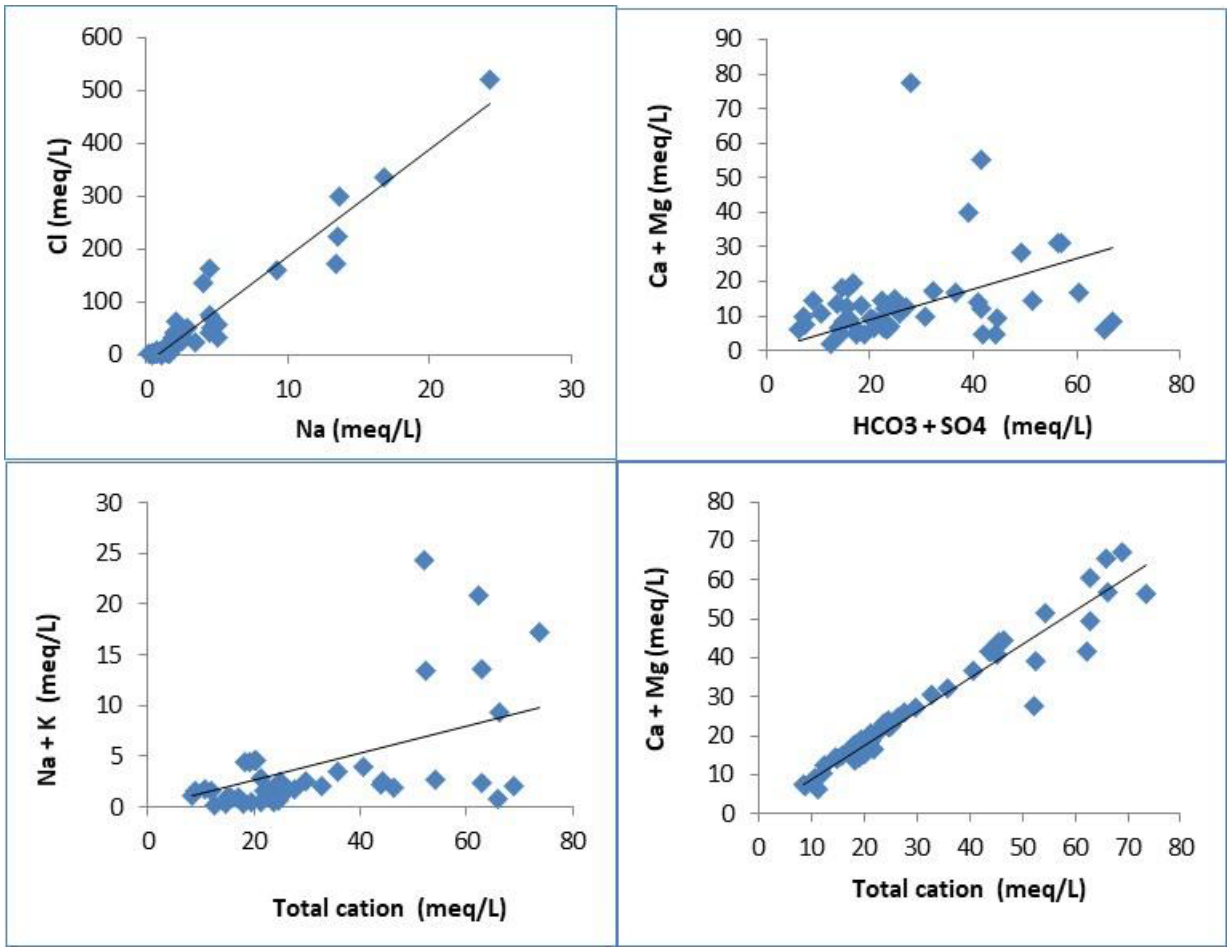

Fig 5.44 Scattered plots of post-monsoon 2019

The scatter plot of the above Ca, Mg Vs HCO3, and SO4 are indicating there is the dominance of the Carbonate type of rock in the area.

The scatter plots of Ca^{2+}+Mg^{2+} vs TZ^+ (Total cations) show that all the water samples of the study area are above the line (1:1), showing the weathering of carbonate minerals (Fig 5.42). Similarly, the relationship between Na^++K^+ vs shows that the samples are plotted very well below the 1:1 line. This suggests that silicate weathering and anthropogenic inputs in soil salts contribute mainly Na^+ and K^+ ions to the water system **(**Stallard and Edmond 1983; Sarin et al., 1989; Datta and Tyagi 1996).

The Na^+ vs Cl^- plot lies above the line (1:1) almost equally distributed but a little more Cl^- is there suggesting that besides some silicate weathering Na^+ may be due to some anthropogenic sources such as sewage, domestic and animal waste. The majority of Cl^-

over Na^+ indicates contamination by anthropogenic activities. The higher content of Cl^- in the groundwater may be attributed to the discharges of industrial effluents and untreated municipal wastes (Fig 5.44).

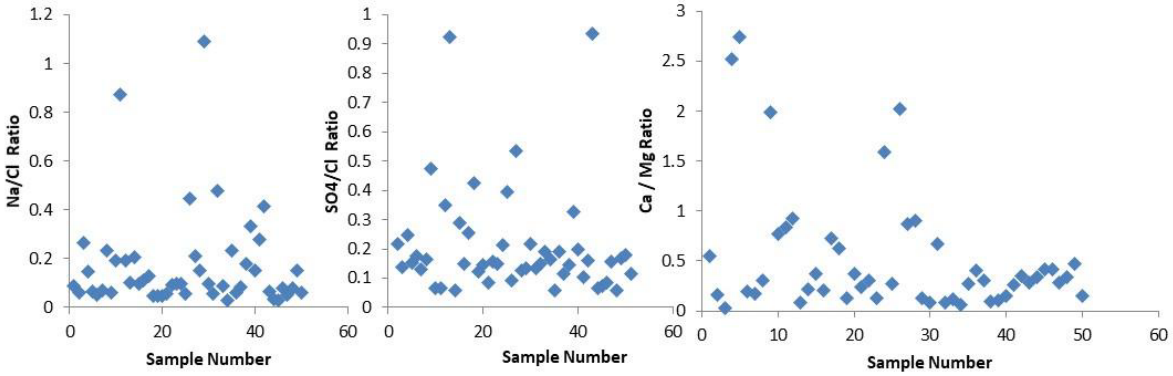

Fig 5.45 Ratio vs Sample number during the post-monsoon 2019

The Na^+/Cl^- molar ratio was used to identify the source of salinity in groundwater. If Na^+/Cl^- ratio is equal to 1 then the source of Na^+ is due to halite dissolution, if the Na^+/Cl^- ratio is greater than 1, the source ofNa^+ is silicate weathering. Here the ratio is below 0.5 in almost the majority of samples hence there is no chance of silicate weathering(Fig 5.45). The ratio of SO_4^{2-}/Cl^- ions was used as a marker to identify the potential pyrite dissolution in groundwater. SO_4^{2-}/Cl^- the ratio of more than 0.5, indicates pyrite oxidation **(**Okiongbo and Douglas 2015**)**. Here most of the values fall below the value of 0.5 hence no Pyrite dissolution is there in the study area (Fig 5.45).

The Ca/Mg ratio is also derived to evaluate the influence of carbonate and silicate weathering on groundwater chemistry. The Ca/Mg ratio equal to one indicates the dissolution of dolomite, while the ratio of more than one depicts the sources of these ions from the dissolution of calcite rocks (Mayo and Loucks 1995). Ca/Mg >2 represents the dissolution of silicate minerals in the groundwater. Here the majority of samples fall below the range of 1 which shows dissolution from dolomite.

Fluoride ion in-situ measurement at selected sites in Mewat district

Fluoride ion in-situ measurements at selected sites in the Mewat district of Haryana were done in June 2022 and details are given in table 5.7 below.

Table 5.7 Fluoride ion in-situ measurement at selected sites in Mewat district during 07-09, June 2022

S.No.	Location	Lat.	Long.	Fluoride	pH	EC
1	Kotla	28°0.7100'N	76°56.8260'E	0.18	7.52	700
2	Kansali	27°58'04.8"N	76°56'24.0"E	0.52	8.21	1180
3	Kansali 2	27°58'04.8"N	76°56'24.0"E	0.58	7.51	1770
4	Ghaghas	27°56'45.6"N	76°56'49.2"E	0.53	7.29	2300

5	Khedi Nuh	27°58'33.6"N	77°00'21.6"E	0.54	8.45	1570
6	Sakras	27°50.9300'N	77°0.0060'E	2.41	7.72	1940
7	Bai-khera(HP)	27°50.9860'N	77°1.6100'E	1.58	8.1	2600
8	Bai-khera(BW)	27°50.9860'N	77°1.6100'E	0.72	7.55	6300
9	Hamzapur	27°49.8220'N	77°0.1450'E	0.11	7.3	3300
10	Raniyali	27°49.0470'N	77°0.1460'E	0.71	7.6	3100
11	Alipur-Tigra	27°46.4470'N	76°59.0380'E	2.26	7.91	3400
12	Basai mev	27°45'21.6"N	77°00'50.4"E	0.25	6.5	850
13	Kameda	27°46.6740'N	76°57.9790'E	0.85	7.3	3100
14	Manduka	27°40.5310'N	76°54.5130'E	2.25	7.1	1090
15	Ravali	27°40'47.6"N	76°57'46.4"E	1.24	7.66	5700
16	Dhoha	27°41.2310'N	76°55.6720'E	2.44	8.1	5400
17	Kolagaun (school)	27°40.4440'N	76°57.4370'E	0.85	8.21	3900
18	Saymer bas	27°40'11.3"N	76°57'17.3"E	1.07	8.35	4400
19	Beria bas	27°42'41.0"N	76°58'18.8"E	1.04	8.01	7200
20	Khedla	27°42.3620'N	76°58.3250'E	1.42	7.51	3300
21	Shahpur	27°42.5960'N	76°58.3130'E	1.80	8.08	1770
22	Agon	27°43.7260'N	76°58.0200'E	0.72	7.81	8300
23	Solpur	27°44.4970'N	76°56.7040'E	2.13	7.51	4400
24	Maholi(RSSB)	27°45.9360'N	76°56.8490'E	1.64	7.2	11300
25	Nasser-bas	27°50.7230'N	76°57.6280'E	1.42	7.54	3900
26	Mandi-khera	27°53.7130'N	76°59.6040'E	0.42	7.82	3908

Fluoride in-situ measured values ranged from 0.11 to 2.44 mg/L with the mean value of 1.14 mg/L at selected sites in the Mewat district in June 2022. The fluoride standard value of 1 ppm has been prescribed by BIS as an acceptable limit for drinking water and the mean value exceeded the permissible limit in the study area which poses a threat of non-carcinogenic risk to people living in the area. Moreover, for better visualization of the fluoride contamination in the study area, a spatial distribution map was prepared using Arc GIS software (Fig. 5.46). The spatial map shows that Block Firozpur Jhirka (southern part of the study area) has the problem of fluoride contamination and yellow to light red color zones have a value greater than 1 ppm, apart from two points namely Hamzapur and Basi Mev where values were found below 1 ppm. The upper portion of the map is Block Nuh shows fluoride values between 0.3 to 0.5 mg/L suggesting no risk related to fluoride contamination. Also, there is a total of 7 measuring points (28%) having values greater than 1.5 ppm i.e BIS permissible limit for drinking water, where the situation was very worse than in another part of the study area.

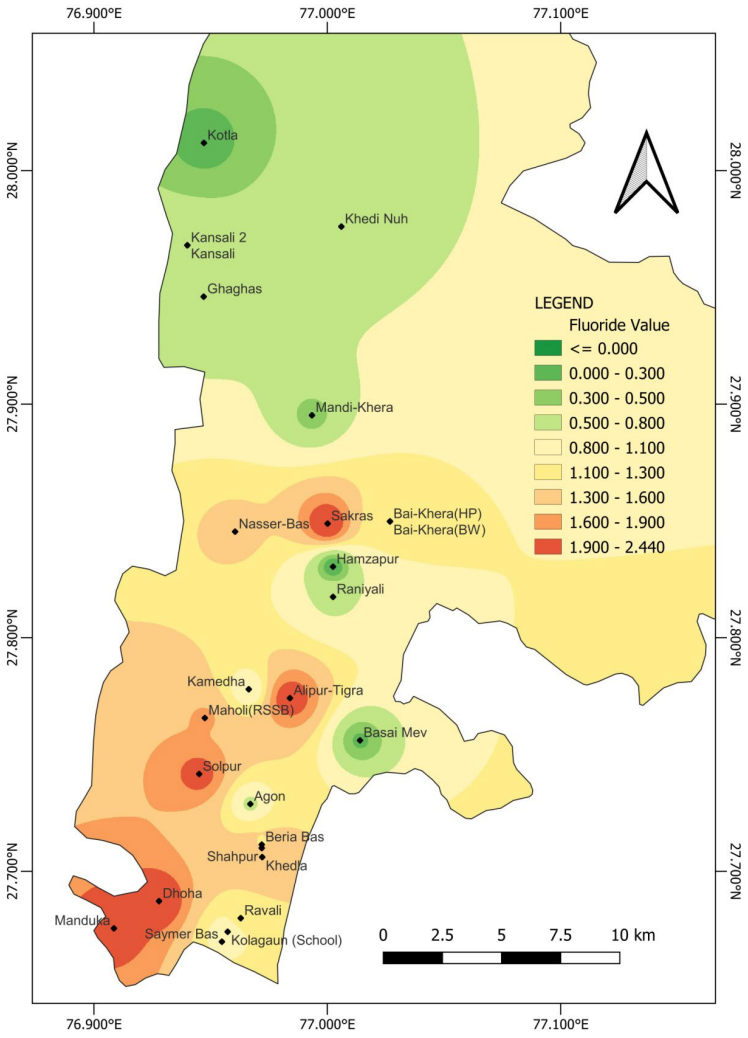

Fig. 5.46 Spatial distribution map of fluoride in Mewat district

5.5 Heavy metal analysis

It is very important to identify the relationship between the presence of heavy metals in drinking water and the prevalence of renal failure, liver cirrhosis, hair loss, and chronic anemia diseases. The prevalence of these diseases has markedly increased in the last few years due to air pollution, water pollution, and hazards over the use of pesticides in agriculture. Trace amounts of metals are common in water and these are normally not harmful to our health. Some metals are essential to sustain life. Calcium, magnesium, potassium, and sodium must be present for normal body functions, and cobalt, copper, iron, manganese, molybdenum, selenium, and zinc are needed at low levels as catalysts for enzyme activities. Naturally occurring metals are dissolved in water when they come into contact with rock or soil material. Other sources of metal contamination are corrosion of pipes and leakage from waste disposal sites. One of the major symptoms of chemical

toxicity seems to be a breakdown of the immune system, which opens the gateway for all kinds of diseases in the body. Also, another major symptom seems to be damage to the nervous system and increased nervousness. Toxic doses of chemicals cause either acute or chronic health effects. The levels of chemicals in drinking water, however, are seldom high enough to cause acute health effects. They are more likely to cause chronic health effects that occur long after exposure to small amounts of a chemical. Examples of chronic health effects include cancer, birth defects, organ damage, disorders of the nervous system, and damage to the immune system. A statistical summary is given in table 5.8.

Table 5.8 Min, max, and the average value of heavy metals with permissible limits defined by WHO (2007) and BIS (2012)

S. No	Metal ion (ppb)	Min.	Max.	Avg.	WHO (2007)	BIS (2012)
1	Pb	1.76	250.52	43.21	10	100
2	Cd	0.38	9.32	4.66	3	10
3	Cu	0.66	75.77	11.47	100	50
4	Ni	0.21	60.73	6.64	20	3000
5	Cr	0.54	28.65	3.37	50	50
6	Mn	3.03	760.95	126.40	100	100
7	Fe	10.0	59870.00	2491.09	300	300
8	Al	38.36	788.05	176.82	NA	NA
9	Zn	32.3	425.69	126.65	3000	5000

5.5.1 Lead and Cadmium

The concentration of lead in the drinking water samples ranged from 1.76 to 250.52 ppb with a mean of 43.21 ppb, the permissible limit of Pb is specified as 100 ppb by BIS (2012) and 10 ppb is specified by WHO (2007) for drinking water. Only one sample exceeded the acceptable limit (table 5.8). It can be inhaled in dust from lead paints, or waste gasses from leaded gasoline. Exposure to lead is cumulative over time. High concentrations of lead in the body can cause death or permanent damage to the central nervous system, the brain, and kidneys. This damage commonly results in behavior and learning problems (such as hyperactivity), memory and concentration problems, high blood pressure, hearing problems, headaches, slowed growth, reproductive problems in men and women, digestive problems, and muscle and joint pain.

On the other hand, the concentration of cadmium in the drinking water samples ranged from 0.38 to 9.32 ppb with a mean of 4.66 ppb, the permissible limit of Cd is specified as 10 ppb by BIS (2012) and 3 ppb is specified by WHO (2007) for drinking water. All the samples were within the acceptable limit by BIS (2012). Cadmium is generally classified as a toxic trace element. Geologic deposits of cadmium can serve as sources of groundwater and surface water, especially when in contact with soft, acidic waters. In low doses, cadmium can produce coughing, headaches, and vomiting. In larger doses, cadmium can accumulate in the liver and kidneys and can replace calcium in bones, leading to painful

bone disorders and renal failure. The kidney is considered to be the critical target organ in humans chronically exposed to cadmium by ingestion.

5.5.2 Copper, Nickel, and Chromium

The concentration of Copper in the drinking water samples ranged from 0.66 to 75.77 ppb with a mean of 11.46 ppb, the permissible limit of Cu is specified as 50 ppb by BIS (2012) and 100 ppb is specified by WHO (2007) for drinking water (table 5.8). Except for 3, all the samples were within the permissible limits of BIS (2012) and all samples were within the limit as per WHO (2007) guidelines. Copper is an essential substance to human life, but chronic exposure to contaminant drinking water with copper can result in the development of anemia, and liver and kidney damage.

Patients suffering from hair loss in this study were related to contaminant drinking water with nickel and chromium. Nickel is used as an alloy product, nickel-plating for anti-corrosion and in the manufacture of batteries. It is regarded as an essential trace metal but toxic in large amounts to human health. It is considered carcinogenic to humans and can cause worsening eczema for humans exposed to high levels of nickel. Hair loss patients are related to nickel contamination in drinking water and nickel can be related to derma toxicity in hypersensitive humans. The concentration of Ni in the drinking water samples ranged from 0.21 to 60.73 ppb with a mean of 6.63 ppb, the permissible limit of Ni is specified as 3000 ppb by BIS (2012) and 20 ppb is specified by WHO (2007) for drinking water. 16 % of the samples exceeded the permissible limits of WHO (2007).

On the other hand, chromium is essential to animals and humans. Chromium in excess amounts can be toxic, especially the hexavalent form. Chromium is used in metal alloys and pigments for paints, cement, paper, rubber, and other materials. Electroplating can release chromic acid spray and air-borne Cr-trioxide, both can result in direct damage to the skin and lungs. Also, chromium dust has been considered a potential cause of lung cancer. Sub chronic and chronic exposure to chromic acid can cause dermatitis and ulceration of the skin. Long-term exposure can cause kidney and liver damage, and damage to circulatory and nerve tissue also. The concentration of Cr in the drinking water samples ranged from 0.54 to 28.65 ppb with a mean of 3.37 ppb, the permissible limit of Cr is specified as 50 ppb by BIS (2012) and WHO (2007) for drinking water. All the samples were within the permissible limits of BIS (2012) and WHO (2007).

5.5.3 Manganese, Iron, Zinc, and Aluminium

Manganese is a known mutagen. The accumulation of Mn may cause hepatic encephalopathy. The concentration of Mn in the drinking water samples ranged from 3.03 to 760.95 ppb with a mean of 126.40 ppb, the permissible limit of Mn is specified as 100 ppb by BIS (2012) and WHO (2007) for drinking water. 30 % of the samples exceeded the permissible limits of BIS (2012) and WHO (2007).

Iron is an essential element in human nutrition. Estimates of the minimum daily requirement for iron depend on age, sex, and iron bioavailability and range from about 10

to 50 mg/day. As a precaution against the storage of excessive iron in the body, the Joint FAO/WHO Expert Committee on Food Additives (JECFA) established a provisional maximum tolerable daily intake (PMTDI) in 1983 of 0.8 mg/Kg of body weight which applies to iron from all sources except for iron oxides used as coloring agents, and iron supplements are taken during pregnancy and lactation. The concentration of Fe in the drinking water samples ranged from 0.01 to 59.87 ppm with a mean of 2.49 ppm, the permissible limit of Fe is specified as 0.3 ppm by BIS (2012) and WHO (2007) for drinking water. 26 % of the samples exceeded the permissible limits of BIS (2012) and WHO (2007).

Zinc occurs in small amounts in almost all igneous rocks. The concentration of Zn in the drinking water samples ranged from 32.30 to 425.69 ppb with a mean of 126.65 ppb, the permissible limit of Zn is specified as 5000 ppb by BIS (2012) and 3000 ppb is specified by WHO (2007) for drinking water. All the samples were within the permissible limits of BIS (2012) and WHO (2007). Acute toxicity arises from the ingestion of excessive amounts of zinc salts, either accidentally or deliberately as an emetic or dietary supplement. Vomiting usually occurs after the consumption of more than 500 mg of zinc sulfate. Fever, nausea, vomiting, stomach cramps, and diarrhea will occur after 3–12 h of ingestion.

Aluminum in drinking water can pose symptoms that are mild and short-lived. No lasting effects on health could be attributed to the known exposure to aluminum in drinking water. Aluminum in groundwater in the study area varies from 38.36 to 788.05 ppb with a mean value of 176.81 ppb.

5.6 Isotope Characterization

To understand the source of seasonal variation in groundwater salinity, 73 samples for pre-monsoon; 78 samples each from monsoon and post-monsoon in the years 2018 and 2019 were collected from different sites in the Mewat district, Haryana, and analyzed for $\delta^{18}O$ and δD. For the pre-monsoon season (April-May), the mean values of $\delta^{18}O$ and δD are -5.5‰ and -41.2‰; in monsoon, $\delta^{18}O$ is -5.6‰ and δD is -40.8‰; whereas for the post-monsoon season (October), $\delta^{18}O$ is -5.5‰ and δD is -42‰. The variation in mean values of the isotopic composition of the three seasons is small. Rozanski et al. (1993) examined the relationship between isotopic composition and temperature (T) for precipitation over India and showed that the seasonal ΔT is low and so there is little variation in isotopic composition $\delta^{18}O$ and δD. There is also a strong influence of Dansgaard's effect in the region. Precipitation during low rainfall months' experiences evaporation in low humid air columns, and d-excess correlates with the seasonal variation in the precipitation. The seasonal variability in the isotopic composition of precipitation gets captured by the groundwater samples.

To further examine the evaporation effect on groundwater of the study area, $\delta^{18}O$ is plotted against δD as shown in Fig 5.47. The slope of 5.64, 6.10, and 5.48 is observed for pre-monsoon, monsoon, and post-monsoon seasons respectively. Since the regression lines are subparallel to Global Meteoric Water Line (GMWL) given by Craig (1961) and LMWL (8.83) with slopes less than 8, it suggests the occurrence of evaporation before the

infiltration of water in the unsaturated zone (Krishan et al., 2020; Huang et al., 2012; Kulkarni et al., 1989).

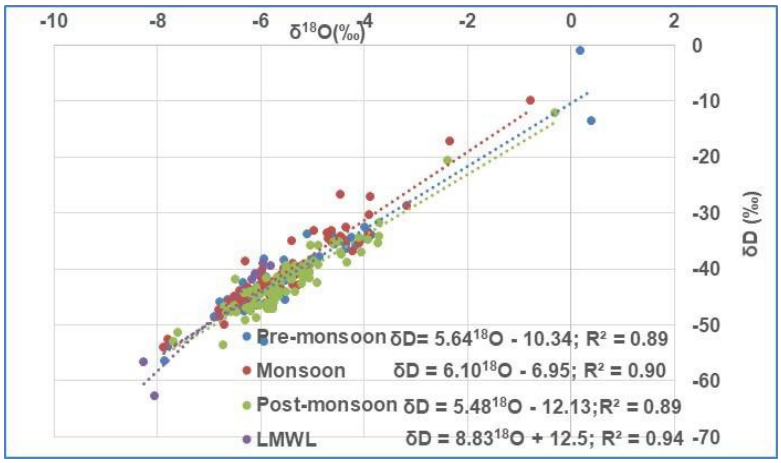

Fig 5.47 Isotope characterization of groundwater in Mewat

D-excess

Dansgaard (1964) proposed the use of deuterium excess (d) represented by:

$d = \delta D - 8\delta^{18}O$…….....(5.5)

Before the precipitation reaches the ground surface it undergoes evaporation and a relative abundance of $\delta^{18}O$ with respect to δD can occur. The decline in deuterium excess represents the evaporation, on the degree of negative correlation in equation (3) represents the intensity of evaporation taking place in the area for a particular season.

During the process of evaporation, equilibrium is set between the surface layer of water reservoir where water molecules are removed and in the adjacent ambient air where water molecules are being exchanged, leads to isotopic fractionation and described by the Rayleigh Equation.
$R = R_O f^{(\alpha v\text{-}l\text{-}1)}$……(5.6) (Clark and Fritz, 1997)
where, f is the remaining fraction of the water body; $\alpha_{v\text{-}l}$-1 is the fractionation factor between product (vapour) and reactant (liquid water) including equilibrium and kinetic fractionation.

Combining equations (5.5) and (5.6) yields
$\delta = (R_O f^{(\alpha v\text{-}l\text{-}1)}/R_{reference} - 1) \times 1000$
$= (\delta_o + 1000) f^{(\alpha\text{-}1)} - 1000$……(5.7) (Huang and Pang, 2012)

Using eqns (5.7) and (5.5), d excess can be obtained, as represented by equation (6)
$d = (\delta oD + 1000) f^{(\alpha D\text{-}1)} - 8 (\delta o^{18}O + 1000) f^{(\alpha 18O\text{-}1)} + 7000$…(5.8) (Huang and Pang, 2012)

where, $\delta_o D$ and $\delta_o{}^{18}O$ are initial δ values of water. Huang and Pang (2012) showed that at constant temperature and constant relative humidity, two water samples with different isotopic compositions the same salinity, when subjected to evaporation, have similar changes in d and f, independent of initial isotopic composition $\delta_o D$ and $\delta_o{}^{18}O$.

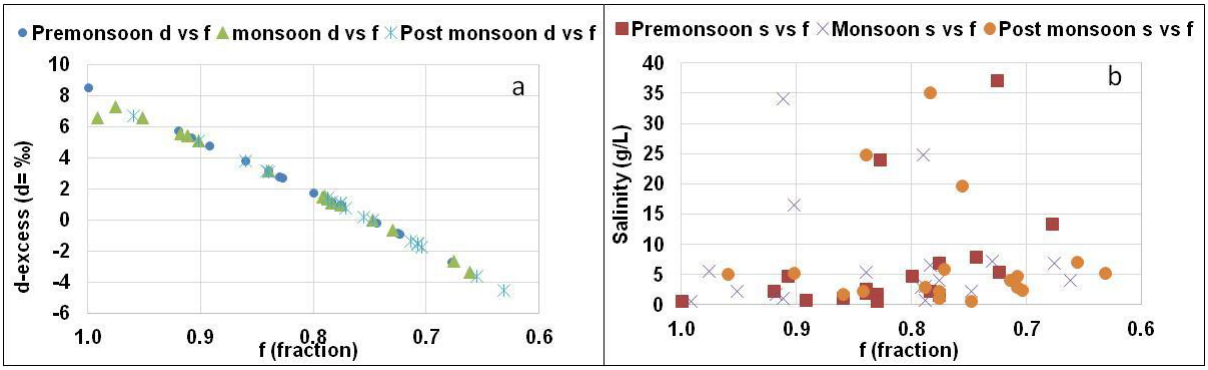

Fig 5.48 Seasonal variations in d-excess (a) and salinity (b) versus remaining fraction in Mewat, Haryana

For every value of d-excess, there is a specific value of fraction 'f', the initial salinity will be salinity of source water as 'S'. Contribution of evapo-concentration (E_c) and mineral dissolution (M_d) will be as below:

$E_c = S/f_i - S$ .....(5.9)

$M_d = S_o - S/f_i$ .....(5.10)

Where S is Initial salinity (salinity of source water); f_i is fraction value of the sample; S_o is salinity value of sample

Table 5.9 Salinity and isotopic parameters for the source water at Kotla

Parameter	Pre-monsoon	Monsoon	Post-monsoon
$\delta^{18}O$	-6.78	-7.88	-7.59
δD	-46	-53.97	-51.33
d-excess	8.24	9.07	9.39
Temperature (K)	305.75	304.88	300.25
Humidity (h)	0.265	0.768	0.493
Salinity (g/L)	0.05	0.53	0.31
Fraction (f)	0.756	0.36	0.45

For a detailed analysis of d-excess and salinity variations in different seasons, the isotope data for the year 2018 was analyzed in detail and seasonal variations in d-excess, remaining fraction, and salinity during evaporation are shown in fig 5.48. It is found that salinity increases and d-excess decreases during evapo-concentration in all seasons. There is a linear relationship between d-excess and remaining fraction in all three seasons in all samples; more scatter is found in salinity and remaining fraction values in 16% of the samples indicate seasonal variations. Huang and Pang (2012) found that the salinity is doubled when half of the water is evaporated due to evapo-concentration and a decrease in deuterium excess from 10‰ to -9.7‰.

Table 5.10 Season-wise salinity (TDS), deuterium excess (d), the remaining fraction (f), contribution percent of initial salinity, evapo-concentration, and mineral dissolution (D) for groundwater in Mewat

	Salinity (S-g/L); d-excess (d-ex ‰); fraction (f)									Salinity source contribution (%) IS-Initial salinity; EC-Evapoconcentration; MD-Mineral Dissolution								
	Pre-monsoon			Monsoon			Post monsoon			Pre-monsoon			Monsoon			Post monsoon		
	S	d-ex	f	S	d-ex	f	S	d-ex	f	IS	EC	MD	IS	EC	MD	IS	EC	MD
Ghagas village	1.8	2.8	0.83	6.6	1.1	0.78	5.3	-4.5	0.63	2.97	0.61	96.42	7.95	2.19	89.87	5.90	3.44	90.66
Kansali	4.7	5.3	0.91	6.9	-2.6	0.68	7.1	-3.6	0.66	1.12	0.11	98.76	7.61	3.65	88.75	4.36	2.29	93.35
Ghagas SF	2.6	3.2	0.84	3.0	1.5	0.79	2.9	-1.5	0.71	2.06	0.39	97.55	17.44	4.58	77.98	10.56	4.36	85.08
Doha	4.8	1.8	0.80	4.1	-3.4	0.66	2.4	-1.7	0.70	1.11	0.28	98.61	12.98	6.63	80.39	12.82	5.39	81.79
Kankarkhedi	24.1	2.7	0.83	24.9	1.6	0.79	24.9	3.1	0.84	0.22	0.05	99.73	2.12	0.56	97.32	1.24	0.24	98.52
Nanglibhundi	6.9	1.0	0.78	5.7	7.3	0.98	5.2	6.8	0.96	0.77	0.22	99.01	9.28	0.23	90.50	5.99	0.25	93.77
Pat khori	1.9	3.0	0.84	0.9	1.4	0.79	1.1	1.1	0.78	2.79	0.53	96.68	60.51	16.28	23.22	27.69	7.99	64.32
Dhadoli	2.3	5.7	0.92	2.4	0.0	0.75	2.4	1.1	0.78	2.29	0.20	97.51	22.41	7.55	70.04	13.18	3.81	83.01
Basai	0.7	2.8	0.83	3.2	1.4	0.79	3.0	1.4	0.79	8.10	1.66	90.23	16.70	4.49	78.81	10.40	2.80	86.81
Naharika	1.2	3.8	0.86	4.0	1.0	0.78	4.1	-1.3	0.71	4.59	0.75	94.66	13.04	3.77	83.19	7.55	3.02	89.43
Kaliketa	1.7	1.0	0.78	1.7	5.6	0.92	5.2	5.1	0.90	3.15	0.91	95.94	30.14	2.69	67.17	5.95	0.65	93.40
Mohmmad Khedi	2.3	1.2	0.78	2.2	6.6	0.95	2.3	3.1	0.84	2.33	0.64	97.03	23.48	1.18	75.34	13.61	2.55	83.84
khurd	0.8	4.8	0.89	1.1	5.4	0.91	1.7	3.8	0.86	6.53	0.79	92.68	47.93	4.63	47.44	17.86	2.91	79.23
Raja kapul	0.7	8.5	1.00	0.6	6.6	0.99	0.6	0.0	0.75	7.75	0.00	92.25	81.76	0.66	17.58	48.65	16.39	34.96
Gouhana	5.5	-0.9	0.72	5.4	3.2	0.84	5.9	0.8	0.77	0.96	0.37	98.67	9.75	1.86	88.40	5.28	1.56	93.17
Nagla shahpur	37.1	-0.8	0.73	34.2	5.4	0.91	35.1	1.2	0.78	0.14	0.05	99.80	1.54	0.15	98.31	0.88	0.24	98.87
Saral	7.9	-0.1	0.74	7.2	-0.7	0.73	4.8	-1.5	0.71	0.67	0.23	99.10	7.32	2.71	89.97	6.50	2.68	90.82
Jaitako	13.4	-2.7	0.68	16.5	5.1	0.90	19.8	0.2	0.76	0.40	0.19	99.42	3.20	0.35	96.46	1.57	0.51	97.93
Min	0.7	-2.7	0.68	0.6	-3.4	0.66	0.6	-4.5	0.63	0.14	0.00	90.23	1.54	0.15	17.58	0.88	0.24	34.96
Max	37.1	8.5	1.00	34.2	7.3	0.99	35.1	6.8	0.96	8.10	1.66	99.80	81.76	16.28	98.31	48.65	16.39	98.87
Mean	6.7	2.4	0.82	7.3	2.6	0.83	7.4	0.8	0.77	2.66	0.44	96.89	20.84	3.56	75.59	11.11	3.39	85.50
Stdev	9.5	2.7	0.08	9.0	3.2	0.10	9.4	2.9	0.08	2.52	0.41	2.79	21.80	3.85	23.63	11.45	3.81	15.13

The summary of water samples collected from Kotla is taken as a reference and given in Table 5.9. As can be seen from Table 5.9, a relation between d-excess, f, and salinity exists. In the monsoon period, the salinity value is highest at 0.53g/L; because these monsoon months have heavy rainfall, mineral dilution occurs, along with higher evaporation which is reflected in the lower values of fraction (f). In the post-monsoon period, with its lower temperatures, the evaporation decreases (f=0.45) and the salinity comes down to 0.31g/L. In the pre-monsoon period, the fraction (f) increases drastically and the salinity shows a decline to 0.05g/L. This was possible because the groundwater level start to rise during pre-monsoon seasons. Dilution of the regional water source by rainfall recharge can be seen in the declining salinity. To understand the contribution of initial salinity, evaporation,

and mineral dissolution, the values of d-excess, TDS, and fraction after evaporation are calculated and tabulated in Table 5.10.

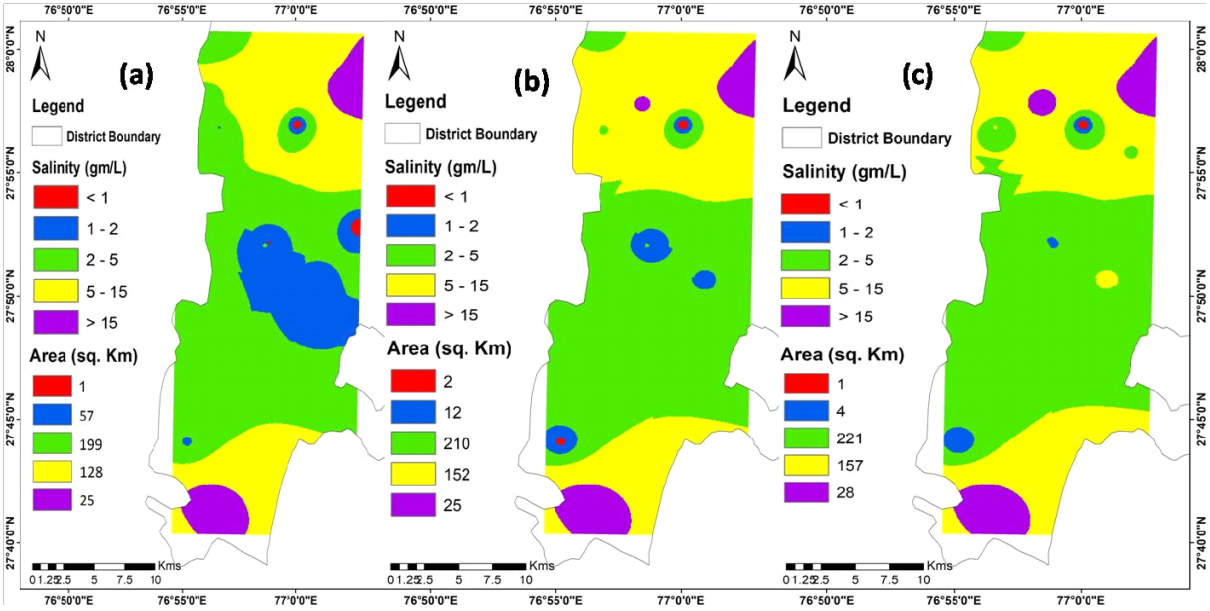

Fig 5.49 Seasonal (a- pre-monsoon; b -monsoon; c- post-monsoon) variation in groundwater salinity in Mewat

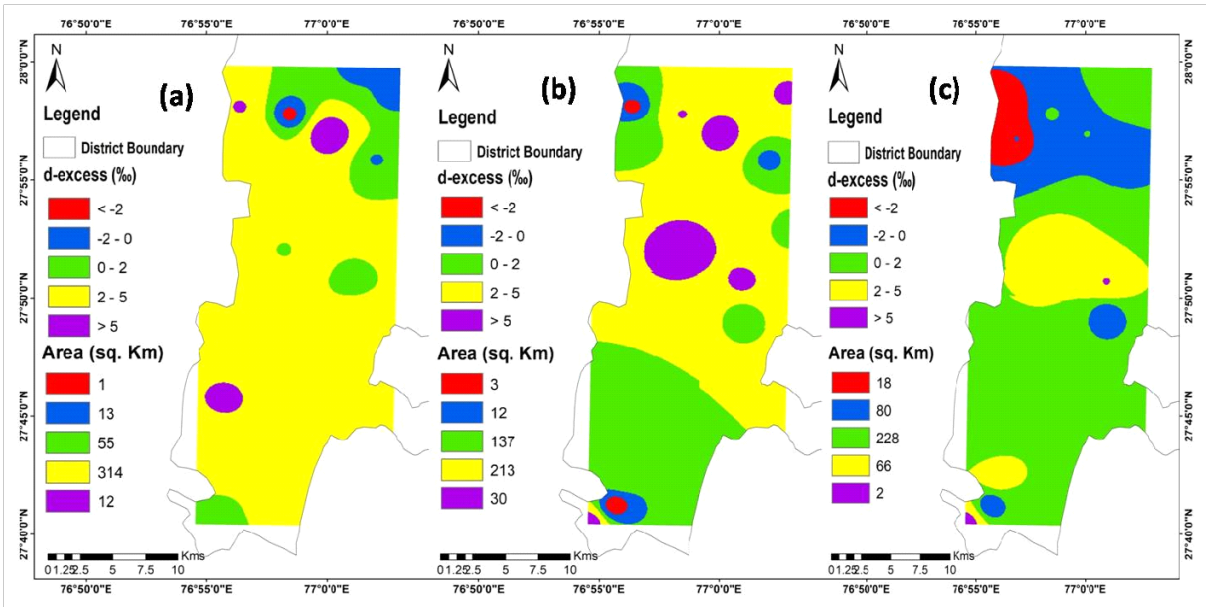

Fig 5.50 Seasonal (a- pre-monsoon; b- monsoon; c- post-monsoon) variation in d-excess in Mewat

The value of d-excess depends upon the temperature and humidity values in the area. The seasonal variability in salinity and d-excess are shown in Fig 5.49 and 5.50, respectively.

It has been observed that the groundwater of the district showed an increase of 0.7g/L salinity from pre-monsoon (6.7g/L) to post-monsoon season (7.4g/L).
The d-excess shows a decline of 1.6‰ in post-monsoon when compared to pre-monsoon, it decreases from 2.4‰in pre-monsoon to 0.8‰ in post-monsoon, which is as per the observations of Dansgaard (1964).

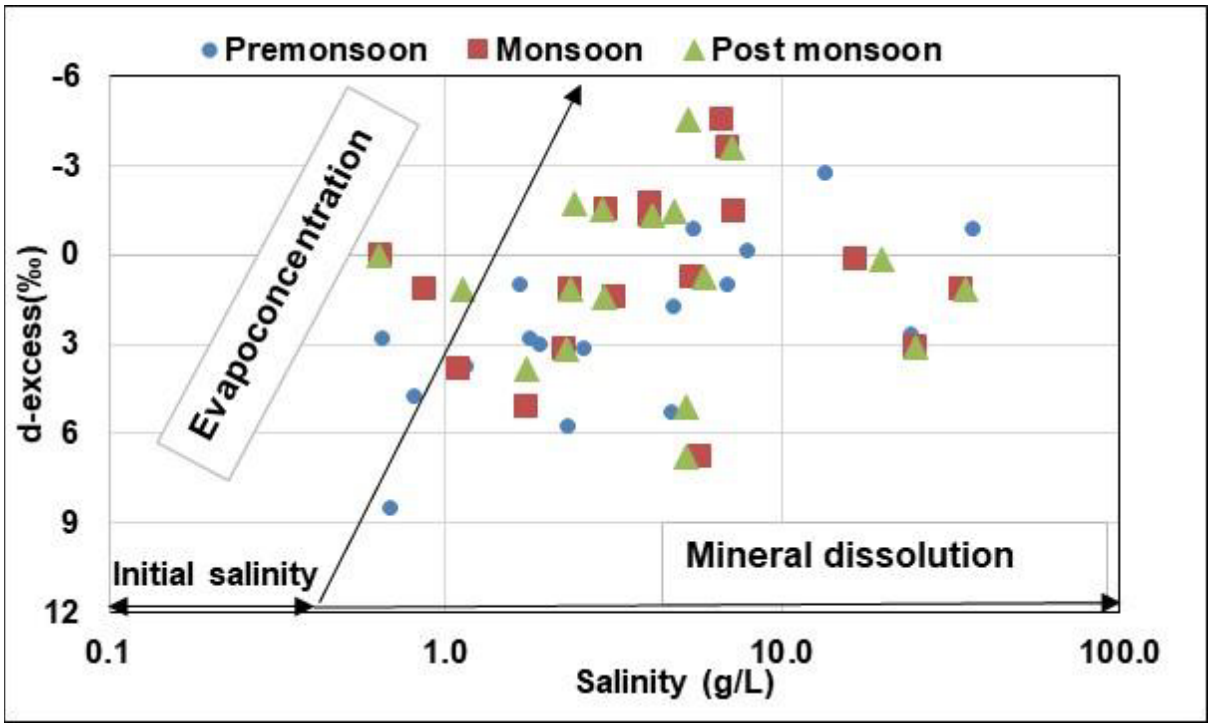

Fig 5.51 Season-wise contribution of evapo-concentration and mineral dissolution to total salinity in Mewat

Similar results showing control of seasons and climates were reported in precipitation and air moisture samples by Unnikrishnan Warrior et al. (2010); Purushothaman et al. (2012); Saranya et al. (2018) and Aneesh et al. (2019). The percent area under salinity values of > 2 g/L increased from 86% in pre-monsoon to 99% in post-monsoon while the percent area with d-excess <0‰ increased from 4% in pre-monsoon to 25% in a post-monsoon season which indicates the increase in the saline affected area.

The sources of salinity (initial salinity, evaporation, and mineral dissolution) in different seasons are shown in Fig 5.51. The contribution of evaporation in total salinity is calculated using d-excess. It was found that in the pre-monsoon season salinity was due to mineral dissolution. However, in the monsoon and post-monsoon seasons, initial salinity also contributes to salinity. Percent area in groundwater salinity with s contribution of >2% from evapo-concentration increased from 0% in pre-monsoon to 94%, with contributions of 2-8% in groundwater salinity.

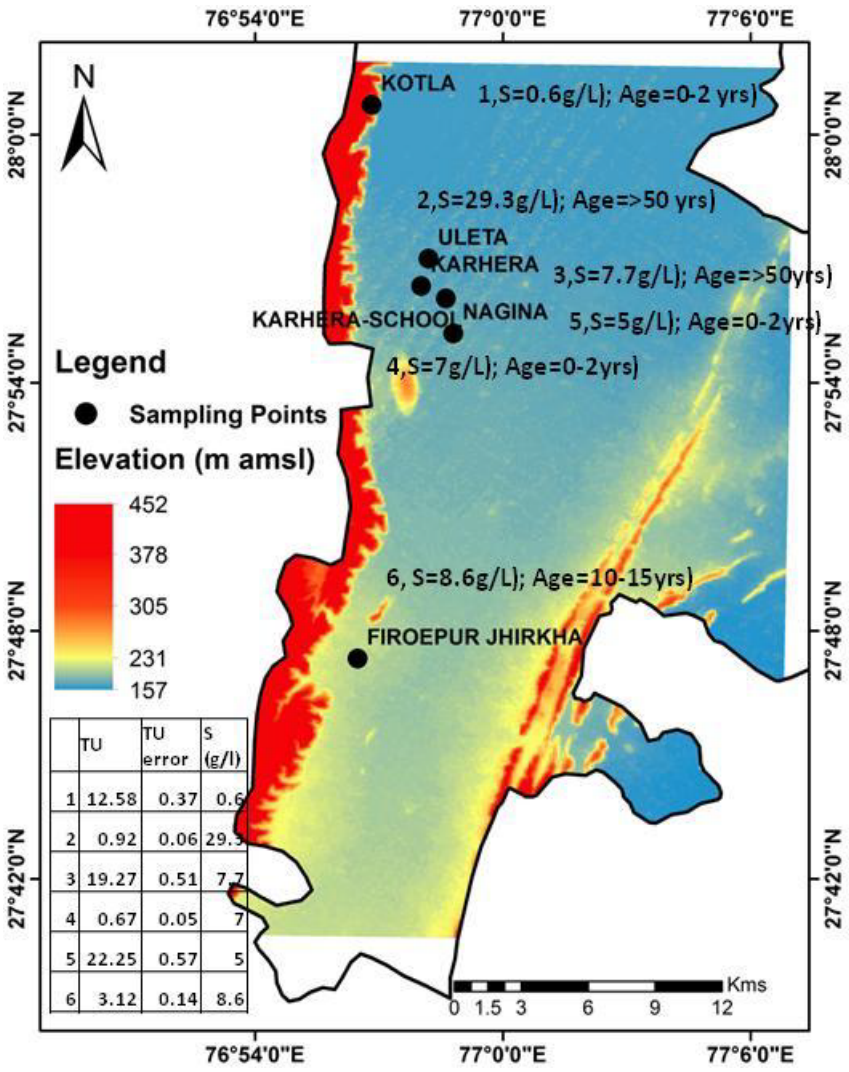

Fig 5.52 Groundwater age distribution using tritium in Mewat

The contribution of mineral dissolution is found by separating the salinity value of evaporation from dissolution; the results were further tested by using Tritium (^3H) to distinguish between modern groundwater (recharge occurring during the last 60 years) and pre-modern groundwater (recharge occurring >60 years). Fig 5.52 shows the groundwater age map for the region along with the contribution of mineral dissolution in different seasons. Considering the ^3H input sequence of precipitation in the region with average values of 8-10 TU but the TU is observed as high as 22. The decayed results show that groundwater ^3H with the content below 2 TU was likely recharged more than 60 years ago. This shows that groundwater has a long residence time in high saline-affected areas. A majority of the samples show a contribution from mineral dissolution in the pre-monsoon season, with a slight decrease in monsoon and post-monsoon seasons. There is wide variation in tritium activities, probably due to discontinuous water flow or poor connectivity between aquifers. In some samples, high tritium activities correspond to percolation from nearby artificial tritium sources (Ramaroson et al., 2018).

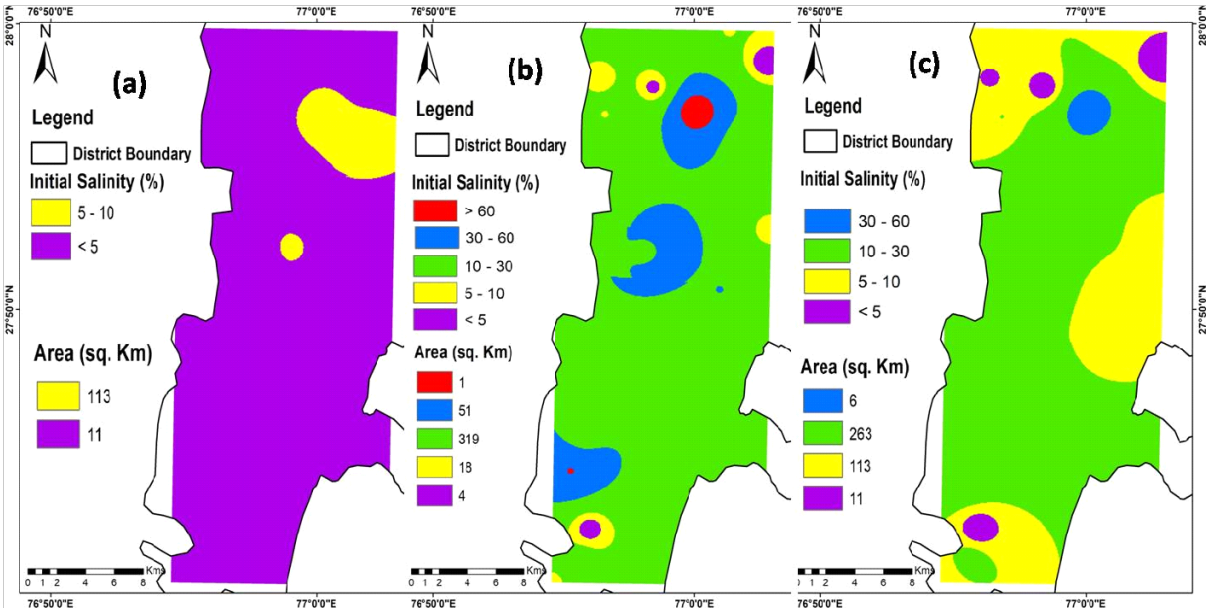

Fig 5.53 Seasonal (a-pre-monsoon; b-monsoon; c- post-monsoon) variation in percent contribution of initial salinity in groundwater salinity in Mewat

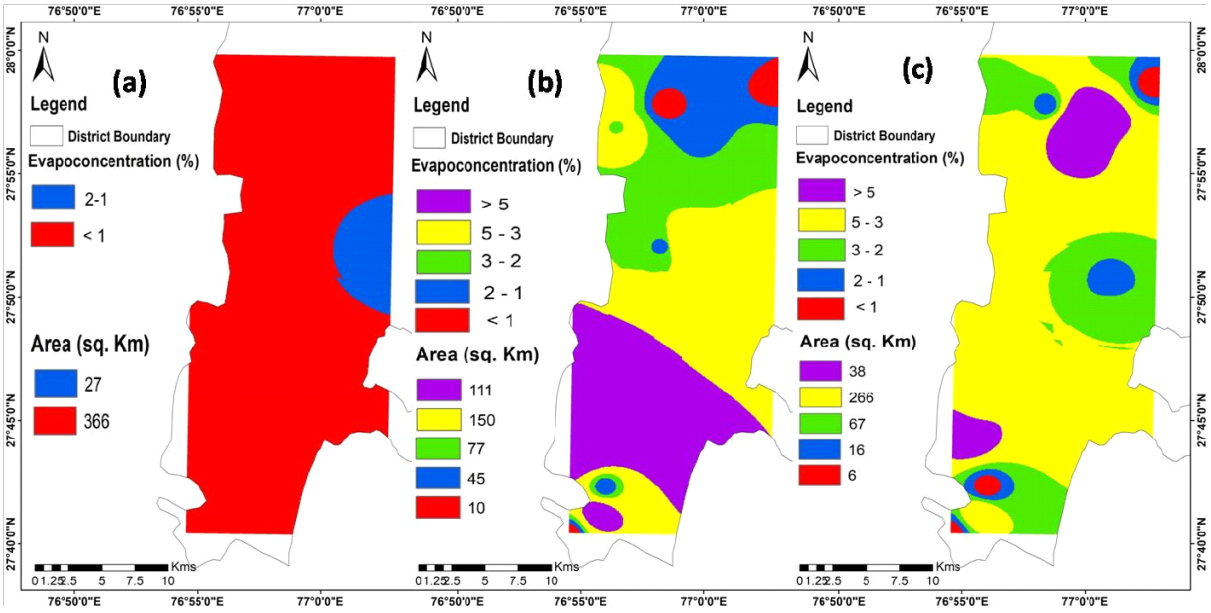

Fig 5.54 Seasonal (a-pre-monsoon; b-monsoon; c- post-monsoon) variation in percent contribution of evapo-concentration in groundwater salinity in Mewat

Similar observations to isotope analysis were found using Principal Component Analysis (PCA), KMO and Bartlett's tests were found valid for both the years 2018 & 2019, and PCA is found suitable for the study area. Three principal components were selected based on the Eigen value which explains 79.58% and 85.08% of total variation in the year 2018 and 2019 respectively. The first Principal component (PC-1) is identified with salinity is

governed by rock-water interactions and agricultural return flow. The second Principal component (PC-2) with alkalinity and the third Principal component (PC-3) described the pollution.

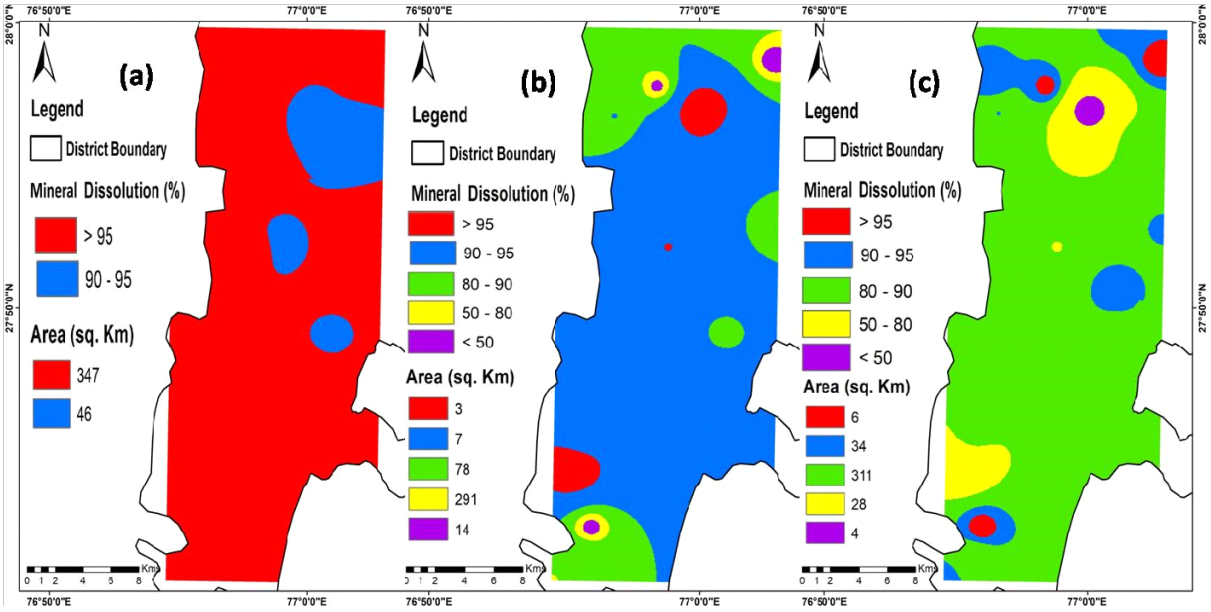

Fig 5.55 Seasonal (a-pre-monsoon; b-monsoon; c- post-monsoon) variation in percent contribution of mineral dissolution in groundwater salinity in Mewat

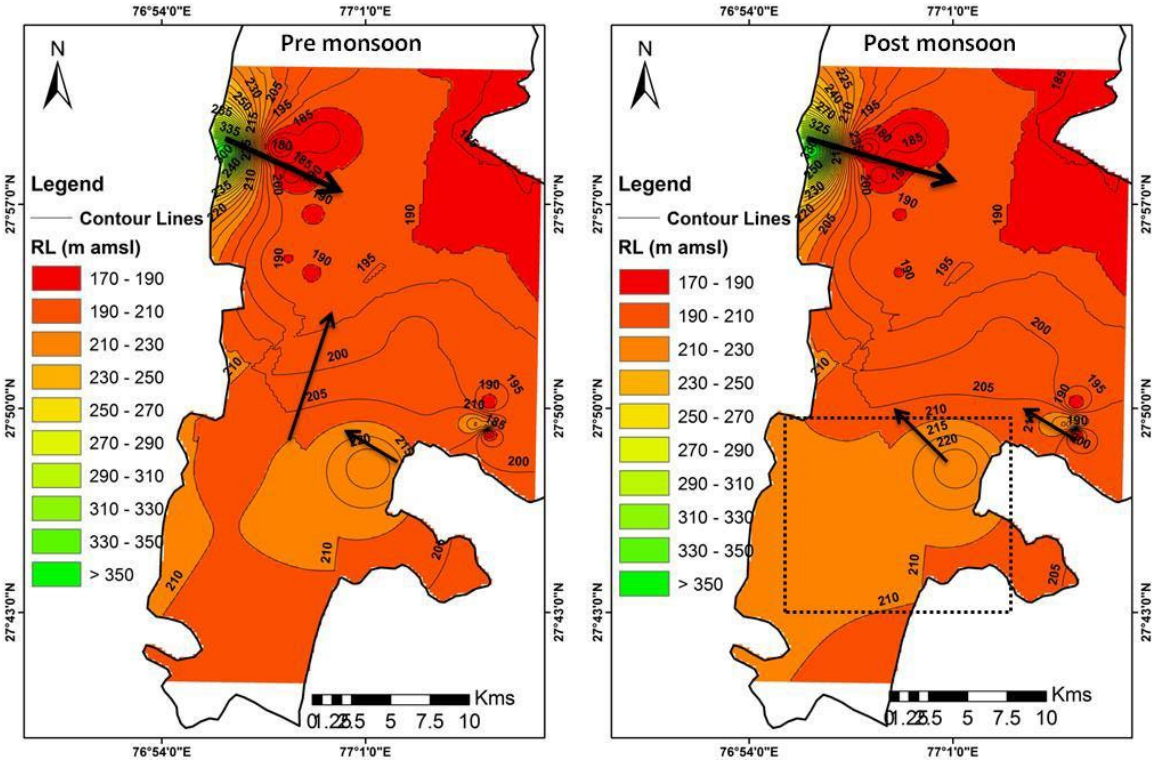

Fig 5.56 Water level map of the study area (2020)

The contributions from initial salinity, evapo-concentration, and mineral dissolution in groundwater in the study area are given in Table 5.10 and their spatial distribution is shown in figs. 5.53, 5.54 and 5.55. Mineral dissolution contributes to most of the groundwater salinity (76–97%). A decrease in the contribution of mineral dissolution occurs in the monsoon season as the initial salinity contribution increases to as high as 21%. This is due to the increased groundwater recharge and mobilization of accumulated salts in soils either naturally or anthropogenic sources. This has also been explained in figure 5.56, showing an increase in water level in salinity affected the central part in the post-monsoon season. Allison and Schonfeldt (1990) and Simpson and Herczeg (1991) have also reported the mobilization of salts in the Murray river basins, Australia due to hydrological regimes and land uses. In addition to land use changes in arid and semi-arid environments, irrigation and groundwater exploitation can also cause an increase in salinity (Williams, 1999).

The percent area in groundwater salinity with contributions of <5% from initial salinity was 93% in pre-monsoon season but changed to 97% of area having a contribution from initial salinity >5% in post-monsoon season (Fig 5.53). This may be due to the spread of mobilized salt to more areas. The percent area in groundwater salinity with contributions of >2% from evapo-concentration increased from 0% in pre-monsoon to 94% with the contribution of 2-8% in groundwater salinity (Fig 5.54). The mineral dissolution contribution of > 95% in groundwater salinity in the pre-monsoon season was in >88% of the area but it reduced to 80-90% contribution in groundwater salinity in 79% of the area (Fig 5.55). These results are very useful in understanding the salinity mechanisms in the area, and their relationship with the surrounding environmental phenomenon like the monsoon can play an important role in making sensible water resource management decisions (Adams et al., 2001).

Fig 5.56 depicts the water level map of the study area. It is evident from the figure that water tables are deeper in the western region. The water is potable in these areas and resulting in higher water withdrawals. In the eastern and southern sides of the study area, water is saline, and water tables are high. The contours of water level show a natural gradient from the Aravalli hills towards the central region but due to high groundwater extraction in the foothills regions of the area, there is the apprehension of movement of water from salinity-affected areas to freshwater areas. Seasonal effects were found in the water levels, in post-monsoon seasons, the water levels increased by 18% in the southern/south-western region of the study area as compared to the pre-monsoon season. This rise was found in the water level class of 210-230 m. There are possibilities of a change in salinity mechanism due to the rise in groundwater levels due to precipitation.

5.7 Aquifer storage and recovery

In face of climate change and the burgeoning human population, keeping an adequate freshwater supply is essential. The sporadic occurrence of freshwater resources is further exacerbated by land-use changes, vast agricultural developments, deforestation, and above all, contamination. Groundwater accounts for 30% of all available fresh water on the earth and is still the most reliable source of water supply. In regions, which have no access to

surface water resources, communities, agriculture, and industries are heavily dependent upon groundwater. However, many such areas are threatened by groundwater scarcity due to over-abstraction, climate change, and groundwater contamination; both anthropogenic and geogenic. All these threats make it more difficult for societies to access free water and do their daily chores. As a resilient society, we have to devise some cost-effective and efficient ways to remediate these natural resources and make them available for common use.

Many methods for groundwater remediation have been invented in the last century. The use of every method depends primarily upon the hydrogeology and chemical, physical, economical, and social feasibility of the technique. Amongst them, one such technique is Aquifer Storage and Recovery which has emerged as a boon to semi-arid areas in providing freshwater supply at a very low cost.

Aquifer Storage and Recovery (ASR) is a water management technique for actively storing excess freshwater during wet periods and recovering during dry periods (fig. 5.57). It presents a viable option to harness the full potential of groundwater. As the name suggests, freshwater from different surface sources like rainwater, reservoirs, ponds, rivers, and desalinated water can be stored temporarily in a subsurface environment for future recovery and use. Think of ASR as a storage unit, which is either physically or chemically bound from all sides to confine freshwater within the unit. Physical boundaries are impermeable stratigraphic units that don't allow the movement of water. However, chemical boundaries are created by the difference in fluid properties like salinity and density, these boundaries emerged as a mixed zone in the system.

Throughout the world, ASR has been successfully implemented at numerous sites and proved very efficient. More than 175 active ASR well fields are operational in the United States (Dillion et al., 2019), followed by Australia, Europe (Sprenger et al., 2017), Latin America, the Arabian peninsula, and South America. ASR is more suitable and effective than other available remediation options because of several reasons:

1. Large quantities of water can be recovered. Since ASR harnesses the potential at the aquifer level, a huge volume of water can be stored and recovered from the ground, providing freshwater supply from household level to state level. The stored water can be used for seasonal or yearly groundwater supply.

2. The biggest advantage of ASR is that it is cost-effective and easy to implement. A simple injection of freshwater with prior subsurface knowledge is required to implement this method. Due to its cost-effectiveness, it's very favorable for developing low-income communities. The easy and handy implementation makes it a very common method of remediation.

3. Stored water is normally free from environmental or organic pollutants. If we store the excess water in open surface storage like ponds, rivers, and lakes. They are prone to develop more organic and inorganic contaminants. Several diseases may rise like malaria and dengue if large quantities of water are left open. To further use

them, we need an extra step to check for contamination and clean for organic pollutants. However, ASR is closed from all sides and it's very unlikely that they develop any organic contaminants but care must be taken in choosing the specific site of the ASR because the presence of organic sediments in the subsurface might pollute the water. Moreover, surficial processes like runoff and dumping cannot affect subsurface storage.

4. It has a negligible surface footprint. Neither it needs any kind of treatment nor any large surface facility, so the surface below which ASR is operating can be used for all purposes and would not affect the community.

5. Lastly, no evapotranspiration losses occur in ASR operations. Since the stored water is not in direct contact with the sunlight or plant species, evaporation losses are negligible in this method. Evaporation is a major concern for water-stressed communities and significantly accounts for losses from surface storage. Some studies have shown that ET can take up to 30 percent of stored water which is very significant and can increase the salinity of the stored water.

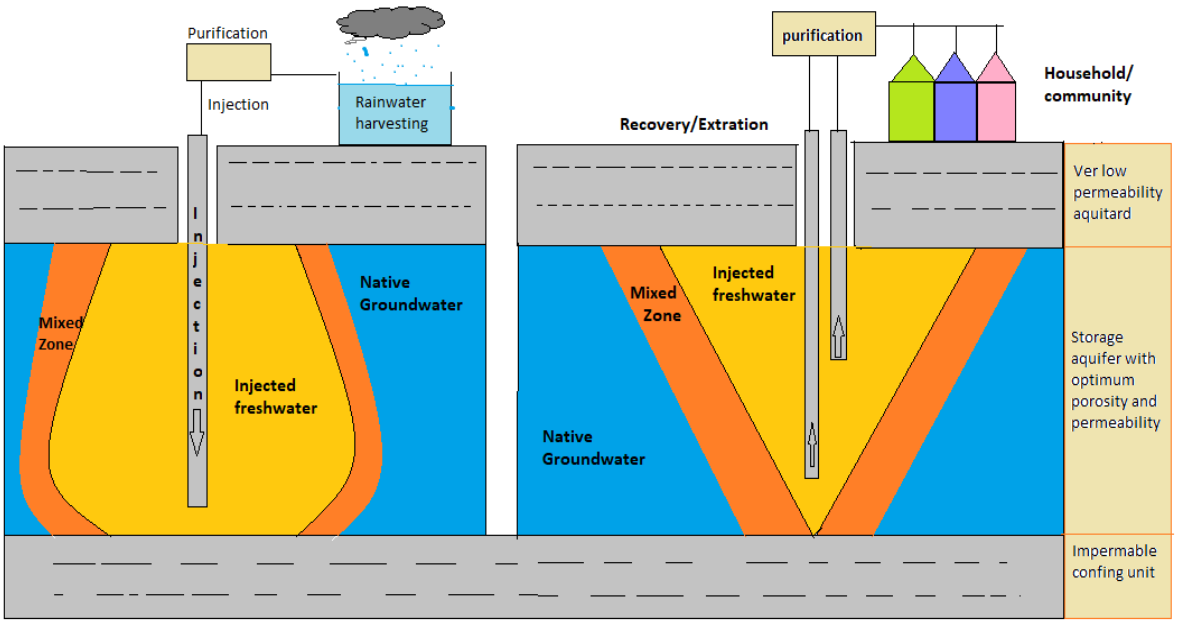

Figure 5.57 Aquifer storage and recovery. The left side image is the injection phase and the right side image is the recovery phase

5.7.1 Historical Development

Historical development and use of ASR are presented in table 5.11. The concept of ASR in brackish water was first proposed by Cederstrom (1947), after which a lot of literature was published describing the phenomenon of water bubbles. The most common factors

that lead to the mixing of freshwater and saline water are dispersion and gravity segregation or free convection. Anthropogenic factors like sporadic pumping lead to mixed/forced convection. According to Esmail and Kimbler (1967), dispersion effects mean if two miscible fluids are in sharp contact, they will slowly diffuse into each other. After some time, initially sharp contact will form a mixed zone. This diffusion results from the random motion of ions of two fluids. The distribution of ions across an arbitrary plane can be represented through Fick's Law. The density contrast between the native saline water and stored freshwater causes the density/buoyancy-driven flow and causes the mixing of the saline and freshwater. Since freshwater is less dense compared to saline water, it tends to flow and remain above the saline-fresh interface. The buoyancy-driven flow causes the saline water to intrude in the lower part of the ASR zone and reduce the recovery efficiency. To reduce these effects, reservoir operation must be taken care of the sites that have very low vertical hydraulic conductivity should be selected to restrict the vertical flow of groundwater. The density effect is also called "gravity segregation" or "buoyancy stratification". experimentally studies the dispersion and gravity segregation in the synthetic sandstone aquifer model and later confirms the observed results with then available computer programs. Esmail and Kimbler (1967) find out that the density effect impacts recovery efficiency more strongly than dispersion effects. They also observed the wider mixing zone suppressing the interface tilt and concluded that storage of fresh water in saline water is feasible under low permeability, small density contrast, low storage period, and high flow rate. The previously thought cylindrical plume is now viewed as a conical plume that reduces the volume of recovered water. For this experiment, they used separate models to study the density and dispersion effects. Later (Kumar and Kimbler, 1970) combined both models and used a pear-shaped model representing 45 degrees of a circle. The major objective of the experiment was to validate the assumption that previously sought the effect of gravitation segregation in the flowing system by expanding it to the radial flow system. Furthermore, it was found that recovery efficiency can be increased by increasing the injection-abstraction cycle.

Furthermore, in an array of papers by Ward, a numerical modeling approach was used to explore the influence of controlling variables on ASR in saline water. Ward et al., 2007 concluded that widening the mixing zone reduces the density contrast and hence the impact of the density effect confirming the assertion of Kumar and Kimbler (1970). Ward et al., (2008) further found that the greater the permeability contrast in layer aquifer and higher the anisotropy inhomogeneous aquifer restrict the vertical flow due to density effect and increase the recovery efficiency. To encounter the negative impacts Zuurbier et al., (2014) set up multiple partially penetrating wells, which inject fresh water into deeper aquifers and recover water from the open well casing in shallow aquifers. The numerical modeling demonstrated that 40% recovery efficiency can be achieved compared to 15% efficiency in a single penetrated well. To further investigate Witt et al., (2021) built a plexiglass tank and dyes to visualize the shape of both fresh and saline water bodies and investigate the recovery efficiency due to multiple penetrating wells. The results corroborate the previous efficiency. To further maximize the recovery efficiency, Zuurbier et al., (2015) experimented with horizontal directional drilled wells (HDDW) in the Netherlands, where they achieved 100% recovery efficiency of injected 4200 m3 injected water, demonstrated by numerical groundwater flow models.

Table 5.11: Aquifer Storage and Recovery- historical perspective (Jay Prakash, 2021)

S.No.	Operating year	Place	Storage zone	Total no. of active ASR systems
1	1956	Israel	Sandstone	100
2	1968, 1972, 1994	Wildwood, Gordons Corner, Murray Avenue- New Jersey	Sand, clay Sand	4
3	1978, 1992	Goleta, Pasadena- California	Clay Sand, Silty sand	11
4	1983	Manatee, Florida	Limestone	15
5	1985, 1987, 1989, 1993	Peace River, Cocoa, Port Malabar, Boynton Beach- Florida	Limestone	15
6	1988	Las Vegas, Nevada	Valley fill	3
7	1989	Scotch College, South Australia	Fractured rock	1
8	1990	Chesapeake, Virginia	Sand	1
9	1990	Netherland	Sand	2
10	1991	Kerrville, Texas	Sandstone	3
11	1992, 1994	Washington	Sand	3
12	1993	Andrew's Farm, South Australia	Tertiary Limestone	1
13	1994	Utah	Sand	1
14	1994	Netherland	Sand	4
15	1995	South Australia	Fractured rock	1
16	1995	The Paddocks, South Australia	Tertiary Limestone	1
17	1999, 2002	Bolivar, South Australia	Limestone	2
18	2001	Northgate, South Australia	Tertiary Limestone	1
19	2012	Australia	Sand	1
20	2019	Sundarbans, India	Sand	1
21	2021	Mewat, India	Sand	1

Laboratory experimentation was done in this study to measure the viability of Aquifer Storage and Recovery (ASR) as a remediation option in the saline aquifers of Mewat, Haryana.

Experiment no. 1

An experimental model was used to conceptualize the aquifer with dimensions of a length of 125 cm, a width of 58 cm, and a height is 153 cm (Fig 5.58). In this experiment, NaCl salt was used to make the solution of the desired concentration. The other materials required for this experiment were two pumps (1HP), P.V.C. pipe, elbow and chuck valve, and a few small tools.

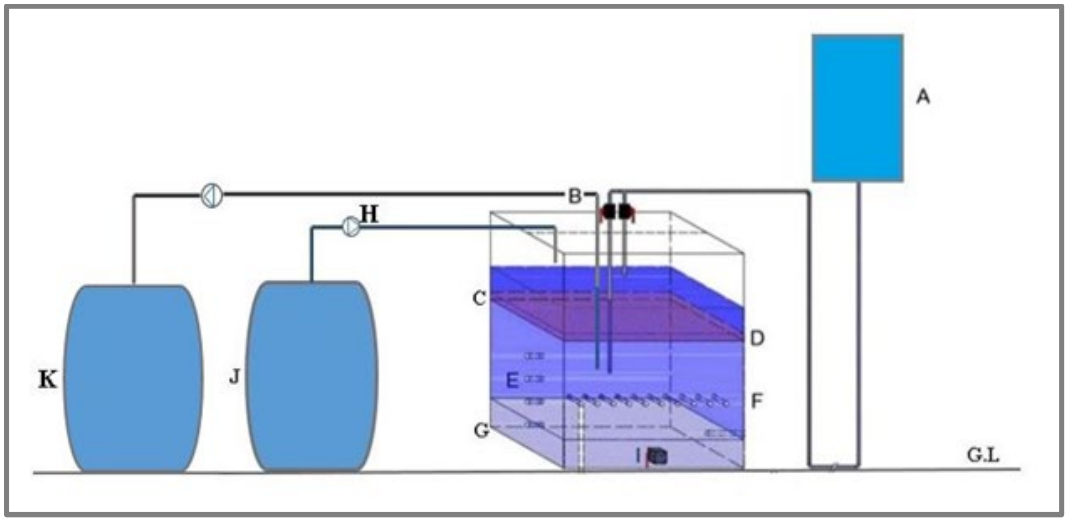

Figure 5.58 Experimental model setup -1

In this model, a prototype aquifer was developed using sand. The tank in the experimental model was used as an artificial aquifer where the sand was filled to half of the total depth (1.0 meters) of the aquifer/model and poured the saline water measuring 100 liters, followed by freshwater about 70 liters at a certain position. Point A, is a freshwater tank with a tank capacity of 1000 liters and installed at a height of 245 cm above the ground level. Point B is a water injection point line. A freshwater carrier pipe was connected to the tank, which was regulated through a tap, and freshwater was injected into the aquifer/model. It is used to control the freshwater injection line. The storage tank becomes empty every time at a fixed interval. Point C is a water level. At point D, the filter screen installed has an important role at the time of water recovery. The recovery pipe was fixed at the bottom of the aquifer along with the injection pipe. Point E is the mixing zone of freshwater and saline water. Point F is the horizontal input port point for checking EC values - before and after injection and at the recovery time. At point G, there is sand and saline water. Point H shows injected saline water with the help of a pump. The point I is an outlet point. Point J is a saline water tank with a storage capacity of 200 liters, to inject saline water with the help of a pump. Point K is a recovery water tank with a storage capacity of 200 liters and water is recovered with the help of a pump.

It has been found that during the initial period, in the recovered water the measured EC was high which does not lie within the permissible limit but it has been decreasing with time.

Consecutively, it started increasing after a certain period due to mixing reactions between saline and freshwater. The volume of water recovered varied between 41.5 to 129.1 liters with an average value of 55 liters. The relationship between EC recovered volume of water with time is shown in Figure 5.59 indicating a decrease in EC with time and becoming constant after a certain period.

The temperature was almost constant with an average value of 18.7ºC. Recovery efficiency ranges from 69.1 to 90.00 % with an average of 83%.

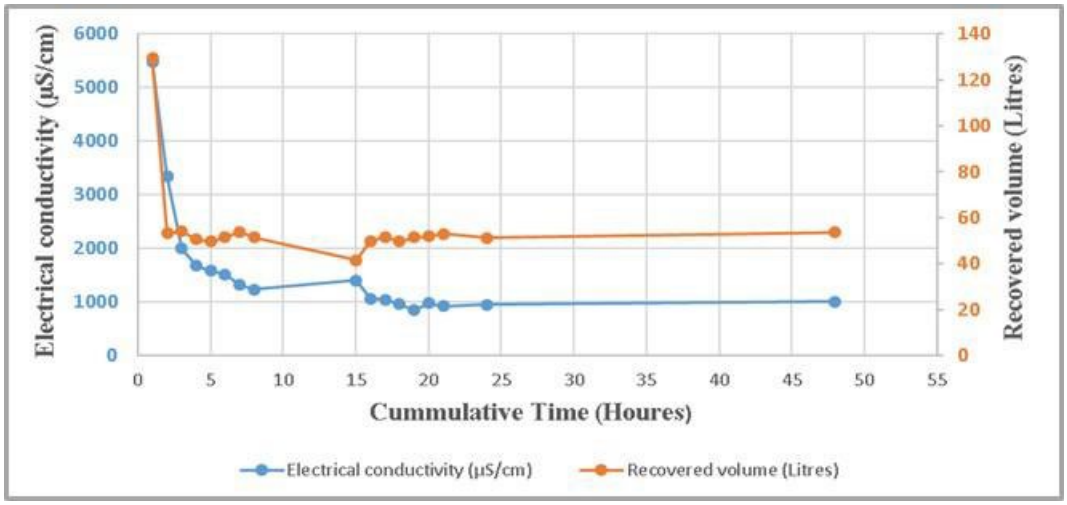

Figure 5.59 Variation in EC and recovered volume with time

Experiment no. 2

The experiment was conducted in an experimental sand-box model having dimensions: 120 cm in length, 60 cm in width, and 120 cm in height (fig 5.60). Separate fresh and saline water injection sources were built. Two sprinklers were used to create saline saturated conditions and four injection wells were used to inject fresh water into the aquifer. The wide distribution of injection wells allows four different pockets of freshwater to observe for ASR phenomenon. A saline solution of concentration 8500 µs/cm was prepared from sodium chloride salt. The temperature was measured with an EC meter (Eutech). 150 liters of this saline solution at a temperature of 25°C was inserted in the sand of size ranging between 0.075 and 1.00 mm till saturation. The sand was kept in the experimental model for a prototype artificial aquifer.

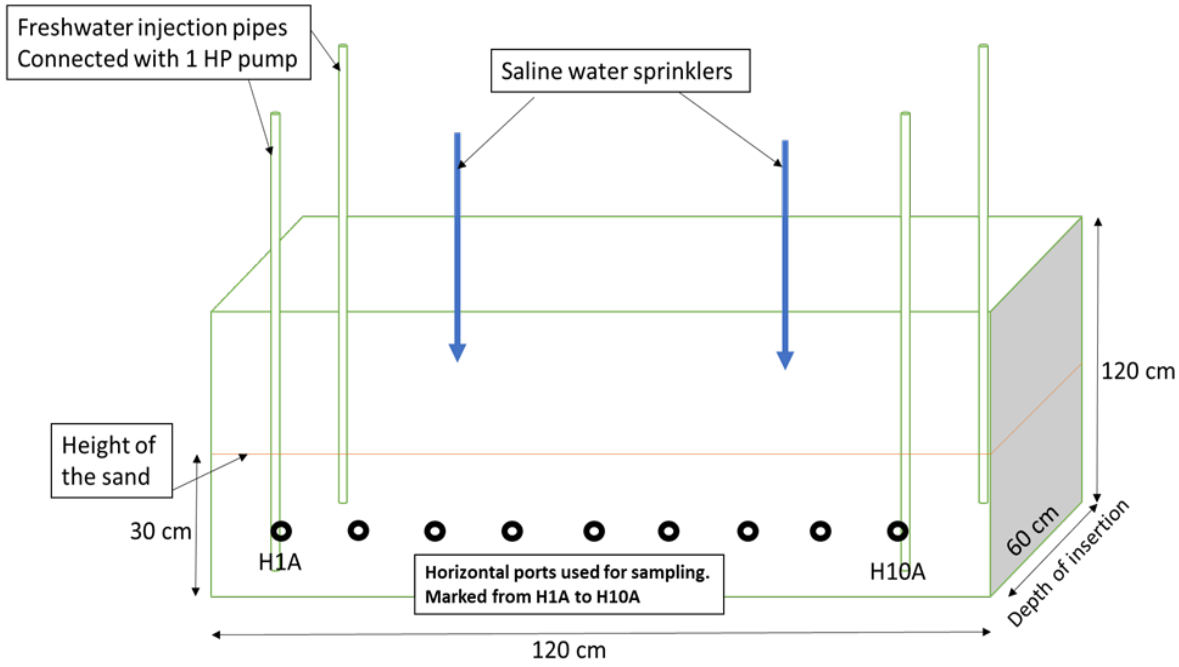

Figure 5.60 Experimental model setup-2

The plots (fig 5.61 – 5.65) present the transverse profile of the model. The x-axis represents the depth inserted for sampling. The z-axis represents the various ports in the horizontal direction. The y-axis represents the electrical conductivity value in micro-siemens per meter. The plot (fig 5.61) shows the spatial variation in EC just after the injection of fresh water in saline water. The middle-high in different plots represents the high salinity. The low mixing between freshwater and surrounding saline water is represented by high relief in salinity variation. The plot (fig 5.62) represents EC values after a few hours of injection. The H1A blue plot and H10A green plot represent the two extreme parts of the model where most of the freshwater is injected. The same can be visualized by sharp highs and lows in the curve. For instance, in the green graph between 25 to 40 cm, we can see the maximum EC value due to the placing of injection points at 10 cm and 45-50 cm distance causing low salinity values at these points. Figure 5.60 shows EC values after one day of experimentation. Due to freshwater saline water mixing, the contrast between middle position values and position values has subsided. For instance, the H10A compared to the previous plot greatly flattened at extreme ends. The gray and yellow plots are taken from extreme middle ports where no injection point was present hence we see an overall constant profile. Figure 5.62 represents the EC observations after two days of injection. Still, at H1A and H10A ports at 45-50 cm depth, we could obtain water of standard quality. Elsewhere, the saline water is thoroughly mixed with fresh water. The slight lower can also be seen at 10 cm depth in the H10A port. After three days of experimentation, the injected freshwater is thoroughly mixed with ambient saline water and the average salinity reaches up to 12500 micro-siemens per meter. Since no pockets of freshwater were found, we decided to halt our experimentation (fig 5.65).

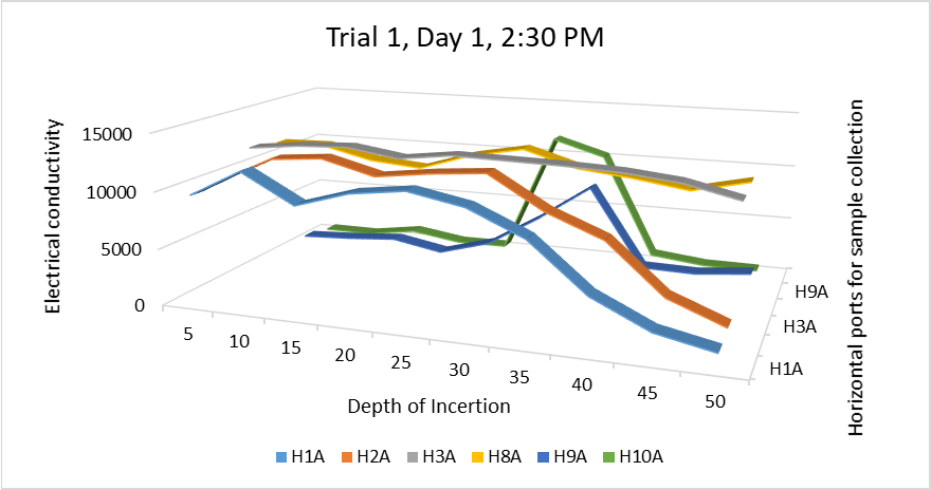

Figure 5.61 Plot 1 (variation of EC with different days and times)

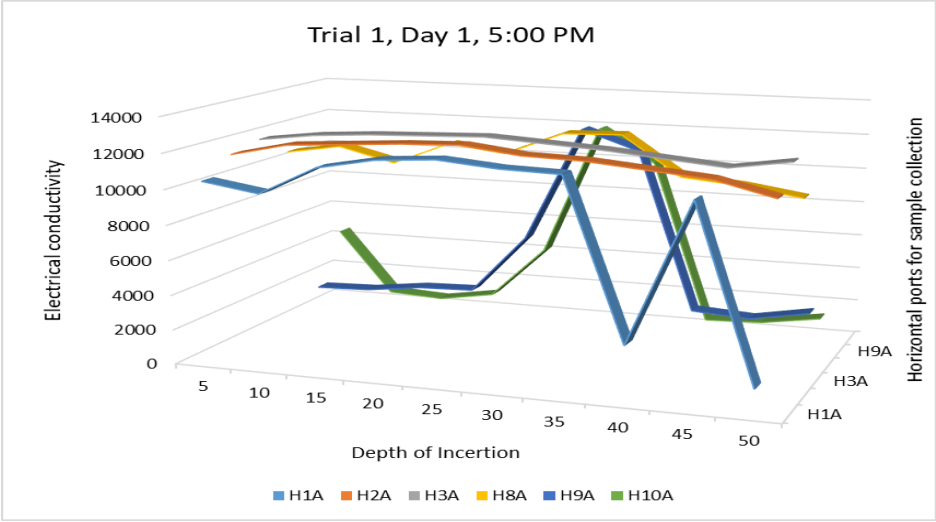

Figure 5.62 Plot 2 (variation of EC with different days and times)

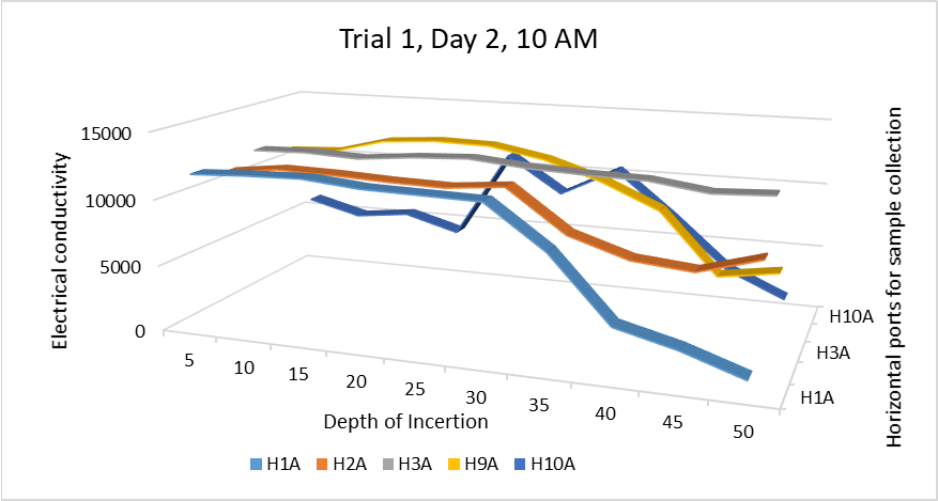

Figure 5.63 Plot 3 (variation of EC with different days and times)

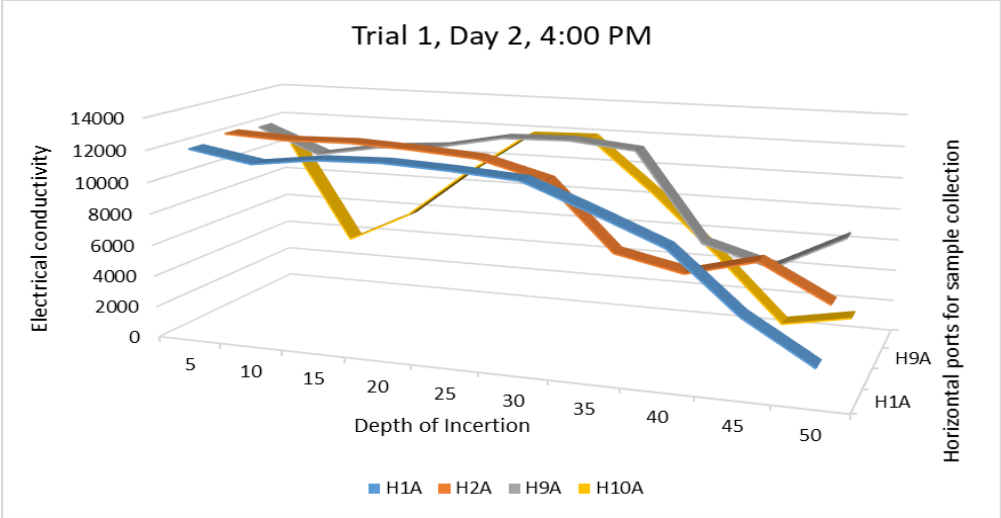

Figure 5.64 Plot 4 (variation of EC with different days and times)

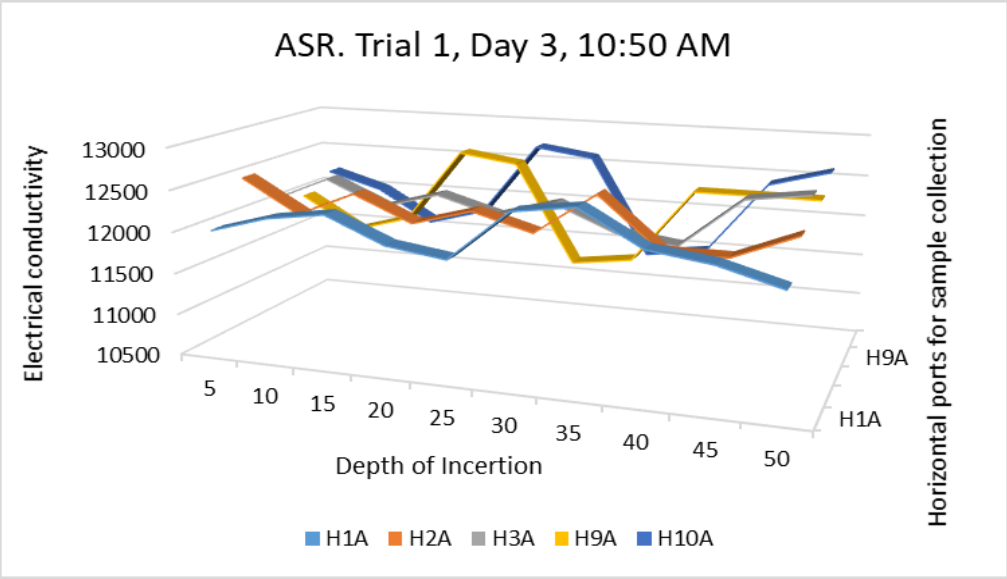

Figure 5.65 plot 5 (variation of EC with different days and times)

Experiment under field conditions

ASR setup was installed at the Karhera site, Mewat district, Haryana. Freshwater was injected into the saline aquifers with the help of an inlet tank (Figure 5.66). In the injection line, the total pipe length is 27 feet. i.e it was performed up to 22.5 feet below the ground surface in the injection well and 4.5 feet is a horizontal pipeline to the connected inlet tank with a capacity of 1000 liters. 1-inch PVC pipe has been used for both injection and recovery lines. An injection pipeline of PVC material conveyed fresh water from the inlet tank to the suction pipe through a sluice valve/gate valve and a T-section was fabricated to connect the injection pipeline. A recovery pipeline was connected to the outlet tank. At a different duration period, freshwater was recovered from the saline aquifer with the help of a pump. Since the density of freshwater is less than saline water; the former floats over the latter. A recovery pipeline is 14.6 feet above ground level. The total length of the recovery line is 43.6 feet. i.e. 5 feet under the ground, 1.5-inch PVC filter pipe, and 24 feet under the ground. A 1-inch PVC pipe has been inserted in the injection well and recovery pipeline related to the recovery tank. i.e., this tank capacity is the same as the inlet tank. Two centrifugal shallow jet pumps were installed for low discharge rates. A high-capacity pump was not used because the force used to extract the water will disturb the pocket and lead to mixing with surrounding saline water. A centrifugal shallow jet pump (1 HP) was installed, 1 foot above the ground surface. The total well depth is 40 feet. Both injection and recovery pipelines were attached with the help of a bore clamp. Two water-metering devices were used for the injected/recovered water. It is connected with the inlet and outlet tank. After the development of the ASR setup, the experiment was performed under field conditions (Figure 5.66).

Figure 5.66 Front view, top view, and side view of ASR setup at Karhera site

The initial injection of freshwater was measured for EC and temperature using an EC meter, and it was injected into the saline aquifer on-site. As shown in figure 5.66, it was observed that the EC of injected freshwater was variable, i in the range of 1200 - 1640 µS/cm with an average value of 1420.45µS/cm. It was slightly saline water in this range. There was no other option at the site, only the above-mentioned EC value range of freshwater was available. The average temperature was 27.42ºC and the total volume of injected freshwater was 19000 liters in the saline aquifer. The volume of injected freshwater in saline aquifer ranged between 1000 and 8000 liters with an average value of 1727.27 liters.

The variation in EC and temperature was taken before and after freshwater pumping. It was observed that the EC value of water was variable before pumping, ranging from 1250 to 5400 µS/cm, with an average value of 3454 µS/cm. The average temperature was 25.32ºC. It has been found that EC values decrease before pumping over time and temperature fluctuates over time. After pumping, the EC value of the water was variable in the range of 8200 and 12800µS/cm, with an average of 10545µS/cm. The average temperature was 25.7ºC (Fig 5.67).

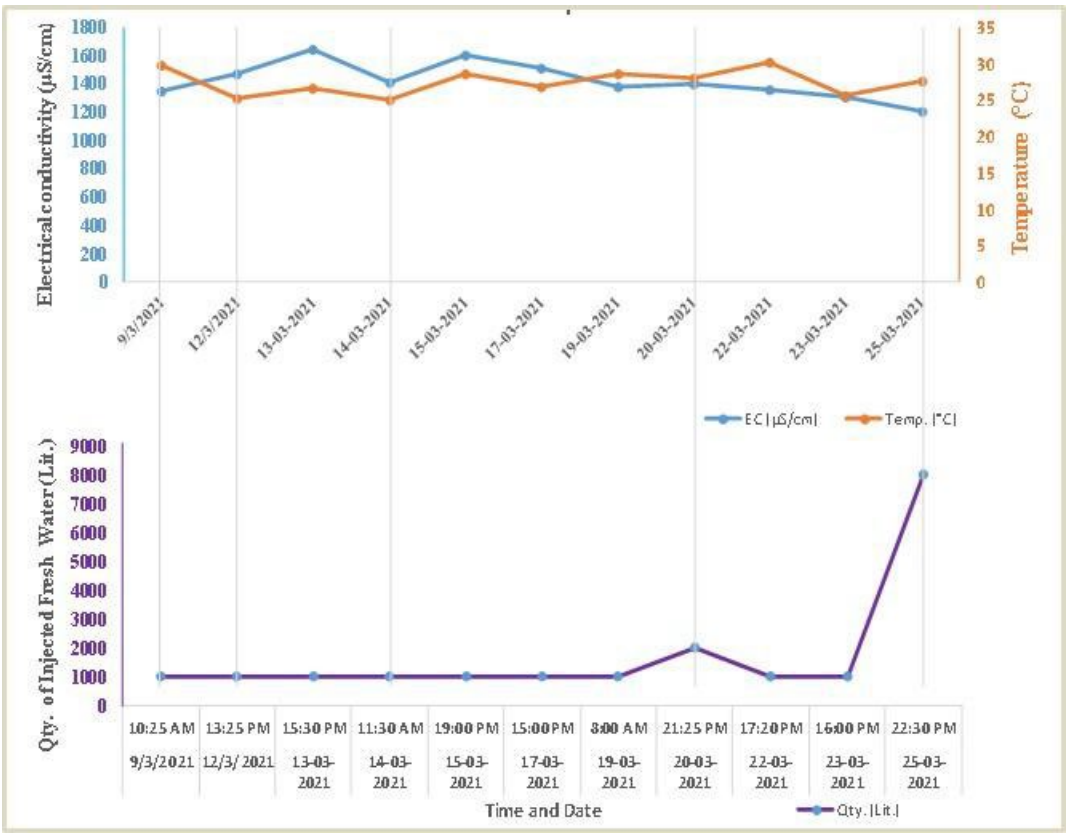

Figure 5.67 Variation in EC and temperature of injected freshwater

Volume and duration time effects on groundwater quality: The average injection rate during every time-injected freshwater was recorded as 0.032 cubic meters per minute, the injection time was found to be 46 minutes for the injected volume of 1000 liters of freshwater and 92 minutes for the injected volume of 2000 liters of fresh water through inlet tank. For the injected volume of 8000 liters of freshwater via a water tanker, it took 85 minutes. In the injection well, the average increase in water level is 0.3 meters. The prime target of the ASR setup was to recharge the saline unconfined aquifer.

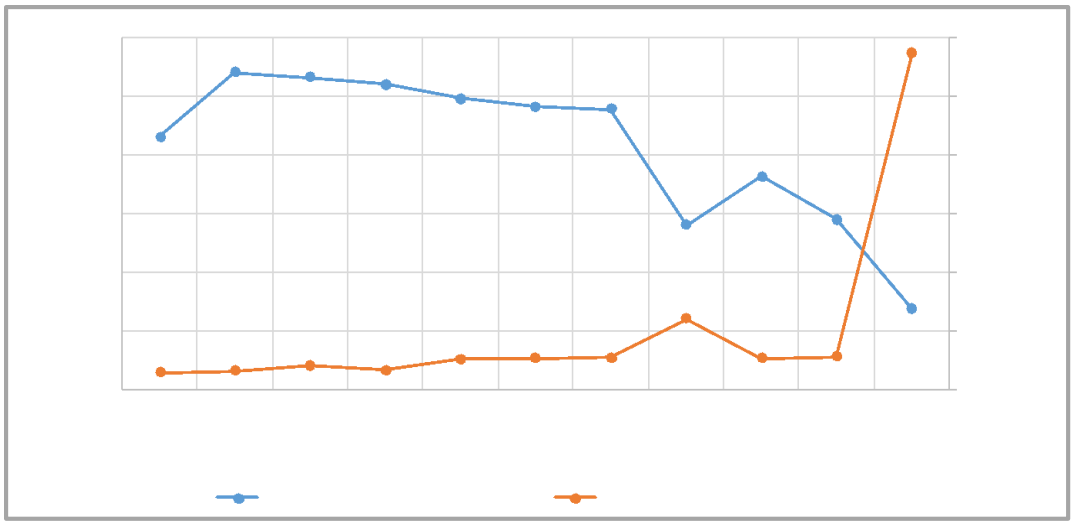

Figure 5.68 Variation in EC and recovered volume with time

As shown in Figure 5.68, the volume of water recovered from EC values is 1365- 4300 µS/cm in the range of 4 hours to 120 hours for retention time. The recovered volume has been observed to increase and the EC value to decrease if the duration is increased. The volume of water recovered varied between 280 to 5735 liters with an average value of 990 liters. Recovery efficiency (RE) ranged from 28 to 71.69 % with an average of 57.32 %. In general, RE is always less than 100 %, and the mechanisms involved are subsurface mixing, density-gradient driven convection, dispersion and diffusion, rate-limited mass transfers, and so on. It was also emphasized that the RE could be increased, but with more contaminations.

Dupit's equation for unconfined aquifer:

For unconfined aquifers, all data are shown in Figure 5.69.
Saturated thickness of unconfined aquifer (H) = 9.512 m
Radius of well, r = 0.915 m
Hydraulic conductivity, K = 0.00111 m/sec
Drawdown in the well, S = 3.03273 m
Length of filter, L_f = 1.525 m

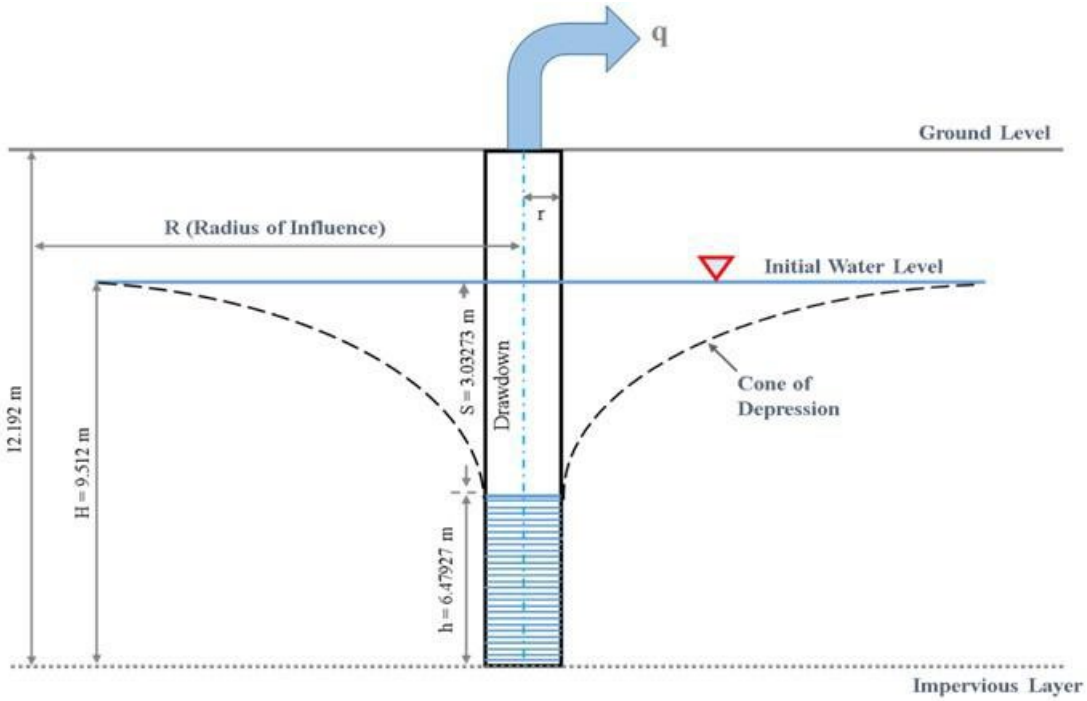

Fig 5.69 Schematic diagram of an unconfined aquifer

The radius of influence 'R', is calculated by using empirical relation:

$R = 3000.S\sqrt{K}$ .....(5.11)

$R = 3000 \times 3.03273 \times \sqrt{0.00111}$

$R = 303.12\ m$

Again, calculating the discharge of the aquifer, substituting the value in equation (i):

$Q_A = \frac{\pi K(H^2 - h^2)}{lnln\ R - lnln\ r}$ .....(5.12)

$Q_A = \frac{\pi \times 0.00111(9.512^2 - 3.03273^2)}{ln\ ln\ 303.12 - ln\ ln\ 0.915}$

$Q_A = \frac{\pi \times 0.00111 \times 48.4972}{5.803}$

$$\boldsymbol{Q_A = 0.02913\ m^3/sec}$$

Again, calculating the discharge of flow, substituting the value in equation (ii):

$Q_F = \frac{2}{15} \times \pi.r.L_f.\sqrt{K}$ .....(5.13)

$Q_F = \frac{2}{15} \times \pi \times 0.915 \times 1.525 \times \sqrt{0.00111}$

$$\boldsymbol{Q_F = 0.01945\ m^3/sec}$$

Hence, $Q_A > Q_F$, means that the injection well is in proper working condition.

CONCLUSIONS, RECOMMENDATIONS, AND SCOPE OF FUTURE WORK

Conclusions

A comprehensive study envisaging analyses of demography, geology, geomorphology, land uses, groundwater usage, hydrometeorology, hydrology, hydrogeology, groundwater quality, isotopic characteristics of water, and socio-economic aspects, etc. has been carried out. Based on the results of analyses of these components, the following conclusions are drawn.

1. Based on the various thematic maps of the study area, it has been found that the central alluvial plain of the study area has very good groundwater potential while the Piedmont plain near Aravali hills has moderate potential and the potential of structural hills and linear ridges ranges have poor to moderate potential. As a result, the created groundwater potential map serves as a starting point for future investigation.

2. The overall irrigation pattern in the study region is found primarily dependent on groundwater resources. The proportion of farmers' own irrigation sources was found to be declined with increasing salinity levels. In all the salinity groups, only 3 percent of farmers were found to be exclusively dependent on rainwater for irrigation.

3. Freshwater zones are found mostly in the villages lying at the foothills of the Aravalli Range. But the cost of extracting such fresh water is high; this has resulted in a number of villages remaining abstained from digging a private bore well.

4. The percentage of households purchasing drinking water is 54% which is more in the high-saline groundwater villages and it remaining 20% in the moderately saline villages and 8% in the villages that have fresh groundwater sources.

5. Private bore wells are the major source of drinking water for households accessing groundwater. These sources are mostly prevalent in moderately saline groundwater villages with 55% of the respondent households utilizing them for drinking water, followed by 51% in the freshwater villages, and 11%t in the high saline groundwater villages.

6. Use of government-supplied water was observed mostly in the high-saline villages; 22 percent of the respondents use it for drinking purposes; while 21 percent of the households in the villages of the freshwater zones use the government water supply, followed by moderately saline villages at percent.

6. For household purposes, 21 percent uses water from a private bore well, and 39 percent of the respondents purchase water to meet the water demand. A general trend in the district showed that people usually construct underground water tanks for storing water from purchased tankers that usually last 20–25 days.

7. Analysis of fluctuation of groundwater levels provides information on the dynamics of recharge and discharge in the short duration; and aquifer conditions (in terms of groundwater potential/depletion) in the long term. The long term (2004-2017 years) average water level trend indicated that the water level in Tauru block depleting at a faster rate i.e 0.40 m/year followed by Firozepur Jhirka block depleting at the rate of 0.33m/year. These 2 blocks have sweet water and the groundwater extraction is maximum. Minimum depletions are found in Nuh (0.08m/year) and Nagina (0.11 m/year) blocks due to groundwater salinity issues in large pockets. The values obtained from the installed loggers in the field showed large variations.

   From the water level map of the study area, it is evident that water tables are deeper in the western region. The water is potable in these areas resulting in higher water withdrawals. In the eastern and southern sides of the study area, water is saline, and water tables are high. The contours of groundwater level show a natural gradient from the Aravalli hills towards the central region but due to high groundwater extraction in the foothills regions of the area, there is the apprehension of movement of water from salinity-affected areas to freshwater areas. Seasonal effects were found in the water level variations; in the post-monsoon seasons, the water levels increased by 18% in the southern/south-western region of the study area as compared to the pre-monsoon season. This rise was found in the places water level ranging between 210-230 m. There are possibilities of a change in salinity mechanism due to the rise in groundwater levels due to precipitation.

8. Salinity has been found in most of the places in the district, however it has been found that the TDS increase per annum varied from 2% (Bich wala well) to 48% (Khalid well) during 2012-2016. Another notable increase of 37% was found in Badru well followed by 20% in Bag wala Kua. During the period 2012 to 2016, there is an increase in TDS values ranging between 500-1000 mg/l in 74% area while 35% increase in area in the category of 1500-2000 mg/l TDS.

9. In addition to the temporal increase in TDS values, seasonal variations are also observed in the groundwater for the years 2018 and 2019. In the year 2018, the TDS vary from 53 to 37051 mg/L with an average value of 6146 mg/L during the pre-monsoon season, 421-34170 mg/L with an average value of 4921 mg/L during monsoon, and 309 to 35108 mg/L with average value 5066 mg/L during the post-monsoon season of the year 2018. About 54%, 93%, and 62% of samples were found above the maximum permissible limit of 2000 mg/L in pre-monsoon, monsoon, and post-monsoon seasons respectively. And about 8%, 7%, and 14% of samples were found within the acceptable limit of 500 mg/L in the pre-monsoon, monsoon, and post-monsoon seasons of the year 2018. Water containing more than 500 mg/L of TDS is not considered desirable for drinking water supplies, though more highly mineralized water is also used where better water is not available.

   In the year 2019, the values of total dissolved solids (TDS) in the groundwater vary from 243 to 36582 mg/L with an average value of 4435 mg/L during the pre-monsoon season, 504-43820 mg/L with an average value of 4482 mg/L during monsoon and

409 to 39845 mg/L with average value 4938 mg/L during the post-monsoon season of the year 2019. About 54%, 62%, and 58% of samples were found above the maximum permissible limit of 2000 mg/L in pre-monsoon, monsoon, and post-monsoon seasons respectively. And about 8%, 0%, and 4% samples were found within the acceptable limit of 500 mg/L in the pre-monsoon, monsoon, and post-monsoon seasons of the year 2019.

To find the daily and seasonal fluctuations in salinity levels, the conductivity loggers were installed in the wells and piezometers. For most of the time period, the loggers were not working due to some technical issues, however, for finding the causes of large variations in the salinity values, long-term monitoring and observations are required.

10. Sodium is considered to be the main ion contributing to the salinity, year-wise seasonal analysis of the groundwater for the sodium concentrations shows that in 2018, concentration of sodium in the study area varies from 2.4 to 10286 mg/L with an average value of 1298 mg/L during the pre-monsoon season, 0 to 5842 mg/L with an average value of 487 mg/L during monsoon and 2.7 to 5168 mg/L with average value 643 mg/L during the post-monsoon season. The high sodium values in the study area may be attributed to the base-exchange phenomenon causing sodium hazards. Groundwater with a high value of sodium is not suitable for irrigation purposes.

    In the year 2019, the concentration of sodium in the study area varies from 12 to 11635 mg/L with an average value of 936 mg/L during the pre-monsoon season, 3 to 448 mg/L with an average value of 61 mg/L during monsoon, and 4 to 557 mg/L with average value 84 mg/L during the post-monsoon season. The high sodium values in the study area may be attributed to the base-exchange phenomenon causing sodium hazards.

11. For the source identifications, salinity mechanism, and residence times of groundwater, the water samples were analyzed for stable isotopes ($\delta^{18}O$ and δD) and tritium (H^3).

    To understand the source of seasonal variation in the groundwater salinity, 73 samples for pre-monsoon; 78 samples each from monsoon and post-monsoon for the years 2018 and 2019 were collected from different sites in the Mewat district, Haryana and analyzed for $\delta^{18}O$ and δD. The mean values of $\delta^{18}O$ and δD for the pre-monsoon season (April-may) are -5.5‰ and -41.2‰; in monsoon, $\delta^{18}O$ is -5.6‰ and δD is -40.8‰; whereas for the post-monsoon season period (October), $\delta^{18}O$ is -5.5‰ and δD is -42‰. The variation in mean values of the isotopic composition during the three seasons is small.

    To examine the evaporation effect on groundwater of the study area, $\delta^{18}O$ is plotted against δD. The slope of 5.64, 6.10, and 5.48 is observed for pre-monsoon, monsoon,

and post-monsoon seasons, respectively. Since the regression lines are sub-parallel to Global Meteoric Water Line (GMWL) and LMWL (8.83) with slopes less than 8, it suggests the occurrence of evaporation before the infiltration of water in the unsaturated zone.

It is found that salinity increases and d-excess decreases during the process of evapo-concentration in all seasons. A linear relationship between d-excess and remaining fraction was found in all three seasons in all samples. However, more scatter is found in the values of salinity and the remaining fraction in 16% of the total samples indicating seasonal variations.

It has been observed that the groundwater of the district showed an increase of 0.7g/L salinity from pre-monsoon (6.7g/L) to post-monsoon season (7.4g/L). The d-excess shows a decline of 1.6‰ in post-monsoon when compared to pre-monsoon, it decreases from 2.4‰ in pre-monsoon to 0.8‰ in post-monsoon.

It was found that in the pre-monsoon season, salinity was due to mineral dissolution. However, in the monsoon and post-monsoon seasons, initial salinity also contributes to salinity. Percent area in groundwater salinity with s contribution of >2% from evapo-concentration increased from 0% in pre-monsoon to 94%, with contributions of 2-8% in groundwater salinity.

The contribution of mineral dissolution is found by separating the salinity value of evaporation from dissolution; the results were further tested by using Tritium (^{3}H) to distinguish between modern groundwater (recharge occurring during the last 60 years) and pre-modern groundwater (recharge occurring >60 years).

This shows that groundwater has a long residence time in high saline-affected areas. A majority of the samples show a contribution from mineral dissolution in the pre-monsoon season, with a slight decrease in monsoon and post-monsoon seasons. There is wide variation in tritium activities which may be due to discontinuous water flow or poor connectivity between aquifers.

Mineral dissolution contributes to most of the groundwater salinity (76–97%). A decrease in the contribution of mineral dissolution occurs in the monsoon season as the initial salinity contribution increases to as high as 21%. This is due to the increased groundwater recharge and mobilization of accumulated salts in soils either naturally or anthropogenic sources.

Similar observations to isotope analysis were found using Principal Component Analysis (PCA), KMO and Bartlett's tests were found valid for both the years 2018 & 2019, and PCA is found suitable for the study area. Three principal components were selected based on the Eigen value which explains 79.58% and 85.08% of total variation in the year 2018 and 2019 respectively. The first Principal component (PC-1) is identified with salinity is governed by rock-water interactions and agricultural

return flow. The second Principal component (PC-2) with alkalinity and the third Principal component (PC-3) described the pollution.

12. On the suggestions of the experts, Fluoride was measured and its in-situ measured values ranged from 0.11 to 2.44 mg/L with mean value of 1.14 mg/L at selected sites in the Mewat district in June 2022. The fluoride standard value of 1 ppm has been prescribed by BIS as an acceptable limit for drinking water and the mean value exceeded the permissible limit in 50% of the samples in the study area which poses a threat of non-carcinogenic risk to people living in the area.

13. The groundwater samples were also analysed for trace metal ions Pb, Cd, Cu, Ni, Cr, Mn, Fe, Zn. It was found that the concentration of Pb in the drinking water samples ranged from 1.76 to 250.52 ppb with a mean of 43.21 ppb, the permissible limit of Pb is specified as 100 ppb by BIS (2012) and 10 ppb is specified by WHO (2007) for drinking water, the ranges found in the study area are far beyond the acceptable limit. Only 1 sample exceeded the limit of 100 ppb specified by BIS (2012).

    The concentration of Cd in the drinking water samples ranged from 0.38 to 9.34 ppb with a mean of 4.38 ppb, the permissible limit of Cd is specified as 10 ppb by BIS (2012) and 3.0 ppb is specified by WHO (2007) for drinking water. All the samples were found in the prescribed limit of 10 ppb by BIS (2012).

    The concentration of Cu in the drinking water samples ranged from 0.66 to 75.77 ppb with a mean of 11.46 ppb, the permissible limit of Cu is specified as 50 ppb by BIS (2012) and 100 ppb is specified by WHO (2007) for drinking water. Except for 3, all the samples were within the permissible limits of BIS (2012) and all samples were within the limit as per WHO (2007) guidelines.

    The concentration of Ni in the drinking water samples ranged from 0.21 to 60.24 ppb with a mean of 6.63 ppb, the permissible limit of Ni is specified as 3000 ppb by BIS (2012) and 20 ppb is specified by WHO (2007) for drinking water. 16 % of the samples exceeded the permissible limits of WHO (2007).

    The concentration of Cr in the drinking water samples ranged from 0.54 to 28.65 ppb with a mean of 3.372 ppb, the permissible limit of Cr is specified as 50 ppb by BIS (2012) and 50 ppb is specified by WHO (2007) for drinking water. All the samples were within the permissible limits of BIS (2012) and WHO (2007).

    The accumulation of Mn may cause hepatic encephalopathy. The concentration of Mn in the drinking water samples ranged from 3.30 to 760.95 ppb with a mean of 126.40 ppb, the permissible limit of Mn is specified as 100 ppb by BIS (2012) and 100 ppb is specified by WHO (2007) for drinking water. 30 % of the samples exceeded the permissible limits of BIS (2012) and WHO (2007).

    The concentration of Fe in the drinking water samples ranged from 0.01 to 59.87 ppm with a mean of 2.49 ppm, the permissible limit of Fe is specified as 0.3 ppm by

BIS (2012) and 0.3 is specified by WHO (2007) for drinking water. 26 % of the samples exceeded the permissible limits of BIS (2012) and WHO (2007).

The concentration of Zn in the drinking water samples ranged from 32.30 to 425.69 ppb with a mean of 126.65 ppb, the permissible limit of Zn is specified as 3000 ppb by BIS (2012) and 3000 ppb is specified by WHO (2007) for drinking water. All the samples were within the permissible limits of BIS (2012) and WHO (2007).

14. Many methods for groundwater remediation have been invented in the last century. The use of each and every method depends primarily upon the hydrogeology and chemical, physical, economical, and social feasibility of the technique. Amongst them, one such technique is Aquifer Storage and Recovery (ASR) which has emerged as a boon to semi-arid areas in providing freshwater supply at a very low cost.

A laboratory experimentation was done to measure the viability of Aquifer Storage and Recovery (ASR) as a remediation option in the saline aquifers of Mewat, Haryana. It has been found that during the initial period, in the recovered water the measured EC was high and, it does not lie within the permissible limit but it decreased with time. Consecutively, it started increasing after a certain period due to mixing reactions between saline water and freshwater. The volume of water recovered varied between 41.5 to 129.1 litres with an average value of 55 litres in the experimental setup.

ASR setup was installed at site Karhera, Mewat district, Haryana to inject fresh water into a saline aquifer with the help of an inlet tank. In the injection line, the total pipe length was 27 feet. i.e., water was injected up to 22.5 feet below the ground surface in the injection well. At 4.5 feet, there was a horizontal pipeline to the connected inlet tank of capacity of 1000 litres. 1-inch PVC pipe was used for both injection and recovery lines. An injection pipeline of PVC material conveyed fresh water from the inlet tank to the suction pipe through a sluice valve/gate valve and a T-section was fabricated to connect the injection pipeline.

The volume of water recovered had EC values ranging from 1365- 4300 µS/cm for 4 to 120 hours of retention time. The recovered volume has been observed to increase and the EC value to decrease if the duration is increased. The volume of water recovered varied between 280 to 5735 litres with an average value of 990 litres. Recovery efficiency (RE) ranged from 28 to 71.69 % with an average of 57.32 %. In general, RE is always less than 100 %, and the mechanisms involved are subsurface mixing density-gradient driven convection, dispersion and diffusion, rate-limited mass transfers, and so on. It was also emphasized that the RE could be increased, but with more contaminations.

Recommendations and future scope of work

In the Mewat district, central part is a closed basin with Aravalli hills on either side, evaporation rates are high and as a result, the ground surface developed saline soils. In the areas where the water table is shallow, the excess drying due to capillary action might have caused salt mineralization. In the subsequent wetting season, these salts are dissolved with the infiltrating water and add salinity to the groundwater resulting in higher salinities with time.

With the above in view, it is necessary to review the availability of water from rain and look for better planning, practice and management to augment the groundwater levels in areas with declining water levels mainly in fresh water pockets and take measures to reduce salinity in the central part of the district.

Augmentation of groundwater

For the areas in Tauru district and part of Nuh district where the groundwater levels are depleting fast, the possibilities of augmentation of groundwater levels are possible as: Mewat district has an average annual rainfall of about 600 mm. Out of this ~ 600 mm, about 80% is received during monsoon period (June through September). Owing to this rainfall, rainwater harvesting can be one of the options, as the concept of 'Catch The Rain' (CTR) has become popular these days and government has also taken initiatives through Jal Shakti Abhiyan. In hilly areas of the district, these rainfalls generate a lot of runoff which should be tapped/stored in both surface and sub-surface reservoirs. Artificial recharge to groundwater can be explored by identifying the suitable recharge sites and constructing infiltration recharge wells/bunds/gullies, etc. It can be done by investigating the infiltration characteristics, groundwater dynamics and assessing the availability of artificially recharged water.

Water management options

This study has found that the salinity is spreading in the district during the last decade. Isotopic results indicated that salinity flushing is possible which can take place in areas where induced freshwater recharge is diluting the salinity during the monsoon seasons but is not effective to remove the deep-seated saline bed. Therefore, it is recommended to continuously remove saline groundwater using the very deep penetration wells and simultaneously refreshing the aquifer through fresh water which will certainly provide some means to wash the deep salt bed. However, such a method needs a more detailed study.

Some of the water management options are discussed here:

- Blending saline groundwater with better quality water from rains to dilute the salinity. Such water could be used for irrigation purposes mainly horticulture, overland applications and gardening. Since in the district, the salinity levels are in different ranges, the areas where salinity is < 3000 mg/l, the saline water can be pumped out

and replaced by precipitation water in due course of time by a careful planning and execution.

- Desalination by conversion of salt water to fresh water is the oldest and most extensive process known to mankind. A number of technologies have been developed for desalination, including distillation, reverse osmosis (RO), electro-dialysis, and vacuum freezing.

- The study has revealed that in addition to salinity issues of groundwater in Mewat district, high fluoride contents have been found. Thus, there is a need to take up immediate measures to reduce these chemical contaminations in groundwater. A detailed study can be carried out in order to understand the possible sources of contamination and remedial measures.

- Introducing crops with lower water requirements; introducing salt tolerant and semi salt tolerant crops may be one of the options. Changes in vegetation can also help improve the water and salt balances in soil, the vadose zone, and shallow groundwater. Since deep tree roots can efficiently pump underlying shallow groundwater, afforestation of grasslands reverses the vertical flux of groundwater from the soil to the saturated zone.

- Aquifer Storage and Recovery (ASR) can be tried where the aquifer is used as an underground reservoir that does not require additional surface space, need only limited maintenance, and losses due to evaporation are minimized, and offer a good alternative to surface water reservoirs. Secondly, ASR can also be approached as a recovery technique.

Mass awareness programs

For the success of any plan/scheme to conserve and manage available water resources, people's participation has been reported the most effective. In Mewat, it should be included as an element to enhance the general level of awareness about the effects of water wastage, optimize its use, and induce community spirit.

REFERENCES

Adams, S., Titus, R., Pietersen, K., Tredoux, G., & Harris, C. (2001). Hydro-chemical characteristics of induc near Sutherland in the Western Karoo, South Africa. *Journal of hydrology*, *241*(1-2), 91-103.

Allison, G.B. and Schonfeldt, C.B., (1990). Sustainability of water resources of the Murray Darling Basin. Aust. Acad. Tech. Sci. Eng. Symp., Oct. 1989, Preprint No. 8, 15 pp.

Aneesh, T. D., Srinivas, R., Singh, A. T., Resmi, T. R., Nair, A. M., & Redkar, B. L. (2019). Stable water isotope signatures of dual monsoon precipitation: A case study of Greater Cochin region, south-west coast of India. *Journal of Earth System Science*, *128*(8), 1-13.

APHA AWWA, W. E. F. (2005). Standard methods for the examination of water and wastewater. APHA WEF AWWA.

Barzegar, R., Adamowski, J., & Moghaddam, A. A. (2016). Application of wavelet-artificial intelligence hybrid models for water quality prediction: a case study in Aji-Chay River, Iran. *Stochastic environmental research and risk assessment*, *30*(7), 1797-1819.

Bennetts, D. A.; Webb, J. A. (2004) Sources of Increased Discharge to a CatchmentAffected by Dryland Salinity, Western Victoria, Using Hydro-chemical andIsotopic Methods. In: *17th Australian Geological Convention;* McPhie, J.,McGoldrick, P., Eds.; Geological Society of Australia: Hobart; pp 4.

BIS (2012) Indian standard drinking water-specification, 2nd revision,IS:10500:2012. Bureau of Indian Standards, New Delhi

Bouchaou, L., Michelot, J. L., Vengosh, A., Hsissou, Y., Qurtobi, M., Gaye, C. B., & Zuppi, G. M. (2008). Application of multiple isotopic and geochemical tracers for investigation of recharge, salinization, and residence time of water in the Souss–Massa aquifer, southwest of Morocco. *Journal of Hydrology*, *352*(3-4), 267-287.

Cartwright, I., Weaver, T. R., Fulton, S., Nichol, C., Reid, M., & Cheng, X. (2004). Hydrogeochemical and isotopic constraints on the origins of dryland salinity, Murray Basin, Victoria, Australia. *Applied Geochemistry*, *19*(8), 1233-1254.

Cederstrom, D.J. (1947). Artificial Recharge of a Brackish WaterWe l l, Vol. 14(No. 14), 31–73. Richmond: Virginia ChamberCommerce.

Central Water Commission. (2017). Problems of salination of land in coastal areas of India and suitable protection measures. *New Delhi, India: Hydrological Studies Organization, Central Water Commission*, *346*.

CGWB (2007). Groundwater information booklet of Haryana.

CGWB (2008). Groundwater yearbook of Channai, India.

CGWB (2012). Ground water information booklet, Mewat district, Haryana**.**

CGWB (2013). Groundwater information booklet, Muktsar district, Punjab.

CGWB (2014). Report on status of Ground water quality in coastal aquifers of India.

CGWB (2019-20). Groundwater year book of Rajasthan, India.

Clark, I.D., Fritz, P.,(1997). Environmental Isotopes in Hydrogeology. Lewis, Boca Raton.

Craig, H. (1961). Isotopic variations in meteoric waters. *Science*, *133*(3465), 1702-1703.

Dansgaard, W. (1964). Stable isotopes in precipitation. *tellus*, *16*(4), 436-468.

Datta, P. S., & Tyagi, S. K. (1996). Major ion chemistry of groundwater in Delhi area: chemical weathering processes and groundwater flow regime. *Journal of Geological Society of India (Online archive from Vol 1 to Vol 78)*, *47*(2), 179-188.

de Montety, V., Radakovitch, O., Vallet-Coulomb, C., Blavoux, B., Hermitte, D., & Valles, V. (2008). Origin of groundwater salinity and hydrogeochemical processes in a confined coastal aquifer: case of the Rhône delta (Southern France). *Applied Geochemistry*, *23*(8), 2337-2349.

Dhar, S., Das, S., & Mazumdar, A. (2010, February). Salt water intrusion into the Piyali river aquifer of the Sundarbans, West Bengal. Proceedings *of the national conference on groundwater resource development and management in hard rocks—supported by DST, GoI* (pp. 35-36).

Dillon, P., Stuyfzand, P., Grischek, T., Lluria, M., Pyne, R. D. G., Jain, R. C., & Sapiano, M. (2019). Sixty years of global progress in managed aquifer recharge. *Hydrogeology journal*, *27*(1), 1-30.

Dimitriadou, S., Katsanou, K., Charalabopoulos, S., & Lambrakis, N. (2018). Interpretation of the factors defining groundwater quality of the site subjected to the wildfire of 2007 in Ilia prefecture, South-Western Greece. *Geosciences*, *8*(4), 108.

Edmunds, W. M., & Milne, C. J. (Eds.). (2001). Palaeowaters in coastal Europe: evolution of groundwater since the late Pleistocene. Geological Society of London.

Elango, L., & Kannan, R. (2007). Rock–water interaction and its control on chemical composition of groundwater. *Developments in environmental science*, *5*, 229-243.

Elmeknassi, M., Bouchaou, L., El Mandour, A., Elgettafi, M., Himi, M., & Casas, A. (2022). Multiple stable isotopes and geochemical approaches to elucidate groundwater salinity and contamination in the critical coastal zone: A case from the Bou-areg and Gareb aquifers (North-Eastern Morocco). *Environmental Pollution*, *300*, 118942.

Esmail, O. J., & Kimbler, O. K. (1967). Investigation of the technical feasibility of storing fresh water in saline aquifers. *Water Resources Research*, *3*(3), 683-695.
Gibbs, R. J. (1970). Mechanisms controlling world water chemistry. *Science*, *170*(3962), 1088-1090.

Foster, S. S. D., & Chilton, P. J. (2003). Groundwater: the processes and global significance of aquifer degradation. *Philosophical Transactions of the Royal Society of London. Series B: Biological Sciences*, *358*(1440), 1957-1972.
Gibbs, R. J. (1970). Mechanisms controlling world water chemistry. *Science*, *170*(3962), 1088-1090.

Giordano, M., & Villholth, K. G. (Eds.). (2007). *The agricultural groundwater revolution: opportunities and threats to development* (Vol. 3). CABI.

Gleeson, T., Wada, Y., Bierkens, M. F., & Van Beek, L. P. (2012). Water balance of global aquifers revealed by groundwater footprint. *Nature*, *488*(7410), 197-200.
Ground water information booklet muktsar district, Punjab (2013). Muktsar district at a glance.

Guo, H., & Wang, Y. (2005). Geochemical characteristics of shallow groundwater in Datong basin, northwestern China. *Journal of Geochemical Exploration*, *87*(3), 109-120.

Herczeg, A.L., Leaney, F.W., Ghomari, R., Davie, R. and Fifield, L.K., (1991). Hydrochemistry of ground waters in the south-western Murray basin with special reference to the Woolpunda ground water mound. Centre for Groundwater Studies, Rep. No. 13. CSIRO, Div. Water Res., Adelaide, 16 pp.

Huang, C., Li, C., & Shi, G. (2012). Graphene based catalysts. *Energy & Environmental Science*, *5*(10), 8848-8868.

Huang, T., & Pang, Z. (2012). The role of deuterium excess in determining the water salinisation mechanism: a case study of the arid Tarim River Basin, NW China. *Applied Geochemistry*, *27*(12), 2382-2388.

Jakeman, A. J., Barreteau, O., Hunt, R. J., Rinaudo, J. D., & Ross, A. (2016). *Integrated groundwater management* (p. 762). Springer Nature.

Katz, J., & Hicks, D. (1997). How much is a collaboration worth? A calibrated bibliometric model. *Scientometrics*, *40*(3), 541-554.

Konikow, L. F., & Person, M. (1985). Assessment of long-term salinity changes in an irrigated stream-aquifer system. *Water resources research*, *21*(11), 1611-1624.

Kim, J. H., Kim, R. H., Lee, J., & Chang, H. W. (2003). Hydrogeochemical characterization of major factors affecting the quality of shallow groundwater in the coastal area at Kimje in South Korea. *Environmental Geology*, *44*(4), 478-489.

Krishan, G., Prasad, G., Kumar, C. P., Patidar, N., Yadav, B. K., Kansal, M. L., ... & Verma, S. K. (2020). Identifying the seasonal variability in the source of groundwater salinization using deuterium excess-a case study from Mewat, Haryana, India. *Journal of Hydrology: Regional Studies*, *31*, 100724.

Krishan, G., Rao, M. S., Kumar, C. P., &Semwal, P. (2013). Identifying salinization using isotopes and ion chemistry in semi-arid regions of Punjab, India. *J GeolGeosci*, *2*(4), 1-6.

Krishan, G., Rao, M. S., Loyal, R. S., Lohani, A. K., Tuli, N. K., Takshi, K. S., ... & Kumar, S. (2014). Groundwater level analyses of Punjab, India: A quantitative approach. *Octa Journal of Environmental Research*, *2*(3).

Kulkarni, K. M., Rao, S. M., Singhal, B. S., Parkash, B., & Navada, S. V. (1989). Origin of saline groundwater of Haryana State, India. *IAHS-AISH publication*, (182), 125-132.

Kumar, A., & Kimbler, O. K. (1970). Effect of dispersion, gravitational segregation, and formation stratification on the recovery of freshwater stored in saline aquifers. *Water Resources Research*, *6*(6), 1689-1700.

Kumar G, Ramanathan AL, Rajkumar K (2010) Textural characteristics of the surface sediments of a Tropical mangrove ecosystemGulf of Kachchh, Gujarat, India. Indian J Mar Sci 39(3):415–422.

Kumar, M., Rao, M. S., Deka, J. P., Ramanathan, A. L., & Kumar, B. (2015). Integrated hydrogeochemical, isotopic and geomorphological depiction of the groundwater salinization in the aquifer system of Delhi, India. *Journal of Asian Earth Sciences*, *111*, 936-947.

Lapworth, D. J., Gopal, K., Rao, M. S., & MacDonald, A. M. (2014). Intensive groundwater exploitation in the Punjab: An evaluation of resource and quality trends.

Louvat, D., Michelot, J. L., & Aranyossy, J. F. (1999). Origin and residence time of salinity in the Äspö groundwater system. *Applied Geochemistry*, *14*(7), 917-925.

MacAllister, D. J., Krishan, G., Basharat, M., Cuba, D., & MacDonald, A. M. (2022). A century of groundwater accumulation in Pakistan and northwest India. *Nature Geoscience*, 1-7.

MacDonald, A. M., Bonsor, H. C., Ahmed, K. M., Burgess, W. G., Basharat, M., Calow, R. C., & Yadav, S. K. (2016). Groundwater quality and depletion in the Indo-Gangetic Basin mapped from in situ observations. *Nature Geoscience*, *9*(10), 762-766.

Malik, A., Parvaiz, A., Mushtaq, N., Hussain, I., Javed, T., Rehman, H. U., & Farooqi, A. (2020). Characterization and role of derived dissolved organic matter on arsenic mobilization in alluvial aquifers of Punjab, Pakistan. *Chemosphere*, *251*, 126374.

Maurya, P. K., Malik, D. S., Yadav, K. K., Kumar, A., Kumar, S., & Kamyab, H. (2019). Bioaccumulation and potential sources of heavy metal contamination in fish species in River Ganga basin: Possible human health risks evaluation. *Toxicology Reports*, *6*, 472-481.

Mayo, A. L., & Loucks, M. D. (1995). Solute and isotopic geochemistry and ground water flow in the central Wasatch Range, Utah. *Journal of Hydrology*, *172*(1-4), 31-59.

McNeill, J. D. (1990). Use of electromagnetic methods for groundwater studies. In *Geotechnical an Environmental Geophysics*: Volume I: Review and Tutorial (pp. 191-218). Society of Exploration Geophysicists.

Mehta, P., Saxena, N., Mangla, B., Birla, S., Hussain, R., & Sultan, A. (2015). Identifying backwardness of Mewat region in Haryana: a block-level analysis. *New Delhi: Sehgal Foundation*.

Misra, A. K., & Mishra, A. (2007). Study of quaternary aquifers in Ganga Plain, India: focus on groundwater salinity, fluoride and fluorosis. *Journal of Hazardous Materials*, *144*(1-2), 438-448.

Mosavi, A., Sajedi Hosseini, F., Choubin, B., Taromideh, F., Ghodsi, M., Nazari, B., & Dineva, A. A. (2021). Susceptibility mapping of groundwater salinity using machine learning models. *Environmental Science and Pollution Research*, *28*(9), 10804-10817.

Mudrakartha, S. (1999). Status and policy framework of groundwater in India. VIKSAT, Nehru Foundation for Development.

Mustari, S., & Karim, A. H. M. (2014). Impact of salinity on the socio-environmental life of coastal people of Bangladesh. *Asian journal of social sciences & humanities*, *3*(1), 12-18.

Okiongbo, K. S., & Douglas, R. K. (2015). Evaluation of major factors influencing the geochemistry of groundwater using graphical and multivariate statistical methods in Yenagoa city, Southern Nigeria. *Applied water science*, *5*(1), 27-37.

Payne, B. R., Quijano, L., & Latorre, D. C. (1979). Environmental isotopes in a study of the origin of salinity of groundwater in the Mexicali Valley. *Journal of Hydrology*, *41*(3-4), 201-215.

Piper, A. M. (1944). A graphic procedure in the geochemical interpretation of water-analyses. *Eos, Transactions American Geophysical Union*, *25*(6), 914-928.

Pulido-Leboeuf, P. (2004). Seawater intrusion and associated processes in a small coastal complex aquifer (Castell de Ferro, Spain). *Applied geochemistry*, *19*(10), 1517-1527.

Purushothaman, G., Marion, R., Li, K., & Casagrande, V. A. (2012). Gating and control of primary visual cortex by pulvinar. *Nature neuroscience*, *15*(6), 905-912.

Rakib, M. A., Sasaki, J., Matsuda, H., & Fukunaga, M. (2019). Severe salinity contamination in drinking water and associated human health hazards increase migration risk in the southwestern coastal part of Bangladesh. *Journal of environmental management*, *240*, 238-248.

Ramaroson, V., Rakotomalala, C. U., Rajaobelison, J., Fareze, L. P., Razafitsalama, F. A., & Rasolofonirina, M. (2018). Tritium as tracer of groundwater pollution extension: case study of Andralanitra landfill site, Antananarivo–Madagascar. *Applied Water Science*, *8*(2), 1-11.

Rao, M. S., Purushothaman, P., Krishan, G., Rawat, Y. S., & Kumar, C. P. (2014). Hydro-chemical and isotopic investigation of groundwater regime in Jalandhar and Kapurthala districts, Punjab, India. *International Journal of Earth Sciences and Engineering*, *7*(01), 06-15.

Richards, L. A. (1954). Diagnosis and improvement of saline and alkali soils (Vol. 78, No. 2, p. 154). LWW.

Rina, K., Datta, P. S., Singh, C. K., & Mukherjee, S. (2012). Characterization and evaluation of processes governing the groundwater quality in parts of the Sabarmati basin, Gujarat using hydrochemistry integrated with GIS. *Hydrological Processes*, *26*(10), 1538-1551.

Rodell, M., Velicogna, I., & Famiglietti, J. S. (2009). Satellite-based estimates of groundwater depletion in India. *Nature*, *460*(7258), 999-1002.

Roy, A. D., & Shah, T. (2002). Socio-ecology of groundwater irrigation in India. *Intensive use of groundwater challenges and opportunities*, 307-335.

Rozanski, K., Araguás-Araguás, L., & Gonfiantini, R. (1993). Isotopic patterns in modern global precipitation. *Geophysical Monograph-American Geophysical Union*, *78*, 1-1.

Sahour, H., Gholami, V., &Vazifedan, M. (2020). A comparative analysis of statistical and machine learning techniques for mapping the spatial distribution of groundwater salinity in a coastal aquifer. *Journal of Hydrology*, *591*, 125321.

Saini, K., Singh, P., & Bajwa, B. S. (2016). Comparative statistical analysis of carcinogenic and non-carcinogenic effects of uranium in groundwater samples from different regions of Punjab, India. *Applied Radiation and Isotopes*, *118*, 196-202.

Saranya, P., Krishan, G., Rao, M. S., Kumar, S., & Kumar, B. (2018). Controls on water vapor isotopes over Roorkee, India: Impact of convective activities and depression systems. *Journal of Hydrology*, *557*, 679-687.

Sarin, M. M., Krishnaswami, S., Dilli, K., Somayajulu, B. L. K., & Moore, W. S. (1989). Major ion chemistry of the Ganga-Brahmaputra river system: weathering processes and fluxes to the Bay of Bengal. *Geochimica et cosmochimica acta*, *53*(5), 997-1009.

Shah, D. G., & Pate, P. S. (2011). Physico-chemical characteristics of bore well drinking water of kathalal territory district kheda, Gujarat, India. Der Chemica Sinica.8-11

Sprenger, C., Hartog, N., Hernández, M., Vilanova, E., Grützmacher, G., Scheibler, F., &

Hannappel, S. (2017). Inventory of managed aquifer recharge sites in Europe: historical development, current situation and perspectives. *Hydrogeology Journal*, *25*(6), 1909-1922.

Villholth, K., & Giordano, M. (2007). Groundwater use in a global perspective–can it be managed. *The agricultural groundwater revolution: opportunities and threats to development*, *3*, 393-402.

Dang, X., Gao, M., Wen, Z., Hou, G., Jakada, H., Ayejoto, D., & Sun, Q. (2022). Saline groundwater evolution in the Luanhe River delta (China) during the Holocene: hydro-chemical, isotopic, and sedimentary evidence. *Hydrology and Earth System Sciences*, *26*(5), 1341-1356.

Parvaiz, A., Khattak, J. A., Hussain, I., Masood, N., Javed, T., & Farooqi, A. (2021). Salinity enrichment, sources and its contribution to elevated groundwater arsenic and fluoride levels in Rachna Doab, Punjab Pakistan: Stable isotope (δ2H and δ18O) approach as an evidence. *Environmental Pollution*, *268*, 115710.

Sharma, P. C., & Singh, A. (2012). ICAR-CSSRI Annual Report 2011-12.

Srinivasamoorthy, K., Chidambaram, S., Prasanna, M. V., Vasanth Vihar, M., Peter, J., & Anandhan, P. (2008). Identification of major sources controlling groundwater chemistry from a hard rock terrain—a case study from Mettur taluk, Salem district, Tamil Nadu, India. *Journal of Earth System Science*, *117*(1), 49-58.

Stallard, R. F., & Edmond, J. M. (1983). Geochemistry of the Amazon: 2. The influence of geology and weathering environment on the dissolved load. *Journal of Geophysical Research: Oceans*, *88*(C14), 9671-9688.

Suarez, D. L. (1989). Impact of agricultural practices on groundwater salinity. *Agriculture, ecosystems & environment*, *26*(3-4), 215-227.

Talsma, T. (1963). The control of saline groundwater (Doctoral dissertation, Veenman).

Thomas, A. C., Reager, J. T., Famiglietti, J. S., &Rodell, M. (2014). A GRACE-based water storage deficit approach for hydrological drought characterization. *Geophysical Research Letters*, *41*(5), 1537-1545.

Thomas, B. F., Caineta, J., &Nanteza, J. (2017). Global assessment of groundwater sustainability based on storage anomalies. *Geophysical Research Letters*, *44*(22), 11-445.

Tran, D. A., Tsujimura, M., Pham, H. V., Nguyen, T. V., Ho, L. H., Le Vo, P., ... & Doan, Q. V. (2022). Intensified salinity intrusion in coastal aquifers due to groundwater over extraction: a case study in the Mekong Delta, Vietnam. *Environmental Science and Pollution Research*, *29*(6), 8996-9010.

van Gend, J., Francis, M. L., Watson, A. P., Palcsu, L., Horváth, A., Macey, P. H., ... & Miller, J. A. (2021). Saline groundwater in the Buffels River catchment, Namaqualand, South Africa: A new look at an old problem. *Science of The Total Environment*, *762*, 143140.

Varadarajan, N., Purandara, B. K., & Kumar, B. (2010). Status of salinity in aquifers of Ghataprabha Command Area, Karnataka, India Slanostnerazmere v vodonosnikihupravl jalnegaob močja Ghataprabha v Karnataki (Indija). *RMZ–Materials and Geoenvironment*,*57*(3), 347-362.

Wada, Y., van Beek, L. P., & Bierkens, M. F. (2012). Nonsustainable groundwater sustaining irrigation: A global assessment. *Water Resources Research*, *48*(6).

Wada, Y., Van Beek, L. P., Van Kempen, C. M., Reckman, J. W., Vasak, S., &Bierkens, M. F. (2010). Global depletion of groundwater resources. *Geophysical research letters*, *37*(20).

Ward, J. D., Simmons, C. T., & Dillon, P. J. (2007). A theoretical analysis of mixed convection in aquifer storage and recovery: how important are density effects?. *Journal of Hydrology*, *343*(3-4), 169-186.

Ward, J. D., Simmons, C. T., & Dillon, P. J. (2008). Variable-density modelling of multiple-cycle aquifer storage and recovery (ASR): Importance of anisotropy and layered heterogeneity in brackish aquifers. *Journal of Hydrology*, *356*(1-2), 93-105.

Warrier, C. U., Babu, M. P., Manjula, P., Velayudhan, K. T., Hameed, A. S., & Vasu, K. (2010). Isotopic characterization of dual monsoon precipitation–evidence from Kerala, India. *Current Science*, 1487-1495.

WHO (2007) Guidelines for drinking water, recommendations. WorldHealth Organization, Geneva.

Wilcox, L. (1955). *Classification and use of irrigation waters* (No. 969). US Department of Agriculture.

Williams, W. D. (1999). Salinisation: A major threat to water resources in the arid and semi-arid regions of the world. *Lakes & Reservoirs: Research & Management*, *4*(3-4), 85-91.

Meybeck, M. (1987). Global chemical weathering of surficial rocks estimated from river dissolved loads. *American journal of science*, *287*(5), 401-428.

Witt, L., Müller, M.J., Gröschke, M. et al. (2021) Experimental observations of aquifer storage and recovery in brackish aquifers using multiple partially penetrating wells. Hydrogeol J 29, 1733–1748. https://doi.org/10.1007/s10040-021-02347-7

World Health Organization & International Programme on Chemical Safety. (1996). Guidelines for drinking-water quality. Vol. 2, Health criteria and other supporting information, 2nd ed. World Health Organization.

Yang, Q., Li, Z., Ma, H., Wang, L., & Martín, J. D. (2016). Identification of the hydrogeochemical processes and assessment of groundwater quality using classic integrated geochemical methods in the Southeastern part of Ordos basin, China. *Environmental Pollution*, *218*, 879-888.

Yousefi, M., Ghoochani, M., &Mahvi, A. H. (2018). Health risk assessment to fluoride in drinking water of rural residents living in the Poldasht city, Northwest of Iran. *Ecotoxicology and environmental safety*, *148*, 426-430.

Zektser, I. S., & Everett, L. G. (2004). Groundwater resources of the world and their use. IHP-VI, Series on Groundwater No. 6. UNESCO, Paris

Zuurbier, K. G., Kooiman, J. W., Groen, M. M., Maas, B., & Stuyfzand, P. J. (2015). Enabling successful aquifer storage and recovery of freshwater using horizontal directional drilled wells in coastal aquifers. *Journal of Hydrologic Engineering*, *20*(3), B4014003.

Zuurbier, K. G., Kooiman, J. W., Groen, M. M., Maas, B., & Stuyfzand, P. J. (2015). Enabling successful aquifer storage and recovery of freshwater using horizontal directional drilled wells in coastal aquifers. *Journal of Hydrologic Engineering*, *20*(3), B4014003.

Zuurbier, K. G., Zaadnoordijk, W. J., & Stuyfzand, P. J. (2014). How multiple partially penetrating wells improve the freshwater recovery of coastal aquifer storage and recovery (ASR) systems: A field and modeling study. *Journal of Hydrology*, *509*, 430-441.

APPENDIX-A Project summary

Table A.1: Summary

Project objectives

1. Assessment of lowering of water table (depletion in groundwater level) in the salinity impacted area using the historical data. 2. Detailed qualitative analysis of the area and the aquifer depth impacted by higher salinity levels, and preparation of maps. 3. To monitor influx of saline groundwater into fresh water zone 4. To assess the impact of groundwater salinity on socio-economic aspects 5. To develop and demonstrate management and resilience building measures	Revised objective **NA**	Reasons for revision **NA**

***Manpower* deployed (against sanctioned manpower)**			
Sanctioned		Deployed	
Designation	Person months	Designation	Person months
JRF 2 nos. PA 1 no.	110 months 55 months	JRF 7 nos. PA 2 nos.	92 months 52 months

JRF worked under the PDS

S.N	Name	From	To	Total Duration
1	Pawan Singh Panwar	12/03/2018	12/09/2018	06 month
2	Mamta Bisht	16/03/2018	15/08/2019	1 year 4 months
3	Gokul Prasad	01/10/2018	31/12/2020	2 year 2 months
4	Priyanka Sejwal	13/11/2019	01/03/2021	1 year 3 months 18 days
5	Ravi Kumar	08/03/2021	04/10/2021	6 months 27 days
6	Mohit Kumar	30/03/2021	30/06/2021	1 year 3 months
7	Rahul Garg	21/10/2021	30/06/2021	8 month 10 days

PA worked under PDS

S.N	Name	From	To	Total Duration
1	Ankur Rohilla	06/03/2018	31/03/2022	4 years 26 days
2	Archit Arora	28/04/2022	31/07/2022	3 months 4 days

Infrastructure/ equipment		
EC probe for soil salinity Water level and conductivity loggers	procured	Reasons for deviation NA
Model for ASR experiment	Developed	
Field work		
Sampling for pre-monsoon, monsoon and post monsoon seasons Field Experiment	Completed	Reasons for deviation NA
Workshop/ Capacity building/ technology transfer		
2 Training workshops on Groundwater salinity	Organized	
July, 2019 February, 2021		
Study area		
Planned	Extended	
Mewat district	NA	
New data generated in the project		
Salinity data Isotope data	Achieved	Reasons for deviation NA

Envisaged contribution of the project

Identify salinity mechanism and suggest remedial measures	Salinity mechanism was identified and ASR technique was suggested in saline areas	Reasons for deviation NA

How research outcome benefited the end user department and society

The experimental model deals with to undertake a demonstrative scheme as resilience building measure towards developing a fresh water pocket in saline aquifers and to predict changes in groundwater salinity as a result of aquifer recharge and extraction.	Benefit derived	Reasons for deviation NA

End-of-project deliverables

Project report Publications	**Achieved**	Reasons for deviation
Total publications	**17**	

Outsourcing (>1 lakh)/ consultancy(All)

Sehgal Foundation Gurgaon	Socioeconomic survey	Estimated cost Rs 3.50 lakhs + GST	Actual cost Rs 3.50 lakhs + GST

Financial achievement

S No	Head	Approved budget	Approved revised budget	Final expenditure	Reasons for deviation
1	Remuneration/Emoluments for Manpower etc.	23.47200	35.97200		Budget of project staff revised
2	Traveling Expenditure	5.00000	4.00000		Limited travelling due to covid 19
3	Infrastructure/Equipment	16.00000	12.00000		LI and GEM purchase
4	Experimental Charges/Field work/Consumables	14.02800	10.52800		Fabrications by local
5	Capacity building/Technology transfer	5.00000	1.00000		Online training due to COVID-19
6	Contingency	1.50000	1.50000		
7	Outsourcing/ consultancy				
	Total	**65.00000**	**65.00000**		

Table A.2: Quantitative outcome

i. Research papers published/ submitted		
S No	Research paper (National/ International Journal/ conferences/ symposium/ workshop/ seminar)	Impact factor for Journal
1	**Krishan, Gopal,** Bhagwat, A, Sejwal, Priyanka, Yadav, BK, Kansal, ML, Bradley, A, Singh, S, Kumar, M, Sharma, LM., Muste, M, 2021. Controls of groundwater salinity, using principal component analysis (PCA)- case study from Mewat (Nuh), Haryana, India. Environment Monitoring and Assessment (revised submitted)	**3.307**
2	Shyam Radhe, **Krishan, Gopal**, Kheraj and Kumar, Amit. 2022. Evaluation of Groundwater quality for life-supporting activities: A case study of Haryana, India, The International Journal of River Basin Management (under review)	Taylor and Francis
3	Pradeep, Gokul and Krishan, Gopal. 2022. Groundwater and Agriculture Potential Mapping of Mewat District, Haryana, India. Discover Water (under review)	Springer

4	**Krishan, Gopal,** Kumar, Bhishm, Rao, MS, Yadav, BK, Kansal, ML. 2021. Environmental tracers in identification of the groundwater salinity – case studies from northwest India. In: International e-conference on "Water source sustainability" held by the Indian Water Resources Society (IWRS) and Department of Water Resources Development and Management IIT-Roorkee during 18-20 June, 2021	IIT-Roorkee
5	**Krishan, Gopal** and Bhattacharya, P. 2021. Arsenic occurrence in soil sediments in Mewat, Haryana, India. In: The 8th International congress and exhibition on arsenic in the environment during 7-9 June, 2021, at Netherlands	Netherlands
6	**Krishan, Gopal**. 2021. Groundwater salinity causes, impact and management solutions. In: International symposium on "Transforming coastal zones for sustainable food and income security" held by the Indian Society of Coastal Agricultural Research in collaboration with ICAR-CSSRI Karnal during 16-19 March, 2021	ISCA-2021
7	**Krishan, Gopal**, Sejwal, P, Anajli, Prasad, Gokul, Yadav, Brijesh, Kumar, C.P., Kansal, M.L., Singh, Surjeet, Sudarsan, N, Bardley, Allen, Sharma Mohan, Lalit, Muste, M. 2021. Role of major ions in aquifer salinization – a case study from a semi-arid region of Haryana, India. Water *13*(5), 617; https://doi.org/10.3390/w13050617.	**3.530**
8	Kaushal, Abhishek Anand, **Krishan Gopal**, Pandey Govind (2020). Recovery efficiency of an aquifer storage and recovery (ASR) experiment from saline aquifer under controlled conditions. Current World Environment 15 (3) 441-445	NAAS Rating 4.98
9	**Krishan, Gopal**, Prasad, Gokul, Anajli, Kumar, C.P., Patidar, Nitesh, Yadav, Brijesh, Kansal, M.L., Singh, Surjeet, Sharma Mohan, Lalit, Bardley, Allen, Verma, S.K. 2020. Identifying the seasonal variability in source of groundwater salinization using deuterium excess- a case study from Mewat, Haryana, India. Journal of Hydrology- Regional Studies, 31: 100724 https://doi.org/10.1016/j.ejrh.2020.100724	**5.119**
10	**Krishan, Gopal**, Ghosh, N.C., Kumar, C.P., Sharma Mohan, Lalit, Yadav, Brijesh, Kansal, M.L., Singh, Surjeet, Verma, S.K., Prasad, Gokul. 2020.Understanding stable isotope systematics of salinity affected groundwater in Mewat, Haryana, India. J Earth Syst Sci 129, 109 (2020). https://doi.org/10.1007/s12040-020-1380-6	**1.423**
11	**Krishan, Gopal,** Kumar, CP, Prasad, Gokul, Kansal, M. L., Yadav, Brijesh and Verma, S.K. 2020. Stable Isotopes and Inland Salinity Evidences for Mixing and Exchange. In: Proceedings of Roorkee Water Conclave (RWC-2020) during 26-28 February, 2020 at IIT Roorkee	IIT-Roorkee
12	**Krishan**, **Gopal,** Kumar, C.P., Prasad, Gokul, Sharma, Lalit Mohan, Kansal, M.L,. Yadav, Brijesh Kumar, Singh, Surjeet, and Bisht, Mamta. 2019. Inland groundwater salinity and its movement towards fresh water aquifers- indicators of saline water intrusion for Mewat, Haryana. In:Proceedings of 2nd International conference on Sustainable Water Resource Management under aegis of National Hydrology Project during 06-08 November, 2019 at Pune	NHP-Pune
13	Bisht, Mamta, **Krishan, Gopal**, Kumar, CP, Prasad, Gokul, Singh, Surjeet. 2019. Evaluation of groundwater quality for irrigation purposes at Mewat, Haryana, India In:Proceedings of International Groundwater Conference (IGWC-2019) Sustainable management of soil and water resources during 21-24 October, 2019 at IIT Roorkee	IIT-Roorkee

14	**Krishan**, **Gopal,** Kumar, C.P., Yadav, Brijesh Kumar, Prasad, Gokul, Sharma, Lalit Mohan, Singh, Surjeet, Kansal, M.L. and Bisht, Mamta. 2019. Groundwater salinity causes and remediation- a case study from Mewat, Haryana.. In:Proceedings of an International conference "India Water Week 2019-Water cooperation-coping with 21st century challenges" (IWW-2019), 24-28 September, 2019at New Delhi, India	IWW-2019
15	**Krishan**, **Gopal,** Ghosh N.C., Bist, Mamta, Prasad, Gokul, Sharma, LM, Yadav, BK, Kansal, ML, Kumar, CP, Singh, Surjeet. 2018. Hydrogeochemical processes in salinity affected groundwater, in Mewat (Nuh), Haryana, India.In:Proceedings of 1st International conference on Sustainable Water Resource Management under aegis of National Hydrology Project during 10-11 December, 2018 at Chandigarh. Pp 678-685	NHP-Chandigarh
16	**Krishan G**, Chandniha S. K, Lohani A. K, Yadav B. K, Arora N. K, Singh S, Kumar C. P, Sharma L. M, Bhardwaj A. K. 2018. Assessment of heavy metals in relation to soil pollution at Mewat, Haryana, India. Curr World Environ **13(3):299-306**	NAAS Rating 4.98
17	Priyanka, **Krishan, Gopal**, Sharma, Ghosh, N.C., Lalit Mohan, and Yadav, Brijesh. 2018. A. survey on the water related issues in arid and semi-arid Mewat district, Haryana. NDC-WWC. Journal. **7 (1): 19-23**.	CBIP Journal

Reports/Monographs/Internal publications brought out

S. No.	Reports/Monographs/Internal publications
1	NIH annual report 2018-19, 2019-20; 2020-21; 2021-22; NHP news letter 2019

ii. New techniques/models/ software/ knowledge developed, if any

Experimental Model for development of fresh water pocket

iii. Web site/ application developed

Name	Web address	Server location	Launch date	Details of information available
	NA			

iv. Patents filed/awarded, if any: " Experimental Model for Development of Fresh water pocket in saline aquifers. "No. UCS&T/PIC/PATENT-33/2018-19; Some observations/objections –will be resolved soon

Workshop/ conferences/ seminars/capacity building programmes organised

S. No.	Topic	Dates, duration, No. of participants	Report published (Y/N)
1	Groundwater issues of Punjab with special emphasis on groundwater salinity	July 16-18, 2019 at Mohali; 34 participants	Submitted to NHP
2	Groundwater salinity issues and management solutions	February 17-19, 2021, online; 21 participants	Submitted to NHP

v. Stake holders feedback and action taken on constructive feed back

S No.	Feedback received	Action taken
Stake holder meet (Topic and date)		

vi. Field observations obtained, thematic maps generated (water quality and salinity, isotope, soil moisture, stage and discharge, sediment, water level, river cross sections, geophysical/ resistivity survey, hydrogeological investigations etc.)			
S No	Parameter, frequency, period, groundwater/ river/ tank/ hand pump/ spring/ sea-water	Number (planned)	Numbers (measured)

vii. Field installations (piezometers, river stage/ discharge, soil moisture etc.)					
S. No	Name, make/ model	Unit price, total price, quantity	Date of installation	% utilization	Remarks regarding maintenance/ breakdown
1	Water level/conductivity loggers (Encardiorites)	Rs. 4,80,000/-	April, 2019		3 times repaired by the company, performance not satisfactory
2	Rain gauges (tipping bucket)	Rs. 1,20,000/-	July, 2020		Installed and data is being recorded

viii. Equipment/ software purchased					
a. Equipment purchased					
S. No	Name, make/ model	Unit price, total price, quantity	Date of installation	% utilization	Remarks regarding maintenance/ breakdown
1	Ion Meter (ISE)/Thermo Fischer model 2140	1,20,000/-	June, 2022	29 samples analysed in the field	
2	Soil EC probe	53,000/-	April, 2019	Used in the field	
b. Software purchased					
S. No	Name, version, license	Unit price, total price, quantity	Date of installation	% utilization	Remarks regarding maintenance/ breakdown
	NA				

ix. Plans for utilizing the equipment facilities in future		
S. No.	Installation/ equipment	Planned future use
1	Will remain installed in field	Readings will be taken periodically

x. Data dissemination policy for data generated in the project

xi. Number of post-graduate/doctoral candidates completed their courses (Please give a list of such candidates)
6 Master dissertation work completed using facility created/data generated under this PDS
DAAD fellowship (1), HTWD, Germany 2019
NIT Manipur (1) - 2021
MMIT, Gorakhpur, UP (2) - 2019, 2020
CU Mahendergarh, Haryana (1) - 2021
KUFOS, Kerala (2) - 2022
xii. Foreign deputation/visit of PI/Co-PIs/students, if any **NA**

A.3 Activity chart

Include activity chart/ modified activity chart, reasons for modification of activity chart.
(FOUR MONTHS WISE FROM JAN. 2018 TO JUL 2022)

Item/Period quarterwise	**1-4**	**5**	**6**	**7**	**8**	**9**	**10**	**11**	**12**	**13**	**14**
Data/literature collection											
Field Surveys											
Sample collection											
Analysis											
Data interpretation											
Suggestions/remedial measures											
Report writing/publications											

Appendix B Supplementary results

Provide supplementary results here, if any






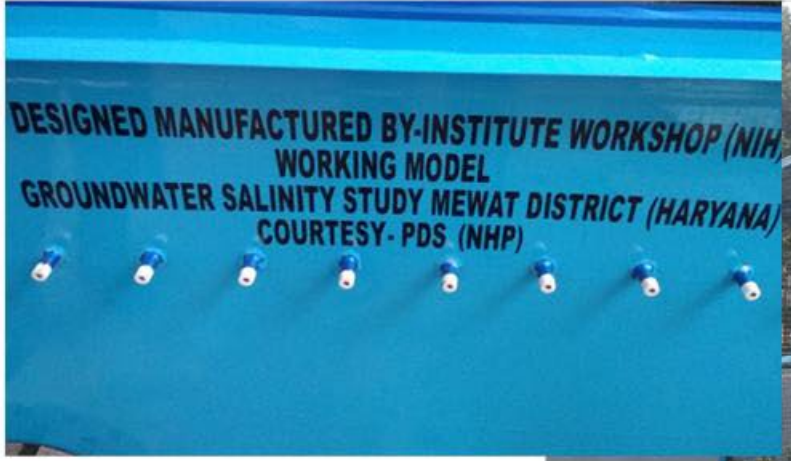
DESIGNED MANUFACTURED BY-INSTITUTE WORKSHOP (NIH)
WORKING MODEL
GROUNDWATER SALINITY STUDY MEWAT DISTRICT (HARYANA)
COURTESY- PDS (NHP)


Diglux


Dr. Allen, IOWA University, USA
01-08-2019


Dr. Peter Dillon, CSIRO, A
25-10-2019


Students IOWA University, USA
17-01-2020







M- 4
SHOT ON REDMI 7
AI DUAL CAMERA
2020/9/8 13:39

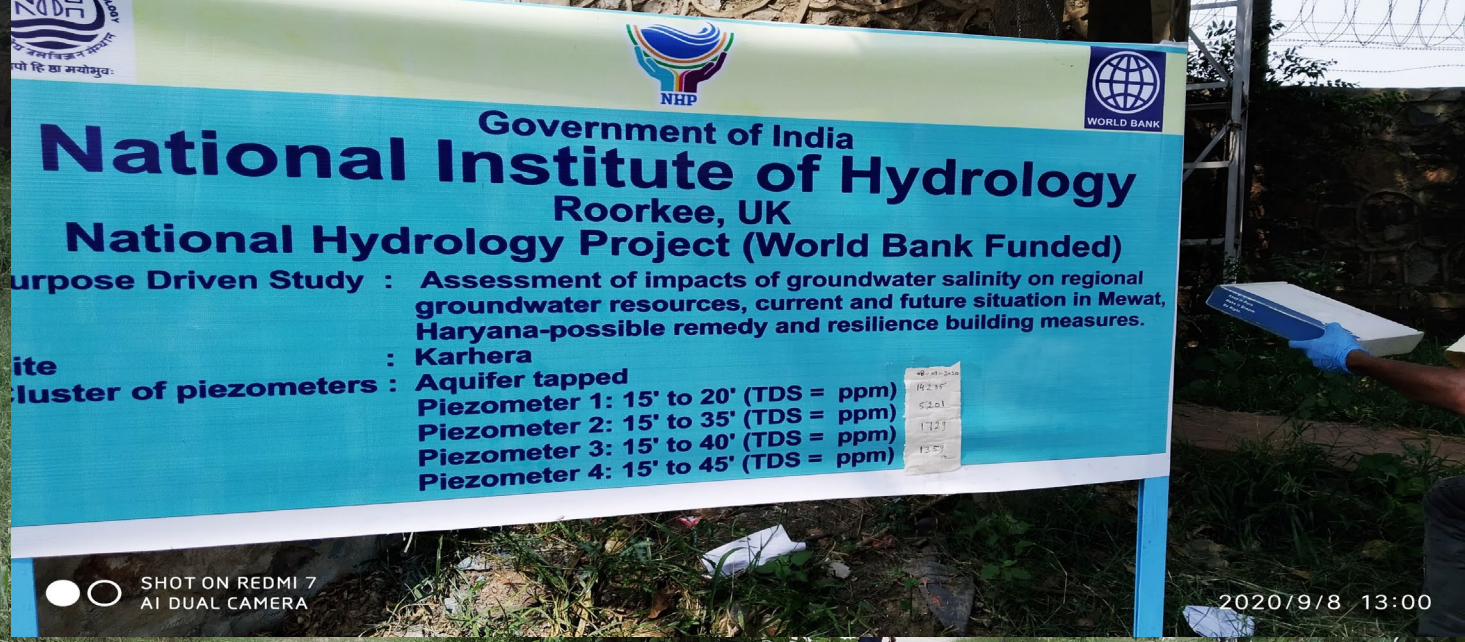
NHP
WORLD BANK
Government of India
National Institute of Hydrology
Roorkee, UK
National Hydrology Project (World Bank Funded)
urpose Driven Study : Assessment of impacts of groundwater salinity on regional groundwater resources, current and future situation in Mewat, Haryana-possible remedy and resilience building measures.
ite : Karhera
luster of piezometers : Aquifer tapped
Piezometer 1: 15' to 20' (TDS = ppm)
Piezometer 2: 15' to 35' (TDS = ppm)
Piezometer 3: 15' to 40' (TDS = ppm)
Piezometer 4: 15' to 45' (TDS = ppm)
SHOT ON REDMI 7
AI DUAL CAMERA
2020/9/8 13:00


राष्ट्रीय जल परियोजना
भारत सरकार द्वारा गठित सोसायटी जल शक्ति मंत्रालय
राष्ट्रीय जलविज्ञान संस्थान
जलविज्ञान भवन, रुड़की - 247667, भारत
DEPTH-35'
DEPTH-20'
SHOT ON REDMI 7
AI DUAL CAMERA
2020/9/8 13:39


Front view of ASR setup
National Institute of Hydrology
PM-1
PM-2
PM-3


Top view of ASR setup


Side view of ASR setup
DEPTH 40'


PM-3
PM-2

TRAINING COURSE
on

GROUNDWATER ISSUES OF PUNJAB WITH SPECIAL EMPHASIS ON GROUNDWATER SALINITY

(July 16-18, 2019)

at

Forest Complex, Mohali

Organized by:

आपो हि ष्ठा मयोभुवः

National Institute of Hydrology

(Under NHP)

Roorkee - 247 667(Uttarakhand)

Dr. Gopal Krishan
Course Coordinator

Dr. A.K. Lohani
Training Coordinator, NHP

Dr. S.K. Jain
NHP Nodal Officer, NHP

GROUNDWATER SALINITY-ISSUES AND MANAGEMENT SOLUTIONS

Training Course: February 17-19, 2021
National Hydrology Project

Course Coordinator
Gopal Krishan
Scientist - C
Groundwater Hydrology Division
NIH, Roorkee
E-mail: drgopal.krishan@gmail.com

Training Coordinator
A.K. Lohani
Scientist - G & Head
Surface water Hydrology Division

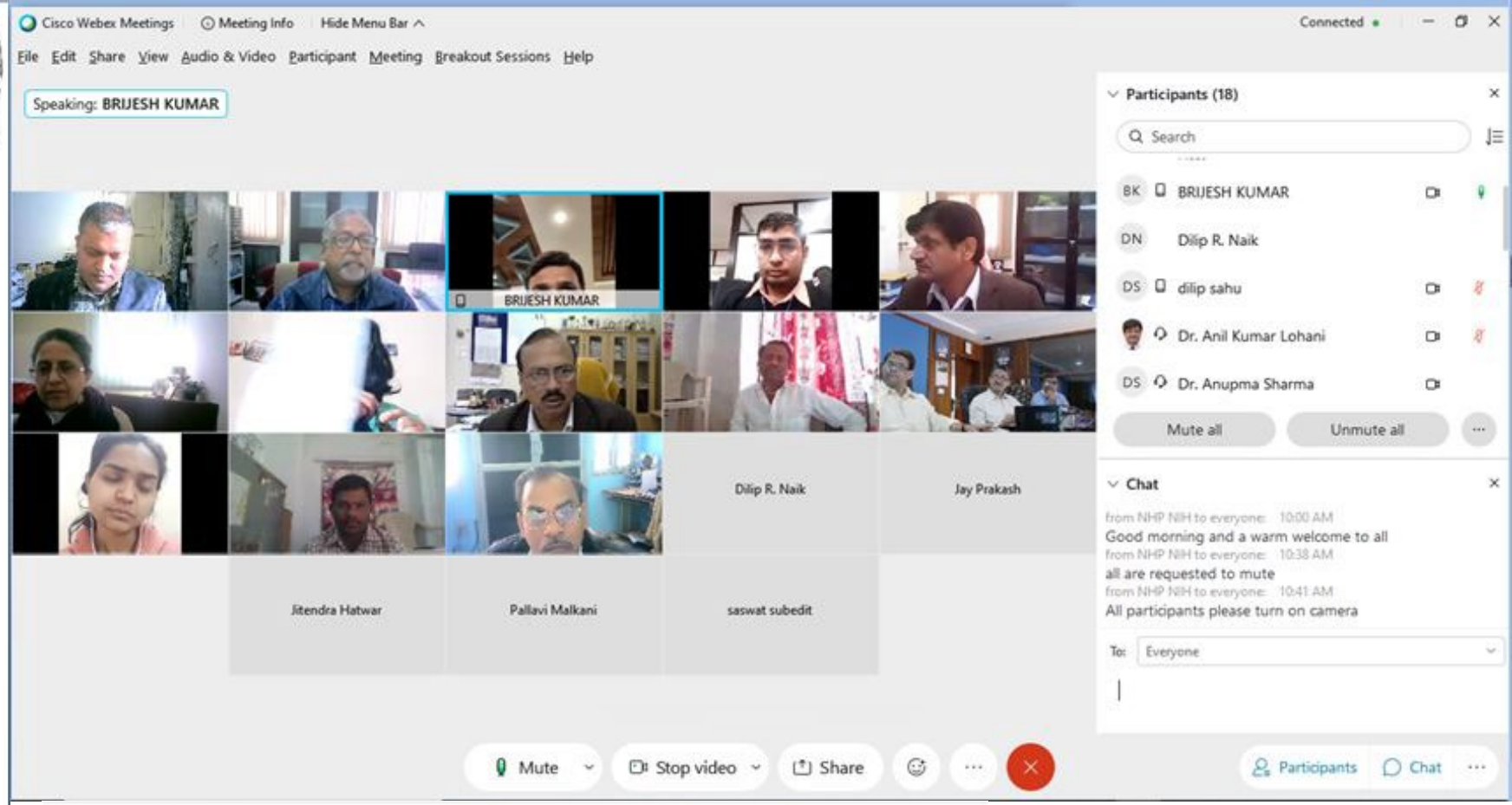

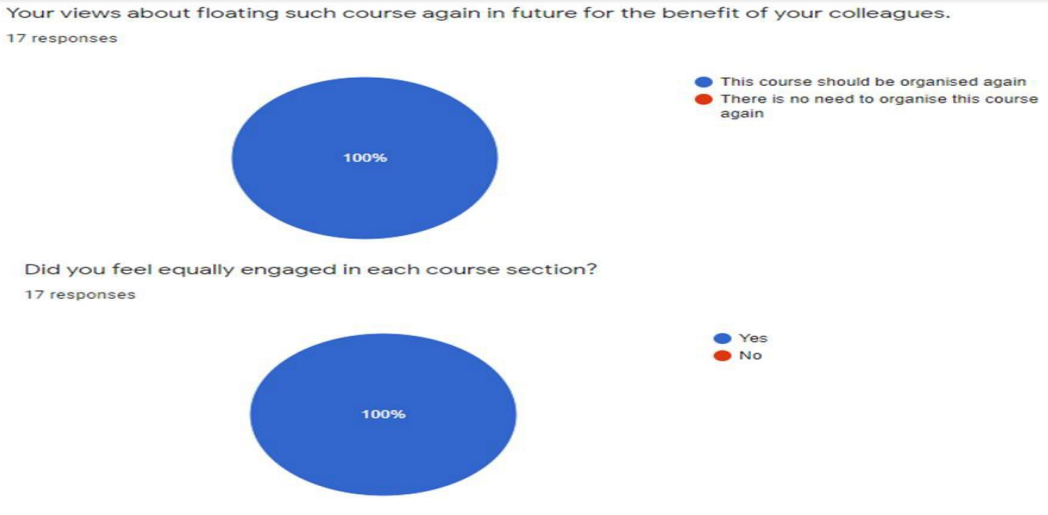

Assessment of impacts of groundwater salinity on regional groundwater resources, current and future situation in Mewat, Haryana – possible remedy and resilience building measures

PDS-ANNUAL PROGRESS

July-2021

IA	:	National Institute of Hydrology, Roorkee
Lead Organisation	:	National Institute of Hydrology, Roorkee
Partner Organisations:		Haryana Irrigation & WRD
		IIT, Roorkee
		Sehgal Foundation, Gurgaon
PI	:	Dr. Gopal Krishan
Budget	:	65 lakhs
2018-2022		

PURPOSE DRIVEN STUDY (PDS) – AN INITIATIVE UNDER NHP

A COMPREHENSIVE STUDY ON HYDROLOGICAL AND HYDROGEOLOGICAL FEATURES FOR GROUNDWATER SALINITY IN MEWAT DISTRICT OF HARYANA

A number of purpose driven studies are ongoing under NHP. One of such studies is dealing with Groundwater salinity at Mewat District, Haryana. Ground water salinity is a global problem, and saline aquifers are most often located in the arid and semi-arid regions of the world. Groundwater salinity in a number of districts in Haryana has given rise to water scarcity for irrigation and domestic uses (CGWB, 2007). Increase of illegal extraction of groundwater from fresh water zones has forced government to intervene for stopping such extractions. Mewat district in Haryana with a geographical coverage of about 1500 sq. km. area with population of 1,089,406 (2011-Census) is one such groundwater salinity effected district. The district lacks in perennial surface water resource and thus, groundwater is being used as the source for irrigation and domestic water, which resulted into aggravation of salinity. If exploited at the current rate, the depleting fresh groundwater in the district can turn into serious water scarcity in next 10-15 years (CGWB, 2007).

Overview of Mewat District, Haryana

Mewat district in Haryana that covers about 1500 sq. km. geographical area with population of 1,089,406 (2011-Census) is major depended on agricultural. The area is devoid of perennial surface water sources making availability of groundwater the critical factor in defining the sustainability of the agro-ecosystem here. Groundwater has become the main source of water for irrigation and domestic use. The major crops grown in the area are wheat, millet and mustard, vegetable crops like onion, tomato, eggplant, chilly, etc. Freshwater aquifer resources in the district are limited, mainly because of low annual rainfall (semi-arid region) and aquifer heterogeneity. On the other hand, the groundwater salinization issues have debilitated the already struggling local economy that relies primarily on groundwater irrigation for farming and adversely affecting the agricultural productivity by deteriorating soil health and limits the choices of crops for farmers.

More than 95% of the population in the district, who live in the rural pockets, and predominantly depend on agriculture as their occupation are dwelling with these unfavourable circumstances. The district also lags behind all other district of Haryana in terms of almost all development indicators, such as education, health, livelihood, etc. The percentage of rural households living Below Poverty Line (BPL) in Mewat area is almost double to that of all other districts in the state. The literacy rate in the district is quite low (41.7%), and also has unequal female to male ratio (907:1000), high infant mortality rate, and poor maternal health. The PDS, that will be carried out at a pilot scale here, will made an interesting contribution to the study of groundwater resources with a regional scope.

National Institute of Hydrology @NIH_Hydrology · Aug 13, 2020

Dr. **Gopal Krishan** scientist NIH Roorkee, and the team have Downloaded data from **loggers** and sampling at Nakodar(Jalandhar) and Sultanpur Lodhi (Kapurthala) under BGS-UK project. #janshakti4jalshakti @MoJSDoWRRDGR

4

National Institute of Hydrology @NIH_Hydrology · Jun 30, 2020

#NIH scientist Dr. **Gopal Krishan** and the team in fieldwork in ongoing Mewat PDS (NHP) for groundwater sampling and **loggers** installation in salinity affected areas.

It was a Pre-COVID 19 fieldwork and to see the change fieldwork will be carried out shortly to see Lockdown effects

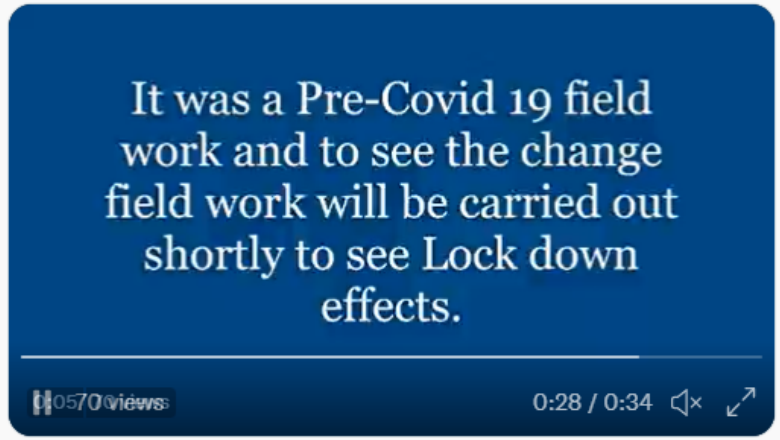

2

National Institute of Hydrology @NIH_Hydrology · Sep 9, 2020

Installation of conductivity and water level **loggers** By NIH Scientist Dr. **Gopal Krishan** and team in newly developed Piezometers under Mewat PDS (NHP) WB funded @MoJSDoWRRDGR

National Hydrology Project @NHPConnect · Jul 8

A Purpose-DrivenStudy under NHP(@NHPConnect)has been undertaken by the @NIH_Hydrology in Mewat,Haryana for understanding the sources of salinization,their relative contributions &to assess seasonal variability for planning best practices in WaterManagement.
#water
@MoJSDoWRRDGR

National Institute of Hydrology @NIH_Hydrology · Jul 24

Construction of cluster of piezometer work started in Mewat purpose-driven study under NHP (WB Funded) to assess salinity variation depth-wise.
#janshakti4jalshakti @MoJSDoWRRDGR

4

National Institute of Hydrology @NIH_Hydrology · Mar 8, 2021

NIH scientist Dr **Gopal Krishan** and the team slowly and steadily, a step towards the final objective of Mewat PDS setting up of experiment developing freshwater bubble/ASR as remediation/management solution for high salinity under **NHP**
#JanShakti4JalShakti @MoJSDoWRRDGR @NHPConnect

4

National Institute of Hydrology @NIH_Hydrology · Mar 31, 2021

#Congratulations to Dr. **Gopal Krishan** and Team.
Under Mewat **PDS**(NHP-WB) the first part of the experiment was successful in reducing groundwater salinity by 7 times.
#JanShakti4JalShakti #waterconservation #watersecurity

Ministry of Jal Shakti #AmritMahotsav

3 2

National Institute of Hydrology @NIH_Hydrology · Sep 1, 2021

Dr. **Gopal Krishan**, Scientist -D made a visit to **Mewat** PDS (NHP) ASR site along with IIT Roorkee partners Prof. Brijesh Yadav and the team for a geophysical survey.
#jalcharcha
@MoJSDoWRRDGR

1 5

National Institute of Hydrology @NIH_Hydrology · Dec 2, 2021

Dr **Gopal Krishan** presented work on "Controls of groundwater salinity, using principal component analysis (PCA)-case study from **Mewat**, Haryana, India". In: International Conference on Recent Advances in Water Science and Technology organized during Dec. 02-03,2021 at @srishakthian

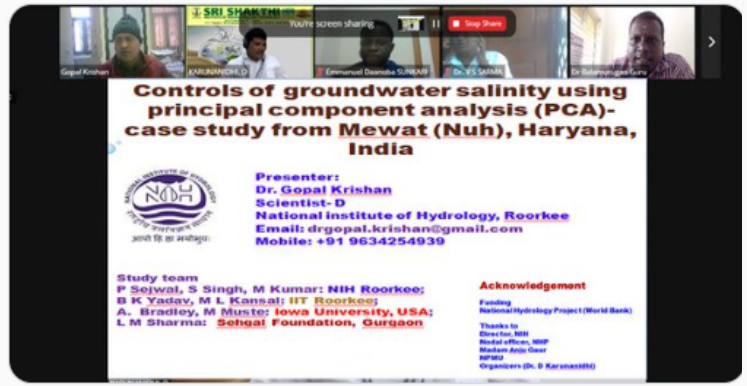

Ministry of Jal Shakti #AmritMahotsav

6 16

National Institute of Hydrology @NIH_Hydrology · Feb 19, 2021

Completed online 3 days training course on Groundwater salinity issues and management solutions under **NHP**, on 3rd-day lectures were delivered by Dr. MK Goel Sc. G & Head, GWHD, NIH, Dr. Brijesh Kumar, Assoc. Prof. DOH, IITR, Dr.Surjeet Singh, Sc. F, and Dr. **Gopal Krishan**, Sc. C

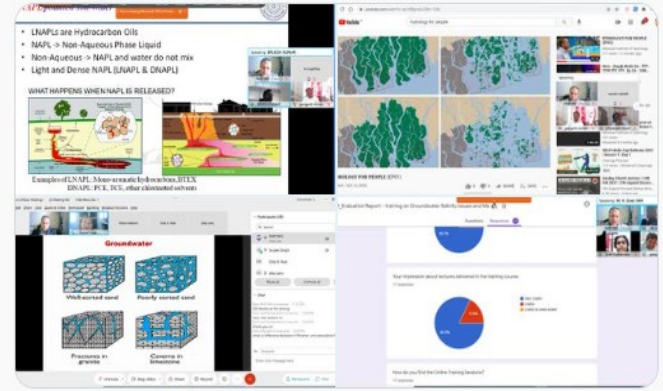

Ministry of Jal Shakti #AmritMahotsav

1

J. Earth Syst. Sci. (2020)129 109
https://doi.org/10.1007/s12040-020-1380-6

Understanding stable isotope systematics of salinity affected groundwater in Mewat, Haryana, India

Gopal Krishan[1,*], N C Ghosh[1], C P Kumar[1], Lalit Mohan Sharma[2], Brijesh Yadav[3], M L Kansal[3], Surjeet Singh[1], S K Verma[1] and Gokul Prasad[1]

water

MDPI

Article

Role of Ion Chemistry and Hydro-Geochemical Processes in Aquifer Salinization—A Case Study from a Semi-Arid Region of Haryana, India

Gopal Krishan [1,*], Priyanka Sejwal [1], Anjali Bhagwat [2], Gokul Prasad [1], Brijesh Kumar Yadav [3], Chander Prakash Kumar [1], Mitthan Lal Kansal [4], Surjeet Singh [1], Natarajan Sudarsan [1], Allen Bradley [5], Lalit Mohan Sharma [6] and Marian Muste [5]

Journal of Hydrology: Regional Studies 31 (2020) 100724

Contents lists available at ScienceDirect

Journal of Hydrology: Regional Studies

journal homepage: www.elsevier.com/locate/ejrh

ELSEVIER

Identifying the seasonal variability in source of groundwater salinization using deuterium excess- a case study from Mewat, Haryana, India

G. Krishan[a,*], G. Prasad[a], Anjali[a], C.P. Kumar[a], N. Patidar[a], B.K. Yadav[b], M.L. Kansal[b], S. Singh[a], L.M. Sharma[c], A. Bradley[d], S.K. Verma[a]

CURRENT WORLD ENVIRONMENT

ISSN: 0973-4929, Vol. 13, No. (3) 2018, Pg. 299-306

Current World Environment

Journal Website: www.cwejournal.org

Assessment of Heavy Metals in Relation to Soil Pollution at Mewat, Haryana, India.

GOPAL KRISHAN[1*], S.K. CHANDNIHA[2], A.K. LOHANI[1], BRIJESH KUMAR YADAV[3], NARESH KUMAR ARORA[4], SURJEET SINGH[1], C.P. KUMAR[1], LALIT MOHAN SHARMA[5] and A.K. BHARDWAJ[4]

Possible methodology for remediation of saline aquifers through fresh water recharge-a new approach

A Dissertation Submitted

In Partial Fulfillment of the Requirements for the Degree of M. Tech.

by

Ashutosh Kumar Yadav

Co-Supervisor	Supervisor
Dr. Gopal Krishan	**Dr. Govind Pandey**
Scientist 'C'	Professor & Head,
Groundwater Hydrology Division	Dept. of Civil Eng.
N.I.H., Roorkee	M. M. M. U. T., Gorakhpur

DEPARTMENT OF CIVIL ENGINEERING

Madan Mohan Malaviya University of Technology,
Gorakhpur (U.P.)- INDIA
May, 2019

Determination of Recovery Rates using Aquifer Storage and Recovery (ASR) Techniques under Controlled Conditions

A Dissertation Submitted

In partial fulfilment of the requirements for the Degree of M. Tech.

in

Environmental Engineering

By

Abhishek Anand Kaushal (Roll No. 2018013201)

Co-Supervisor	Supervisor
Dr. Gopal Krishan	**Dr. Govind Pandey**
Scientist 'C'	Professor & Head,
Groundwater Hydrology Division	Dept. of Civil Eng.
N.I.H., Roorkee	M. M. M. U. T., Gorakhpur

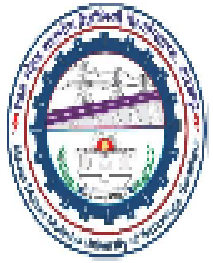

Department of Civil Engineering
Madan Mohan Malaviya University of Technology
Gorakhpur- 273010 (U.P.)- India

राष्ट्रीय जलविज्ञान संस्थान
(जल संसाधन, नदी विकास और गंगा संरक्षण मंत्रालय के अधीन भारत सरकार की समिति)
जलविज्ञान भवन, रूड़की – 247667, (उत्तराखण्ड), भारत
National Institute of Hydrology
[Government of India Society under Ministry of Water Resources, River Development & Ganga Rejuvenation)
Jalvigyan Bhawan, Roorkee - 247 667, (Uttarakhand), INDIA
(An ISO 9001 : 2008 Certified Organization)
Phone : +91-1332-272106, 272106
Fax : +91-1332-272123, 273976

Dr. Gopal Krishan
Scientist-C
Groundwater Hydrology Division,
National Institute of Hydrology, Roorkee
247667 (Uttarakhand)
Mobile: +91 9634254939, 7906057455
Email: drgopal.krishan@gmail.com; drgopal.krishan.nihr@gov.in

TESTIMONIALS

I have known Mr. Johannes Malte Medick for about 2 years. He has assisted in salinity experiments on an in-house model developed in a Purpose Driven Study "Assessment of impacts of groundwater salinity on regional groundwater resources, current and future situation in Mewat, Haryana – possible remedy and resilience building measures" under National Hydrology Project funded by World Bank. The work was done during November 2018 to January 2019 part of his DAAD fellowship period at National Institute of Hydrology, Roorkee under my supervision and guidance. Mr Johannes took keen interest to learn and execute the work efficiently. He has been found efficient in management and coordinated efforts which he proved through working at the institute. I wish him all success for the best of his future.

(Gopal Krishan) 10/2020

Dr. Gopal Krishan
Scientist
Groundwater Hydrology Div.
National Institute of Hydrology
Roorkee

A STUDY ON FEASIBILITY OF AQUIFER STORAGE AND RECOVERY TECHNIQUE IN SALINE AQUIFER OF MEWAT HARYANA

A Thesis submitted to

National Institute of Technology Manipur

for the award of the Degree

of

Master of Technology

in Environmental and Water Resources Engineering

by

JAY PRAKASH

19201003

DEPARTMENT OF CIVIL ENGINEERING

NATIONAL INSTITUTE OF TECHNOLOGY MANIPUR

IMPHAL -795004

MAY, 2021

GROUNDWATER QUALITY EVALUATION FOR DRINKING AND IRRIGATION PURPOSES IN MEWAT, HARYANA

A Thesis submitted to
Central University of Haryana, Mahenderagarh
For the award of the Degree
of

Master of Science
in Geography
by

RADHE SHYAM
Roll No.- 190754
Under Supervision of

Dr. Kheeraj
Assistant Professor
CUH, Mahendergarh

Dr. Gopal Krishan
Scientist-D,
NIH Roorkee

DEPARTMENT OF GEOGRAPHY
CENTRAL UNIVERSITY OF HARYANA
MAHENDERGARH -123031
JUNE, 2021

A STUDY ON MANAGEMENT OF GROUNDWATER SALINITY: AN EXPERIMENT UNDER CONTROLLED CONDITIONS

Project Submitted to **Cochin University of Science and Technology (CUSAT)** for partial fulfillment of MSc Degree in MARINE GEOLOGY, 2020-2022.

Submitted by

Ms. GAYATHRI B S

Reg. No. 31620007

Department of Marine Geology and Geophysics, CUSAT

Under the Guidance of:

Dr. Gopal Krishan
Scientist-D, Groundwater Hydrology Division
National Institute of Hydrology
Roorkee
India -247667

GROUNDWATER AND AGRICULTURE POTENTIAL MAPPING OF MEWAT DISTRICT, HARYANA, INDIA

DISSERTATION SUBMITTED FOR THE PARTIAL FULFILLMENT OF REQUIREMENT FOR THE DEGREE OF MASTER OF SCIENCE IN APPLIED GEOLOGY

SUBMITTED BY

GOKUL PRADEEP

SCHOOL OF OCEAN STUDIES AND TECHNOLOGY

KERALA UNIVERSITY OF FISHERIES AND OCEAN STUDIES, KOCHI – 682506.

UNDER THE GUIDANCE OF

DR. GOPAL KRISHAN

SCIENTIST-D, GROUNDWATER HYDROLOGY DIVISION,NATIONAL INSTITUTE OF HYDROLOGY,

ROORKEE – 247667